© 2018

John Thomas Szilagyi

ALL RIGHTS RESERVED

LIPID REGULATION OF PLACENTAL MYCOTOXIN TRANSPORT

By

JOHN THOMAS SZILAGYI

A dissertation submitted to

The School of Graduate Studies

Rutgers, The State University of New Jersey

In partial fulfillment of the requirements

For the degree of

Doctor of Philosophy

Graduate Program in Toxicology

Written under the direction of

Drs. Lauren M. Aleksunes and Jeffrey D. Laskin

And approved by

_____

_____

_____

_____

_____

New Brunswick, New Jersey

October, 2018

ABSTRACT OF THE DISSERTATION

Lipid Regulation of Placental Mycotoxin Transport

By: JOHN THOMAS SZILAGYI

Dissertation Directors: Lauren Aleksunes, PharmD, PhD, DABT; Jeffrey Laskin, PhD

During pregnancy, the placental BCRP/*ABCG2* efflux transporter prevents the transplacental transfer of chemicals and protects the fetus from exposure to toxicants. Prior studies have demonstrated that BCRP can transport zearalenone, an estrogenic mycotoxin produced by fungi that grows on cereal crops. However, there is little known regarding the neonatal outcomes of compromised placental BCRP function in pregnant women exposed to zearalenone. Because of its estrogenic activity, *in utero* exposure to zearalenone could potentially increase the risk of altered sexual development and certain cancers. The purpose of this dissertation was to determine the influence of lipids on the expression and function of placental BCRP and its impact on the placental distribution of zearalenone during pregnancy. In both *in vitro* transwell models of the placental barrier (Marine Darby Canine Kidney cells and BeWo trophoblasts) and *in vivo* experiments with C57BL/6 mice, BCRP/Bcrp prevented the maternal-to-fetal transfer of zearalenone. Anandamide, an endocannabinoid, is known to influence placental development and function and may play a role in certain diseases of pregnancy. Studies using both human term placental explants and BeWo trophoblasts revealed that anandamide can down-regulate BCRP mRNA transcription and protein expression via a CB2-cyclic AMP signaling pathway. In BeWo trophoblast cells, anandamide increased the retention of Hoechst 33342, a fluorescent BCRP substrate, and zearalenone without directly inhibiting BCRP. Anandamide also decreased the basolateral-to-apical transport of glyburide, a BCRP substrate prescribed for gestational diabetes. Detailed analysis of

human placenta specimens and BeWo trophoblasts also revealed that BCRP function is dependent on membrane cholesterol. Specifically, lipid raft isolation by density gradient ultracentrifugation demonstrated that BCRP is localized to lipid rafts in both BeWo trophoblasts and human placentas. Pre-treatment with cholesterol lowering agents pravastatin and methyl-β-cyclodextrin decreased BCRP efflux of both Hoechst 33342 and zearalenone without altering BCRP surface expression. Taken together, these data provide evidence that BCRP is important in protecting the fetus from exposure to zearalenone and that this function can be influenced by certain classes of lipids.

DEDICATION

This dissertation is dedicated to my grandparents, Ildefonso Quintero (Abuelo), Ada Quintero (Abuela), John Szilagyi Sr. (Poppup), and Elizabeth Szilagyi (Baka).

ACKNOWLEDGEMENTS

I would first like to acknowledge my advisors, Drs. Lauren Aleksunes and Jeffrey Laskin. Dr. Aleksunes, you have defined for me what it means to be a mentor. Your door is always open and you have always listened to what I have to say as if I was your equal. You have always pushed me to do more than I ever thought I could. I will carry the lessons you have taught me over these past 5 years for the rest of my life. Dr. Laskin, I am in the Joint Graduate Program for Toxicology because 5 years ago you took a chance on me, and I am truly grateful. In my time here, you have taught me to be skeptical, humble, and deliberate in my research. You have been always willing to share your wisdom and experience with me, and that has been so valuable to my development. Whatever success I can find after I defend I owe to the both of you. I would also like to thank my thesis committee. Drs. Brian Buckley, Troy Roepke, and Kary Thompson have taken so much time out of their own busy lives for my own benefit, and I am truly grateful. Your insight and suggestions have kept my project moving forward and helped shaped it into what it is today. I would also like to acknowledge here Drs. Vladimir Mishin and Laurie Joseph, whose mentorship helped me to overcome significant hurdles in my research. Thanks to the both of you for truly caring about my work and providing me truly instrumental advice in more than a few instances.

To all of my labmates, both past and present, it has been a pleasure to work beside you. I have never once asked anything of anyone and received a “no” in response. The environment in both of my labs has been collaborative, helpful, supportive, and inspiring. Beyond that, each and every one of you displays such work ethic that it drives me to do better and work harder. Each piece of work I have produced has the fingerprint of your collective minds. I would like here to especially acknowledge Dr. Kristin Bircsak, who has

laid the foundation for my dissertation with her own work on placental transporters. Her own efforts have made my own work exponentially simpler.

To all of my colleagues here at the JGPT, past and present, that have become some of my best friends: Dr. Justin Schumacher, Dan Rizzolo, Alexa Murray, Dr. Alessandro Venosa, Dr. Laura Armstrong, Dr. Sara Fournier, Dr. Ley Smith, Sheryse Taylor, Stephanie Marco, Gabriella Composto, Nicole Renkel, Brittany Karas. Your friendships have kept me sane. Be it game night, softball, or Park Pub, I am grateful for the time we have spent together, and I will miss you all.

To all of my friends outside of this program, thank you for keeping me grounded and reminding me to enjoy myself, even through this process. Thank you also for reminding me that no matter how hard I have worked for this Ph.D., I am still not a “real” doctor.

To the Rutgers Pharmacology/Toxicology Department and EOHSI staff, thank you for all of your effort. You have helped to ensure that this process went as smoothly as possible.

Most of all I owe my biggest thanks to my family. To my mother, Aimee Corzo, thank you for pushing me from day one and never expecting anything less than my best. You have instilled in me the confidence not only to take on challenges but to thrive in doing so. To my father, John Szilagyi, Jr., who has always believed I can do anything. You have always referred to yourself as the “stage 1 rocket” whose purpose is to help me travel to where I am meant to go. You have always been so much more to me, and I can only hope to emulate your selflessness and integrity throughout the rest of my life. To my stepfather, Antonio Corzo, thank you for helping me to find strength within myself. You

have always been someone I can count on, and you have treated me like nothing less than your own son. To my sister, Larissa Szilagyi, thank you for your companionship and contention; you have always reminded me to play fair and think carefully about my own opinions. To my grandparents, for whom this dissertation is dedicated, Ildefonso Quintero (Abuelo), Ada Quintero (Abuela), John Szilagyi Sr. (Poppup), and Elizabeth Szilagyi (Baka), thank you for believing that I could do something great. I was fortunate enough to have grown up around these four incredible people who were integral in raising me into the man I am today. Thank you also to all of my aunts, uncles, and cousins who have always given me their unwavering support. To my fiancée, my best friend, and the love of my life, Rosalba Perricone, thank you for absolutely everything. I cannot begin to say how truly grateful I am to have you in my life. Through this process, you have given to me your support, compassion, and unconditional love. You have put up with me through some of the toughest parts in my life and have never left my side. This dissertation is as much your effort as mine, and I can honestly say that I could not have come this far without you.

ACKNOWLEDGEMENT OF PUBLICATIONS

CHAPTER 2

John T. Szilagyi, Ludwik Gorczyca, Anita Baker, Brian Buckley, Jeffrey D. Laskin, Lauren M. Aleksunes (2018). Placental BCRP/ABCG2 transporter reduces fetal exposure to the estrogenic mycotoxin zearalenone. *(In preparation for submission to Drug Metabolism and Disposition)*

CHAPTER 3

John T. Szilagyi, Gabriella M. Composto, Laurie B. Joseph, Bingbing Wang, Todd Rosen, Jeffrey D. Laskin, Lauren M. Aleksunes (2018). Anandamide down regulates placental transporter expression through CB2 receptor-mediated inhibition of cAMP synthesis. (*In preparation for submission to Biochemical Pharmacology*)

CHAPTER 4

John T. Szilagyi, Anna Vetrano, Jeffrey D. Laskin, Lauren M. Aleksunes (2017). Localization of the Placental BCRP/ABCG2 Transporter to Lipid Rafts: Role for Cholesterol in Mediating Efflux Activity. *Placenta.* 55: 29-36.

APPENDIX 1

John T. Szilagyi, Vladimir Mishin, Diane E. Heck, Yi-Hua Jan, Jason R. Richardson, Lauren M. Aleksunes, Debra L. Laskin and Jeffrey D. Laskin (2016). Selective Targeting of Heme in Cytochrome P450s and Nitric Oxide Synthase by Diphenyleneiodonium. *Toxicological Sciences.* 151(1); 150-9.

APPENDIX 2

John T. Szilagyi, Yun Wang, Vladimir Mishin, Diane E. Heck, Yi-Hua Jan, Lauren M. Aleksunes, Debra L. Laskin and Jeffrey D. Laskin (2018). Redox Cycling Agents Inhibit Cytochrome b5 Reductase. (*Submitted to Toxicology and Applied Pharmacology*)

Blessy George, **John T. Szilagyi**, Lauren M. Aleksunes (2018). Regulation of Renal Calbindin Expression in Mice with Cisplatin Nephrotoxicity. (*In preparation*)

Guadalupe Herrera-Garcia, Jamie E Moscovitz, **John T. Szilagyi**, Kathleen Schroeder, Sabrina Scroggins, Mark Santillan, Donna Santillan, Grace L Guo, Lauren M Aleksunes (2018). Estradiol-Mediated Suppression of Fibroblast Growth Factor (FGF) 19 During Pregnancy. (*In preparation*)

TABLE OF CONTENTS

LIST OF FIGURES

LIST OF TABLES

Abbreviations

ABC, ATP binding cassette; AEA, anandamide; AhR, aromatic hydrocarbon receptor; ASCT, alanine, serine, cysteine transporter; BCRP, breast cancer resistance protein; CB, cannabinoid receptor; CML, chronic myeloid leukemia; CNT, concentrative nucleotide transporter; CREB, cAMP response element binding protein; CRH, corticotropin releasing hormone; CT, cytotrophoblastl; CYP, cytochrome P450; EGFR, epidermal growth factor receptor; ENT, equilibrative nucleoside transporter; ER, estrogen receptor; EVT, extra-villous trophoblast; FAAH, fatty acid amide hydrolase; GPR, G-protein coupled receptor; hCG, human choriogonadotropin; HEK, human embryonic kidney; HIF1α, hypoxia inducible factor 1α; hPL, human placental lactogen; MATE, multidrug and toxin extrusion protein; MDCK, Marin-Darby canine kidney; MDR, multidrug resistance transporter; MRP, multidrug-associated resistance protein; MβCD, methyl-β-cyclodextrin; NAPE-PLD, N-acyl phosphatidylethanolamine-specific phospholipase D; NF-κB, nuclear factor kappa-light-chain-enhancer of activated B cells; NHERF, Na+/H+ exchanger regulatory factor; NRF2, nuclear factor erythroid 2–related factor 2; OAT, organic anion transporter; OATP, organic anion transporting polypeptide; OCT, organic cation transporter; OCTN, carnitine transporter; P-gp, P-glycoprotein; PKA, protein kinase A; PPAR, peroxisome proliferator activated receptor; PXR, pregnane X receptor; SLC, solute carrier; ST, syncytiotrophoblast; TM, transmembrane; TRPV1, transient receptor potential cation channel subfamily V member 1.

CHAPTER 1: INTRODUCTION

1.1 Human Placenta Physiology

The placenta is an organ that connects the conceptus with the maternal blood supply through the endometrium. It regulates the flow of nutrients in and waste out of the fetal compartment, thereby meeting the high metabolic demand of the developing fetus. Currently, it is understood that the placenta also contributes to a healthy pregnancy through endocrine signaling, producing hormones such as choriogonadotropin (hCG), and regulating the maternal immune system. Unless otherwise stated, the following information has been adapted from Williams Obstetrics (Cunningham *et al.*, 2014) which describes the anatomy and function of the human placenta in detail.

1.1.1 Structure and Development

Upon implantation of the blastocyst in the endometrium, the placenta forms from the differentiation of pluripotent embryonic stem cells into trophoblasts. The outermost layer of the embryo is comprised of trophoblasts by days 3 to 4 post fertilization. Inside the embryo, cells differentiate into the three germ cell types (ectoderm, endoderm, and mesoderm) which ultimately give rise to all fetal tissues. Within 5 to 8 days of conception, trophoblasts invade into and remodel uterine blood vessels in order to lay the foundation for placental attachment and growth. The placenta continues to grow throughout pregnancy up to an average diameter of 22 cm and a thickness of 2 to 2.5 cm.

Blood Flow

The placenta has two separate circulatory systems: the uteroplacental circulation and the fetoplacental circulation. The uteroplacental system carries oxygenated maternal

blood from spiral arteries into the intervillous space and deoxygenated blood into uterine veins. The fetoplacental circulation originates in chorionic villi. Fetal capillaries receive nutrients and gases through the villi, which serve as the physical and chemical barrier between the two circulations. Blood is then carried back to the fetus through arteries in the umbilical cord, and deoxygenated blood is fed back into the placenta via fetal veins. Uteroplacental circulation is fully established by the end of the first trimester, and blood flow increases throughout pregnancy as the placenta increases in size. Echo planar imaging has shown that the average perfusion rate of a normal human placenta from 20 weeks of gestational age to term is about 176 mL/min/100 g of placenta (Gowland *et al.*, 1998). Phase-contrast magnetic resonance imaging has determined that the rate of flow in umbilical arteries and vein is 140 mL/min/kg of fetal weight and 155 mL/min/kg of fetal weight, respectively (Krishnamurthy *et al.*, 2017). The increase in blood flow to the fetus throughout gestation is accompanied by a 30-50% increase in maternal cardiac output by full term, which together function to fulfill the metabolic demand of the fetus throughout pregnancy.

Cell Types

Within the placenta, trophoblasts are the parenchymal cells responsible for nutrient and waste transfer, hormone production, and remodeling of the uterine spiral arteries. Cytotrophoblasts (CTs) lie within the chorionic villi and serve as precursor cells that ultimately differentiate into syncytiotrophoblasts and extravillous trophoblasts. Cytotrophoblasts migrate to the surface of the villi and fuse into a multinucleated cells known as syncytiotrophoblasts (STs). Syncytialization provides a cohesive physical barrier between the maternal and fetal circulations. Extravillous trophoblasts (EVTs) invade into the decidua and remodel the maternal spiral arteries in order to establish uteroplacental blood flow. Fetal endothelial cells line capillaries that flow within the

chorionic villi. The fetal side of the placenta is lined with the amnion and chorion which together form the chorionic plate and serve to house the conceptus and the amniotic fluid. The placenta also contains several populations of stromal cells including fibroblasts, Hofbauer cells (villous macrophages), and fetal macrophages.

Trophoblast Differentiation

Trophoblast differentiation into STs and EVTs is a critical process in placentation. Syncytialization is responsible not only for the formation of the physical barrier that the placenta provides, but STs also produce the primary hormones of the placenta. STs are a terminal cell type and therefore lack the capacity to proliferate. Therefore, the maintenance of the placental barrier is reliant on the continuous syncytialization of CTs. The syncytial epithelium undergoes tightly-regulated cell turnover through intrinsic and extrinsic apoptosis and the formation of nuclei-dense syncytial sprouts which themselves detach from the syncytium. The ratio of STs to CTs remains constant throughout pregnancy (about 9:1), and the turnover rate is proportional to the overall mass of the placenta throughout gestation, reaching a maximum of 4.5 million cells per day at term. hCG produced by STs binds to luteinizing hormone receptor on CTs and trigger a signaling cascade through activation of adenylyl cyclase and the intracellular messenger cyclic adenosine monophosphate (cAMP) (Grinwich *et al.*, 1976; Wang *et al.*, 1988; Yang *et al.*, 2003). This signaling pathway activates protein kinase A (PKA), which then phosphorylates the transcription factor cAMP response element binding protein (CREB) (Delidaki *et al.*, 2011; Knofler *et al.*, 1999; Yoshie *et al.*, 2010). Phosphorylated CREB translocates into the nucleus, binds to cAMP response elements in the regulatory regions of targets, and induces the expression of a number of genes involved in regulating syncytialization.

While the entire mechanism behind trophoblast fusion is not fully understood, it is recognized that syncytins are necessary for this process. Syncytins are fusion proteins upregulated in response to hCG signaling (Delidaki, et al., 2011). Syncytin-1 and -2, encoded by the *ERVW-1* and *-2* genes, respectively, were originally a result of an ancient retroviral infection that caused its integration into the primate genome (Knerr *et al.*, 2002; Mi *et al.*, 2000). Syncytins are expressed on the cell surface of STs and bind to neutral amino acid transporters ASCT1 and ASCT2 receptors on adjacent cells (Holder *et al.*, 2012; Tailor *et al.*, 1999). Although the exact mechanism of pore formation and ultimately cell fusion are unknown, syncytins do share structural domains with class I viral fusogens. Proteins classified as class I fusogens, like influenza hemagglutnin, bind to the surface of two cells, trimerize, and undergo a conformational change to open and fuse adjancent plasma membranes. The syncytialization process is also self-perpetuating. The DNA sequence for hCG itself contains a cAMP response element, and hCG signaling stimulates its own production (Licht *et al.*, 1993; Silver *et al.*, 1987). *In vitro*, syncytialization and expression of syncytialization genes can be induced not only by treatment with hCG but also by stimulating PKA directly with addition of cAMP or forskolin, an adenylyl cyclase activator.

Invasion of EVTs into the uterine decidua is similarly intricate and regulated in part by uterine natural killer cells (Gupta *et al.*, 2016; Matsumoto *et al.*, 2016). In particular, uterine natural killer cells produce cytokines, growth factors, leptin, vascular endothelial growth factor, and tumor necrosis factor alpha, which together induce trophoblast differentiation, migration, and contribute to decidual remodeling (Matsumoto, et al., 2016). The invading trophoblasts secrete matrix metalloproteinases which digest extracellular matrix proteins in order to migrate and remodel the uterine endothelium to establish adequate blood flow to the placenta. The interaction between EVTs and uterine

endothelial cells also serves to anchor the placenta to the uterine wall during gestation. Conversion of CTs to the EVT phenotype is similar to the epithelial-mesenchymal transition of invading tumor cells; both processes involve increased expression of epithelial-mesenchymal transition markers vimentin, E-cadherin, and β-catenin (Duzyj *et al.*, 2015; Tang *et al.*, 2015).

Dysregulation of trophoblast invasion is also involved in placental pathologies. Over-invasion into the decidua and attachment to the myometrium, known as placenta accreta, can compromise the ability of the placenta to detach during birth and may be life threatening to the mother (Duzyj, et al., 2015). By comparison, under-invading trophoblasts provide inadequate blood flow to the placenta can lead to preeclampsia, a condition that manifests primarily as increased maternal blood pressure and proteinuria (reviewed in Saito and Nakashima, 2014). Placentas from preeclamptic pregnancies therefore often lack the oxygen content required for fetal development.

1.1.2 Placental Function

The primary function of the placenta is to ensure that the conceptus develops properly throughout pregnancy. In order to accomplish this, the placenta itself performs endocrine, immune, and chemical exchange functions that maintain conditions in which a developing fetus can thrive.

Transport

The placenta coordinates the bidirectional exchange of gasses, nutrients, waste, and xenobiotics between the maternal and fetal circulations. As stated previously, the syncytium is the physical and biochemical barrier between the uteroplacental and fetoplacental circulations. It is therefore the sole responsibility of the STs to regulate the

trafficking of nutrients in and waste out of the fetal circulation, and it accomplishes this with an array of membrane transporters. STs are polarized cells; the apical membrane of STs faces the maternal blood supply and their basolateral membrane faces the fetus.

The mode of transport through the ST layer is determined by the chemical properties of each compound (reviewed in Eshkoli *et al.*, 2011). Small (<500 Da), neutral molecules are exchanged by passive diffusion and are therefore driven by their concentration gradient. Some molecules, like glucose, are transported by a facilitative mechanism through glucose transporters, which are expressed on ST plasma membranes. Other molecules are driven against their concentration gradient, often coupled to ATP hydrolysis or a secondary active transport mechanism.

STs express transporters responsible for the fetal uptake of fatty acids, amino acids, nucleotides, and metals. STs also highly express a number of xenobiotic transporters which remove waste products (like urea) from and transport certain endogenous molecules (like nucleotides) to the fetal blood supply (reviewed in Vähäkangas and Myllynen, 2009). The majority of these transporters belong to either the solute carrier (SLC) or ATP-binding cassette (ABC) superfamilies. SLC genes expressed in STs include organic cation transporters (OCT3/*SLC22A3*), organic anion transporters (OAT4/*SLC22A11*), organic anion-transporting polypeptides (OATP2B1/*SLCO2B1*, OATP4A1/*SLCO4A1*), concentrative nucleoside transporters (CNT1/*SLC28A1*), equilibriative nucleoside transporters (ENT1/*SLC29A1*, ENT2/*SLC29A2*), multidrug and toxin extrusion protein (MATE1/*SLC47A1*), and carnitine transporters (OCTN1/*SLC22A4*, OCTN2/*SLC22A5*). ABC genes encode proteins that serve as efflux transporters, which, using ATP hydrolysis, drive endogenous waste (e.g. heme breakdown products and uric acid) and xenobiotics (both pharmaceutical and

environmental) out of the cytoplasm and against their concentration gradient. Toxicological studies in the placenta emphasize the role of apical ABC transporters multidrug resistance protein 1 (MDR1/*ABCB1*) or P-glycoprotein (P-gp) and the breast cancer resistance protein (BCRP/*ABCG2*) because they both are abundantly expressed and contribute to protecting the fetus from xenobiotic exposure. ABC transporters in the ST also include the multidrug resistance-associated proteins (MRP1/*ABCC1*, MRP2/*ABCC2*, MRP3/*ABCC3*, MRP4/*ABCC4*, MRP5/*ABCC5*) which are expressed on either or both the apical and basolateral ST membranes.

Endocrine

The production of hormones by placenta STs is critical for the maintenance of a healthy pregnancy (reviewed in Costa, 2016b). Production of hCG regulates syncytialization, as stated previously, but also functions to maintain the corpus luteum after implantation. Similar to its action in trophoblasts, hCG binds to luteinizing hormone receptors in the ovary, which, in response, secretes progesterone that acts to enrich the uterus with blood. The concentration of hCG peaks at the 10^{th} week of pregnancy and then plunges as the placenta itself produces progesterone.

STs also secrete corticotrophin releasing hormone (CRH) and human placental lactogen (hPL). CRH is a polypeptide stress response hormone that works along the hypothalamic-pituitary-adrenal axis to trigger the release of adrenocorticotropic hormone (ACTH) and ultimately glucocorticoid hormones. CRH levels rise toward the end of pregnancy (up to 4-5 ng/mL), which is thought to regulate parturition by stimulating the release of dehydroepiandrosterone and activating cervical contractions (Mastorakos and Ilias, 2003). hPL production rises throughout pregnancy and reaches peak concentration (5-7 µg/mL) near the end of gestation (Mastorakos and Ilias, 2003). hPL functions to

decrease maternal glucose utilization and increase free fatty acid lipolysis, which in turn increases glucose availability for the fetus. hPL is an agonist for the prolactin receptor and helps prepare mammary tissue for lactation. Therefore, placental hormone synthesis and secretion contributes to human development both during and after gestation.

Immune

The placenta provides a barrier for the fetus against the maternal immune cells. Fetal tissues express antigens of both maternal and paternal lineage, and circulating maternal antigen-recognizing cells may construe the conceptus as foreign. To prevent an immune response, STs lack many of the proteins that circulating immune cells detect, such as major histocompatibility complexes and human leukocyte antigens. Cloaking the fetus from the maternal immune system is critical because the placenta needs to maintain intimate contact with the maternal blood supply.

Like many permanent organs, the placenta also contains a population of resident macrophages. Placental macrophages, known as Hofbauer cells, are localized in the chorionic villi often along fetal endothelium and can be seen as early as 4 weeks post-conception. Hofbauer cells have recently been discovered to contribute to placental health in a number of ways, although further characterization is necessary. For instance, this phagocytic cell population has been implicated in the regulation of placental morphogenesis and differentiation, stromal water content, regulation of the maternal immune system, and protein trafficking across the placenta. Dysregulation of these cells may therefore contribute to inflammatory placental pathologies such as chorioamnionitis.

1.2 The Breast Cancer Resistance Protein (BCRP/*ABCG2*) Transporter

BCRP is an efflux transporter that translocates a wide range of substrates against their concentration gradient and across the plasma membrane by utilizing ATP hydrolysis. Placental BCRP protects the fetus from toxic xenobiotic exposures, and it is therefore important to understand the processes that regulate BCRP expression and function.

1.2.1 Structure, Function, Localization

Structure

BCRP, also classified as ABCP, ABCG2 and CDw338, is a 72 kDa protein localized in the plasma membrane and consists of a cytoplasmic (1-395), and a transmembrane region (396-655) (Allikmets *et al.*, 1998a; Taylor *et al.*, 2017). The cytoplasmic region of BCRP constitutes its nucleotide (ATP) binding domain and a hinge region that contributes to BCRP conformational changes (Jackson *et al.*, 2018). The transmembrane region anchors BCRP to the plasma membrane with six transmembrane α-helices that also form the substrate binding site. It is generally understood that BCRP is a half transporter that homodimerizes through disulfide bridges (C284, C374, C438) to be functional (Khunweeraphong *et al.*, 2017). There are also three other cysteine residues (C592, C603, C608) in the third extracellular loop of the BCRP protein that form intra-molecular bonds that are important to both protein folding and transport function. The cytoplasmic-facing substrate binding pocket is formed upon dimerization by the TM2 and TM5a transmembrane domains of each BCRP monomer. ATP hydrolysis in the cytoplasmic domain is driven by cytoplasmic substrate binding to TM2 and TM5a, and the energy released induces a conformational change in BCRP from inward-facing to outward facing. This drives the bound substrate past the plasma membrane and into the extracellular space. When the substrate is released, BCRP returns to an inward facing conformation. Crystal structure analysis of BCRP also revealed six distinct cholesterol-binding residues in the substrate binding pocket (F432 and F439 from TM2 and L539,

I543, V546, and M549 from TM5a) bound to two cholesterol molecules (Jackson, et al., 2018; Taylor, et al., 2017). These residues are conserved or replaced by other hydrophobic amino acids in the ABCG subfamily. ABCG1, ABCG4, and ABCG5/G8 are well known sterol transporters, but BCRP does not itself catalyze cholesterol transport (Matsuo, 2010). Alternatively, cholesterol may be critical for BCRP substrate transport, and the evidence for this effect will be covered in detail in **Section 1.4**. Because of the hydrophobicity of substrate binding region and the geometry of the cavity formed by TM2 and TM5a, the BCRP dimer is well suited for flat, polycyclic, and hydrophobic structures.

Localization

In humans, BCRP is widely expressed throughout the body, with detectable transcripts in the liver, kidneys, gut lungs, heart, brain, mammary glands, testis, ovaries, placenta and uterus (reviewed in Klaassen and Aleksunes, 2010). Its highest expression is found in the placenta, followed by the uterus and liver. BCRP localizes to apical, brush border membranes in polarized cells such as renal tubule epithelial cells, hepatocytes, and enterocytes. In the placenta, BCRP is expressed on the apical surface of both syncytiotrophoblasts and, to a lesser extent, fetal endothelial cells (reviewed in Mao, 2008). The mechanism by which BCRP is selectively expressed on the apical surface has not been fully characterized, but it is likely a result of post-translational modification and Golgi-driven trafficking. Trafficking of proteins to the apical surface is often a result of covalent attachment to lipids and carbohydrates such as palmitic acid and glycans. N-glycosylation of BCRP (N596) is required for protein maturation; a loss of function mutation at N596 increases BCRP ubiquitin-mediated degradation (Jani *et al.*, 2014). BCRP localization is also dependent on regulation by Na+/H+ exchanger regulatory factor 2 and 3 (NHERF2/3), which also mediates the apical sorting of MDR1 and certain MRPs (Walsh *et al.*, 2015). However, BCRP lacks the canonical NHERF binding

element, so the precise mechanism involved in apical trafficking of BCRP is not yet clear (Walsh, et al., 2015). The consequence of this subcellular localization is that BCRP serves as a fetoprotective transporter. However, BCRP also impairs the delivery of certain medicines to the fetus that may be necessary for fetal health, such as antiretrovirals prescribed to pregnant women with human immunodeficiency virus.

Function

BCRP was so named because it was originally characterized as a survival factor in MCF-7 cells against treatment with mitoxantrone, a chemotherapeutic agent commonly used in the treatment of breast cancer (Doyle *et al.*, 1998a). Mitoxantrone–selected MCF-7 cells were also found to be resistant to chemotherapeutics doxorubicin, bisantrene, and topotecan (Rabindran *et al.*, 1998b). The same year, BCRP was also discovered and named ABCP for its enrichment in the placenta (Allikmets, et al., 1998a). After more than twenty years of screening and characterizing BCRP, the list of substrates is extensive and involves endogenous substrates, environmental toxicants, and pharmaceuticals. BCRP more than likely evolved to protect cells from toxic dietary and endogenous breakdown products like pheophorbide a, a toxic chlorophyll metabolite that results from consumption of leafy green vegetables (Jonker *et al.*, 2002a). BCRP also transports redox active heme breakdown products such as protoporphyrin IX (Jonker, et al., 2002a). BCRP has also been shown to transport dietary toxicants bisphenol a, a plasticizer, and zearalenone, a fungal mycotoxin (Mazur *et al.*, 2012; Xiao *et al.*, 2015). BCRP is most often considered, however, as a critical pharmacokinetic determinant in the pharmaceutical industry (Prueksaritanont *et al.*, 2013). Characterization of BCRP transport or inhibition is required in drug development according to FDA guidelines as certain SNPs like 421C>A (Q141K) reduce BCRP function and can influence drug pharmacokinetics (Prueksaritanont, et al., 2013).

As stated previously, placental BCRP is important in protecting the fetus from toxic exposure to common environmental toxicants as well as pharmaceuticals prescribed during pregnancy. For instance, BCRP substrates glyburide and nitrofurantoin are routinely prescribed during pregnancy for gestational diabetes and urinary tract infection, respectively (Christensen, 2000; Ogunyemi *et al.*, 2011). Two hours after retro-orbital injection, Bcrp$^{-/-}$ FVB mice exhibited a five- and two-fold increase in the fetal-to-maternal AUC ratio of glyburide and nitrofurantoin, respectively, compared to wild type (Zhang *et al.*, 2007b; Zhou *et al.*, 2008). Ko143, a pharmacological inhibitor of BCRP, also decreased glyburide transport in both *in vitro* trophoblast cultures and microvillous membrane vesicles prepared from human term placenta (Bircsak *et al.*, 2016). In an *ex vivo* human placental perfusion model, the fetal-to-maternal concentration ratio of glyburide was increased in the presence of Ko143, from 0.32 to 0.56 (Pollex *et al.*, 2008). In the same model, Ko143 also increased the fetal-to-maternal concentration ratio of 2-amino-1-methyl-6-phenylimidazo(4,5-b)pyridine, a potential carcinogen commonly found in cooked meat, from 0.72 to 0.90 (Myllynen *et al.*, 2008). Glyburide transport was also reduced in HEK293 cells that expressed the Q141K variant of BCRP versus wild type (Bircsak, et al., 2016). These data make evident that placental BCRP decreases the transplacental transport of certain toxicants during pregnancy. Further, these studies highlight the importance of understanding the factors that regulate *ABCG2* expression and activity in the placenta.

1.2.2 Regulation

Transcriptional Regulation

The gene sequence for BCRP contains an array of response elements to which transcription factors bind and induce transcription. Therefore, BCRP expression can be

regulated on the transcriptional level through receptor activation. For instance, activation of the pregnane x receptor (PXR) or aromatic hydrocarbon receptor (AhR) by ligand binding induces BCRP expression in the placentas of C57BL/6 mice and JEG3 trophoblasts, respectively (Gahir and Piquette-Miller, 2011; Neradugomma *et al.*, 2017). PXR is typically activated by endogenous and exogenous steroids dexamethasone, and AhR is activated by polar, planar aromatic compounds with multiple ring structures, such as benzopyrenes and napthoflavones. BCRP transcription can also be activated by estrogen receptor (ERα/β), peroxisome proliferator-activated receptor (PPARα/γ), and epidermal growth factor (EGFR) receptor agonism (Lin *et al.*, 2016; Porcelli *et al.*, 2014; Wang *et al.*, 2008a). BCRP expression is also regulated by homeostatic changes of the cell. Hypoxia, for instance, can change BCRP transcription through HIF1α signaling. However, it has been reported that hypoxia (3% and 8% O_2) can both increase and decrease BCRP transcription, and the specific effect of hypoxia may be dependent on the model of placenta used and the stage of placental development (Francois *et al.*, 2017; Koritzinsky *et al.*, 2006; Lye *et al.*, 2013). BCRP can also be up-regulated in response to oxidative stress (via nuclear factor (erythroid-derived 2)-like 2, NRF2) and inflammation (via nuclear factor kappa-light-chain-enhancer of activated B cells, NF-κB) (Gibson *et al.*, 2012). Taken together, these studies indicate that BCRP can be regulated by a wide range of cellular conditions and toxic exposures, but the coding sequence of BCRP can itself affect BCRP expression.

Genetic Variation

As with most drug metabolizing enzymes, endogenous BCRP expression varies in the human population resulting in a range of pharamacokinetic responses. This is particularly concerning during pregnancy, as placental BCRP expression is not screened for prior to prescribing medications. Further, the consequence of such variation in

placental BCRP expression is an unidentified population sensitive not only to prescribed pharmaceuticals but also environmental contaminants that may be developmental toxicants. Genetic variation in BCRP is most often the result of polymorphisms that alter BCRP expression or activity. The most common (allele frequency = 35.7%) and most extensively characterized polymorphism is 421C>A (Q141K), which is located in the nucleotide binding domain (Prasad *et al.*, 2013; Zamber *et al.*, 2003). This residue may also be involved in protein stability and turnover; the 421C>A polymorphism decreases BCRP expression and transport (Imai *et al.*, 2002). The 34G>A polymorphism (V12M, allele frequency = 29.8%) in the N-terminus is also common, but, despite lower expression, bears no impact on efflux activity (Zamber, et al., 2003). Interestingly, other genetic variants exist in transmembrane or extracellular regions that increase BCRP expression but alter substrate specificity such as 1711T>A (F571I, allele frequency = 0.5%), 1768A>T (N590Y, allele frequency = 9.7%), and 1858G>A (D620N, allele frequency = 11.1%) (Zamber, et al., 2003).

Post Transcriptional Regulation

BCRP expression and function are also dependent on post-transcriptional and post-translational regulatory mechanisms. Several miRNAs have been identified for their capacity to inhibit BCRP expression, such as miR-328 and has-miR-520, by binding to mRNA transcripts and forming RNA-induced silencing complexes that include the endoribonuclease Dicer (Li *et al.*, 2011). It is important to note is that the BCRP DNA sequence includes a miRNA response element to which some miRNAs can bind, and this sequence is lost in some multidrug-resistant cancer cells. Post-translational modification in the Golgi is critical for BCRP. For instance, N-glycosylation is required for BCRP function and trafficking in both human and mice. Mutations at Arg 596, the site N-glycosylation in the human isoform, will result in BCRP ubiquitination and degradation

(Mohrmann *et al.*, 2005). Further, glycosylation is known to promote protein association with cholesterol and lipid rafts, and the importance of this process to BCRP function will be covered in detail in **Section 1.4.2**.

1.3 Zearalenone

Zearalenone ((S-(E))-3,4,5,6,8,10-Hexahydro-14,16-dihydroxy-3-methyl-1H-2-benzoxacyclo-tetradecin-1,7(8H)-dione) is an estrogenic mycotoxin synthesized by *Fusarium* fungi that occur naturally on cereal crops like corn (Kuiper-Goodman *et al.*, 1987). Zeranol, a metabolite of zearalenone, is a highly estrogenic, synthetic agent used in cattle farming to increase feed to meat ratio (Mader, 1994). While BCRP has been shown to transport zearalenone in overexpressing systems (Xiao, et al., 2015), there is no data demonstrating the influence of BCRP on the disposition of zearalenone or zeranol during pregnancy. Because of zearalenone and zeranol are potently estrogenic, there exists crucial need for further analysis into the disposition of zearalenone across the placenta.

1.3.1 Structure and Occurrence

Structure

Zearalenone, a resorcylic acid, is a closed 18 carbon multi-ring structure with one six-membered aromatic ring (C12-17) and one double bond (C11-12) (**Fig. 1.1**). The aromatic ring is bonded to two hydroxide groups (C14, 16) that are oriented para to one another. Additionally, zearalenone contains one ester group (C1), one ketone (C7), and an additional methyl group (C8). At room temperature, zearalenone is a white odorless colorless crystalline solid with a solubility of 20 mg/L.

Prevalence

The European Union (EU) has set the allowable limit for zearalenone in food at 4 µg/kg (Commision, 2006). However, as seen in studies across several continents, common foods exceed this limit. A study in Korea found 163 contaminated foods at levels between 3-17 µg/kg including noodles, cereal, and infant formula (Ok *et al.*, 2014). A study in Pakistan found 30% of foods surveyed were contaminated with zearalenone, and 20% of those foods exceeded the EU limit (Iqbal *et al.*, 2014). Analysis of wheat crops in Brazil found that 84% of crops from the Rio Grando do Sul region of Brazil were contaminated with zearalenone with a median concentration of 70.9 µg/kg (Tralamazza *et al.*, 2016). Sorghum marketed in Tunisia was detected in 30% of samples tested (n = 64), and the concentration varied between 3.7 and 64.5 µg/kg (Lahouar *et al.*, 2018). Zearalenone is also prevalent in the domestic market as well. A comprehensive study of a cohort of pre-pubescent girls in New Jersey (Jersey Girl Study, ages 9-10 yrs old at recruitment) was performed to measure mycotoxin exposure and correlated with dietary composition. An analysis of zearalenone in the urine of New Jersey girls (n = 163) showed a range of 0.2-8.4 ng/mL, and this exposure was connected to popcorn and beef intake (Bandera *et al.*, 2011). It should also be noted that the synthetic metabolite zeranol is routinely administered to cattle in the U.S. and Canada under the brand name Ralgro, whereas use has been banned in the EU.

1.3.2 Pharmacokinetics and Pharmacodynamics

Pharmacokinetics

Phase I and II metabolic enzymes catalyze the biotransformation and, in turn, facilitate the elimination of zearalenone (described in Mukherjee *et al.*, 2014). The phase I enzymes CYP2D6, CYP2C9, and CYP3A4, can catalyze aromatic hydroxylation of zearalenone forming 13- and 15- hydroxyl catechol metabolites. Hydroxy steroid dehydrogenase (HSD, both the 3α and 3β isoforms) mediate the reduction of the double

bond (C11-12) or the ketone group (C7) in zearalenone, converting the parent compound to α-zearalenol or β-zearalenone. The parent compound as well as the HSD-catalyzed metabolites can all be glucuronidated by the phase II enzyme uridine 5'-diphospho-glucuronosyltransferase (UGT). Glucuronidation (O7, O14) is the major phase II metabolic pathway for zearalenone (V_{max}/K_m = 4.7 x 10^{-3}), and the most active isoforms for conjugation are UGT1A1, 1A3, 1A8, and 2B7. Hydroxylated metabolites of zearalenone can also be further modified by s-adenosine methionine and catechol-O-methyltransferase which methylate the newly added hydroxyl group. The methylated metabolites can spontaneously convert to quinones, which may be redox-active and produce reactive oxygen species.

The role of xenobiotic transporters in the disposition of zearalenone has not been fully characterized *in vivo*, but some studies offer insight on the potential mechanism. BCRP has been shown to transport zearalenone in the BeWo choriocarcinoma cell line and HEK cells (Xiao, et al., 2015). Zearalenone (10 μM) also induces expression of BCRP, MRP1, MRP2, and MDR1 mRNA by 24 h in BeWo cells (Prouillac *et al.*, 2009). In Caco-2 transwell cultures, the transepithelial transport of zearalenone and its metabolites are mediated by MRP1 and MRP2 (Videmann *et al.*, 2009). Another study demonstrated the interaction of zearalenone with various mouse and human uptake transporters (OATs/Oats and OCTs/Octs) in transfected *Drosophila* cells (Tachampa *et al.*, 2008). Zearalenone is most efficiently transported by OAT/Oat 1 and 3, with no difference between species. Zearalenone also inhibited OAT 1-4 and OCT 1 and 2. OCT1 was most sensitive to inhibition by zearalenone (IC_{50} = 0.62 μM) and OAT2 was least sensitive (IC_{50} = 149 μM).

The major route of excretion for zearalenone in humans is urinary, whereas in other species zearalenone is most efficiently excreted in the feces. This may make pharmacokinetic data in from rodent studies difficult to interpret. Pharmacokinetic studies in male Sprague-Dawley rats (8-10 wks) have shown that oral bioavailability of zearalenone is fairly low (2.7%) (Shin *et al.*, 2009a). Following a 6 h iv infusion at 1.13 mg/kg/h, zearalenone was detectable in all tissues sampled (lung, liver, spleen, kidney, heart, testis, brain, muscle, adipose, stomach, small intestine, blood, and serum) (Shin, et al., 2009a). The highest concentrations were found in the small intestine, liver, and kidney and the lowest levels were observed in the muscle, testis, and brain. The half ($t_{1/2}$) of zearalenone, but not the clearance (Cl) or volume of distribution (V_d) were dependent on oral dose. At 1 mg/kg, $t_{1/2}$ = 0.6 h, Cl = 5.6 L/h/kg, and V_d = 2.6 L/kg, whereas at 8 mg/kg $t_{1/2}$ = 2.8 h, Cl = 5.0 L/h/kg, and V_d = 2.0 L/kg. Daily oral dosing of male Sprague-Dawley rats (8-10 wks) with 0.1 mg/kg yielded a mean steady state serum concentration of 0.014 ng/mL (Shin *et al.*, 2009b). Pharmacokinetic modeling of rodent parameters suggests that a daily human dose of 0.0312 mg/kg would achieve the equivalent steady state serum concentration. In the Jersey Girl Study, the $t_{1/2}$ of zearalenone was estimated to be 11.89 h, significantly more than the *in vivo* rodent studies (Bandera, et al., 2011). Humans are therefore potentially more sensitive to the effects of zearalenone due to longer exposure periods, and understanding the potential risk that zearalenone poses to human health from rodent studies requires careful extrapolation that accounts for the divergent inter-species pharmacokinetic parameters.

Pharmacodynamics and Toxicology

Zearalenone demonstrates only low acute toxicity (LD_{50} = 2,000-20,000 mg/kg after oral administration in adult mice, rats, and guinea pigs), but chronic studies with zearalenone reveal that it is a developmental toxicant at lower doses in mice, rats, hamsters, and

rabbits (Reviewed in Zinedine *et al.*, 2007). For instance, in female ICR neonatal (1-10 d) mice, zearalenone (i.p. daily for 3-5 d) induced ovarian follicle atresia, persistent estrous, delayed vaginal opening, and uterine proliferation later in life (Ito and Ohtsubo, 1994). *In utero* exposure to zearalenone reduces embryonic survival, and decreases fetal weight, uterine luteinizing hormone and progesterone secretion. Pharmacokinetic studies show that zearalenone can cross the placenta in both Sprague-Dawley rats and CBA mice (Appelgren *et al.*, 1982; Bernhoft *et al.*, 2001). *In utero* exposure to zearalenone during critical development windows of gestation causes precocious puberty and mammary proliferation in both female Wistar rats and C57/BL mice (Belli *et al.*, 2010; Hilakivi-Clarke *et al.*, 1998). Although the impact of *in utero* exposure to zearalenone on humans has not been assessed, the previously mentioned Jersey Girl Study correlated the presence of zearalenone and zeranol in the urine to a slowed onset of puberty, as measured by breast size (Bandera, et al., 2011). *In utero* exposure to zearalenone may therefore pose a risk to human health, and there exists a clear need to characterize the pharmacokinetics of zearalenone during pregnancy.

The developmental effects of zearalenone are primarily mediated by estrogen receptor activation. Zearalenone is an estrogenic compound and has been shown to interact with both isoforms of the nuclear estrogen receptor (ERα and ERβ) as well as the cell surface g-protein coupled estrogen receptor (GPR30) (Nakamura and Kadokawa, 2015; Takemura *et al.*, 2007). Zeranol is more estrogenic than the parent compound, making it useful as a non-steroidal cattle supplement, and is as potent as 17β-estradiol. In one study, the K_d values of zearalenone and zeranol for binding to human ERα were found to be 240 and 22 nM, respectively, 166 and 43 nM for ERβ, respectively (Takemura, et al., 2007). Because zearalenone is not as potent as endogenous hormones, the toxic effects from zearalenone may be due to either the agonism or antagonism of estrogen

receptors, depending on the concentration of estrogens, co-activators, and co-repressors present in the cell. Their interaction with GPR30, however has not been as fully characterized. In two studies, both zearalenone and zeranol were shown to inhibit GPR30 signaling in bovine and pig pituitary cells (He *et al.*, 2018; Nakamura and Kadokawa, 2015). In these studies however, GPR30 signaling was characterized by measuring the release of follicle stimulating hormone and luteinizing hormone after stimulation with gonadotropin releasing hormone. Zearalenone directly binds to GPR30, but a comparison has not yet been made with its affinity toward the nuclear estrogen receptor isoforms. Through estrogen receptor activation, chronic, *in utero* exposure to zearalenone poses a risk to human health and requires further characterization.

1.4 Cholesterol and Lipid Rafts

During pregnancy, circulating cholesterol concentrations increase by 25-50%, beginning in the second trimester (reviewed in Bartels and O'Donoghue, 2011). Concentrations of cholesterol peak in the third trimester and return to baseline levels at about four weeks after parturition. Cholesterol is incorporated into every cell in the human body, and a developing fetus cannot synthesize all of the cholesterol it requires for development *de novo*. Therefore, the placenta is tasked with trafficking cholesterol into the fetal circulation. This is evident in the case of Smith-Lemli-Opitz syndrome, a congenital defect in cholesterol biosynthesis. Despite being unable to synthesize cholesterol, there is still cholesterol present in the neonatal blood supply. Further, STs express LDL receptors and apolipoprotein B which control the process of transplacental cholesterol transport. Cholesterol, however, also critically controls membrane fluidity and the formation of lipid rafts within the placenta (Kahya *et al.*, 2005; Riquelme *et al.*, 2011).

Lipid rafts are rigid, ordered microdomains in the plasma membrane that are rich in cholesterol and contain a unique array of proteins (Simons and Sampaio, 2011). Due to their structure, cholesterol molecules tightly cluster in cell membranes compared to phospholipids and are thus less fluid than the surrounding membrane (Lingwood and Simons, 2010). The clustering together of lipid rafts promotes the intimate interaction of proteins and lipids with co-dependent functions. By promoting protein-protein and protein-lipid interactions, lipid rafts are key mediators of signal transduction, mechanosensing, and cell differentiation (Simons and Toomre, 2000). The role of lipid rafts in protein function has been shown with a number of established techniques to determine 1) what proteins are localized to lipid rafts and 2) if cholesterol contributes to the function of those protein.

Methods for Lipid Raft Analysis

Localization techniques center around lipid raft isolation methods, whereby the plasma membrane is disrupted, typically using a detergent or sonication, and subjected to high speed density gradient centrifugation. Lipid rafts are resistant to solubilization by a nonionic detergent and will separate by density (lower density) from the detergent soluble non-raft membrane (Brown and London, 1998). Western blot is then typically used to determine whether a protein floats with other known lipid raft proteins. The method of membrane disruption varies widely between studies, and the observed profile of lipid raft-associated proteins will depend on detergent type and concentration or sonication power and time. Contemporary techniques also utilize confocal microscopy and fluorescent resonance energy transfer techniques to directly study the *in situ* co-localization of transmembrane proteins and lipids, thereby determining their association with lipid rafts.

Three models of cholesterol depletion are routinely utilized to study protein function: 1) methyl-β-cyclodextrin (MβCD), 2) statins, and 3) ω-3-polyunsaturated fatty acids. MβCD sequesters cholesterol directly from cell membranes, thereby disrupting lipid raft integrity after short treatment times (30-120 min). Statins are pharmacological inhibitors of cholesterol synthesis and can also disrupt lipid raft integrity (Hillyard *et al.*, 2007). Lastly, ω-3-polyunsaturated fatty acids have also been shown to reduce cholesterol both *in vitro* and *in vivo* by increasing ubiquitination of cholesterol synthesis enzymes and simple displacement of cholesterol from the plasma membrane (Gelsomino *et al.*, 2013; Kuan *et al.*, 2011; Shaikh, 2012). Fish oil and vitamins containing ω-3-polyunsaturated fatty acids are commonly included in a prenatal regimen, but their effects on placental drug transport have not been established.

Lipid Rafts in the Placenta

Evidence for lipid rafts in the placenta and their role in fetal development have been extensively studied (reviewed in Riquelme, 2011). Lipid rafts are present in the apical, microvillous membrane of the STs and, to a lesser extent, in the fetal endothelium. By contributing to the polarization of STs, lipid rafts along with other factors coordinate directional transport between the maternal and fetal circulation, and regulate the function of apical membrane proteins. For instance, a number of studies have correlated membrane lipid composition of trophoblasts and the function of ion channels, which, as determined by gradient centrifugation, are localized in lipid rafts (Godoy and Riquelme, 2008; Nothdurfter *et al.*, 2010; Riquelme *et al.*, 2012). Transplacental folate transport is also dependent on lipid rafts, and folate is well known as a critical component of fetal neural tube formation. Lipid rafts in the syncytium have also been implicated in the function of flotillins, which contribute to transcytosis of larger molecules, cell mobility, and cell matrix interactions.

Lipid raft-protein interactions have also been studied as a contributing factor in diseases of pregnancy. Riquelme et al. (2011) analyzed placental lipid rafts collected from normal (n = 7), preeclamptic (n = 6) and growth-restricted (n = 5) pregnancies by density gradient centrifugation and determined that β-actin has increased association with lipid rafts in pathological placentas. In another study, Riquelme et al. (2012) reported that potassium channel $K_{ir}2.1$ is less associated with lipid rafts in placentas from patients with growth restriction (n = 4) and preeclampsia (n = 4) versus normal placentas (n = 8). Additionally, galectin-13, a placental regulator of T cells, has been shown through immunofluorescent co-localization studies to exhibit decreased lipid raft localization in placentas from preeclamptic pregnancies with and without HELLP (hemolysis, elevated liver enzymes, low platelet count) (Balogh *et al.*, 2011).

1.4.1 Lipid Rafts and Efflux Transporters

Lipid rafts have been shown to contribute to non-placental efflux transporter function in a number of cancer and primary cell lines (reviewed in Klappe *et al.*, 2009). Although there is no evidence specifically linking placental BCRP and lipid raft integrity, BCRP has been shown to be dependent on membrane cholesterol in other cell types (Herzog *et al.*, 2011; Storch *et al.*, 2007). Therefore, a thorough analysis of the interaction placental BCRP and lipid rafts is needed.

Evidence for Localization of Efflux Transporters to Lipid Rafts

Several distinct methods of density gradient analysis demonstrate that BCRP is localized in lipid rafts of plasma membranes in a number of immortalized and primary cells. Centrifugation methods employing digestion with Triton X-100, a harsh and selective detergent, demonstrate this localization by Western blot analysis in BCRP transfected

MDCK cells (Herzog, et al., 2011; Storch, et al., 2007). BCRP was also shown to co-immunoprecipitate with caveolin-1, a scaffolding protein found in caveolae, a subset of lipid rafts characterized by their cave- or flask-like shape (Herzog, et al., 2011). Proteomic analysis has shown BCRP localization in Triton-resistant lipid rafts generated from human T cells, C2C12 mouse muscle cells, and mouse embryonic fibroblasts (Lin *et al.*, 2010; Nixon *et al.*, 2009). Similar analysis also demonstrated this localization in Brij-35-resistent lipid rafts from mouse sperm cells (Nixon, et al., 2009). Brij-35 and other detergents such as Brij-98 and Lubrol WX are also used in lipid raft analysis and are generally considered less harsh than Triton and more inclusive of proteins weakly associated with lipid rafts.

Similarly, MDR1 and MRP1 may localize to lipid rafts, but conflicting results have been published (reviewed in Klappe, et al., 2009). Differences between studies, however, are dependent on cell type and detergent (Schuck *et al.*, 2003). Generally, stronger association with lipid rafts was evident for both transporters when Lubrol was used rather than Triton, and MDR1 was more consistently demonstrated in lipid rafts than MRP1. MDR1 localized to lipid rafts in CEM-CCRF T-cells, transfected MDCK cells, MCF-7 breast cancer cells, 2780AD ovarian cancer cells, Ht29G+ colon adenocarcinoma cells, human lymphoblastic leukemia cells, and AUXB1 chinese hamster ovary cells (Barakat *et al.*, 2005; Demeule *et al.*, 2000; Hinrichs *et al.*, 2004; Kamau *et al.*, 2005; Klappe *et al.*, 2010; Klappe, et al., 2009; Zhang *et al.*, 2015). MDR1 also co-immunoprecipitated with caveolin-1 in MCF-7 cells and SGC7901 human gastric cancer cells (Zhang, et al., 2015). MRP1 was localized to detergent-resistant lipid rafts in transfected baby hamster kidney cells (BHK), transfected human embryonic kidney cells (HEK293), and neuro2a mouse neuroblastoma cells but not Ht29G+, or BHK lipid rafts generated by sonication (Cerf *et al.*, 2007; Klappe, et al., 2010; Klappe,

et al., 2009; Meszaros *et al.*, 2011). Despite conflicting data on lipid raft localization, membrane cholesterol plays an important role in the function of BCRP, MDR1, and MRP1.

Evidence for Functional Relevance

Depletion of cellular cholesterol by MβCD inhibits BCRP activity *in vitro* (Storch, et al., 2007). MβCD increased the cellular retention of BCRP substrate pheophorbide in BCRP-MDCK cells, BCRP-HEK293 cells, primary human peripheral blood mononuclear cells, CCD 841 human colon cells and WRL-68 human cervical cells (Storch, et al., 2007; Telbisz *et al.*, 2014; Telbisz *et al.*, 2007; Telbisz *et al.*, 2013; To *et al.*, 2014). Cholesterol content increases BCRP ATPase activity in membrane preparations from Sf9 insect cells (Telbisz, et al., 2013). Importantly, peripheral blood mononuclear cells from patients with high low density lipoprotein levels have greater BCRP function and expression than those from normal patients (To, et al., 2014). Additionally, treatment with statins both *in vivo* and *in vitro* reduced BCRP function and expression in peripheral blood mononuclear cells from these patients (To, et al., 2014). While there has been no data on primary, whole tissue, the data presented in these studies suggest that cholesterol may play a role in the pharmacokinetics of BCRP substrate *in vivo.*

Cholesterol depletion also inhibited the efflux activity of both MDR1 and MRP1 in several models. MβCD decreased efflux of MDR1 substrates rhodamine-123 in MDR1-MDCK cells and daunomycin in human CML acute lymphoblastic leukemia cells (Gayet *et al.*, 2005; Kamau, et al., 2005). Peripheral blood mononuclear cells from patients treated with statins similarly had decreased MDR1-mediated rhodamine efflux activity (Glodkowska-Mrowka *et al.*, 2014). MβCD and statins also increased retention of MRP1 substrate CFDA in neuro2a and MRP1-BHK cells (Klappe, et al., 2010; Klappe, et al.,

2009; Meszaros, et al., 2011). The data presented in these studies demonstrate that, similar to BCRP, MDR1- and MRP1-mediated efflux is dependent on membrane cholesterol content.

Ω-3-polyunsaturated fatty acids, often prescribed as part of a prenatal vitamin regimen, are known to lower cholesterol *in vivo.* Importantly, treatment with ω-3-polyunsaturated fatty acids has been shown to inhibit the function of BCRP, MDR1, and MRP1 (Gelsomino, et al., 2013). Docosahexaenoic acid supplementation increased the efficacy of FEC 75 chemotherapy in breast cancer patients, which is a regimen that includes the BCRP, MDR1, and MRP1 substrates cyclophosphamide, epirubicin, and 5-fluorouracil, respectively (Gelsomino, et al., 2013). Arachidonic acid, eicosapentaenoic acid, and docosahexaenoic acid also increase retention of Calcein AM and paclitaxel, MRP1 and MDR1 substrates, respectively, in Caco-2 human colorectal adenocarcinoma cells (Kuan, et al., 2011). The effect of ω-3-polyunsaturated fatty acids on drug disposition during pregnancy has not yet been assessed, and, because of their widespread use, their interaction with drug transporters may require consideration by prescribing obstetricians.

1.5 Endocannabinoid System

The endocannabinoid system is composed of lipid signaling molecules, receptors, synthetic enzymes, and hydrolytic enzymes that control a variety of physiological and cognitive processes including energy homeostasis, pain, temperature regulation, and memory (Pagotto *et al.*, 2006; Pertwee, 2015; Woodhams *et al.*, 2015). During pregnancy, the endocannabinoid system plays a key role in regulating implantation, placentation, and fetal development. It has therefore been hypothesized that

endocannabinoid dysregulation may contribute to pathological pregnancies (Costa, 2016a).

The primary lipid signaling molecule of the endocannabinoid system is N-arachidonoylethanolamide (anandamide, AEA). AEA is synthesized *de novo* from phosphatidyl ethanolamine, which is converted to N-acyl-phosphatidylethanolamine (NAPE) by transacylase (Liu *et al.*, 2008). NAPE is then cleaved primarily by phospholipase d (NAPE-PLD) to convert it to AEA. NAPE-PLD$^{-/-}$ mice (C57BL/6), however, are able to produce AEA from NAPE, and it has been suggested that NAPE cleavage can be catalyzed by phospholipase A2 and C (Liu, et al., 2008). The primary hydrolytic enzyme of the endocannabinoid system is fatty acid amide hydrolase (FAAH), an intracellular protein which cleaves AEA to yield arachidonic acid and ethanolamine (Giang and Cravatt, 1997). Both NAPE-PLD and FAAH are expressed in mammalian tissues ubiquitously, which demonstrates the biological importance and widespread function of AEA.

In humans, AEA has a steady state plasma concentration of 0.18-0.24 ng/mL, but these levels can fluctuate based on certain physiological stimuli (Wood *et al.*, 2008). Human participants (n = 71) subjected to a standardized psychosocial stress procedure (Trier Social Stress Test) were found to have a 3 fold increase of circulating AEA concentrations compared to a control test group (Dlugos *et al.*, 2012). AEA levels in venous blood was also increased 30% during intense exercise and 60% 15 min after intense exercise in healthy, trained male cyclists (n = 11) (Heyman *et al.*, 2012). Another study found that circulating AEA concentrations were increased by 35% in obese women (n = 20) versus lean women (n = 20) (Engeli *et al.*, 2005). Adipose expression of FAAH mRNA from obese subjects was also decreased by 59%. The numerous physiological

effects of AEA have also been characterized after administration *in vivo.* In male Sprague-Dawley rats, intravenous AEA (0.5-10 mg/kg) decreased arterial pressure and increased portal venous flow and pressure. AEA also reduced gastric emptying in male ICR mice, as measured by phenol red recovery after oral challenge (Di Marzo *et al.*, 2008). Daily, oral AEA administration of male CD-1 mice prior to weaning (up to post-natal day 21, 20mg/kg) increased food intake, body weight, epididymal fat, and insulin resistance in adulthood (Aguirre *et al.*, 2012). Taken together, these studies demonstrate how AEA can regulate a wide array of biological processes.

AEA signaling is mediated primarily by the cannabinoid receptors CB1 and CB2. CB1 and CB2 are expressed throughout the body, including the central and peripheral nervous system, liver, GI, endocrine organs, placenta, fat and muscle cells, testis, and ovaries (Pagotto, et al., 2006). The cannabinoid receptors are coupled to g-proteins and are activated not only by AEA but also tetrahydrocannabinol (THC), the active compound in cannabis. CB1 and CB2 possess seven transmembrane regions connected by three extracellular and three intracellular loops (Galiegue *et al.*, 1995; Shao *et al.*, 2016). Both receptors activate G_i, which in turn inhibits the adenylate cyclase-mediated production of cyclic adenosine monophosphate (cAMP). Downstream, G_i inhibits activation of protein kinase A (PKA) and phosphorylation of the PKA target cAMP response element binding protein (CREB) (Pisanti *et al.*, 2013b). G_i also inhibits Ras homolog gene family A (RhoA) and β-catenin, which then inhibits angiogenesis and epithelial-mesenchymal transition, respectively. CB1 and CB2 can also activate the p38/c-Jun N terminal kinase/extracellular signal-regulated kinase and inhibit the phosphoinositide 3-kinase/protein kinase B/target of rapamycin pathway (Pisanti, et al., 2013b). The downstream result of both pathways is an increase in apoptosis and

decrease in proliferation. The complex CB receptor signaling pathways can explain, in part, the array of effects mediated by AEA.

More recently, it has been shown that AEA can bind to other receptors as well, further diversifying its biological utility. For instance, AEA can inhibit the activity of TRPV1, a calcium channel activated by capsaicin that provides a sensation of pain and heat (Toth *et al.*, 2009). By inhibiting TRPV1-mediated calcium influx, AEA as well as THC can dampen the pain response (Pertwee, 2015; Woodhams, et al., 2015). AEA also activates peroxisome proliferator activated receptors (PPARs) α and γ, which in turn regulates differentiation and lipid metabolism (Simon and Cota, 2017). AEA likewise interacts with serotonin, muscarinic, glycine, and nicotinic receptors *in vitro,* although the implications of those interactions are poorly understood *in vivo* (Christopoulos and Wilson, 2001; Kimura *et al.*, 1998; Lozovaya *et al.*, 2005; Oz *et al.*, 2003; Xiong *et al.*, 2008). It has also been suggested that GPR55, an orphan receptor, may be a third cannabinoid receptor, but there are conflicting studies on the potency and efficacy of AEA binding to GPR55 (Johns *et al.*, 2007; Oka *et al.*, 2007; Ryberg *et al.*, 2007; Waldeck-Weiermair *et al.*, 2008).

In conclusion, AEA, which is produced and broken down ubiquitously throughout the body, can regulate a vast array of biological processes. The diversity of responses to AEA signaling is mediated by both cannabinoid receptor signal transduction and an array of identified and unidentified intracellular and extracellular receptors that interact with AEA. It is therefore no surprise that AEA signaling is a crucial component of fetal development and placentation during pregnancy, as discussed below.

Endocannabinoids During Pregnancy

During pregnancy, CB1 and CB2 are expressed on the decidua, fetal membranes, and placenta (Habayeb *et al.*, 2008). Immunohistochemical staining of human term placenta reveals that CB1, CB2, and FAAH are expressed in cytotrophoblasts, syncytiotrophoblasts, and mesenchymal cores (Habayeb, et al., 2008). CB1 and FAAH expressions are consistent throughout pregnancy, except through GW9-10, during which CB1 and FAAH protein increases before returning to basal levels (Habayeb, et al., 2008). AEA plays a critical role in female reproduction; plasma AEA concentration changes throughout both the menstrual cycle and gestation. One study demonstrated that circulating AEA during the first, second, and third trimester (n=77) were 0.89, 0.44, and 0.42 nM, respectively (Habayeb *et al.*, 2004). AEA then increased to 2.5 nM during labor, indicating a potential role in the role of AEA in initiating parturition. AEA levels during gestation were lower when compared to non-pregnant women (n=25, 1.68 nM and 0.87 nM during the follicular and luteal phase, respectively). Importantly, however, the endometrium, which maintains intimate contact with the placenta, produces AEA throughout pregnancy. However, the local AEA concentration in the placenta has not been investigated, and high levels of AEA can interfere with a number of placental functions. For instance, AEA reduces trophoblast hCG, cAMP, and alkaline phosphatase secretion by a CBR-dependent mechanism *in vitro*, suggesting that AEA can inhibit trophoblast syncytialization (Costa, 2016a; Costa *et al.*, 2015a). AEA also decreased the expression of galectin-13, aromatase, and leptin and increased nitric oxide synthase activity *in vitro* through a CBR-independent mechanism (Battista *et al.*, 2015; Chan *et al.*, 2013; Cinar *et al.*, 2017; Costa, et al., 2015a). High concentrations of AEA (>50 μM) induces apoptosis in primary trophoblasts and reduces BeWo cell proliferation by a CB-dependent mechanism as well (Aban *et al.*, 2016; Costa *et al.*, 2015b). The endocannabinoid system is also involved in trophoblast invasion; $CB1^{-/-}$ mice (C57BL/6J) displayed reduced trophoblast invasion into the decidua basalis on GD14 compared to

WT (Sun *et al.*, 2010). Primary $CB1^{-/-}/CB2^{-/-}$ trophoblasts are also less invasive *in vitro* compared to WT trophoblasts (Sun, et al., 2010). Dysfunctions in trophoblast invasion, syncytialization, and apoptosis have all been implicated in the etiology of placental pathologies. Taken together with these studies, it is evident that diseases of pregnancy are driven in part by aberrant endocannabinoid signaling.

In general, placentas from pregnancies with complications, such as preeclampsia, have increased endocannabinoid signaling compared to normal placentas (Battista, et al., 2015). One study demonstrated that preeclamptic placentas (N=14 preeclamptic placentas) express higher levels of NAPE-PLD and lower levels of FAAH but no difference in CB1 protein expression compared to normal placentas (N=14 normal placentas) (Aban *et al.*, 2013). Contrary to this, another study (N=18 normal, 18 preeclamptic placentas) showed that CB1 expression is higher in placentas from preeclamptic patients (Fugedi *et al.*, 2014). In preeclampsia, trophoblast invasion into the uterine spiral arteries is inadequate, leading to a decrease in uteroplacental blood flow and hypoxic conditions in the placenta (Tal, 2012). Hypoxia activates the transcription factor HIF1α, and HIF1α increases FAAH expression in trophoblasts *in vitro* (Aban, et al., 2016). Moreover, inhibition of CB1 using AM251 inhibited *in vitro* apoptosis induced by cobalt chloride, a HIF1α activator (Aban, et al., 2016). Hypoxia-driven changes in the endocannabinoid system in preeclampsia may therefore contribute to the etiology of the disease.

The endocannabinoid system has been implicated in other pathologies of pregnancy as well. Placentas from spontaneous miscarriage (N=15 miscarriages) have higher CB1 and lower FAAH protein expression compared to voluntary terminations (N=15 voluntary terminations), again an indication of increased endocannabinoid signaling. EVTs from

women who suffer from recurrent miscarriage (N=45 miscarriages) express FAAH, while those from voluntary terminations (N=17 voluntary termination) do not (Chamley *et al.*, 2008). In ectopic pregnancies (N=38 ectopic, 38 controls), peripheral FAAH activity was decreased (19%) while circulating AEA (24%) was increased along with AEA analogs oleoylethanolamine (41%) and palmoylethanolamine (63%) (Gebeh *et al.*, 2013). $FAAH^{-/-}$ mice (C57BL/6) have a higher rate (35%) of preterm birth compared to wild type in an Lipopolysaccaride-induced preterm birth model. $CB1^{-/-}$ mice (C57BL/6J/129) also have a higher rate of preterm birth (mean GD = 19.5 vs 20.0 for WT), but, interestingly, $CB2^{-/-}$ mice do not (Wang *et al.*, 2008b). This demonstrates that both increased and decreased endocannabinoid signaling can both contribute to pathological pregnancies.

1.6 Research Objective and Hypothesis

Considering all of the information presented in this introduction, a central hypothesis was developed: endogenous lipids influence the capacity for placental BCRP to prevent fetal exposure to the mycotoxin zearalenone by 1) directly impacting BCRP efflux or 2) altering the transcription of the BCRP/*ABCG2* gene. Three specific aims were employed to evaluate the hypothesis presented in this thesis:

Aim 1. Comprehensively assess the role of BCRP in the transport of zearalenone and its metabolites across the blood-placenta barrier.

Aim 2. Determine the effect of lipid signaling molecules on BCRP transcription, expression, and activity.

Aim 3. Investigate the post-transcriptional regulation of placental BCRP by membrane cholesterol and lipid rafts.

The prevalence of zearalenone in the environment and the specific potential toxic effects make the risk of exposure during pregnancy a significant concern. This work aims to shed light on the potential risks that may result from gestational disease states that alter maternal endocannabinoid or cholesterol homeostasis. My thesis research fills knowledge gaps in the fields of transporter biology, developmental toxicology, and environmental health sciences. These studies enlist complementary methods to assess the regulation of the placental BCRP transporter by lipids and how this may affect the *in utero* exposure to zearalenone and its metabolites. This work is aimed at identifying the mechanisms underlying the function and expression of BCRP, a critical fetoprotective transporter that may prevent the fetal accumulation of the developmental toxicant, zearalenone.

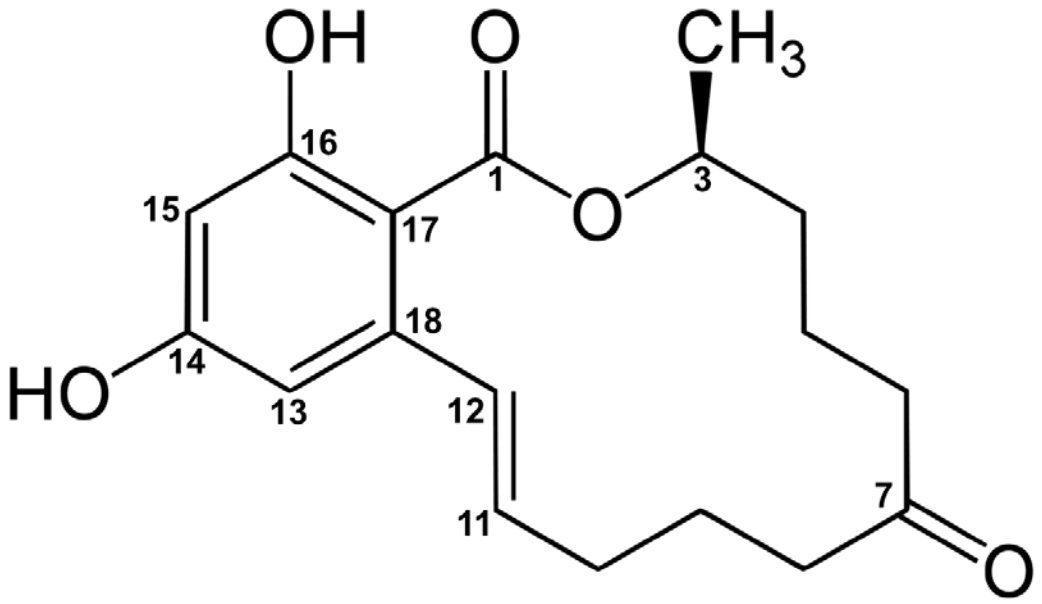

Fig 1.1 Numbered structure of zearalenone.

Table 1.1 List of BCRP Substrates

Substrates	References
Mycotoxins	
Aflatoxin B_1	van Herwaarden et al., 2006a
Zearalenone	Xiao, et al., 2015
Ochratoxin A	Schrickx et al., 2006
Beauvericin	Dornetshuber et al., 2009
Anticancer drugs	
Etoposide	Allen et al., 2003
Imatinib	Burger et al., 2004
Sunitinib	Kunimatsu et al., 2013
Axitinib	Reyner et al., 2013
Erlotinib	de Vries et al., 2012
Gefitinib	Zaher et al., 2006
Sorafenib	Agarwal et al., 2011
Mitoxantrone	Allikmets et al., 1998a; Doyle et al., 1998a; Rabindran et al., 1998a
Methotrexate	Volk et al., 2002b
Daunorubicin	Doyle, et al., 1998b
Doxorubicin	Doyle, et al., 1998b
Irinotecan	Maliepaard et al., 1999
Topotecan	Jonker et al., 2002a
SN-38	Brangi et al., 1999
Leflunomide	Kis et al., 2009
Teriflunomide	Kis, et al., 2009
Temozolomide	de Gooijer et al., 2018
Endogenous compounds	
Estrone-3-sulfate	Imai et al., 2003
Dehydroepiandrosterone-sulfate	Lee et al., 2005
Protoporphyrin IX	Krishnamurthy et al., 2004
Uric acid	Nakayama et al., 2011
Cholate	Janvilisri et al., 2005
Deoxycholate	Janvilisri et al., 2005
Taurocholate	Janvilisri et al., 2005
Fluorescent/luminescent dyes	
Hoechst 33342	Scharenberg et al., 2002
D-luciferin	Zhang et al., 2007a
Rhodamine 123	Litman et al., 2000
Other pharmaceutical drugs	
Cimetidine	Pavek et al., 2005
Glyburide	Gedeon et al., 2006

Diclofenac	Lagas et al., 2009
Apixaban	Zhang et al., 2013
Rivaroxaban	Gong et al., 2018
Edoxaban	Hodin et al., 2018
Sulpiride	Bai et al., 2017
Chlorothiazide	Beery et al., 2012
Sulfasalazine	Kawamura et al., 2009
Prazosin	Zhou et al., 2009
Ketamine	Ganguly et al., 2018
HMG CoA Reductase Inhibitors	
Cerivastatin	Matsushima et al., 2005
Pitavastatin	Hirano et al., 2005
Rosuvastatin	Huang et al., 2006
Antibacterials	
Ciprofloxacin	Merino et al., 2006
Danofloxacin	Schrickx and Fink-Gremmels, 2007
Grepafloxacin	Ando et al., 2007
Norfloxacin	Merino, et al., 2006
Ofloxacin	Merino, et al., 2006
Nitrofurantoin	Merino et al., 2005
Antivirals	
Abacavir	Pan et al., 2007
Lamivudine	Ceckova et al., 2016
Zidovudine	Pan, et al., 2007
Acyclovir	Gunness et al., 2011
Other Dietary Compounds	
Pheophorbide a	Jonker, et al., 2002a; Robey et al., 2004
2-Amino-1-methyl-6-phenylimidazo(4,5-b)pyridine (PhIP)	Pavek, et al., 2005
Genistein	Enokizono et al., 2007; Imai et al., 2004
Daidzein	Cooray et al., 2004a; Enokizono, et al., 2007
Folic acid	Chen et al., 2003
Quercetin	Cooray et al., 2004b; Sesink et al., 2005
Resveratrol	Cooray, et al., 2004b
Hesperetin	Cooray, et al., 2004b
Silymarin	Cooray, et al., 2004b
Riboflavin	van Herwaarden et al., 2007
Butyrate	Goncalves et al., 2011
Perfluorooctanoic acid	Dankers et al., 2013

CHAPTER 2: PLACENTAL BCRP/*ABCG2* TRANSPORTER PREVENTS FETAL EXPOSURE TO THE ESTROGENIC MYCOTOXIN ZEARALENONE

John T. Szilagyi[a], Ludwik Gorczyca[a], Anita Baker[c], Brian Buckley[b,c], Jeffrey D. Laskin[b,c,d], Lauren M. Aleksunes[b,c]

[a] Joint Graduate Program in Toxicology, Rutgers University Graduate School of Biomedical Sciences, 170 Frelinghuysen Rd, Piscataway, NJ 08854, USA

[b] Department of Pharmacology and Toxicology, Rutgers University, 170 Frelinghuysen Rd, Piscataway, NJ 08854, USA

[c] Environmental and Occupational Health Sciences Institute, Rutgers University, 170 Frelinghuysen Rd, Piscataway, NJ 08854, USA

[d] School of Public Health, Rutgers University 170 Frelinghuysen Rd, Piscataway, NJ 08854, USA

2.1 Abstract

In the placenta, the BCRP/*ABCG2* efflux transporter is responsible for preventing the maternal-to-fetal transfer of chemicals. Previous research has pointed to the estrogenic mycotoxin, zearalenone as a potential substrate for BCRP. The purpose of this study was to assess the role of the BCRP transporter in the transplacental disposition of zearalenone during pregnancy. *In vitro* transwell transport assays employing BCRP/Bcrp-transfected MDCK cells and BeWo trophoblasts with reduced BCRP expression were used to characterize the impact of BCRP on the bidirectional transport of zearalenone. In transwell experiments, the presence of BCRP protein increased the basolateral-to-apical transport of the probe BCRP substrate glyburide by 42-89% after 2 h. The presence of BCRP protein in transwell cultures also decreased the apical-to-basolateral transport of zearalenone by and increased its basolateral-to-apical transport up to 24%. *In vivo* pharmacokinetics analyses were then performed on pregnant wild-type and Bcrp$^{-/-}$ mice after a single tail vein injection of zearalenone. Zearalenone and its metabolite α-zearalenol were detectable in serum, placentas, and fetuses from all animals, and β-zearalenol was detected in serum and fetuses but not placentas. There were no significant differences in the maternal serum concentrations of any analytes between the two genotypes. In Bcrp$^{-/-}$ mice, the free fetal concentrations of zearalenone, α-zearalenol, and β-zearalenol were increased by 115%, 84%, and 150%, respectively, when compared to wild-type mice. Placental concentrations of free zearalenone and α-zearalenol were increased by 145% and 78%, respectively, when compared to wild-type mice. Taken together, these data indicate that the placental BCRP transporter functions to prevent the fetal accumulation of zearalenone, which may impact susceptibility to developmental toxicities associated with *in utero* zearalenone exposure.

Abbreviations

ABC, ATP-binding cassette; MDCK, Marine-Darby canine kidney; BCRP, breast cancer resistance protein; CYP, cytochrome P450; ENT, equilibrative nucleoside transporter; GAPDH, glyceraldehyde 3-phosphate dehydrogenase; GusB, glucuronidase B; HEK, human embryonic kidney; MATE, multidrug and toxin extrusion protein;MDR, multidrug resistance protein; MRP, multidrug resistance-associated protein; OAT, organic anion transporter; OATP, organic anion transporting polypeptide; OCT, organic cation transporter; OCTN, organic cation transporter, novel; P_{app}, apparent permeability coefficient; RPL13a, ribosomal protein 13a; SULF, sulfatase; SULT, sulfotransferase; TEER, transepithelial electrical resistance.

2.2 Introduction

During pregnancy, the placenta develops from the blastocyst and regulates the flow of nutrients, waste, and gases between the maternal and fetal circulations. Trophoblasts, the parenchymal cell of the placenta, fuse to form a syncytium that inhibits direct contact of the two blood supplies providing a physical and biochemical barrier that protects the developing fetus (Gupta, et al., 2016). The breast cancer resistance protein (BCRP/*ABCG2*) is an efflux transporter enriched on the maternal-facing surface of syncytiotrophoblasts. On the apical membrane, BCRP prevents the transepithelial passage of xenobiotics. Substrates of BCRP include endogenous chemicals, such as certain steroids and bile acids, pharmaceuticals, such as the diabetes drug glyburide and the antibiotic nitrofurantoin, and dietary contaminants, such as the plasticizer bisphenol A and phytoestrogen genistein. Compromised BCRP function in the placenta may consequently increase the risk of the fetus to chemical exposures during pregnancy. It is therefore critical to characterize the interaction of environmental and dietary contaminants with placental BCRP.

Recently, *in vitro* screening performed by our laboratory identified zearalenone as a substrate of the human BCRP transporter (Xiao, et al., 2015). Zearalenone is an estrogenic mycotoxin produced by *Fusarium* fungi that grows on cereal crops in moist climates. The European Union has determined the acceptable maximum for zearalenone in food at 4 µg/kg (Commision, 2006), but multiple studies worldwide have demonstrated that commonly consumed foods often exceed this level (Iqbal, et al., 2014; Lahouar, et al., 2018; Ok, et al., 2014; Tralamazza, et al., 2016). Further, analysis of urine from a cohort of pre-pubescent girls in New Jersey demonstrated that free zearalenone was present in the range of 0.2-8.4 ng/mL and was correlated with delayed puberty onset (Bandera, et al., 2011). It should also be noted that α-zearalanone, a zearalenone

metabolite marketed under the tradename Ralgro®, is commonly used to increase feed-to-weight ratios in cattle. Ralgro® is current used as a growth promoter in the United States but has been banned by the European Union. Exposure to xenoestrogens *in utero* is well-understood to induce adverse developmental effects (Hines, 2011). *In utero* exposure to zearalenone causes precocious puberty and mammary proliferation in both female Wistar rats and C57BL/6 mice (Belli, et al., 2010; Hilakivi-Clarke, et al., 1998). Zearalenone exposure is potentially common during pregnancy, with one study reporting detectable levels of zearalenone in the urine of 11 out of 30 pregnant women tested (Fleck *et al.*, 2016).

From prior *in vivo* rodent studies, zearalenone does cross the placenta into the fetal compartment, but the transplacental transfer of zearalenone appears to be limited (Appelgren, et al., 1982; Bernhoft, et al., 2001; Koraichi *et al.*, 2012). While multiple factors can regulate xenobiotic disposition, these data could point to placental efflux as a potential mechanism for regulating fetal exposure to zearalenone. To date, no studies have evaluated the ability of the BCRP transporter to regulate the fetoplacental disposition of zearalenone. Therefore, the purpose of this study was to comprehensively assess whether BCRP restricts the maternal-to-fetal transfer of zearalenone using *in vitro* and *in vivo* models of the human placental barrier.

2.3 Materials and Methods

Chemicals

Unless stated otherwise, all chemicals were purchased from Sigma-Aldrich (St. Louis, MO).

Cell Culture and Lentiviral Knockout of BCRP

All cell culture and transport experiments were performed in an incubator at 37°C with 5% CO_2 in HEPA-filtered air. Marine-Darby Canine Kidney (MCDK) cells transfected with human (hBCRP) or mouse (mBcrp) BCRP constructs or empty vector were provided by Dr. Alfred Schinkel (Netherlands Cancer Institute) and maintained in DMEM (Life Technologies, Carlsbad, CA) supplemented with 10% fetal bovine serum (Atlantic Biologicals, Frederick, MD) and 1% penicillin-streptomycin (Durmus *et al.*, 2012). BeWo-b30 human choriocarcinoma cells were provided by Dr. Nicholas Illsley (Hackensack University Medical Center) and maintained in DMEM:F12 (Life Technologies) supplemented with 10% fetal bovine serum and 1% penicillin-streptomycin (Vardhana and Illsley, 2002). Stable BeWo knockdown cells were generated using ABCG2 (sc-41151-V, Santa Cruz) or control (sc-108080) lentiviral shRNA particles. Cells were grown to 70% confluence on a 96-well plate before incubation for 24h in DMEM:F12 containing 5 µg/mL polybrene (Santa Cruz) and 2 viral particles per cell (60,000 particles/well). Subsequently, cells were sub-cultured in a 24-well plate, and stable transfected clones were selected using 6.5 µg/mL puromycin over 48 h.

Animal treatment

$Bcrp^{-/-}$ mice were obtained from Taconic Biosciences (Taconic, NY) and backcrossed to the C57BL/6 background (027 strain, Charles River Laboratories, Wilmington, MA) until >99% congenic (Rutgers RUCDR Infinite Biologics, Piscataway, NJ). Adult female and

male C57BL/6 wild-type and Bcrp$^{-/-}$ mice were mated overnight with the same genotype. The presence of the sperm plug denoted gestational day 0. Mice were provided phytoestrogen-free food and water *ad libitum*. At gestation day 14, mice were administered 10 mg/kg zearalenone dissolved in DMSO:PEG400:Saline (1:5:4 v/v) by tail vein injection (n = 6-8 dams per genotype). Two additional dams per genotype received vehicle to generate tissue matrices used for standard curves. At one hour post injection, dams were sacrificed by pentobarbital overdose, and blood (cardiac puncture), placentas, and fetuses were collected. Blood samples were centrifuged for 15 min at 600 x *g* to isolate sera. All samples were stored at -80°C until analysis by LC-MS.

Western Blotting

MDCK and BeWo cell lysates for Western Blot were collected and stored in buffer containing 20 mM Tris-HCl, 150 mM NaCl, 5 mM ethylenediaminetetraacetic acid, 1% Triton X-100 and a protease inhibitor cocktail (Sigma P8340, 1%, v/v). Mouse placenta homogenates were prepared in sucrose-Tris-HCl buffer (250 mM sucrose and 10 mM Tris-HCl, pH 7.5) supplemented with protease inhibitor cocktail (Sigma P8340, 1%, v/v) using a bead homogenizer (Tissue-Lyser LT, Qiagen) for 3 min at 40 Hz. Unless indicated otherwise, all Western blotting was performed with equipment from BioRad (Hercules, CA) as previously described (Zheng *et al.*, 2013b). All samples were spun down at 1000 x *g* for 10 min. Thirty µg of protein homogenates were loaded onto 4-12% Tris-HCl gels, electrophoretically separated, and transferred to nitrocellulose membranes. After blocking in 5% nonfat milk for 2 h, membranes were incubated overnight at 4°C in 2% nonfat milk containing primary antibodies used to detect BCRP (BXP-53, 1:5000; Enzo Life Sciences, Farmingdale, NY), β-actin (ab8227, 1:2000, Abcam, Cambridge, MA) or glyceraldehyde 3-phosphate dehydrogenase (GAPDH, ab9485, Abcam), followed by incubation with either HRP-linked rabbit or HRP-linked rat

secondary antibodies (1:1000, 2 h, Cell Signaling Technologies, Danvers, MA). After incubating membranes briefly with Luminata Forte Western HRP substrate (Millipore, Billerica, MA), protein-antibody complexes were visualized using a Fluorchem Imager (ProteinSimple, Santa Clara, CA).

Hoechst 33342 Transport

For Hoechst 33342 transport studies, BeWo or MDCK cells were added to 96-well round-bottom plates (100,000 cells/well). *Uptake phase.* Cells were incubated in 100 µL DMEM (MDCK) or DMEM:F12 (BeWo) containing 5 µM Hoechst 33342, a fluorescent BCRP substrate, for 30 min. A parallel treatment group included cells also incubated with 1 µM Ko143, an established BCRP inhibitor (Bircsak *et al.*, 2013). *Efflux phase.* The substrate-containing media was removed and replaced with substrate-free media. Cells were then incubated an additional 1 h. The cells were then washed and re-suspended in 50 µL ice cold HBSS and set on ice for analysis. A Cellometer Vision automated cell counter (Nexcelom Bioscience, Lawrence, MA) fitted with a VB-450-302 filter (excitation/emission = 375/450 nm) was used to quantify intracellular fluorescence. The total number of cells analyzed for each sample ranged from 500-2000, and fluorescence was normalized for cell size.

Transwell Transport

MDCK or BeWo cells were seeded at a density of 100,000 and 200,000 cells per well, respectively, on a collagen-coated 24-well multiwall insert system (Cat# 351181, 1.0 µM pore, high density PET membrane, Corning, Tewksbury, MA). Transport assays were performed on day 3-4 post seeding on those wells with a TEER value greater than 250 $\Omega*cm^2$ for MDCK cells (Yang *et al.*, 2016) and 80-160 $\Omega*cm^2$ for BeWo cells (Li *et al.*, 2013a) as measured immediately before and after the experiment. Monolayer integrity

was also assessed by measuring the rejection percentage of Lucifer Yellow (20 μM) (Hidalgo *et al.*, 1989) using % Rejection = $(1 – C_r / (C_r + C_D) * 100$, where C_r is the final concentration in the receiver compartment and C_d is the final concentration in the donor compartment (Nkabinde *et al.*, 2012). On the day of experiments, media in both the apical and basolateral compartment were replaced with HBSS. The test compound (1 μM BODIPY-glyburide, 50 μM zearalenone, or 10 μM Rhodamine 123) was added to the donor compartment at time = 0 and a 100 μL aliquot was collected from the receiver compartment every 30 min. Fluorescence was measured using a SpectraMax M3 spectrophotometer (Molecular Devices, San Jose, CA). BODIPY-glyburide and Lucifer Yellow were measured using Ex/Em: 428/540 nm, and Rhodamine was measured using Ex/Em: 507/529 nm. Zearalenone was quantified by HPLC-UV. Permeability coefficients were calculated using P_{app} (cm/s) = (Q / t) / ($A*C_0$), where Q is glyburide (nmol) transported to the receiver compartment at time t (s), A is the cell surface area (cm^2) and C_0 is the initial concentration of test substrate (μM) (Li, et al., 2013a).

Messenger RNA Quantification

Mouse placentas were homogenized using a bead homogenizer (Tissue-Lyser LT, Qiagen) for 4 min at 40 Hz in RNAzol RT. Total RNA was isolated from lysates according to the manufacturer's protocol. RNA content and purity was determined by measuring absorbance at 260 nm using a NanoDrop (Fisher Scientific). cDNA was generated from total RNA (1000 ng) with the High-Capacity cDNA Reverse Transcription Kit (ThermoFisher) and a MultiGene OptiMax Thermal Cycler (Labnet International Inc., Edison, NJ) according to the manufacturer's instructions. Quantitative PCR was performed with cDNA, Sybr Green dye (Life Technologies), forward and reverse primers (see **Supplemental Table 2.1**) (Integrated DNA Technologies, Inc., Coralville, IA), and a

ViiA7 RT-PCR System (Life Technologies). Ct values were converted to ΔΔCt values by comparison with the housekeeping gene ribosomal protein 13A (Rpl13A).

Quantification of Zearalenone and Metabolites

Quantification of free zearalenone (parent compound only) in aliquots from transwell transport experiments was performed using an HPLC-UV system (Jasco, Easton, MD) equipped with a PU-4185 binary pump, UV 4075 detector (254 nm), AS-2055 autosampler, Zorbax Eclipse 3 mm x 15 cm C18 column (Agilent, Santa Clara, CA) (adapted from De Baere *et al.*, 2012). Peak areas were quantified using ChromNav V2 and compared to a standard curve. The mobile phase consisted of H_2O:acetonitrile (3:2, formic acid added to pH = 3.0).

In order to quantify free and total zearalenone and metabolites from in vivo experiments, analyte extracts were prepared and measured by LC-MS. For sera, samples were added onto ChemElut solid phase extraction columns (1 mL, unbuffered, 12198002, Agilent), and analytes were eluted using methyl tert-butyl ether. Samples were then dried under N_2, re-dissolved in methanol, added onto pre-conditioned Discovery DSC-NH_2 solid phase extraction columns, and eluted with methanol. Samples were dried again before being re-dissolved in LC-MS mobile phase (see below). Placentas and fetuses were first weighed and homogenized in sodium acetate buffer (0.2 M, pH 4.65) before incubating overnight in the presence or absence of β-glucuronidase (1000 U/sample) at 37°C with gentle shaking. Liquid-liquid extraction was then performed on the homogenates by adding methyl tert-butyl ether (2x volume of sample), vortexed for 30 sec, and centrifuged at 1000 x g for 10 min. The ether phase was removed and the extraction was repeated two more times. Extracts were dried under N_2, reconstituted in n-hexane:dichloromethane (3:2), and added onto pre-conditioned silica Sep-Pak solid

phase extraction columns (500mg/3cc, 186004615, Waters, Milford, MA). Samples were washed with ethyl acetate:n-hexane (6:94), and then the analytes were eluted with ethyl acetate:n-hexane (25:75) then ethyl acetate (neat). Eluates were dried under N_2 before being re-dissolved in LC-MS mobile phase (see below).

Quantification of zearalenone and its metabolites in extracts prepared from mouse tissues and serum was performed using an LC-MS system (Thermo Fisher) equipped with an Accela UPLC pump and autosampler (4°C), a 100 x 4.6 mm betasil phenyl hexyl column (35°C) (Phenomenex, Torrance, CA), and an LTQ XL mass spectrometer with an atmospheric pressure chemical ionization source. The mobile phase used was water:methanol (0.1% formic acid added):acetonitrile (2:1:1). Spiked sample matrices were used for quality control (>80% recovery) and run with each sample batch. The inter/intra-day variability (%RSD) was 4.5/4.0, 3.2/3.1, and 2.6/2.5 for zearalenone, α-zearalenol, and β-zearalenol, respectively. The detection limit for this method was 0.05 ng/mL. Peak areas were quantified using Xcalibur and normalized to mL (serum) or mg (tissues).

Statistical Analysis

Data are presented as mean ± SE and analyzed using GraphPad Prism 5.0 software (GraphPad Software Inc., La Jolla, CA). Depending upon the number of comparisons, either one-way or two-way analysis of variance with Newman-Keuls or Bonferroni post-test, respectively, or an unpaired student's t test was used to assess statistical significance ($p < 0.05$).

2.4 Results

Transporter Expression and Activity in Transfected hBCRP and mBcrp MDCK Cells

The ability of human BCRP and mouse Bcrp proteins to transport zearalenone was first assessed in MDCK cells transfected with full-length *BCRP/Bcrp* plasmids (Durmus, et al., 2012). Western blot analysis of MDCK cells demonstrated that only the hBCRP and mBcrp transfected cell lines expressed BCRP/Bcrp protein, with no detectable bands in the empty vector control cells (**Fig 2.1A**). H33342, a fluorescent substrate of BCRP, was used to assess BCRP activity using a cell accumulation assay. The intracellular retention of H33342 was reduced 80-90% in MDCK cells transfected with hBCRP and mBcrp (**Fig 2.1B**). Ko143, an inhibitor of BCRP, increased the cellular accumulation of H33342 by 20%, 1000%, and 425% in control, hBCRP, and mBcrp MDCK cells, respectively (**Fig 2.1B**).

Transepithelial Transport of Zearalenone in Transfected hBCRP and mBcrp MDCK Cells

As an efflux transporter that localizes to the apical membrane of cells, BCRP/Bcrp enables the basolateral-to-apical transport of chemicals in polarized epithelium. In transwell cultures, BODIPY-glyburide was used as a probe BCRP/Bcrp substrate (Bircsak, et al., 2016; Gedeon *et al.*, 2008; Hemauer *et al.*, 2010; Zhou, et al., 2008) to confirm the polarization and activity of BCRP/Bcrp. For these experiments, BODIPY-glyburide was added to the donor compartment and fluorescence quantified in the receiver compartment. The time-dependent increase of glyburide in the receiver compartment was linear (**Fig 2.2**, R^2 = 0.95 – 0.99). When grown in transwell inserts, MDCK cells exhibited minimal apical-to-basolateral transport of glyburide that was unaffected by expression of BCRP/Bcrp (**Fig 2.2A**). As expected, both hBCRP and mBcrp MDCK cells significantly increased the basolateral-to-apical transport of glyburide (**Fig 2.2A**).

Similar to experiments with glyburide, the increase of zearalenone in the receiver compartment was linear and time-dependent (**Fig 2.2B**, R^2 = 0.98 – 0.99). While zearalenone was transported in the apical-to-basolateral direction, this transfer was minimally affected by expression of BCRP/Bcrp (**Fig 2.2B**). By comparison, both hBCRP- and mBcrp-transfected MDCK cells exhibited significantly increased basolateral-to-apical transport of zearalenone (**Fig 2.2B**).

MDCK cells express endogenous canine multidrug resistance protein 1 (MDR1, P-glycoprotein) (Li *et al.*, 2013b). In this study, we confirmed canine MDR1 activity using the MDR1 substrate, Rhodamine 123. In MDCK cells, the MDR1 inhibitor PSC833 significantly reduced the basolateral-to-apical transport of Rhodamine 123 at all time points (**Supplemental Fig 2.1A**) but had no impact on the disposition of zearalenone (**Supplemental Fig 2.1B**).

BCRP Expression and Activity in Human Placental Cells Following Lentiviral Knockdown

To recapitulate the human placental barrier, a second set of transwell studies were performed using human BeWo b30 trophoblast cells. Consistent with prior reports (Ceckova *et al.*, 2006; Mitra and Audus, 2010), BeWo cells highly express BCRP protein (**Fig 2.3A**). Lentiviral knockdown of BCRP in BeWo b30 cells using targeted shRNAs reduced BCRP protein to levels below detection (**Fig 2.3A**). Similarly, compared to BeWo b30 cells infected with control shRNAs, BCRP mRNA expression was reduced 88% (data not shown). As a result of BCRP knockdown, H33342 retention was increased by 53% in BeWo b30 cells (**Fig 2.3B**). The enhanced accumulation of H33342 in BCRP knockdown cells was similar to the pharmacological inhibitor of BCRP, Ko143 (**Fig 2.3B**).

Transepithelial Transport of Zearalenone in Human Placental Cells Following Lentiviral Knockdown of BCRP

In the placenta, BCRP mediates the fetal (basolateral) to maternal (apical) translocation of xenobiotics. When grown in transwell inserts, BeWo b30 cells exhibited greater transfer of BODIPY-glyburide in the basolateral-to-apical direction compared to the apical-to-basolateral direction. While there was no difference in the apical-to-basolateral transport of glyburide between control and shBCRP BeWo cells (**Fig 2.4A**), the basolateral-to-apical transport of glyburide was significantly decreased by 50% in shBCRP BeWo cells (**Fig 2.4A**). These data confirm that BCRP was properly polarized to the apical surface of BeWo b30 cells and functional in transferring the known substrate glyburide. By comparison, the apical-to-basolateral transport of zearalenone was significantly increased in shBCRP BeWo cells compared to control cells (**Fig 2.4B**), and this difference was observed when the starting concentration was as low as 5 μM (**Supplemental Fig 2.2**). The basolateral-to-apical transport of zearalenone also tended to decrease in shBCRP cells (**Fig 2.4B**).

For all transwell experiments, the observed effects of BCRP on glyburide and zearalenone transport were reflected in the respective permeability coefficients and flux ratios, presented in **Table 2.1**. Lucifer yellow was used in transwell experiments to confirm monolayer integrity (determined by TEER values), and the percent rejection of Lucifer yellow was 98.6 ± 1.5% and 95.0 ± 0.6% and in MDCK and BeWo cell transwell cultures, respectively. BCRP expression did not impact Lucifer yellow rejection in either MDCK or BeWo cells (data not shown).

Distribution of Zearalenone and its Metabolites in Wild-Type and Bcrp$^{-/-}$ Mice

After confirming that both mouse and human BCRP proteins could transport zearalenone and that BCRP can influence the directional transfer of the mycoestrogen in placental cells, the transplacental transfer of zearalenone was assessed in pregnant wild-type and Bcrp$^{-/-}$ mice. In placentas from gestation day 14, Bcrp protein was detected in wild-type but not Bcrp$^{-/-}$ mice (**Fig 2.5A**). Placentas from Bcrp$^{-/-}$ mice also displayed a >99% reduction in Bcrp mRNA (data not shown).

After an IV injection of zearalenone to pregnant wild-type and Bcrp$^{-/-}$ mice, zearalenone and its metabolites were quantified in mouse serum, placenta, and fetuses by LC-MS. After 1 h, serum concentrations of free zearalenone, α-zearalenol, and β-zearalenol ranged from 108 – 588, 4 – 7, and 1 – 2 ng/mL, respectively (**Fig 2.5B**). There were no significant differences in the serum concentrations of any analyte between wild-type and Bcrp$^{-/-}$ mice (**Fig 2.5B**). For placental and fetal tissues, both free and total (free + deconjugated) zearalenone and its metabolites were quantified. In fetal tissues of Bcrp$^{-/-}$ mice, free/total zearalenone, α-zearalenol, and β-zearalenol increased by 115/118%, 84/53%, and 150/100%, respectively, compared to wild-type mice (**Fig 2.5C**). In matched placentas of Bcrp$^{-/-}$ mice, free/total zearalenone and α-zearalenol were increased by 145/99% and 122/114%, respectively, compared to wild-type mice (**Fig 2.5D**). β-zearalenol was not detected in placental samples of either genotype (data not shown). All samples were also assessed for the presence for zearalenone, α-zearalanol, and β-zearalanol, but these analytes were below the detectable limit (data not shown).

Relative Expression of Transporters and Drug Metabolizing Enzymes in Wild-Type and Bcrp$^{-/-}$ Mouse Placentas

To rule out compensatory changes in placental gene expression that could impact the metabolism and disposition of zearalenone *in vivo*, the mRNA expression of transporters

and drug metabolizing enzymes were compared between wild-type and Bcrp$^{-/-}$ placentas (**Table 2.2**). The majority of transcripts analyzed demonstrated no statistically significant difference between genotypes. Oatp2b1, Oatp3a1, and Oatp5a1 mRNA levels were significantly but minimally altered in Bcrp$^{-/-}$ placentas (+31%, +29%, and -27% compared to wild-type placentas, respectively). Cyp1a1 and sulfatase 1 were also significantly altered in Bcrp$^{-/-}$ placentas (+37% and -24%, respectively). Transcripts for Cyp3a11, Oatp1a5, and Oatp2a1 were also analyzed but could not be detected.

2.5 Discussion

In the placenta, BCRP protects the fetus from toxicant exposure by preventing transport from the maternal to the fetal circulation. Therefore, we sought to determine whether BCRP can prevent the maternal-to-fetal transfer of the mycotoxin, zearalenone. Previous work from our laboratory demonstrated that zearalenone is a novel substrate of BCRP using basic screening techniques including BCRP substrate retention and ATPase activity (Xiao, et al., 2015). Zearalenone inhibited BCRP activity in membrane vesicles (using ATPase activity with sulfasalazine and Lucifer yellow uptake) and in BeWo cells (using the H33342 retention assay) (Xiao, et al., 2015). Further, the presence of the BCRP inhibitor Ko143 increased zearalenone retention in BeWo cells (Xiao, et al., 2015). Building on these initial data, the current study employed complementary *in vitro* and *in vivo* approaches to address whether BCRP could limit the transplacental transfer of zearalenone. We compared transport of zearalenone by mouse Bcrp and human BCRP isoforms, utilized an *in vitro* model of the human placental barrier, and quantified placental and fetal zearalenone concentrations in wild-type and Bcrp$^{-/-}$ dams.

In order to determine if BCRP prevents fetal exposure to zearalenone, this study utilized techniques designed to more accurately represent the human placental barrier than cell retention-based transport methods. MDCK cells transfected with the *hBCRP* and *mBCRP* genes were used to elucidate the specific effect of BCRP on zearalenone disposition and to account for differences between homologues (human and mouse). After establishing that BCRP was present and functional in transfected MDCK cells, glyburide, a previously published substrate of BCRP in BeWo cells (Bircsak, et al., 2016), was used to probe the impact of BCRP on vectoral transport. In MDCK cells, BCRP greatly increased the basolateral-to-apical transport of glyburide. The flux ratios of glyburide in control, hBCRP, and mBcrp MDCK cells were 6.38, 14.87, and 17.70,

respectively. Only minimal glyburide was transported from the apical to the basolateral compartment, which could account for a lack of difference between the transfected and non-transfected MDCK cells. MDCK cells also express the canine Mdr1 transporter, which can transport glyburide. In MDCK cells, the presence of BCRP increased the basolateral-to-apical transport and decreased the apical-to-basolateral transport of zearalenone. Importantly, the MDR1 inhibitor PSC833 had no impact on the basolateral-to-apical transport of zearalenone, indicating that our observations with MDCK cells are specific to BCRP/Bcrp.

B30 cells, a sub-clone of the BeWo cell line that can form a monolayer, were used to recapitulate syncytiotrophoblasts. It has been previously demonstrated that BeWo cells secrete hormones including human chorionic gonadotropin similar to syncytiotrophoblasts (Pattillo and Gey, 1968; Pattillo *et al.*, 1968). After confirming that shBCRP knockdown successfully reduced BCRP protein expression and activity, we examined the impact of BCRP on the bidirectional transport of glyburide and zearalenone. Similar to our observations with MDCK cells, BCRP knockdown reduced the basolateral-to-apical transport of glyburide by BeWo cells but had no effect in the opposite direction. BeWo b30 cells have been reported to express MDR1 protein (Albekairi *et al.*, 2015), but, contrary to those studies, we did not detect MDR1 protein or activity (data not shown). In BeWo cells, the genetic knockdown of BCRP decreased the basolateral-to-apical transport and increased the apical-to-basolateral transport of zearalenone.

The flux ratios of zearalenone ranged from 0.91-1.06 when BCRP was expressed and 0.59-0.65 when BCRP was absent or reduced. Traditionally, a flux ratio of >1.5 indicates active transport, but the results observed in this study make evident the importance of

BCRP in zearalenone distribution during pregnancy. Further, in considering the data presented here, it is also important to recognize the potential role of other uptake and efflux transporters present at both the apical and basolateral membranes of either cell line. Zearalenone has also been shown to interact with MRP1-3, OAT1-4, OCT1 and OCT2 *in vitro* (Tachampa, et al., 2008; Videmann, et al., 2009). This study focused specifically on the role of BCRP, and further work is needed to fully characterize involvement by other transporters in the transplacental disposition of zearalenone.

Pharmacokinetics studies with nitrofurantoin and glyburide in Bcrp$^{-/-}$ mice demonstrate that BCRP/Bcrp activity in the placenta prevents the fetal accumulation of BCRP substrates (Zhang, et al., 2007b; Zhou, et al., 2008). The findings from the *in vivo* experiments in this study reflect those observed from *in vitro* transwell assays. Bcrp$^{-/-}$ mice displayed greater placental retention and maternal-to-fetal transfer of zearalenone and its metabolites compared to control without any significant differences in sera concentrations, placental weights litter size, or fetal weights. It is therefore evident that Bcrp plays a role in protecting the fetus from exposure to zearalenone present in the maternal circulation. In considering the impact of BCRP on zearalenone pharmacokinetics, it is also important to note any compensatory transcriptional changes to transporters and enzymes that result from deleting the *Bcrp* gene. Bcrp$^{-/-}$ placentas displayed a similar transcriptional profile of transporters to those of wild-type mice, with a few exceptions. Oatp2b1 and 3a1 were both slightly up-regulated (29-31%) and Oatp5a1 was slightly down-regulated (27%). Oatp2b1 is basolateral transporter, and, if zearalenone is an Oatp2b1 substrate, an increase in transcript levels would decrease the transplacental transfer of zearalenone. However, the subcellular localization of Oatp3a1 and 5a1 in mouse syncytiotrophoblasts and their contribution to zearalenone disposition are not currently understood. It is also unclear in this study if the metabolites

of zearalenone cross the placenta or are formed from fetal hepatic metabolism of the parent compound. By gestation day 17, fetal livers of C57BL/6 mice do express a number of Cyps, including 2d26, 2d10, 2c68, and 2c69, but these isoforms have not yet been shown to metabolize zearalenone (Peng *et al.*, 2012). It is known that zearalenone is metabolized to α-zearalenol and β-zearalenol by 3α- and 3β-hydroxysteroid dehydrogenase, and both the parent compound and its metabolites can be glucuronidated in humans by UGT 1A1, 1A3, 1A8, and 2B7. Sulfonation of the parent compound also occurs but to a much lesser extent. BCRP is known to transport both glucuronidated and sulfonated phase II metabolites of other compounds (An and Morris, 2011; Imai *et al.*, 2003b; Wu *et al.*, 2012; Zamek-Gliszczynski *et al.*, 2011). While the glucuronidated metabolites have not been shown to be estrogenic, human fetal livers do express glucuronidase enzymes that can deconjugate the glucuronide-conjugated zearalenone metabolites. Additional work is therefore needed to thoroughly characterize the transport of these metabolites individually.

The effects of *in utero* exposure to zearalenone are not fully understood, but *in vivo* studies note developmental effects similar to other estrogens. Prior studies have demonstrated that zearalenone crosses the placenta and impacts reproductive development in both female Wister rats and C57BL/6 mice (Belli, et al., 2010; Hilakivi-Clarke, et al., 1998). Specifically, zearalenone (0.2-5000 µg/kg/day for Wistar rats on GD9-PND5 and 2 µg/day for C57BL/6 mice on GD15-20) induced precocious puberty and mammary proliferation in both studies, raising the concern that similar effects may be seen in humans. Conversely, however, urinary zearalenone concentration has been correlated to delayed puberty in a cohort of New Jersey girls (Bandera, et al., 2011). It is possible, however, that urinary concentrations of zearalenone indicate an increase in excretion rather than an increase in consumption. Alternately, zearalenone may act as

an antagonist to endogenous estrogens. Zearalenone interacts with all three isoforms of estrogen receptor (ERα, ERβ, and GPR30) but is not as potent as 17β-estradiol (Kuiper-Goodman, et al., 1987; Takemura, et al., 2007; Zinedine, et al., 2007). The specific effects of zearalenone, therefore, may depend on the presence of endogenous estrogens.

There exist genetic, pathological, and toxicological factors that decrease placental BCRP activity and may therefore increase fetal exposure to zearalenone. The 421C>A BCRP polymorphism, for instance, significantly decreases BCRP protein expression (40-50%) but not transcription (Bircsak *et al.*, 2018). The 421C>A allele varies between ethnic groups, but is relatively common among Asian (32%) and Hispanic (28%) populations (Bircsak, et al., 2018). Previous *in vitro* experiments with Q141K BCRP expressing HEK cells demonstrate increased retention of H33342, glyburide, and zearalenone compared to those expressing wild-type BCRP protein (Bircsak, et al., 2016; Xiao, et al., 2015). However, further studies are needed to determine the impact of the Q141K polymorphism on fetal drug accumulation *in vivo*. BCRP activity can also be directly inhibited by the previously mentioned substrates glyburide, genistein, and bisphenol A, which can all be encountered during pregnancy (Bircsak, et al., 2016; Dankers *et al.*, 2013). Moreover, BCRP expression is reduced by diseases of pregnancy involving placental dysfunction. Placentas from pregnancies with preeclampsia and intrauterine growth restriction, for instance, have demonstrated a marked reduction in BCRP mRNA and protein expression (Evseenko *et al.*, 2007a; Jebbink *et al.*, 2015b).

Using a complement of *in vitro* and *in vivo* approaches, we have demonstrated that zearalenone is a substrate of human BCRP and mouse Bcrp and that BCRP/Bcrp in the placenta reduces the maternal-to-fetal transfer of zearalenone. There are a number of

conditions in which placental BCRP function can be compromised which could potentially increase the maternal-to-fetal transfer of zearalenone. Taken together, these data suggest that women with compromised BCRP efflux may be at risk for higher fetal zearalenone exposure during pregnancy. Therefore, further studies are needed to characterize the effects of real world *in utero* exposure to zearalenone.

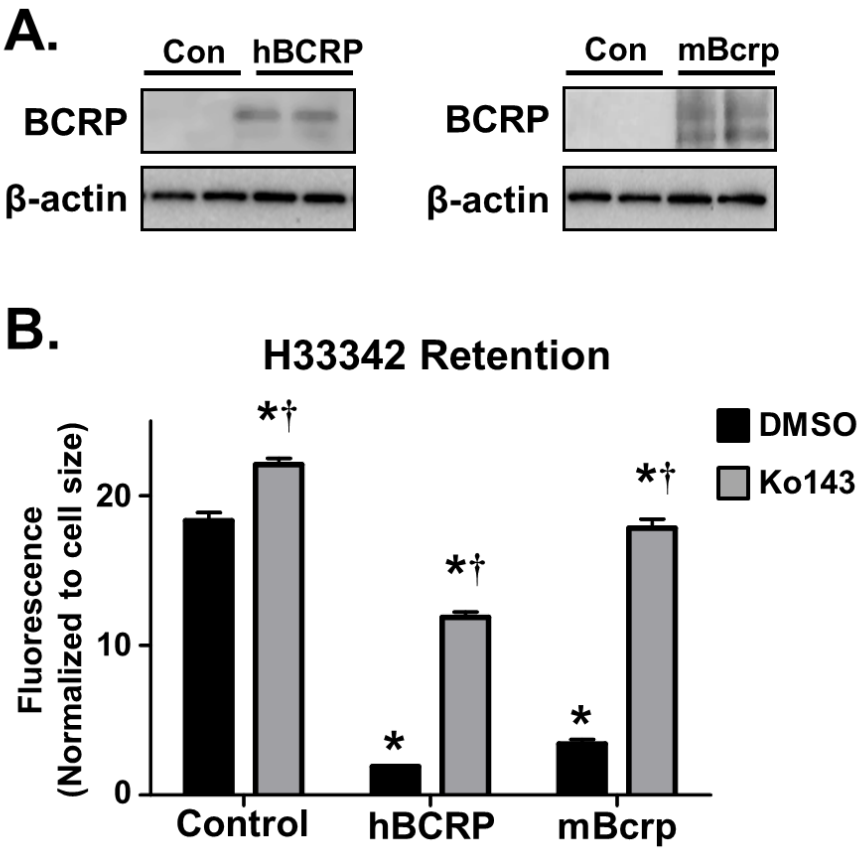

Fig 2.1. Characterization of BCRP expression and activity in hBCRP- and mBcrp-transfected MDCK cells.

A. Western Blot of transfected and control MDCK cells analyzing BCRP/Bcrp protein expression (72 kDa). β-actin (42 kDa) was used as a loading control. **B.** Retention of H33342 (10 μM) in empty vector control and transfected MDCK cells. Ko143 (1 μM) was used as a pharmacological inhibitor of BCRP/Bcrp. Data represent the mean ± SE (n = 6) and were analyzed using a two-way ANOVA followed by post-hoc Bonferroni analysis. Asterisks (*) represent statistically significant differences ($p < 0.05$) compared to control/vehicle (control black bar). Daggers (†) represent statistically significant differences ($p < 0.05$) compared to vehicle within treatment group (black bars within group).

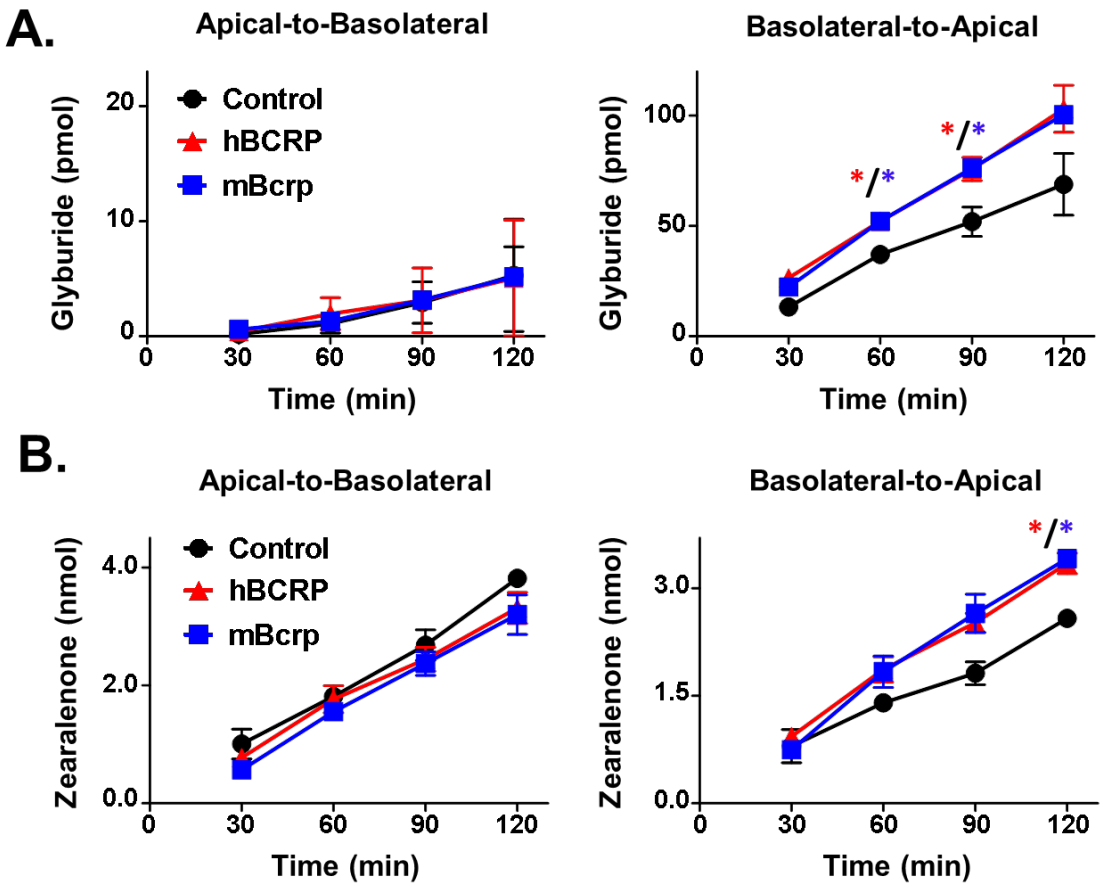

Fig 2.2. Transport of glyburide and zearalenone by MDCK cells in transwell cultures.

MDCK cells grown on transwell inserts were assessed for translocation of **A.** BODIPY-glyburide (1 μM) and **B.** zearalenone (50 μM) across cell monolayers for 2 h as described in the Materials and Methods. Data represent the mean pmol detected in the receiver compartment ± SE (n = 3 independent experiments) and were analyzed using a one-way ANOVA followed by post-hoc Newman-Keuls analysis (*$p < 0.05$ compared to control).

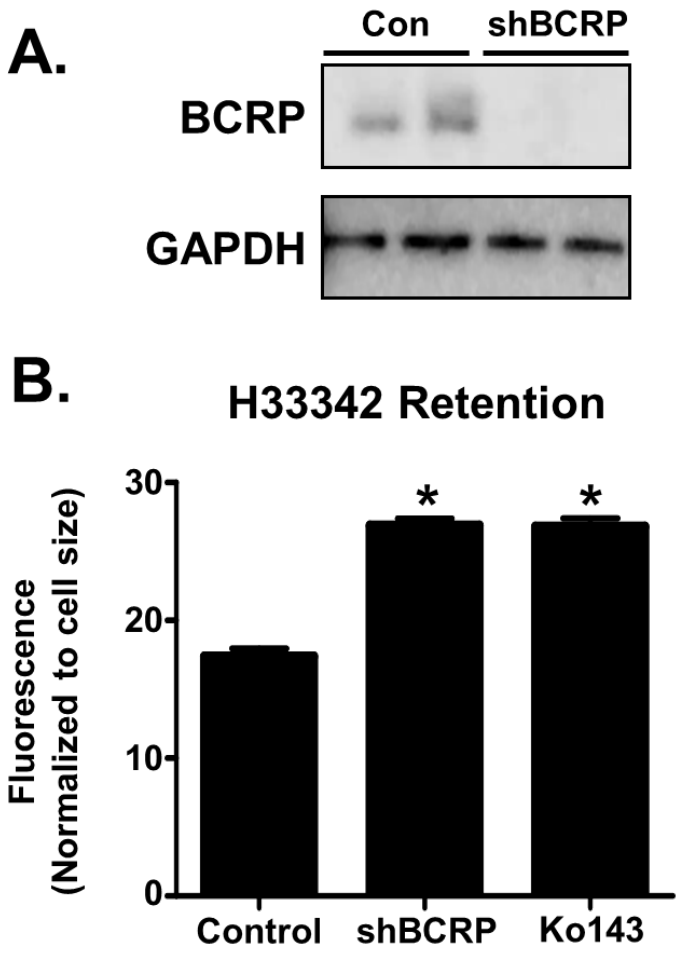

Fig 2.3. Characterization of BCRP protein and activity in BeWo shBCRP cells.

A. Western blot of BCRP protein (72 kDa) in lysates from BeWo cells after treatment with control or shBCRP lentiviral particles. GAPDH (37 kDa) was used as a loading control. **B.** Retention of H33342 (10 μM) in control and shBCRP BeWo cells. Ko143 (1 uM) was used as a pharmacological inhibitor of BCRP. Data represent the mean ± SE (n = 6) and were analyzed using a one-way ANOVA followed by post-hoc Newman-Keuls analysis (*$p < 0.05$ compared to control).

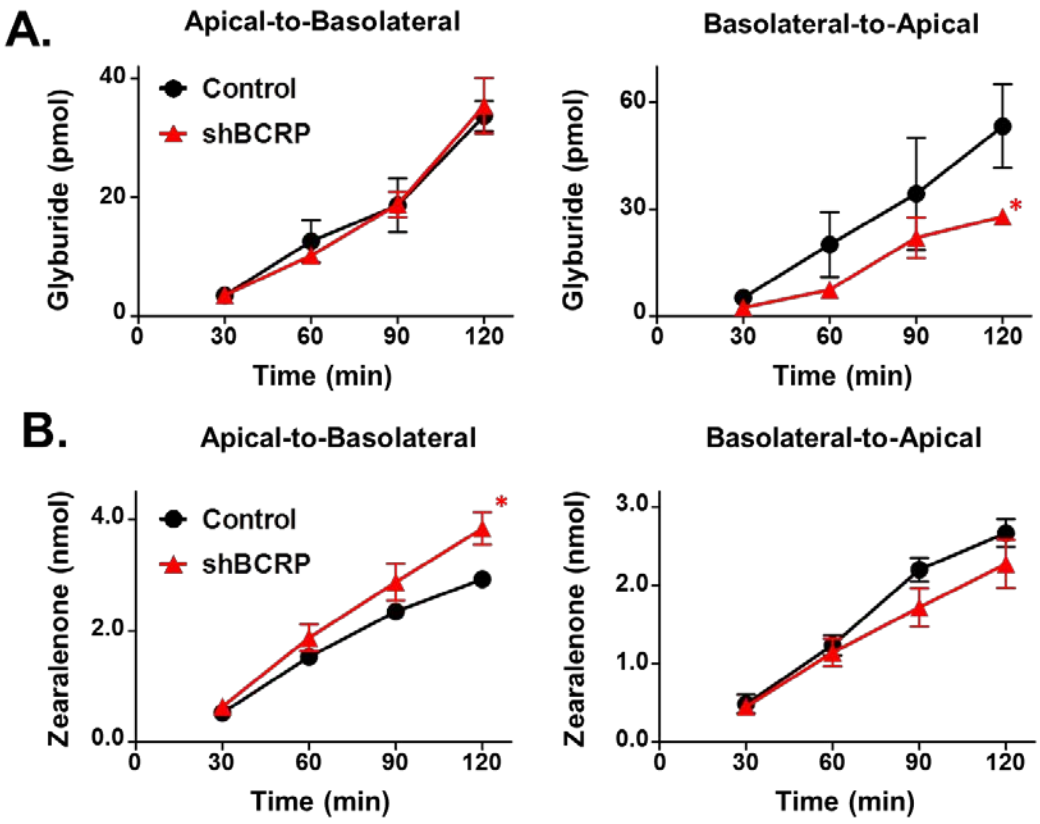

Fig 2.4. Transport of glyburide and zearalenone by BeWo cells in transwell cultures.

BeWo cells grown on transwell inserts were assessed for translocation of **A.** BODIPY-glyburide (1 µM) and **B.** zearalenone (50 µM) across cell monolayers for 2 h as described in the Materials and Methods. Data represent the mean pmol/nmol detected in the receiver compartment ± SE (n = 3 independent experiments) and were analyzed using a Student's t-test (*$p < 0.05$ compared to control).

Table 2.1 Permeability coefficients of glyburide and zearalenone in BeWo and MDCK transwell culture experiments

	Glyburide[a]		
	P_{app} A-B	P_{app} B-A	Flux Ratio
BeWo	1.42×10^{-5}	2.33×10^{-5}	**1.64**
BeWo BCRP-kd	1.49×10^{-5}	1.21×10^{-5}	**0.81**
MDCK	4.54×10^{-6}	2.90×10^{-5}	**6.38**
MDCK hBCRP	2.83×10^{-6}	4.21×10^{-5}	**14.87**
MDCK mBCRP	2.39×10^{-6}	4.23×10^{-5}	**17.70**

[a]P_{app} expressed in cm/s

	Zearalenone[a]		
	P_{app} A-B	P_{app} B-A	Flux Ratio
BeWo	2.46×10^{-5}	2.25×10^{-5}	**0.91**
BeWo BCRP-kd	3.23×10^{-5}	1.92×10^{-5}	**0.59**
MDCK	3.34×10^{-5}	2.17×10^{-5}	**0.65**
MDCK hBCRP	2.79×10^{-5}	2.82×10^{-5}	**1.01**
MDCK mBCRP	2.69×10^{-5}	2.87×10^{-5}	**1.06**

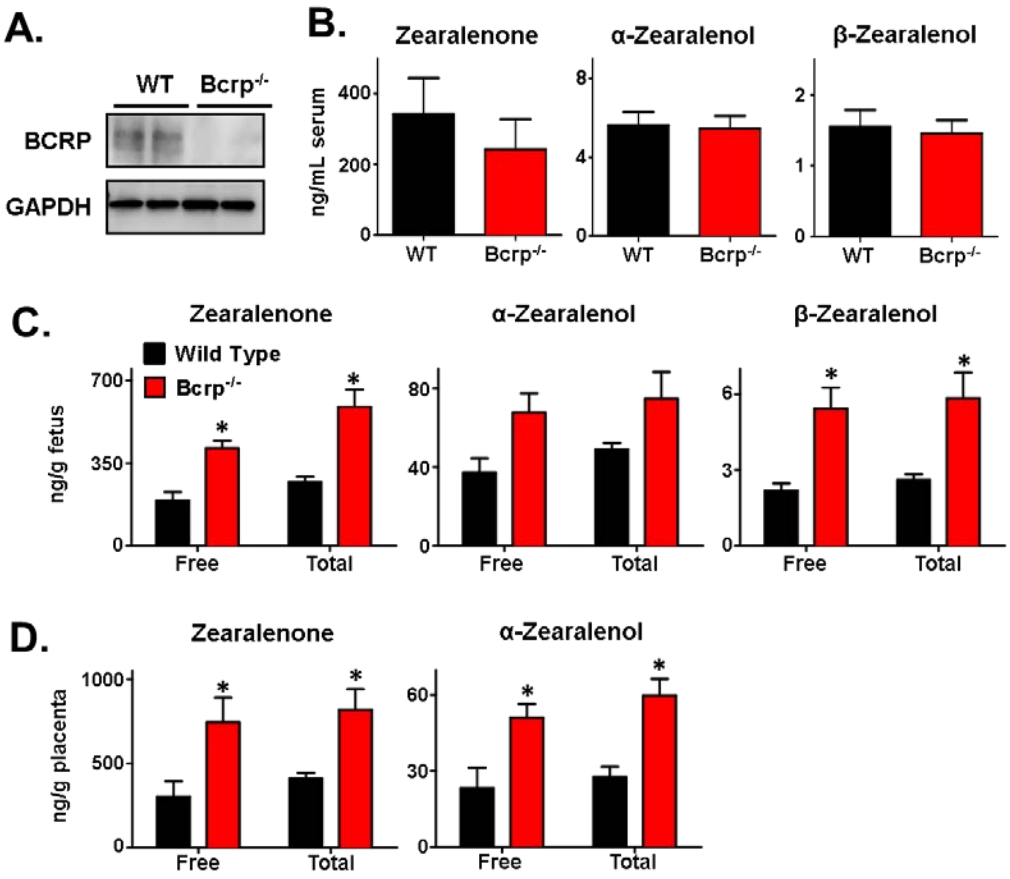

Fig 2.5. Quantification of zearalenone and its metabolites in pregnant wild-type and Bcrp-/- mice.

A. Western Blot of placental homogenates from pregnant wild-type and Bcrp$^{-/-}$ mice analyzing BCRP protein expression (72 kDa) on gestation day 14. GAPDH (37 kDa) was used as a loading control. **B-D.** Concentration of zearalenone and its metabolites detected in serum (B), fetuses (C), and matched placentas (D) 1 h after tail vein injection as determined by LC-MS. Total concentration was determined after incubation of samples with β-glucuronidase overnight at 37°C. Data represent the mean ± SE (n = 4-6 dams) and were analyzed using a two-way ANOVA followed by post-hoc Bonferroni analysis (*$p < 0.05$ compared to control).

Table 2.2 Changes in mRNA transcription of transporters and drug metabolizing enzymes in placentas from Bcrp-/- mice versus wild-type mice.

Slc Transporters		
Gene	Fold Change	P < 0.05
Oct1	1.12	N
Oct2	0.87	N
Oct3	0.88	N
Oat1	0.95	N
Oat2	0.92	N
Oat3	1.13	N
Octn1	0.97	N
Octn2	0.97	N
Octn3	0.96	N
Ent1	1.07	N
Mate1	1.07	N
Mate2	0.96	N
Oatp1a4	0.89	N
Oatp2b1	1.31	Y
Oatp3a1	1.29	Y
Oatp4a1	1.05	N
Oatp5a1	0.73	Y

Abc Transporters		
Gene	Fold Change	P < 0.05
Abca1	1.19	N
Mdr1a	1.08	N
Mdr1b	1.13	N
Mrp1	1.16	N
Mrp2	0.79	N
Mrp3	1.27	N
Mrp4	1.23	N
Mrp5	1.14	N
Mrp6	1.19	N
Mrp7	1.13	N

Phase I & II Enzymes		
Gene	Fold Change	P < 0.05
Cyp1a1	1.37	Y
Cyp1a2	1.31	N
Cyp1b1	0.94	N
Cyp27a1	1.01	N
Cyp2b10	1.19	Y
Cyp2e1	1.57	N
Gusb	1.02	N
Sulf1	0.76	Y
Sulf2	1.02	N
Sult1a1	1.09	N
Sult1e1	1.03	N

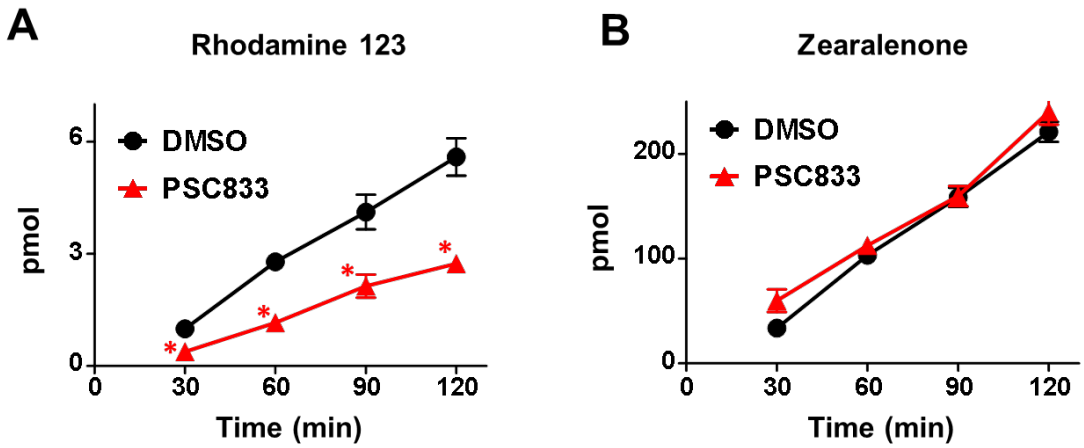

Supplemental Fig 2.1. Basolateral-to-apical transport of zearalenone and Rhodamine 123 in MDCK cells in the presence of a MDR1 inhibitor.

Control MDCK cells grown on transwell inserts were assessed for translocation of the MDR1 substrate Rhodamine 123 (10 µM, **A**) and zearalenone (50 µM, **B**) across cell monolayers for 2 h as described in the Materials and Methods. PSC833 (5 µM) was used as a pharmacological inhibitor of MDR1. Data represent the mean pmol detected in the receiver compartment ± SE (n = 3-4) and were analyzed using a Student's t-test (*$p < 0.05$ compared to control).

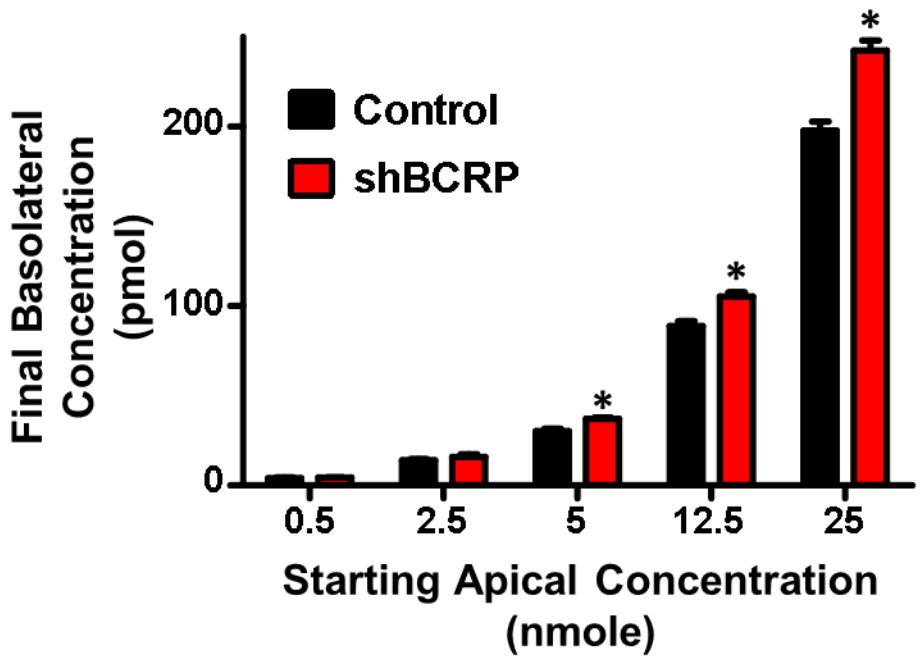

Supplemental Fig 2.2. Concentration-dependent apical-to-basolateral transport of zearalenone by BeWo b30 cells in transwell cultures.

Control and shBCRP BeWo b30 cells grown on transwell inserts were assessed for translocation of zearalenone across cell monolayers for 2 h as described in the Materials and Methods. Data represent the mean pmol detected in the receiver compartment at 2 h ± SE (n = 3-4) and were analyzed using a Student's t-test (*$p < 0.05$ compared to control).

Supplemental Table 2.1. Primer Sequences for qPCR (5' → 3')

Abca1	AAAACCGCAGACATCCTTCAG	CATACCGAAACTCGTTCACCC
Bcrp/Abcg2	GCGGAGGCAAGTCTTCGTTGC	TCTCTCACTGTCAGGGTGCCCA
Cyp1a1	TGGAAGGGCATAGGCAGCCAC	ACCAATGAAGGGCAAGCCCCA
Cyp1a2	CCCTGCCCTTCAGTGGTACAGATG	TCCGGGTGGATTCTTCAGGCC
Cyp1b1	GCTCATCCTCTTTACCAGATACC	GCAAAAAGCTGGAGAATCGC
Cyp27a1	GCCTCACCTATGGGATCTTCA	TCAAAGCCTGACGCAGATG
Cyp2b10	TGCTGTCGTTGAGCCAACCTTCA	GGGGCTCCCTGGGATTTCCG
Cyp2e1	TTCTGCAGGAAAGCGCGTGTGT	GCGTGGGATACTGCCAAAGCCAA
Cyp3a11	TCACACACACAGTTGTAGGGAGAA	GTCCATCCCTGCTTGTTTGTC
Ent1	CAAGTATTTCACAAACCGCCTGGAC	GAAACGAGTTGAGGCAGGTGAAGAC
Gusb	GGGTGAATGGGATTCATGTGG	TTGGGATACATGGAGGTGTCAG
Mate1	GTTGGCCTTACGGAGAGGAC	AATCCCACCCACCAAGACTAA
Mate2	AGTGGAGCTCCTACACGCGC	AGGGCACCATGTAGGCGACAG
Mdr1a	TGCCCCACCAATTTGACACCCT	ATCCAGTGCGGCCTGAACCA
Mdr1b	GTGTTAAAGGGGCGATGGGCG	AGGCTTGGCCAGACAACAGCTT
Mrp1	GCTGTGGTGGGCGCTGTCTA	CCCAGGCTCAGCCACAGGAA
Mrp2	AGCAGGTGTTCGTTGTGTGT	AGCCAAGTGCATAGGTAGAGAAT
Mrp3	CTGGGTCCCCTGCATCTAC	GCCGTCTTGAGCCTGGATAAC
Mrp4	CCAGACCCTCGTTGAAAGAC	TGAAGCCGATTCTCCCTTC
Mrp5	AGGGCAGCTTGTGCAGGTGG	TGCTGTTCCCGCTTCCTTGCT
Mrp6	TGTCTGCAAGCCATCGGACTGTTTG	TGGAAAAGCGGTTCAGCAGGTTCC
Mrp7	TGGAAACCTCTACACCCCAC	TGAGGAGTCGATGCAGTAGG
Oat1	TAATACCGAGGGGCCATACA	ATGCTTATCAGTGGGCTCAC
Oat2	GTGCTCAGACAGACAGGAAT	AGCTGTGCTTTCTTCGTCTC
Oat3	CTTCAGAAATGCAGCTCTTG	ACCTGTTTGCCTGAGGACTG
Oatp1a4	GCTTTTCCAAGATCAAGGCATTT	GCTTTTCCAAGATCAAGGCATTT
Oatp1a6	GCTGTGTAGACTGAGTTCCAT	CCAACAGAAACACCTTGATCTT
Oatp2a1	CTGTGGAGACAATGGAATCGAG	CACGATCCTGTCTTTGCTGAAG
Oatp2b1	CTCAGGACTCACATCAGGATGC	CTCTTGAGGTAGCCAGAGATCA
Oatp3a1	CGTTTGTTGGGTTTCATCCC	GAGGATGAAGGCAAAGGACT
Oatp4a1	CCAGCGCTACGTTGTTATGAGAG	CAATGAGTGTGGCTTCAGTGG
Oatp5a1	CACCCTGGGACCAACCTATT	ACTCCACCAGTTTCCGATGA
Oct1	TGTCGGCTCTGGCTACAGGAGA	GGGGGATTCTGGGACAAACCAGTAA
Oct2	ATTTCTGGTGCATACCGGAGTCTCC	AGGGGTTCTGACCAAGTCCAGGA
Oct3	ATCCTGAGGCGCGTGGCTAA	GCGCTCGTGAACCAAGCAAACAT
Octn1	GCGCCTATAACAGACTCCTAC	TTTTTCCCACATCTGAACCCTC
Octn2	ACTTTGTTTACCTAGGTGCCTA	TTGTCTGGCTTTGGATTTGC
Octn3	CGTGGGTGTGCTCTTAGGC	CGTGGGTGTGCTCTTAGGC
Rpl13a	GGGCAGGTTCTGGTATTGGAT	GGCTCGGAAATGGTAGGGG
Sulf1	TGAGTGCTTGAGGACGTGTT	CCCTCAGCACCTGAAAATACTG
Sulf2	AAAGTGACCCATCGGTGCTA	TTGAGACGGCCTTTGTGTTG
Sult1a1	CCCGTCTATGCCCGGATAC	GGGCTGGTGTCTCTTTCAGAGT
Sult1e1	TAA AAA CTC ACC TGC CAC CCA	ACC ATA CGG AAC TTG CCC T

CHAPTER 3: ANANDAMIDE DOWN-REGULATES PLACENTAL TRANSPORTER EXPRESSION THROUGH CB2 RECEPTOR-MEDIATED INHIBITION OF CAMP SYNTHESIS

John T. Szilagyi[a], Gabriella M. Composto[a], Laurie B. Joseph[b], Bingbing Wang[d], Todd Rosen[d], Jeffrey D. Laskin[b,c,f], Lauren M. Aleksunes[b,c,e]

[a] Joint Graduate Program in Toxicology, Rutgers University Graduate School of Biomedical Sciences, 170 Frelinghuysen Rd, Piscataway, NJ 08854, USA

[b] Department of Pharmacology and Toxicology, Rutgers University, 170 Frelinghuysen Rd, Piscataway, NJ 08854, USA

[c] Environmental and Occupational Health Sciences Institute, 170 Frelinghuysen Rd, Piscataway, NJ 08854, USA

[d] Division of Maternal-Fetal Medicine, Department of Obstetrics, Gynecology and Reproductive Sciences, Rutgers Robert Wood Johnson Medical School, New Brunswick, NJ 08901, USA

[e] Rutgers Center for Lipid Research, New Jersey Institute for Food, Nutrition, and Health, Rutgers University, New Brunswick, NJ 08901, USA

[f] School of Public Health, Rutgers University 170 Frelinghuysen Rd, Piscataway, NJ 08854, USA

3.1 Abstract

The breast cancer resistance protein (BCRP/*ABCG2*) is an efflux transporter expressed in placental syncytiotrophoblasts that protects the fetus from toxicant exposure. Syncytiotrophoblasts arise from the fusion of trophoblasts, a process negatively regulated by the endocannabinoid, anandamide (AEA). It is currently unknown whether AEA can influence fetal concentrations of xenobiotics by modulating the expression of transporters in syncytiotrophoblasts. Here, we sought to characterize and identify the mechanism(s) responsible for AEA-mediated down-regulation of the BCRP transporter in human placental explants and BeWo trophoblasts. Treatment of human placental explants with AEA (1 μM, 24 h) reduced hCGα, syncytin-1, and BCRP mRNAs by ~30%. Similarly, treatment of BeWo trophoblasts with AEA (0-10 μM, 3-24 h) coordinately down-regulated hCGß, syncytin-2, and BCRP mRNAs. In turn, AEA increased the sensitivity of trophoblasts to the cytotoxicity of mitoxantrone, a known BCRP substrate, and environmental and dietary contaminants including mycoestrogens and perfluorinated chemicals. AEA-treated trophoblasts also demonstrated reduced BCRP transport of the mycoestrogen zearalenone and diabetes drug glyburide. The AEA-mediated reduction of BCRP mRNA was abrogated when placental cells were co-treated with AM630, a CB2 receptor inhibitor, or 8-Br-cAMP, a cAMP analogue. AEA reduced intracellular cAMP levels in trophoblasts by 75% at 1 hr, and completely inhibited forskolin-induced cAMP response element binding protein (CREB) phosphorylation. AEA also decreased p-CREB binding to the *BCRP* promoter. Taken together, our data indicate that the endocannabinoid AEA down-regulates placental transporter expression and activity via CB2-cAMP signaling. This novel signaling mechanism may explain the repression of placental BCRP expression observed during diseases of pregnancy.

Abbreviations

ABC, ATP binding cassette; AEA, anandamide; AKT, protein kinase B; ALP, alkaline phosphatase; BCRP, breast cancer resistance protein; cAMP, cyclic adenosine monophosphate; CB, cannabinoid receptor; CREB, cAMP response element binding protein; DAB, 3,3'-diaminobenzidine; ERK, extracellular signal–regulated kinases; JNK, c-Jun N-terminal kinase; FAAH, fatty acid amide hydrolase; hCG, human choriogonadotropin; HELLP, hemolysis, elevated liver enzymes, low platelet count; HIF1α, hypoxia inducible factor 1α; H33342, Hoechst 33342; mTOR, mammalian target of rapamycin; NF-κB, nuclear factor kappa-light-chain-enhancer of activated B cells; PFOS, perfluorooctanesulfonic acid, PFOA, Perfluorooctanoic acid; PI3K, phosphatidylinositol-4,5-bisphosphate 3-kinase; PKA, protein kinase A; PPAR, peroxisome proliferator-activated receptors; RPL13A, ribosomal protein 13A; TEER, transepithelial electrical resistance; TRPV1, transient receptor potential cation channel subfamily V member 1.

3.2 Introduction

Fetal exposure to environmental toxicants can result in developmental disorders, congenital malformations, or preterm birth (Gluckman and Hanson, 2004). In fact, it has been estimated that 1 in 250 infants are born with malformations due to environmental exposures (Brent, 2001). The placenta helps protect the fetus from these exposures by utilizing an array of efflux xenobiotic transporters that prevent the transplacental trafficking of toxicants. The breast cancer resistance protein (BCRP/*ABCG2*) is one such efflux transporter that, in the placenta, limits exposure of the fetus to certain toxicants (reviewed in Mao, 2008). BCRP was simultaneously discovered by three groups, one of which identified it in the placenta and originally named it the placental ABC transporter (ABCP) (Allikmets, et al., 1998a). In the placenta, BCRP is highly expressed on the apical surface of syncytiotrophoblasts where it plays a key role protecting the fetus from exposure to xenobiotics present in the maternal circulation (Hahnova-Cygalova *et al.*, 2011). It is well known that BCRP transports a wide array of toxicants, including zearalenone, an estrogenic mycotoxin commonly found on cereal crops, glyburide, a prescription drug used for gestational diabetes, as well as the synthetic fluorosurfactants, perfluorooctanoic acid (PFOA) (Dankers, et al., 2013; Gedeon, et al., 2008; Jonker, et al., 2002a; Xiao, et al., 2015).

Placental BCRP expression is down-regulated in a number of gestational diseases including preeclampsia, intrauterine growth restriction, and HELLP (hemolysis, elevated liver enzymes, low platelet count) syndrome (Evseenko, et al., 2007a; Gormley *et al.*, 2017; Jebbink *et al.*, 2015a; Mason *et al.*, 2011; Nishizawa *et al.*, 2011). Clinically, disruption of BCRP activity has the potential to increase fetal exposure to toxicants (Mao, 2008). While the exact mechanism(s) responsible for altering placental BCRP expression in gestational disorders are unknown, multiple regulatory factors have been

shown to modulate BCRP levels in trophoblasts, including hormones, hypoxia, prostaglandins, membrane cholesterol, and dietary constituents (Bircsak, et al., 2016; Francois, et al., 2017; Mason *et al.*, 2014; Szilagyi *et al.*, 2016; Wang, et al., 2008a; Wang *et al.*, 2006).

One approach to identifying critical mediators involved in placental BCRP dysregulation is to interrogate pathways known to be disrupted during pregnancy disorders. The endocannabinoid system has an established role in regulating appetite, memory, pain, and mood. More recently, however, the endocannabinoid system was identified as a regulator of placentation and has therefore been suggested as a potential therapeutic target for diseases of pregnancy (reviewed in Costa, 2016a). The endocannabinoid receptors cannabinoid receptors 1 and 2 (CB1 and CB2) as well as the catabolic enzyme fatty acid amide hydrolase (FAAH) are expressed in cytotrophoblasts, syncytiotrophoblasts, and the mesenchymal core throughout gestation (Habayeb, et al., 2008; Park *et al.*, 2003; Trabucco *et al.*, 2009). The signaling molecule anandamide (AEA), an endogenous ligand for CB1 and CB2, is produced by the endometrium throughout pregnancy (Liu *et al.*, 2002). In general, biochemical responses elicited by endocannabinoids exhibit biphasic responses; high or low levels of AEA can be harmful to placental development and function (Cella *et al.*, 2008; Liu, et al., 2002; Wang *et al.*, 1999; Xie *et al.*, 2012). Assessment of placentas from preeclamptic women, for instance, has shown increased CB1 and decreased FAAH protein expression, both which enhance AEA signaling (Aban, et al., 2013; Fugedi, et al., 2014). Key roles for AEA have been shown during trophoblast syncytialization, invasion, and apoptosis (Costa, 2016a). Likewise, fetal endothelial vascular tone and nitric oxide synthase activity are modulated by AEA signaling (Cella, et al., 2008). However, the precise role

of endocannabinoid dysregulation in the etiology of gestational diseases has yet to be identified.

The function and localization of BCRP within the placenta provides protection of the fetus from exposure to toxicants. It is therefore critical to understand the underlying cellular mechanisms that drive BCRP expression. Recognizing that BCRP expression is down-regulated in gestational disorders associated with perturbed endocannabinoid signaling, we sought to determine whether the endocannabinoid AEA regulates the placental expression and activity of BCRP and characterize the underlying molecular mechanism(s) involved.

3.3 Materials and Methods

Chemicals

Unless stated otherwise, all chemicals were from Sigma-Aldrich (St. Louis, MO).

Patient Selection, Tissue Processing and Placental Explant Culture

Placentas were obtained from healthy women between the ages of 18–45 years following term delivery by scheduled Cesarean section. Placentas from patients with complication of pregnancies such as diabetes, preeclampsia, infection, hypertension, autoimmune disease, and fetal growth restriction were excluded. The study was approved by the Institutional Review Board of Rutgers University Robert Wood Johnson Medical School (protocol #20150001445)

Within 2 h of delivery, placentas were collected and processed. Villous tissue to be used for immunohistochemical staining was placed in PaxGene containers according to the manufacturer's protocol and later embedded in paraffin for slide processing. Explants were collected and cultured as previously described (Bircsak, et al., 2016). Placentas were examined for discernible irregularities and location of umbilical cord. The maternal decidua and the chorionic plate along the overlying membranes were removed, and sections of villous tissue were washed in sterile PBS to remove maternal blood before dissection into individual 8 mm^3 pieces. In a 24-well tissue culture plate, explants were cultured and maintained in an incubator at 37°C with 5% CO_2 in air in 1 mL of a phenol red-free DMEM and F12 1:1 mixture (Life Technologies, Carlsbad, CA), and with 10% charcoal-stripped, dextran-treated fetal bovine serum (Atlanta Biologicals, Miami, FL) and 1% penicillin-streptomycin (Life Technologies). Cell culture medium was replaced every 24 h. Because it was the purpose of this study to examine the effects of AEA on both BCRP expression and syncytialization, treatment of explants with AEA occurred

during days 2-3 post-collection, which falls within the window of syncytium regeneration (Miller *et al.*, 2005). Circulatory AEA has a short half-life in vivo (< 5 min), and homogenates of rat placenta have been shown to hydrolyze AEA (~200-500 pmol/min/mg protein) (Fonseca *et al.*, 2014; Willoughby *et al.*, 1997). Therefore, explant cultures, which were incubated with AEA (0.1-10 μM) for a total of 24 h, were replenished once with fresh AEA during the incubation period. AEA was dissolved in ethanol with a final ethanol concentration of 0.05% (v/v) in treatment media. Following the 24-hour treatment, explants were removed from culture plates, washed in PBS, snap frozen, and stored at -80°C until use.

BeWo cell culture

BeWo human choriocarcinoma cells (B30 sub-clone) were generously provided by Dr. Nicholas Illsley (Hackensack University Medical Center) and maintained in an incubator at 37°C with 5% CO_2 in air in a DMEM and F12 1:1 mixture (Life Technologies, Carlsbad, CA), supplemented with 10% fetal bovine serum (Atlantic Biologicals) and 1% penicillin-streptomycin (Life Technologies) (Baumann *et al.*, 2014). This cell line recapitulates first trimester trophoblasts because of their ability to undergo syncytialization, secrete human choriogonadotropin (hCG), and express transporters such as BCRP (Ceckova, et al., 2006; Kudo *et al.*, 2003; Pattillo and Gey, 1968). For all experiments, cells were grown to 70-80% confluence before treatment with AEA in combination with rimonabant (100 nM), a CB1 inverse agonist, AM630 (100 nM), a CB2 antagonist, forskolin (50 μM), a stimulator of adenylate cyclase, or 8-Br-cAMP (1 mM), a stable, cell-permeable cAMP analog. AEA was dissolved in ethanol, and all chemicals were dissolved in DMSO. The final concentration of solvent in culture media did not exceed 0.1% (v/v). Treatment media differed from culture media and consisted of phenol red free DMEM:F12 (Life Technologies) supplemented with 10% charcoal-stripped,

dextran-treated fetal bovine serum (Atlanta Biologicals) and 1% penicillin-streptomycin (Life Technologies).

Western Blotting

Explants were thawed on ice and placed in 200 µL of homogenization buffer (250 mM sucrose, 10 mM Tris-HCl buffer (pH 7.4)) supplemented with protease inhibitor cocktail (Sigma P8340, 1%, v/v), and lysed in a using a bead homogenizer (Tissue-Lyser LT, Qiagen) for 3 min at 40 Hz. BeWo cell lysates for Western blotting were collected in buffer containing 20 mM Tris-HCl, 150 mM NaCl, 5 mM ethylenediaminetetraacetic acid, 1% Triton X-100 and a protease inhibitor cocktail (Sigma P8340, 1%, v/v). Lysates were centrifuged at 1000 x g for 10 min to remove cellular debris before use. Unless otherwise stated, all Western blotting was performed using equipment from BioRad as previously described (Zheng, et al., 2013b). Proteins were resolved on Tris-HCl polyacrylamide gels and transferred to nitrocellulose membranes. Membranes were incubated overnight in primary antibodies used to detect BCRP (BXP-53, 1:5000; Enzo Life Sciences, Farmingdale, NY), β-actin (ab8227, 1:2000, Abcam, Cambridge, MA), CREB (9197, 1:1000, Cell Signaling Technologies, Danvers, MA), p-CREB (9198, 1:1000 Cell Signaling Technologies), CB1 (10006590, 1:1000, Cayman Chemical, Ann Arbor, MI), or CB2 (10006590, 1:1000, Cayman Chemical) followed by incubation with either HRP-linked rabbit or HRP-linked rat secondary antibodies (1:1000, 2 h, Cell Signaling Technologies). After the addition of a Luminata Forte Western HRP substrate (Millipore, Billerica, MA), chemiluminescent protein-antibody complexes were visualized using a Fluorchem Imager (ProteinSimple, Santa Clara, CA). Semi-quantitative analysis of protein band intensity was performed using AlphaView Software (ProteinSimple).

RNA Isolation and Analysis Using Quantitative Polymerase Chain Reaction (qPCR.

Explants to be used for mRNA expression analysis were thawed on ice and placed in 500 µL of RNAzol, and homogenized using a bead homogenizer (Tissue-Lyser LT, Qiagen) for 4 min at 40 Hz. BeWo cells were also collected in RNAzol and homogenized using a pipette. Nuclease-free water (200 µL) was added to lysates, which were then centrifuged at 13,000 x g for 15 min to precipitate DNA, lipids, and proteins. RNA was precipitated from the supernatant by adding 500 µL isopropanol and centrifuging at 13,000 x g for 15 min. The resulting pellet was washed twice with 500 µL ethanol, allowed to dry, and resuspended in 50 µL nuclease-free water. RNA content and purity was determined by measuring absorbance at 260 nm using a NanoDrop (Fisher Scientific). RNA was converted to cDNA using the High-Capacity cDNA Reverse Transcription Kit (ThermoFisher) and a MultiGene OptiMax Thermal Cycler (Labnet International Inc., Edison, NJ). RNA (1000 ng) was combined with RT buffer, RT random primers, 4 mM dNTP mix, 2.5 U MultiScribe Reverse transcriptase, 20 U RNase inhibitor, and nuclease free water to a final volume of 20 µL. Samples were incubated in the thermocycler with the following steps: 10 min at 25°C, 120 min at 37°C, 5 min at 85°C, and held at 4°C until samples were removed. Quantitative PCR was performed with specific forward and reverse primers (see **Supplemental Table 3.1**, Integrated DNA Technologies, Inc., Coralville, IA), cDNA, Sybr Green dye (Life Technologies), and a ViiA7 RT-PCR System (Life Technologies). Ct values were converted to ΔΔCt values by comparison with ribosomal protein 13A (RPL13A) as a reference gene and normalized to the control group for each respective experiment.

Cell Viability Assay

Cell viability was assessed as an indirect approach to determine the effect of AEA on BCRP efflux activity. BeWo cells were seeded at 10,000 cells/well in 96-well plates and allowed to adhere overnight. BeWo cells were incubated for 24 h with either AEA (10

μM) or Ko143 (1 μM) in combination with a range of concentrations for mitoxantrone (0.6-600 μM), zearalenone (0.5-500 μM), α-zearalanol (0.5-500 μM), perfluorooctanoic acid (2-2000 μM), or perfluorooctanesulfonic acid (2-2000 μM). At the end of treatment, cell viability was assessed using the Alamar Blue assay (Invitrogen) (Page *et al.*, 1993). Cells were incubated in 100 μL HBSS containing Alamar Blue (0.1 mg/mL resazurin) for 4 h. Fluorescence was then measured using Ex/Em: 535/580 nm. These values were normalized to the vehicle control group and used to calculate LC_{50} values for each substrate in the presence of AEA, Ko143, or vehicle control. Neither AEA nor Ko143 treatment alone had a significant effect on BeWo cell viability after 24 h (data not shown).

Hoechst 33342 Transport

For Hoechst 33342 transport studies, BeWo cells were incubated in the presence or absence of AEA (10 μM) and 8-Br-cAMP (1 mM) for 24 h, detached from the culture plates with trypsin and added to a 96-well round bottom plate at a density of 100,000 cells/well. Plates were centrifuged (500 x g, 5 min, 5°C) to remove media and cells were washed using ice cold HBSS. Cells were then re-suspended in 100 μL of treatment media containing Hoechst 33342 (5 μM), an established fluorescent BCRP substrate, in the presence or absence of the BCRP-specific inhibitor, Ko143 (1 μM) (Bircsak, et al., 2013). Both plates were incubated at 37°C for 30 min, during which Hoechst 33342 was taken up into BeWo cells. Cells were then centrifuged and washed with ice cold HBSS. At this point, cells used to measure relative fluorescence unit $(RFU)_{UPTAKE}$ were resuspended in 50 μL HBSS and set aside on ice for analysis. The remaining wells were re-suspended in substrate-free growth medium with or without Ko143 and incubated an additional 1 h at 37°C, during which Hoechst 33342 was actively transported from cells. Cells were then washed and re-suspended in 50 μL HBSS and set aside on ice for

measurement of RFU_{EFFLUX}. Quantification of intracellular fluorescence was performed using a Cellometer Vision automated cell counter (Nexcelom Bioscience, Lawrence, MA) fitted with a VB-450-302 filter (excitation/emission = 375/450 nm). The total number of cells analyzed for each sample ranged from 100 to 1000. Fluorescence was normalized for cell size. Percent efflux was calculated using: $\%efflux = ((RFU_{UPTAKE} - RFU_{EFFLUX})/(RFU_{UPTAKE}))*100\%$.

Zearalenone Transport and HPLC Measurement

After experimental treatments, BeWo cells were detached from the culture plates with trypsin, washed, resuspended in medium, and added to 2 x 96-well round bottom plates at a density of 200,000 cells/well. Plates were centrifuged (500 x g, 5 min, 5°C) to remove media and cells were washed using cold HBSS. Cells were then re-suspended in 100 µL of growth medium containing zearalenone (50 µM) in the presence or absence of the BCRP-specific inhibitor, Ko143 (1 µM) (Bircsak, et al., 2013). Both plates were incubated at 37°C for 60 min. Cells were then centrifuged and washed with ice cold HBSS. At this point, one of the plates was re-suspended in 50 µL HBSS and set aside on ice. The remaining plate was re-suspended in substrate-free growth medium with or without Ko143 and incubated an additional 30 min at 37°C. The cells were then washed and re-suspended in 50 µL HBSS. For both plates, cells from 3 wells were pooled into one sample and combined with ethanol (50% final concentration). Cells were passed through a 26 gauge needle 10x and then incubated for 1 h at -20°C. Samples were centrifuged at 1000 x g for 10 min and the resulting supernatants were analyzed for zearalenone content. Zearalenone was quantified by HPLC using a method adapted from a previous publication (De Baere, et al., 2012). A Jasco (Easton, MD) HPLC system equipped with a PU-4185 binary pump, UV 4075 detector (254 nm), AS-2055 autosampler, Zorbax Eclipse 3 mm x 15 cm C18 column (Agilent, Santa Clara, CA), and

Spectra-Physics (Santa Clara, CA) FL2000 fluorescent detector (Ex/Em: 275/440) was used. Peak areas were quantified using ChromNav V2 and compared to a standard curve. Zearalenone (ZLN) values were normalized to protein concentration before being used to calculate %efflux using: %efflux = $((ZLN_{UPTAKE} - ZLN_{EFFLUX})/(ZLN_{UPTAKE}))*100\%$. The mobile phase used was H_2O:acetonitrile at a ratio of 60:40 which was titrated to pH = 3.0 using formic acid. The retention time of zearalenone was 13-14 min.

BODIPY-Glyburide Transwell Transport

BeWo cells were seeded on collagen-coated 24-well multiwall inserts (Cat# 351181, 1.0 µM pore, high sensity PET membrane, Corning, Tewksbury, MA) at a density of 200,000 cells per well. Media was changed daily and wells were assessed for transepithelial electric resistance (TEER). On day 2 post-seeding, culture media was replaced with treatment media that contained AEA (10 µM, 24 h) or solvent only. Transport assays were performed on day 3 post seeding on those wells with a TEER value of 80-160 $\Omega*cm^2$ (Li, et al., 2013a). Monolayer integrity was confirmed by measuring the permeability of Lucifer yellow (20 µM) (Hidalgo, et al., 1989). The percent of Lucifer yellow rejection for these experiments was 95.3 ± 3.7% as calculated using % rejection = $(1 - (C_r / (C_r + C_D))) * 100$, where C_r is the final concentration in the receiver compartment and C_d is the initial concentration in the donor compartment (Nkabinde, et al., 2012). Anandamide pre-treatment did not affect TEER values or Lucifer Yellow transport. On the day of the experiment, both compartments of each well were washed with HBSS. Cells were then incubated in HBSS with 1 µM BODIPY-glyburide (Thermo-Fisher) in the basolateral compartment. Ko143 (1 µM) was included during the assay as a control for BCRP inhibition. One hundred µL samples were collected from the apical compartments at 30 min intervals and fluorescence was measured using Ex/Em: 428/540 nm. Data were corrected for pmol of glyburide removed at each time point.

TEER was measured in each well immediately prior to and after the experiment to ensure membrane integrity throughout the assay. Permeability coefficients were calculated using P_{app} (cm/s) = (Q / t) / (A*C_0), where Q is the initial nmol of glyburide transported to the receiver compartment at time t (s), A is the cell surface area (cm^2) and C_0 is the initial concentration of glyburide (μM) (Li, et al., 2013a).

^{3}H-Anandamide Transport

AEA transport was assessed in BeWo cells from a modified, previously published protocol (Maccarrone *et al.*, 2003). BeWo cells were added to a 96-well round bottom plate at a density of 100,000 cells/well. Plates were centrifuged (500 x g, 5 min, 5°C) to remove media. Cells were then re-suspended in 100 μL of serum- and phenol red-free treatment medium containing 100 nM ^{3}H-AEA (Movarek Biochemicals, Brea, CA) in the presence or absence of the BCRP-specific inhibitor, Ko143 (1 μM) (Bircsak, et al., 2013), or MM-22, a biotinylated AEA analog that blocks AEA uptake (Fezza *et al.*, 2008). Plates were incubated at 37°C or 4°C (inhibiting active transport) for 30 min. Cells were then centrifuged and washed with ice cold HBSS with 1% bovine serum albumin Cells were then re-suspended in substrate-free medium with or without inhibitors and incubated an additional 15 min at 37°C or 4°C. After the 15 min incubation, cells were centrifuged, washed, lysed using 1M NaOH, neutralized using 1M HCl, and added to 4 mL ScintiSafe Econo 1 liquid scintillation fluid (Fisher Scientific, Waltham,MA). Radioactivity was detected using a TriCarb 2100TR Liquid Scintillation Analyzer (PerkinElmer-Packard, Waltham, MA). Anandamide was quantified using a standard curve and normalized to protein concentrations as determined using the detergent-compatible assay (BioRad).

Immunohistochemistry

Tissue sections (5 µm) were deparaffinized, and blocked with 25% normal goat serum (Invitrogen, Grand Island, NY) and 1% bovine serum albumin at room temperature for 2 h. Sections were then incubated overnight at 4°C with antibodies used to detect CB1 (1:250, Cayman Chemical) and CB2 (1:250, Cayman Chemical). Blocking peptides against CB1 and CB2 (1:25, Cayman Chemical) were incubated with the primary antibody mixture for 1 h at room temperature prior to use. Sections were than washed and incubated at room temperature for 30 min with biotinylated goat anti-rabbit secondary antibody (Vector Labs, Burlingame, CA). Antibody-protein binding was visualized using a DAB Peroxidase Substrate Kit (Vector Labs) and counterstained with hematoxylin. Slides were imaged by light microscopy on an Olympus BX51 microscope (Waltham, MA) fitted with a ProgRes C14+ camera (Jenoptik, Jena, Germany), and images were white-balanced in Adobe Photoshop CS2 (Adobe Systems, San Jose, CA).

Measurement of Intracellular cAMP

BeWo cells grown to 70-80% confluence on 100 mM plates were treated with AEA (10 µM) and/or the adenylyl cyclase activator forskolin (FOR, 50 µM) in treatment media. After 1 h at 37°C, the cells were then washed with HBSS and scraped into 200 µL 0.1M HCl. Extracts were agitated using a vortex mixer for 10 sec and incubated at room temperature for 20 min. cAMP concentrations in the extracts was determined using a cAMP enzyme-linked immunosorbent assay kit (ELISA, Cayman Chemical). Data were normalized to protein concentrations in the HCl extracts as determined using the detergent-compatible assay (BioRad).

Chromatin Immunoprecipitation (ChIP)

ChIP was performed on BeWo cells using the SimpleChIP Enzymatic Chromatin IP Kit (Agarose Beads) (Cell Signaling Technologies). Cells were grown on 150 mm plates to

80% confluence, washed, then incubated in the presence or absence of AEA (10 μM) and forskolin (50 μM) in treatment media for 60 min. Cells were then crosslinked in 1% formaldehyde and ChIP was performed according to the manufacturer's protocol. Immunoprecipitation of crosslinked, digested DNA-protein complexes was performed using a rabbit monoclonal antibody to pCREB (9198, 1:200, Cell Signaling Technologies) or rabbit IgG as a negative control. Purified DNA from ChIP preparations and corresponding 2% input samples was quantified by qPCR using SYBR Green and primers for NR4A3 (4829, Cell Signaling Technologies), a positive control for pCREB ChIP, α-satellite repeats (4486, Cell Signaling Technologies), a negative control for pCREB ChIP, and the *BCRP* cAMP response element (CRE) (Xie *et al.*, 2015). Primer sequences for the *BCRP* CRE can be found in **Supplemental Table 3.1**. Percent input was calculated using PI = 2% x 2^($Ct_{2\%\ input} - Ct_{sample}$).

Statistical Analysis

Data are presented as mean ± SE and analyzed using GraphPad Prism 5.0 software (GraphPad Software Inc., La Jolla, CA). According to the number of comparisons and variables, either one-way analysis of variance with Newman-Keuls post-test or a two-tailed student's t test was used to assess statistical significance ($p < 0.05$). LC_{50} values were generated by plotting log (inhibitor) vs. response using a variable slope (Hill slope = -4.69 to -0.28) and robust fitting method.

3.4 Results

AEA Down-Regulates the Expression of Syncytialization Markers and the BCRP Transporter in Human Placental Explants

To recapitulate human placenta AEA signaling *in situ*, we cultured explants from healthy, term placentas and exposed them to AEA *ex vivo*. Transcripts of syncytins and hCG are well-established markers of trophoblast syncytialization in both placental explants and BeWo cells and as a result were quantified to confirm the repressive effects of AEA on syncytialization (Gupta, et al., 2016). While BCRP protein is expressed primarily in the syncytium (Szilagyi *et al.*, 2017), it is not known whether BCRP is coordinately regulated with markers of syncytialization. Exposure of human placental explants to AEA (1 μM) for 24 h reduced hCGα, syncytin-1, and BCRP mRNA expression by 48%, 25%, and 46%, respectively (**Fig 3.1A**). BCRP mRNA expression was also reduced at other concentrations of AEA (0.1 and 10 μM, 24 h) although not statistically significant (data not shown). By comparison, syncytin-2 mRNA expression was unchanged by AEA treatment (data not shown) and little to no hCGβ transcripts were detected in any of the placentas (Ct > 30 cycles, data not shown). Similar to its mRNA expression, BCRP protein was down-regulated by 30% in placental explants treated with AEA (1 μM) for 24 h (**Fig 3.1B**). Anandamide treatment did not induce any visible changes to the morphology of the explants (data not shown).

Time- and Concentration-Dependent Down-Regulation of Syncytialization Markers and the BCRP Transporter by AEA in Human Trophoblasts

In subsequent studies, immortalized BeWo cells were used to recapitulate first trimester trophoblasts and identify the mechanism by which AEA down-regulates BCRP. Similar to a prior report (Costa, et al., 2015a), we demonstrated that AEA inhibits BeWo syncytialization using time- and concentration-dependent studies. AEA (10 μM)

decreased the mRNA expression of hCGβ and syncytin-2 by 40-50% at 18 and 24 h (**Fig 3.2A**). Both transcripts returned to control levels by 48 h, likely due to the hydrolysis of AEA by FAAH, which has been previously detected in BeWo cells (Habayeb, et al., 2008). Down-regulation of syncytialization markers were also dependent upon the concentration of AEA (24 h). AEA significantly lowered the mRNA expression of hCGβ at 10 nM (71%) and syncytin-2 at 1 μM (40%), with both transcripts similarly repressed at higher concentrations (**Fig 3.2B**). AEA did not alter the expression of syncytin-1 or hCGα mRNAs in BeWo cells (data not shown).

Similar to syncytin-2 and hCGβ, BCRP expression was also down-regulated by AEA. In the presence of AEA (10 μM), there was a maximal reduction of BCRP mRNA at 24 h with a return to control levels by 48 h (**Fig 3.2A**). Evaluation of AEA concentrations between 10 nM and 10 uM revealed that the expression of BCRP mRNA in BeWo cells was decreased 30-50% at all concentrations of AEA tested (**Fig 3.2B**).

AEA Reduces the Protein Expression and Transport Activity of BCRP in Human Trophoblasts

Similar to the regulation of BCRP mRNA, treatment of BeWo cells with AEA (10 μM) for 24 h reduced protein expression by ~30% (**Fig 3.3A**). Using Hoechst 33342 (5 μM) and Ko143 (1 μM), a well-established fluorescent substrate and inhibitor of BCRP, respectively, we quantified the ability of AEA to alter BCRP activity. Vehicle-treated BeWo cells were able to efflux 35% of the Hoechst 33342 dye that was taken up (**Fig. 3.3B**, left). By comparison, exposure to AEA (10 μM) for 24 h decreased BCRP efflux activity to 15% which was similar to the functional inhibitor Ko143 (8%). The cellular retention of zearalenone, a known BCRP substrate and developmental toxicant, was also quantified in BeWo cells treated with AEA (Xiao, et al., 2015; Zhao *et al.*, 2013). In

vehicle-treated cells loaded with zearalenone, BeWo cells were able to efflux 71% of accumulated zearalenone. By comparison, AEA (10 μM, 24h) and Ko143 (1 μM) reduced the efflux of zearalenone to 33% and 49%, respectively.

In order to better understand how anandamide may affect transplacental drug trafficking during pregnancy, we quantified the basolateral-to-apical transport of the BCRP substrate, glyburide (Bircsak, et al., 2016). The appearance of glyburide in the apical compartment increased over time up to 7.9 pmol after 2 h (**Fig 3.3D**). AEA (10 μM, 24h) and Ko143 (1 μM, present during assay) reduced the transepithelial transport of glyburide by 20% and 32%, respectively, after 2 h (**Fig 3.3D**). The apparent permeability (P_{app}) of glyburide in this experiment was $3.3*10^{-3}$ cm/s under control conditions, which was reduced to $2.7*10^{-3}$ cm/s and $2.2*10^{-3}$ cm/s by AEA and Ko143, respectively. Reductions in the basolateral-to-apical transport of glyburide by AEA could potentially increase placental and/or fetal exposures to this chemical.

The ability of BCRP to transport AEA is unknown. Using ^{3}H-AEA (100 nM) and MM-22 (50 μM), a known inhibitor of AEA uptake, the intracellular retention of AEA was reduced 27% (**Fig 3.4A**). By comparison, exposure to the BCRP inhibitor Ko143 (1 μM) had no impact on AEA retention (**Fig 3.4A**). A separate group of cells were incubated at 4°C to inhibit active transport, which resulted in a 44% reduction in the intracellular concentration of AEA (**Fig 3.4A**). Additionally, the presence of AEA (10 μM) did not impact BeWo Hoechst 33342 activity without a 24 h pre-incubation (**Fig 3.4B**).

Down-Regulation of BCRP Expression by AEA Heightens the Sensitivity of Human Trophoblasts to Chemical-Induced Cytotoxicity

We measured BeWo cell viability by Alamar Blue to screen for the ability of AEA to alter placental toxicity by reducing BCRP expression. Twenty four hour pre-incubations were performed in the presence of vehicle or AEA (10 μM) along with the environmental contaminants zearalenone (0.5-500 μM), α-zearalanol (0.5-500 μM), perfluorooctanoic acid (2-2000 μM), and perfluorooctanesulfonic acid (2-2000 μM). It has been shown that these chemicals are potential substrates or inhibitors of BCRP (Dankers, et al., 2013). Mitoxantrone (0.6-600 μM), a commonly used cytotoxic substrate of BCRP, was used a positive control for this experiment, and Ko143 (1 μM) was used as a known pharmacological inhibitor of BCRP for comparison. LC_{50} values for 50% cytotoxicity in BeWo cells are presented in **Table 1**. Neither Ko143 nor AEA alone affected BeWo cell viability (data not shown). The LC_{50} value of mitoxantrone in BeWo cells was 10.7 μM. In the presence of Ko143 and AEA, BeWo cells were more sensitive to mitoxantrone (LC_{50} = 3.1 and 3.2 μM for Ko143 and AEA, respectively). In the absence of AEA, BeWo cells were most sensitive to the cytotoxicity of α-zearalanol and least sensitive to the cytotoxicity of perfluorooctanesulfonic acid. Following exposure to either Ko143 or AEA for 24h, BeWo cells were 2- to 3-fold more sensitive to all tested environmental chemicals. These data suggest that the down-regulation of BCRP by AEA inhibits their efflux and sensitizes placental cells to chemical toxicity.

Down-Regulation of BCRP Expression by AEA in Human Trophoblasts Involves CB2 Receptor Signaling

In order to delineate the mechanism by which AEA reduces BCRP expression, we assessed the role of the CB1 and CB2 cannabinoid receptors. Consistent with previous publications (Habayeb, et al., 2008; Park, et al., 2003; Trabucco, et al., 2009), the staining of CB1 was localized mainly to syncytiotrophoblasts and fetal endothelium in term placentas from healthy pregnancies (**Fig 3.5A**). CB2 showed similar staining, but

was additionally expressed on the surface of fetal erythrocytes (**Fig 3.5A**). Consistent with these findings, CB1 and CB2 proteins were also expressed in the lysates of naïve BeWo cells as determined by Western blot (**Fig 3.5B**).

To test the involvement of CB1 and CB2 receptors in the regulation of BCRP by AEA, pharmacological modulators of each receptor were employed. Notably, the down-regulation of BCRP mRNA by AEA (10 μM, 24 h) in BeWo cells was completely inhibited by AM630 (0.1μM, co-treatment with AEA), a CB2-selective inhibitor, but only partially inhibited by rimonabant (0.1μM, co-treatment with AEA), a CB1 inverse agonist (**Fig 3.5C**).

Regulation of BCRP by AEA is Mediated by cAMP

The signal transduction pathways of CB2 involve a number of well-known intracellular messengers, including cAMP, ERK/JNK, ceramides, PI3K/AKT/mTOR, and β-catenin (Pisanti *et al.*, 2013a). In order to identify the downstream AEA-CB2 signals involved in regulating BCRP, inhibitors of TRPV1 (SB366791, 1 μM), PPARα (GW6471, 5 μM), PPARγ (GW9662, 5 μM), and ERK (PD98059) were tested though none of these chemicals reversed the effects of AEA (data not shown). Capsaicin (1 μM, 24 h), a well-known agonist of TRPV1, also had no effect on BCRP expression in BeWo cells (data not shown). AEA has also been shown to inhibit NF-κB, but SN-50, a peptide inhibitor of NF-κB, did not alter BCRP expression (data not shown).

Interestingly, AEA (10 μM, 1 h) reduced basal intracellular levels of cAMP in BeWo cells from 34.8 to 12.4 pmol/mg protein (**Fig 3.6A**). Forskolin (50 μM, 1 h), an activator of adenylyl cyclase, increased intracellular levels of cAMP to 12,800 pmol/mg protein which was also reduced by AEA to 8,250 pmol/mg protein (**Fig 3.6A**). These data suggested

that cAMP-mediated signaling may be involved in the repression of BCRP by AEA. Interestingly, 8-Br-cAMP (1 mM, 24 h), a stable analog of cAMP, completely attenuated the down-regulation of BCRP expression and efflux activity by AEA (10 μM, 24 h) in BeWo cells (**Fig 3.6B**). In measuring the BCRP-mediated Hoechst 33342 efflux by BeWo cells, control cells transported an average of 33% of the Hoechst 33342 dye that was taken up (**Fig 3.6C**). 8-Br-cAMP itself had no effect on Hoechst 33342 transport, but it completely prevented the ability of AEA (10 μM) to lower Hoechst 33342 efflux from BeWo cells (**Fig 3.6C**). Forskolin (50 μM, 24h) partially inhibited the AEA-mediated reduction of BCRP transcription but had no effect on the AEA-mediated reduction of Hoechst 33342 efflux (data not shown).

Signal transduction by intracellular cAMP involves phosphorylation of CREB (cAMP response element binding protein), which then binds to promoter sequences to increase transcription of target genes (Montminy and Bilezikjian, 1987). CREB phosphorylation in BeWo cells after 1 h treatment with AEA (10 μM), forskolin (50 μM), or both was examined by Western blot. As determined by densitometry, control cells had varying levels of p-CREB relative to total CREB protein, but no pCREB was detected in cells treated with AEA (10 μM, 1 h) (**Fig 3.7A**). Exposure to forskolin (50 μM, 1 h) consistently increased CREB phosphorylation (73% increase in pCREB/CREB ratio relative to control), which was again abolished when cells were co-treated with AEA (**Fig 3.7A**). ChIP was used to assess p-CREB binding to the *BCRP* promoter region (base pairs –504 to –403) (Xie, et al., 2015). P-CREB precipitated samples yielded a significantly higher signal compared to an IgG control for the BCRP cAMP response element and NR4A3, a positive control for p-CREB ChIP, but not α-satellites, a negative control for p-CREB ChIP (**Fig 3.7B**). Importantly, treatment of trophoblasts with AEA (10 μM, 1 h) decreased p-CREB binding to the *BCRP* promoter by 68% (**Fig 3.7C**). Co-treatment of

cells with AEA and forskolin (50 μM, 1 h) partially reversed the effects of AEA and resulted in only a 12% reduction in p-CREB binding.

3.5 Discussion

Because of its enrichment on the apical surface of syncytiotrophoblasts and its ability to efflux a wide range of xenobiotics, BCRP protects the fetus from chemical toxicities during development. Recognizing this critical role in the placental barrier, it is necessary to elucidate the biochemical pathways that regulate BCRP expression and activity under healthy and pathological conditions. While it has been shown that phytocannabinoids such as cannabidiol and Δ9-tetrahydrocannabinol, both found in *Cannabis sativa*, can decrease BCRP expression and activity, there is no research demonstrating this same relationship with endogenous cannabinoids (Feinshtein *et al.*, 2013b; Holland *et al.*, 2007; Spiro *et al.*, 2012). Our studies demonstrate for the first time that AEA down-regulates BCRP mRNA and protein expression in both human BeWo trophoblast cells and human term placental explants. This repression was observed at concentrations as low as 10 nM AEA in BeWo cells. Notably, AEA is an agonist for both the CB1 and CB2 receptors, and previous studies have demonstrated a potential role for both isoforms in regulating trophoblast differentiation (Costa, et al., 2015a; Habayeb, et al., 2008; Sun, et al., 2010). In a primary culture of human trophoblasts, AEA was found to decrease alkaline phosphatase (ALP) activity and hCG release through both receptors (Costa, et al., 2015a). Importantly, however, the AEA-mediated reduction of cAMP was found to be CB2-mediated (Costa, et al., 2015a). Using CB1 and CB2 signaling modulators, we have similarly shown that only inhibition of CB2 fully reversed the AEA-induced down-regulation of BCRP (Barth and Rinaldi-Carmona, 1999; Ross *et al.*, 1999). Recently the *BCRP* promoter was shown to possess a functional cAMP response element (BP –504 to –403), which taken together may explain the selectivity of this mechanism toward CB2 in comparison to CB1 (Xie, et al., 2015). We have also demonstrated that AEA decreases intracellular cAMP concentrations in BeWo cells and that 8-Br-cAMP can reverse the repressive effects of AEA on BCRP expression and activity. Further, we

have shown that AEA inhibits both CREB phosphorylation and reduces p-CREB promoter binding and the subsequent transcription of BCRP. Collectively, these data point to AEA's ability to repress BCRP expression in the placenta via CB2-mediated inhibition of cAMP-pCREB signaling.

The effects of AEA treatment on trophoblast syncytialization in placental explants and BeWo trophoblast cells largely mirrored observations from prior studies where AEA reduced syncytialization as indicated by a reduction hCG secretion and intracellular cAMP (Costa, et al., 2015a; Gupta, et al., 2016; Wang, et al., 1999). However, in the current study, the specific genes that were sensitive to AEA treatment varied between explants (hCGa, syncytin-1) and BeWo cells (hCGB, syncytin-2). This inconsistency may be due to the fact that BeWo cells reflect the signaling of first trimester trophoblasts (Pattillo, et al., 1968), whereas explants were isolated from term placentas, which express little or no hCGβ (Lin *et al.*, 1995). Conversely, the discrepancy in target syncytialization genes may also be due to the influence of other cell types (i.e. Hofbauer and endothelial cells) in explants that are not present in BeWo cell cultures.

There is increasing attention placed on identifying environmental and dietary chemicals whose transplacental transfer as well as placental toxicity may be reduced by BCRP efflux from syncytiotrophoblasts. We have demonstrated indirectly that a cell viability assay can be used to screen environmental contaminants as potential substrates. While this experiment is useful, the concentrations required for cytotoxicity *in vitro* far exceed those expected in human exposures. Nonetheless, this approach allows us to identify potentially novel BCRP substrates (i.e., zeranol and perfluorooctanesulfonic acid) using Ko143 as well as point to the ability of AEA to sensitize trophoblasts to the toxicities of chemicals by repressing BCRP expression. We further confirmed the ability of AEA to

lower the functionally activity of BCRP in BeWo cells using cell accumulation and Transwell assays. Notably, AEA increased the cellular retention of BCRP substrates Hoechst 33342 and zearalenone and decreased the basolateral-to-apical transport of glyburide. We have also demonstrated that AEA retention in BeWo cells was not altered by Ko143, indicating that AEA is not a substrate of BCRP. Therefore, we can conclude that AEA reduces BCRP activity by inhibiting its transcription rather than through competitive or functional inhibition.

There is substantial, albeit varying, evidence that dysregulation of the endocannabinoid system may be a driving factor behind diseases of pregnancy (reviewed in Costa, 2016a). AEA regulates trophoblast differentiation, apoptosis and invasion, and disruption of these tightly coordinated processes is generally associated with placental disorders leading to poor neonatal outcomes (Costa, et al., 2015a; Costa, et al., 2015b; Gupta, et al., 2016; Roland *et al.*, 2016; Sitras *et al.*, 2009; Sun, et al., 2010; Zhang *et al.*, 2016). In one study, preeclamptic placentas showed higher expression of n-arachidonyl phosphatidyl ethanolamine phospholipase D an enzyme essential for AEA synthesis, and lower FAAH expression but no changes in CB1 or CB2 (Aban, et al., 2013). Another study published that CB1 expression was higher in placentas from pregnancies complicated by preeclampsia compared to controls, with no change in CB2 receptor levels (Fugedi, et al., 2014). Contradictory to these data is one study that demonstrated circulating levels of AEA are lower in preeclampsia (Molvarec *et al.*, 2015). Blood AEA concentration, however, is not necessarily an indicator of local AEA concentration or AEA signaling within the placenta and may be under the control of feedback mechanisms. Regardless, the endocannabinoid system is also an emerging regulator of the hypoxic response, which is a known factor in preeclampsia due to restrictive blood flow in the placenta (Aban, et al., 2016). Hypoxia inducible factor-1α (HIF1α), for

instance, regulates FAAH expression (Aban, et al., 2016). Further, cobalt chloride-induced apoptosis in placental explants, an *ex vivo* model of hypoxia, was abrogated by inhibition of CB1 receptor signaling using AM251 (Aban, et al., 2016). Hypoxia also down-regulates BCRP expression in BeWo cells by a HIF-1α related mechanism, and it has been shown that BCRP levels are reduced in the placentas of preeclamptic patients (Francois, et al., 2017; Gormley, et al., 2017; Jebbink, et al., 2015a; Nishizawa, et al., 2011). We therefore propose that hypoxic conditions in the placenta during preeclampsia may be responsible for the reduction in BCRP expression, and this mechanism could result from aberrant endocannabinoid signaling. Ectopic pregnancies and spontaneous miscarriage have also been linked to aberrant endocannabinoid signaling, but no studies have yet been performed to assess placental BCRP expression in these gestational disorders (Gebeh, et al., 2013; Gebeh *et al.*, 2012; Trabucco, et al., 2009).

Placentas from pregnancies complicated by intrauterine growth restriction (IUGR) exhibit decreased BCRP mRNA expression (Evseenko, et al., 2007a; Ruebner *et al.*, 2012). While a specific role for AEA has not been identified, it is now commonly recognized that IUGR is a complication of cannabis exposure during pregnancy (Davitian *et al.*, 2006; El Marroun *et al.*, 2009; Warner *et al.*, 2014). Unfortunately, cannabis has been misleadingly suggested as a safe remedy for nausea and emesis during pregnancy and 34-60% of cannabis users continue use during pregnancy (Jaques *et al.*, 2014; Moore *et al.*, 2010; Passey *et al.*, 2014; Schempf and Strobino, 2008). Chronic cannabis exposure has also been shown to affect endocannabinoid signaling up to 6 months after complete cessation, highlighting the importance of understanding how the endocannabinoid system regulates placentation and the placental barrier (Muhl *et al.*, 2014).

Endocannabinoids can dysregulate placentation and in turn, neonatal outcomes. Taken together, our data suggest that the expression and activity of BCRP may also be regulated by endocannabinoid signaling. This novel observation may point to a potential explanation for the altered placental expression of BCRP previously observed in gestational diseases. With reduced BCRP expression, there is potential for altered xenobiotic disposition in the placenta, higher fetal xenobiotic exposures, and increased risk of adverse outcomes in newborns.

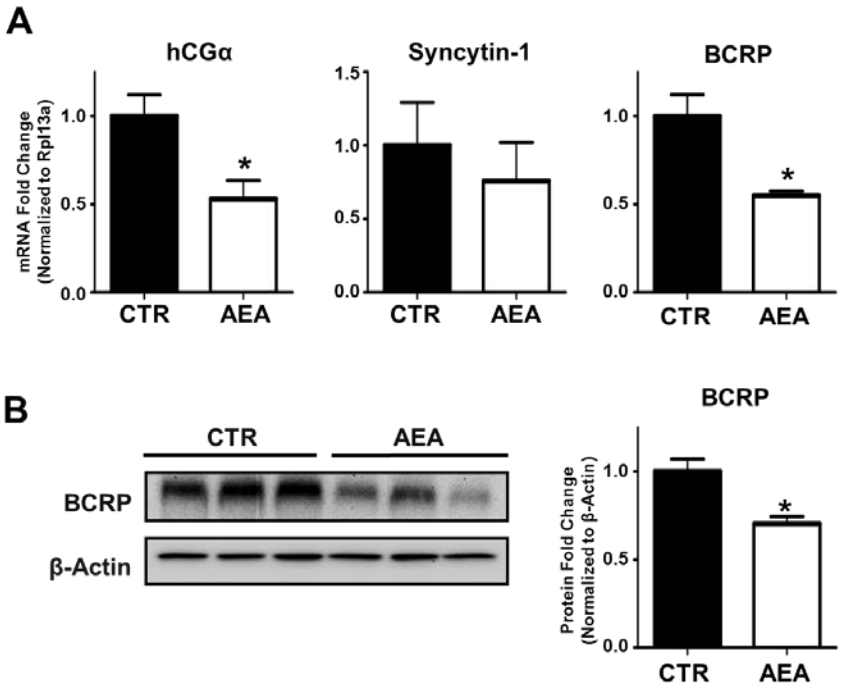

Fig 3.1. Expression of syncytialization-related genes and the BCRP transporter in human placental explants treated with anandamide.

A. mRNA expression of BCRP and syncytialization-related genes. qPCR was performed on total RNAs extracted from term placental explants treated with AEA (1 μM) for 24 h as described in the Materials and Methods. Data represent the mean of 3 placentas (3-6 samples from each placenta) ± SE. **B.** *Left*. Protein expression of BCRP in AEA-treated explants. Protein homogenates were prepared from control and AEA (1 μM, 24 h) treated term placental explants and analyzed for expression of BCRP (72 kDa) by Western blotting. β-actin (42 kDa) was used as a loading control. *Right.* Densitometry analysis of BCRP Western blots from control and AEA (10 μM, 24 h) treated explants. Data represent the mean of 3 placentas (3-5 samples from each placenta) ± SE and were analyzed using a Student's t-test (*$p < 0.05$ compared to control).

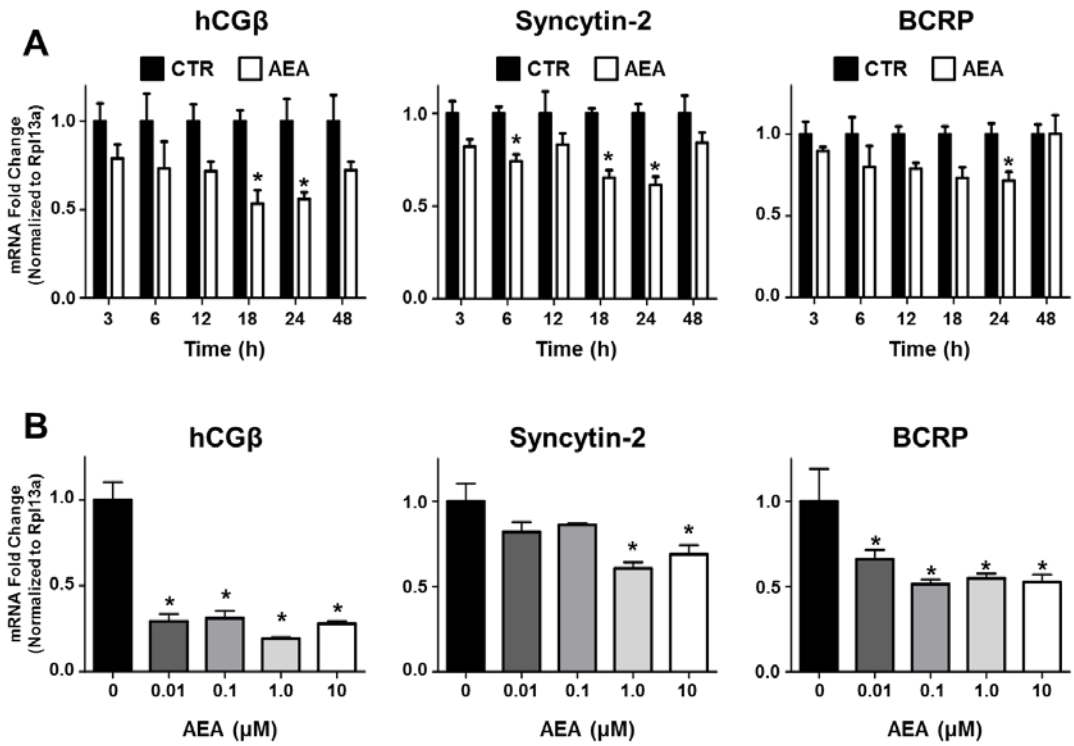

Fig 3.2. Expression of syncytialization-related genes and the BCRP transporter in human BeWo trophoblast cells treated with anandamide.

A. Time-dependent mRNA expression of syncytialization markers and BCRP. qPCR was performed as described in the Materials and Methods in BeWo cells treated with AEA (10 μM) at various time points. Black bars represent vehicle-treated cells and white bars represent AEA-treated cells. Data are presented as mean ± SE (n = 4) and were analyzed using a Student's t-test (*$p < 0.05$ compared to control). **B.** Concentration-dependent mRNA expression of syncytialization–related genes and BCRP. qPCR was performed in BeWo cells treated with AEA (0.01-10 μM) for 24 h. Data are presented as mean ± SE (n = 4) and were analyzed using a one-way ANOVA followed by post-hoc Newman-Keuls analysis (*$p < 0.05$ compared to control).

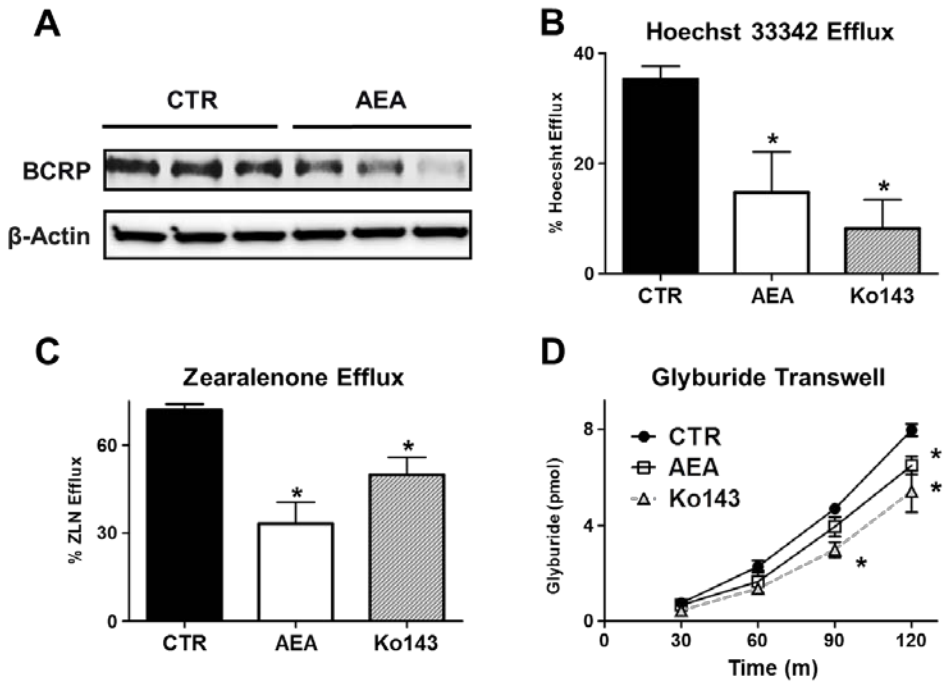

Fig 3.3. BCRP protein expression and efflux activity in human BeWo trophoblast cells treated with anandamide.

A. Protein expression of BCRP in AEA-treated cells. Lysates were prepared from control and AEA (10 μM, 24 h) treated BeWo cells and analyzed for expression of BCRP protein (72 kDa) by Western blotting. β-actin (42 kDa) was used as a loading control. B and C. Inhibition of BCRP Hoechst 33342 and zearalenone efflux activity by AEA. Control and AEA (10 μM, 24 h) treated BeWo cells were trypsinized and subjected to either the Hoechst 33342 (5 μM, **B**) or zearalenone (50 μM, **C**) cell accumulation assay as described in the Materials and Methods. Data are presented as mean ± SE (n = 3-5). **D.** Inhibition of BODIPY-glyburide transport across BeWo monolayers. Control and AEA (10 μM, 24 h) treated BeWo cells in transwell inserts were assessed for basolateral-to-apical translocation of BODIPY-glyburide (1 μM) over 2 h as described in the Materials and Methods. One group of cells in each experiment were incubated in the presence Ko143 (1 μM) during the assay to provide a positive control for BCRP inhibition. Data represent

the mean ± SE (n = 3 independent experiments) and were analyzed using a Student's t-test (*$p < 0.05$ compared to control).

Table 3.1. Effect of AEA on cell viability in the presence of BCRP substrates and environmental contaminants.

	LC_{50} values (μM)		
	Control	*Ko143*[a]	*AEA*
MTX[b]	10.7 ± 1.1	3.1 ± 1.8*	3.2 ± 1.3*
ZLN	182.9 ± 3.7	84.8 ± 19.3*	73.9 ± 33.3*
α-ZRN	77.4 ± 6.4	36.0 ± 10.1*	27.4 ± 9.1*
PFOA	672.9 ± 58.2	450.0 ± 163.9	326.3 ± 47.3*
PFOS	724.7 ± 56.8	438.3 ± 87.7*	277.5 ± 74.6*

LC_{50} values are presented as the mean of three experiments +/- SEM.

**Statistically significant differences ($p < 0.05$) compared to control cells as determined by* Student's t-test.

[a]BeWo cells were incubated in the presence of Ko143 (1 μM), AEA (10 μM), or vehicle (rows) and various concentrations of known or potential BCRP substrates (columns)

[b]Abbreviations: MTX, mitoxantrone; ZLN, zearalenone; α-ZRN, α-zearalanol; PFOA, perfluorooctanoic acid; PFOS, perfluorooctanesulfonic acid

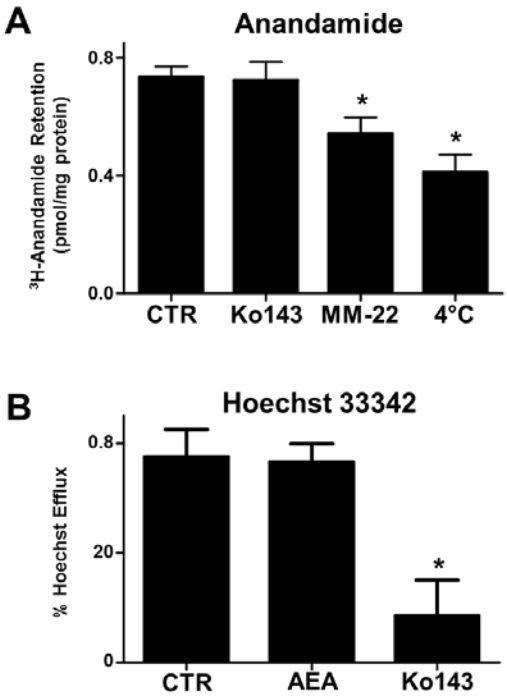

Fig 3.4. AEA is not a substrate or direct inhibitor of BCRP.

A. ^{3}H-Anandamide accumulation in human BeWo trophoblast cells. Untreated BeWo cells were trypsinized and subjected to the ^{3}H-Anandamide (100 nM) transport assay as described in Materials and Methods. During the uptake and efflux phase, cells were incubated in the presence of Ko143 (1 μM), MM-22 (25 μM), or DMSO. One set of cells was incubated at 4°C for the duration of the assay. Data are presented as mean ± SE (n = 6). **B.** Competitive inhibition of Hoechst 33342 efflux in BeWo cells. Untreated BeWo cells were trypsinized and subjected to either the Hoechst 33342 (5 μM) cell accumulation assay as described in the Materials and Methods in the presence of vehicle, AEA (10 μM), or Ko143 (1 μM). Data are presented as mean ± SE (n = 3) and were analyzed using a Student's t-test (*$p < 0.05$ compared to control).

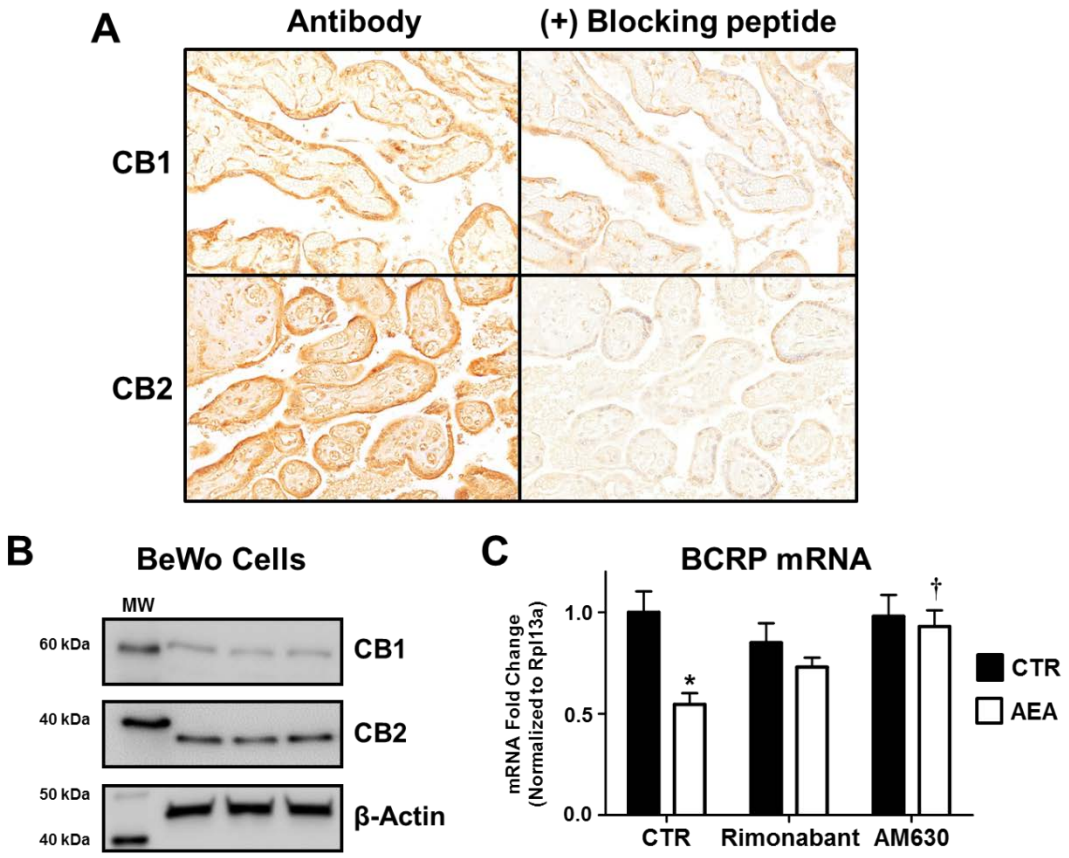

Fig 3.5. Expression and function of cannabinoid receptors in human term placentas and human BeWo trophoblast cells.

A. Immunohistochemical staining of the CB1 and CB2 receptors in term human placentas. Sections of paraffin-embedded healthy term placentas (5 µm) were prepared and stained with antibodies against CB1 and CB2 as well as respective blocking peptides and visualized using a Vectastain DAB kit *(brown staining)* as described in the Materials and Methods. Magnification 20x. **B.** Protein expression of the CB1 and CB2 receptors in BeWo cells. Lysates were prepared from naïve BeWo cells and analyzed for expression of CB1 (60 kDa) and CB2 (38 kDa) by Western blotting. β-actin (42 kDa) was used as a loading control. **C.** CB-receptor dependence of AEA down-regulation of BCRP. qPCR was performed on cells treated with vehicle control (CTR), rimonabant (0.1

μM), or AM630 (0.1 μM) with or without AEA (10 μM) for 24 h. Black bars represent vehicle-treated cells and white bars represent AEA-treated cells. Data are presented as mean ± SE (n = 4) and were analyzed using a one-way ANOVA followed by Newman-Keuls post-hoc analysis (*$p < 0.05$ compared to control, †$p < 0.05$ compared to AEA-treated cells).

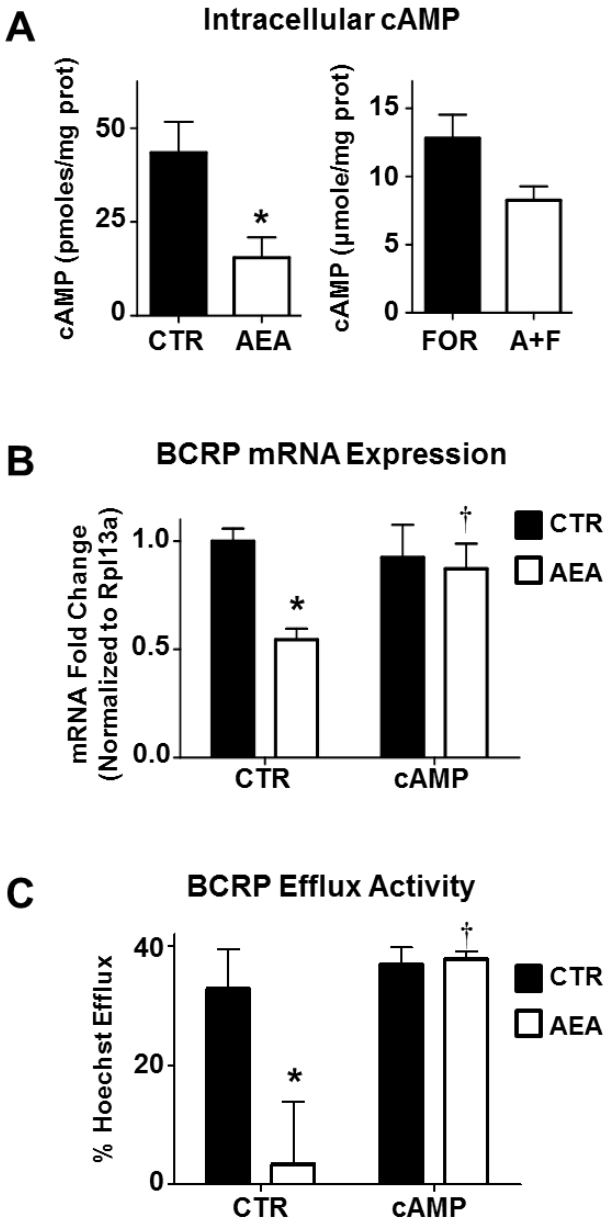

Fig 3.6. cAMP regulation of BCRP expression and activity in human BeWo trophoblast cells treated with anandamide.

A. Effects of AEA on intracellular cAMP levels. BeWo cells were treated (± 10 µM AEA; ± 50 µM forskolin, FOR) for 1 h and collected in 0.1 M HCl. Intracellular concentrations of cAMP were determined by ELISA and normalized to protein concentration. Data are presented as mean ± SE (n = 4) and were analyzed using a Student's t-test (*$p < 0.05$

compared to control). **B.** 8-Br-cAMP abrogates AEA effects on BCRP mRNA. qPCR was performed on BeWo cells treated with AEA (10 μM), 8-Br-cAMP (1 mM), or both for 24 h. Black and white bars represented samples treated in the absence or presence of AEA, respectively. Data are presented as mean ± SE (n = 4) and were analyzed using a one-way ANOVA followed by Newman-Keuls post-hoc analysis (*$p < 0.05$ compared to control, †$p < 0.05$ compared to AEA-treated cells). **C.** Inhibition of BCRP efflux activity by AEA is cAMP-dependent. BeWo cells were treated with either AEA (10 μM), 8-Br-cAMP (1 mM), or both for 24 h. Cells were then trypsinized and subjected to the Hoechst 33342 transport assay as described in Materials and Methods. Data represent the mean ± SE (n = 3-5) and were analyzed using a one-way ANOVA followed by Newman-Keuls post-hoc analysis (*$p < 0.05$ compared to control, †$p < 0.05$ compared to AEA-treated cells).

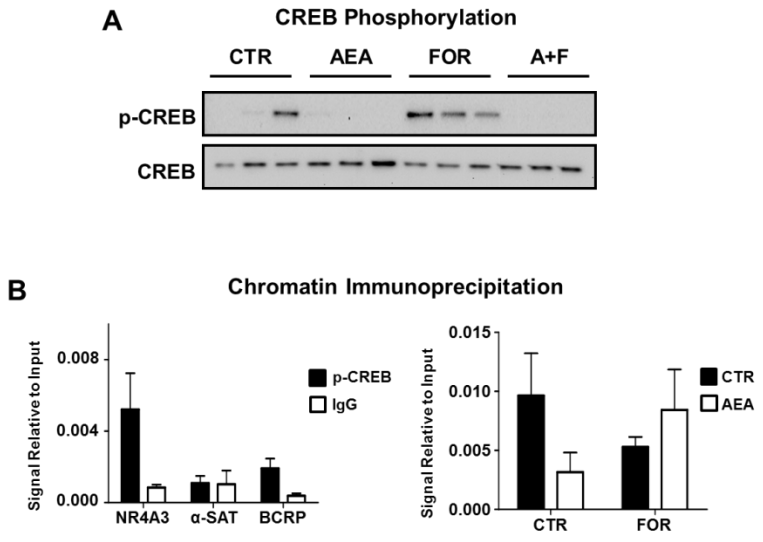

Fig. 3.7. AEA inhibits p-CREB signaling and BCRP promoter binding in BeWo cells.

A. Western blot of pCREB signaling in AEA- and FOR-treated cells. Lysates were prepared from BeWo cells treated for 1 h with AEA (10 μM), FOR (50 μM), or both, and analyzed for pCREB and CREB (37 kDa) by Western blot. B. Validation of chromatin immunoprecipitation. ChIP was performed on untreated cells using a p-CREB antibody (black bars) or an IgG control (white bars), and samples were analyzed by qPCR for NR4A3, a positive control for pCREB ChIP, α-satellites, a negative control, and the unique BCRP cAMP response element sequence. Data are presented as mean ± SE (n = 3-4) and were analyzed using a Student's t-test (*$p < 0.05$ compared to p-CREB). C. ChIP analysis of p-CREB binding to the *BCRP* promoter region. BeWo cells treated for 1 h with AEA (10 μM), FOR (50 μM), or both. ChIP was performed using a p-CREB antibody and samples were analyzed by qPCR for the unique BCRP cAMP response element sequence. Data are presented as mean ± SE (n = 3-5). Ct values for each sample were compared against respective 2% input controls.

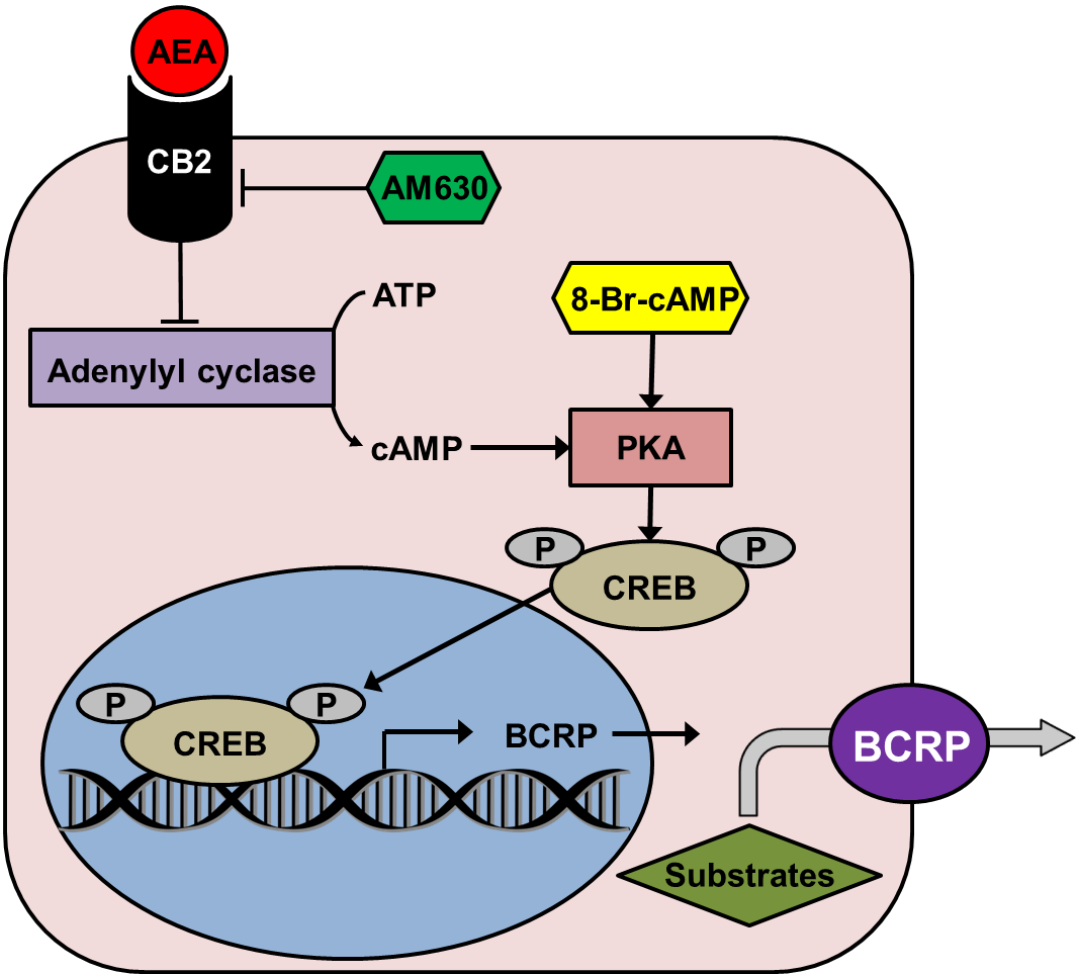

Fig. 3.8. Proposed mechanism of AEA-mediated down-regulation of BCRP and syncytialization-related genes.

AEA binds to and activates the CB2 receptor, which in turn inhibits adenylyl cyclase. The corresponding decrease in cAMP production reduces basal protein kinase A (PKA) activation and, therefore, CREB phosphorylation. The DNA sequence for *BCRP*, along with genes involved in trophoblast syncytialization, contain a cAMP response element (BP –504 to –403) to which p-CREB would normally bind. Decreased p-CREB signaling would therefore reduce BCRP transcription and efflux activity.

Supplemental Table 3.1. Primer Sequences for qPCR (5' → 3')

Human Gene	Forward Primer	Reverse Primer
BCRP	ATCAGCTGGTTATCACTGTGAGGCC	AGTGGCTTATCCTGCTTGGAAGGC
hCGα	CAGAATGCACGCTACAGGAA	CGTGTGGTTCTCCACTTTGA
hCGβ	GCACCAAGGATGGAGATGTT	GCACATTGACAGCTGAGAGC
Syncytin-1	CCCCATCGTATAGGAGTCTT	CCCCATCAGACATACCAGTT
Syncytin-2	GCCTGCAAATAGTCTTCTTT	ATAGGGGCTATTCCCATTAG
BCRP CRE	CCCTTTCCTTCCTTGGGTTA	AAATGGGTGGTTTCTGGTGA

CHAPTER 4: LOCALIZATION OF THE PLACENTAL BCRP/*ABCG2* TRANSPORTER TO LIPID RAFTS: ROLE FOR CHOLESTEROL IN MEDIATING EFFLUX ACTIVITY

John T. Szilagyi[a], Anna M. Vetrano[b], Jeffrey D. Laskin[a], Lauren M. Aleksunes[c]

Affiliations

[a]Department of Environmental and Occupational Health, Rutgers University School of Public Health, 170 Frelinghuysen Rd, Piscataway, NJ 08854, USA

[b]Department of Pediatrics, Rutgers University Robert Wood Johnson Medical School, 1 Robert Wood Johnson Place, New Brunswick, NJ 08901, USA

[c]Department of Pharmacology and Toxicology, Rutgers University, 170 Frelinghuysen Rd, Piscataway, NJ 08854, USA

1.1 Abstract

Introduction: The breast cancer resistance protein (BCRP/*ABCG2*) is an efflux transporter in the placental barrier. By transporting chemicals from the fetal to the maternal circulation, BCRP limits fetal exposure to a range of drugs, toxicants, and endobiotics such as bile acids and hormones. The purpose of the present studies was to 1) determine whether BCRP localizes to highly-ordered, cholesterol-rich lipid raft microdomains in placenta microvillous membranes, and 2) determine the impact of cholesterol on BCRP-mediated transport *in vitro*.

Methods: BCRP expression was analyzed in lipid rafts isolated from placentas from healthy, term pregnancies and BeWo trophoblasts by density gradient ultracentrifugation. BeWo cells were also tested for their ability to efflux BCRP substrates after treatment with the cholesterol sequestrant methyl-β-cyclodextrin (MβCD, 5mM, 1 h) or the cholesterol synthesis inhibitor pravastatin (200μM, 48 h)**.**

Results and Discussion: BCRP was found to co-localize with lipid raft proteins in detergent-resistant, lipid raft-containing fractions from placental microvillous membranes and BeWo cells. Treatment of BeWo cells with MβCD redistributed BCRP protein into higher density non-lipid raft fractions. Repletion of the cells with cholesterol restored BCRP localization to lipid raft-containing fractions. Treatment of BeWo cells with MβCD or pravastatin increased cellular retention of two BCRP substrates, the fluorescent dye Hoechst 33342 and the mycotoxin zearalenone. Repletion with cholesterol restored BCRP transporter activity. Taken together, these data demonstrate that cholesterol may play a critical role in the post-translational regulation of BCRP in placental lipid rafts.

Abbreviations

BCRP, breast cancer resistance protein; ABC, ATP binding casette; MβCD, methyl-β-cyclodextrin; PRAV, pravastatin; MVM, microvillous membrane; GAPDH, glyceraldehyde 3-phosphate dehydrogenase; PLAP, placental alkaline phosphatase; TFR, transferrin receptor.

1.2 Introduction

The breast cancer resistance protein (BCRP/*ABCG2*) is highly expressed on the apical membrane of placental syncytiotrophoblasts, serving a fetoprotective function at the interface of the maternal and fetal circulations (Hahnova-Cygalova, et al., 2011; Maliepaard *et al.*, 2001). BCRP transports substrates away from the placenta and prevents the accumulation of potentially harmful xenobiotics in the fetus (Jani, et al., 2014). Substrates include commonly prescribed drugs such as the hypoglycemic agent glyburide, the chemotherapeutic drug doxorubicin and the antibiotic nitrofurantoin (Bircsak, et al., 2016; Doyle, et al., 1998a; Kruijtzer *et al.*, 2002; Zhang, et al., 2007b). BCRP also transports estrogenic dietary chemicals that affect sexual differentiation of the fetus including the fungal toxin zearalenone (Bircsak and Aleksunes, 2015; Hilakivi-Clarke, et al., 1998; Jefferson and Williams, 2011; Xiao, et al., 2015). Additionally, BCRP critically prevents cytokine-induced apoptosis and facilitates syncytial formation in placental cells (Evseenko, et al., 2007a; Evseenko *et al.*, 2007b).

Few studies have offered insight into the post-translational regulation of BCRP by cholesterol and its organization in the plasma membrane. Cholesterol in the plasma membrane aggregates in structures called lipid rafts, which are ordered microdomains rich in sphingolipids and proteins (Simons and Sampaio, 2011). Lipid raft order creates a phase-separation between its contents and the disordered phospholipid bilayer (Lucero and Robbins, 2004; Simons and Sampaio, 2011). Lipid rafts are critical in a number of membrane processes including signal transduction, biochemical synthesis and transport (Simons and Toomre, 2000).

There is some evidence linking lipid raft integrity and membrane cholesterol content to BCRP function. In cells transfected to overexpress BCRP, the BCRP protein localizes in

lipid raft fractions after density gradient ultracentrifugation (Storch, et al., 2007). Proteomic analysis of lipid rafts in primary human T cells and mouse spermatozoa also point to the detergent resistance of the BCRP protein (Lin, et al., 2010; Nixon, et al., 2009). Further, BCRP efflux activity is dependent on lipid raft integrity and cholesterol content in canine kidney cells and membrane vesicles overexpressing BCRP (Hegedus *et al.*, 2015; Storch, et al., 2007; Telbisz, et al., 2007). It is known that cholesterol is critical for fetal development; mothers with chronically low cholesterol are at higher risk for premature delivery and low birth weight babies (Bream *et al.*, 2013; Mudd *et al.*, 2012). However, it is possible that cholesterol also plays a critical role in regulating placental BCRP and therefore influence drug transfer from the maternal to the fetal circulation.

To date, the majority of studies of the BCRP transporter have investigated the localization of the protein in lipid rafts and the ability of cholesterol to regulate its activity using overexpressing cell-based systems, with little attention paid to native human tissues. Therefore, we hypothesized that BCRP localizes to lipid rafts in microvillus membranes from healthy term placentas and cultured placental cells. Further, we expected that disruption of cholesterol content in placental cells would alter BCRP function and enrichment in lipid rafts, which could potentially enhance drug transfer across the placental barrier

1.3 Materials and Methods

Chemicals

Unless stated otherwise, all chemicals were from Sigma-Aldrich (St. Louis, MO).

Cell Culture

BeWo human choriocarcinoma cells (American Type Culture Collection, Manassas, VA) were maintained in an incubator at 37°C with 5% CO_2 in air in a DMEM and F12 1:1 mixture (Life Technologies, Carlsbad, CA), supplemented with 10% fetal bovine serum (Atlantic Biologicals, Miami, FL) and 1% penicillin-streptomycin (Life Technologies). This cell line recapitulates first trimester trophoblasts by secreting placental hormones and expressing transporters such as BCRP (Pattillo and Gey, 1968). For all experiments, cells were grown to 70-80% confluence before use. For cholesterol modulation studies, cells were cultured in the presence or absence of pravastatin (PRAV, 10-200 μM) for 48 h or methyl-β-cyclodextrin (MβCD, 5 mM) for 1 h and then HBSS in the absence and presence of cholesterol-MβCD (Sigma C4951) for 30 min (Simons and Toomre, 2000). Time points and doses used were based on previous literature and preliminary studies indicating a reduction in cholesterol but no effect on cell viability (**Supplemental Fig 4.1**) (Simons and Toomre, 2000). Cells were lysed in buffer containing 20 mM Tris-HCl, 150 mM NaCl, 5 mM ethylenediaminetetraacetic acid, 1% Triton X-100 and a protease inhibitor cocktail (Sigma P8340).

Patient Selection and Sample Collection

Placentas (n = 3) were obtained with written informed consent from healthy women meeting all criteria following term delivery by scheduled Cesarean section. Inclusion criteria included healthy women between the ages of 18–40 years, term gestation (≥ 36 weeks), and scheduled Cesarean section without labor. Exclusion criteria included

chronic medical conditions, pregnancy-induced medical conditions, maternal infection, clinical chorioamnionitis, medication use (with the exception of prenatal vitamins), maternal smoking, alcohol or drug abuse, multiple pregnancies, and known fetal chromosomal abnormalities (Memon *et al.*, 2014). The study was approved by the Institutional Review Boards of Robert Wood Johnson Medical School (Protocol #0220100258) and Rutgers University (Protocol #E12-024).

Upon collection, placenta samples for lipid raft analysis were snap frozen and stored at -80°C until use. Samples for immunohistochemistry were stored in PAXgene Tissue Containers containing PAXgene tissue stabilizer (Qiagen, Germantown, MD).

Assays for Cholesterol, Protein and Cell Viability and Growth Inhibition

All colorimetric and fluorescent assays were performed using a SpectraMax M3 Multimode Microplate Reader and analyzed with SpectraMax SoftMax Pro 6.3 software (Molecular Devices, Sunnyvale, CA). For analysis of cholesterol in cell lysates and lipid raft fractions, an Amplex Red based detection kit was used according the instructions provided by Sigma-Aldrich. Samples were compared to a standard curve generated from human low density lipoprotein prepared in either cell lysis buffer (20 mM tris-HCl, 150 mM NaCl, 5 mM EDTA, pH = 7.4) or lipid raft extraction buffer (see below). Protein content of cell lysates and lipid raft fractions was quantified using a Detergent Compatible analysis kit (BioRad, Hercules, CA) based on the Lowry method (Lowry *et al.*, 1951).

Viability was measured as a function of the ability of the cells to convert resazurin to fluorescent resorufin as previously described (Fields and Lancaster, 1993). To assess growth, cell number quantified using a Beckman Coulter Z1 Particle Counter

(Indianapolis, IN). At all concentrations used, pravastatin had no effect on either cell growth or viability (**Supplemental Fig. 4.1**).

Subcellular Fractionation

Ultracentrifugation and density gradient methods were employed to obtain total cell membranes from BeWo cells, brush border membranes from human term placenta, and lipid rafts using a Beckman L7-55 ultra-centrifuge (Beckman Coulter, Brea, CA) (Bayyareddy *et al.*, 2012; Jimenez *et al.*, 2004; Smart *et al.*, 1995).

Membrane Isolation from BeWo Cells

Plasma membranes were collected from BeWo cells using a Percoll-based ultra-centrifugation method as previously described (Smart, et al., 1995). All ultra-centrifugation steps for membrane isolation were performed using a Type 40.1 Ti rotor (Beckman Coulter, Indianapolis, IN).

Placental Brush Border Membrane Extraction

Crude brush border MVM extracts were prepared from human term placentas using an $MgCl_2$-based centrifugation method as previously described (Jimenez, et al., 2004). Pure MVM were prepared by subjecting the crude MVM to the protocol a second time. All ultra-centrifugation steps for brush border membrane extractions were performed using a Type 60 Ti rotor (Beckman Coulter). Whole homogenates, nuclear fractions, and crude and pure MVM were analyzed for markers of apical and endothelial membranes, cytoplasm, nuclei and mitochondria using techniques in Western blotting.

Lipid Raft Extraction

Lipid raft fractions were prepared using a method adapted from a prior report (Bayyareddy, et al., 2012). Brush border membrane extracts and BeWo plasma membranes were incubated in TNE buffer (25 mM Tris HCl, 150 mM NaCl, 5 mM EDTA), supplemented with 1% Lubrol or 1% Triton X-100, respectively, on ice for 1 h. The mixtures were then mixed with OptiPrep (60% iodixanol) to a final concentration of 40% iodixanol in a final volume of 3 mL. This was added to the bottom of an open-top ultra-centrifuge tube and overlayed with 6 mL of 30% iodixanol and then 2 mL of 5% iodixanol. Samples were centrifuged at 260,000 g for 4 h at 4°C using an SW41 swinging bucket rotor (Beckman Coulter). Detergent-resistant lipid rafts migrated up the tube and concentrated at the 30-5% interface. Ten 1.4 mL fractions were collected from each tube with a pipette, starting from the least dense fractions at the top of the tube.

Western Blotting

Unless otherwise stated, all Western blotting was performed using equipment from BioRad as previously described (Zheng *et al.*, 2013a). Primary antibodies were used to detect BCRP (BXP-53, 1:5000; Enzo Life Sciences, Farmingdale, NY), β-actin (ab8227, 1:2000, Abcam, Cambridge, MA), transferrin receptor 1 (TFR-1, ab108985, 1:5000 Abcam), placental alkaline phosphatase (PLAP, ab133602, 1:10,000, Abcam), multidrug resistance-associated protein 1 (MRP1, ab3368, 1:2000, Abcam), cluster of differentiation 34 (CD34, ab81289 1:10,000, Abcam), histone H2A (25785, 1:1000, Cell Signaling, Danvers, MA), and glyceraldehyde 3-phosphate dehydrogenase (GAPDH, G8795, 1:1000, Sigma-Aldrich). HRP-linked secondary antibodies (anti-rabbit, anti-rat or anti-mouse, 1:2000 Sigma-Aldrich) were used to detect primary antibodies. After the addition of a Luminata Forte Western HRP substrate (Millipore, Billerica, MA), chemiluminescent protein-antibody complexes were visualized using a Fluorchem

Imager (ProteinSimple, Santa Clara, CA). Semi-quantitative analysis of bands of the blots was performed using AlphaView Software (ProteinSimple).

Flow Cytometry

Phycoerthyrin-labeled anti-BCRP antibody (5D3) (R&D Systems, Minneapolis, MN) was used to detect BCRP expression in BeWo cells according to the manufacturer's protocol. Phycoerthyrin-labeled IgG antibody was used as a negative control. Cells were washed three times and then resuspended in 2% paraformaldehyde/PBS for flow cytometric analysis using a Gallios/FC500 Cytometer (Beckman Coulter, Indianapolis, IN) (excitation wavelength, 488 nm; emission wavelength, 575 nm).

Transporter Function

The transport activity of BCRP in BeWo cells was measured by analyzing the cellular retention of two BCRP transporter substrates, Hoescht 33342 and zearalenone, an estrogenic mycotoxin (Bircsak, et al., 2013; Xiao, et al., 2015).

Hoescht 33342 Transport

After experimental treatments, BeWo cells were detached from the culture plates with trypsin, washed, resuspended in medium, and added to a 96-well round bottom plate at a density of 200,000 cells/well in a final volume of 200 µL. Plates were centrifuged (500 g, 5 minutes, 5°C) and the medium removed. Cells were then resuspended in 200 µL of growth medium containing Hoechst 33342 (5 µM). After 30 min at 37°C in the presence or absence of the BCRP-specific inhibitor, Ko143 (1 µM), cells centrifuged, washed and re-suspended in substrate-free growth medium with or without Ko143. After 1 h at 37°C, the cells were washed and resuspended in 50 µL ice cold PBS for analysis. Quantification of intracellular fluorescence was performed using a Cellometer Vision

automated cell counter (Nexcelom Bioscience, Lawrence, MA) fitted with a VB-450-302 filter (excitation/emission = 375/450 nm). The total number of cells analyzed for each sample ranged from 200 to 2000 and were normalized for cell size.

Zearalenone Transport

For zearalenone transport studies, BeWo cells, grown and treated in 6 well culture dishes, were loaded with zearalenone (10 μM) in HBSS in the presence or absence of Ko143 (1 μM). After 1 h at 37°C, cells were washed with HBSS, and then incubated in zearalenone-free HBSS in the absence and presence of Ko143. After 30 min at 37°C, cells were washed, collected in lysis buffer and stored at -80°C. Quantification of intracellular zearalenone was performed using an ELISA kit (Abnova, Taipei City, Taiwan), and standards were prepared in lysis buffer (Xiao, et al., 2015).

Immunohistochemistry

For immunohistochemistry, tissue was embedded in paraffin and 5 μm thick sections prepared. After deparaffinization, tissue sections were quenched in 2% H_2O_2 (10 min, room temperature). Tissue sections were then blocked with an avidin/biotin blocking kit (Vector Laboratories, Burlingame, CA) followed by 5% serum corresponding to the source of the primary antibody. After 2 h at room temperature, tissues sections were incubated with primary antibodies to BCRP (BXP-21, 1:100; abcam), TFR-1 (ab108985, 1:200 Abcam), PLAP (ab133602, 1:1000, Abcam), or CD34 (ab81289 1:10,000, Abcam). After 16 h at 4°C, tissue sections were washed and incubated with biotinylated secondary antibodies for 60 min at room temperature (Vector Laboratories). Tissue sections were then stained using a 3,3'-diaminobenzidine peroxidase substrate kit (Vector Laboratories). After counterstaining with hematoxylin, tissue sections were dehydrated and imaged by light microscopy on a Olympus BX51 microscope (Waltham,

MA) fitted with a ProgRes C14+ camera (Jenoptik, Jena, Germany). Negative controls for each secondary antibody are provided (**Supplemental Fig 4.2**).

Statistical analysis

Data are presented as mean ± SE and analyzed using Graphpad Prism 5.0 software (Graphpad Software Inc., La Jolla, CA). Data were normally distributed, and two-way analysis of variance post-test or one-way analysis of variance with Bonferroni post-test was used to determine significance, which was set at $p < 0.05$.

1.4 Results

Localization of the BCRP Transporter in Human Term Placentas

BCRP protein was highly expressed on syncytiotrophoblasts and fetal endothelial cells (**Fig 4.1**). Placental alkaline phosphatase (PLAP) and transferrin receptor (TFR), markers for raft and non-raft regions of cell membranes, respectively, were also expressed in syncytiotrophoblasts. TFR was also present on fetal endothelial cells while CD34, a marker for endothelial membranes, was localized only in the fetal endothelium (**Fig 4.1**).

Localization of the BCRP Transporter to Lipid Raft-Enriched Fractions in Human Term Placentas

MVM was extracted and purified from healthy term placentas and tested for contamination using Western blotting (**Fig 4.2A**). PLAP, also a marker for MVM, was highly enriched in both crude and purified MVM fractions of the tissue when compared to whole placenta homogenates. MRP1, a marker of syncytiotrophoblast basolateral membranes, was present in whole homogenates and crude MVM, but little or no expression of this protein was evident in purified fractions. Similar results were obtained for GAPDH, a marker of cytoplasmic contamination. CD34 was present only in whole placenta homogenates and nuclear fractions. Low levels of CD34 remained in crude MVM preparations but were not detected following further purification. H2A, a nuclear protein marker, was found only in nuclear fractions. These data confirmed that pure MVM were prepared.

Detergent-based density gradient ultracentrifugation was then performed on pure MVM to isolate lipid raft, and non-lipid raft fractions. Ten fractions were collected starting from

the least dense fractions at the top of the gradient and analyzed for overall protein and cholesterol content. Lower density fractions at the top (fractions 1-3) typically represent detergent-resistant raft microdomains, while higher density fractions at the bottom (fractions 7-10) typically represent detergent-soluble cell components, including non-raft membranes (Smart, et al., 1995). Protein and cholesterol analysis of lipid raft fractions showed that only 11.7% of total protein was localized to fractions 1-3 while 96.0% of cholesterol (normalized to protein) was localized to the same fractions (**Fig 4.2B**).

Western blotting of the density gradient fractions showed that approximately 84.8% of total PLAP protein content was found in fractions 2 and 3 while 84.3% of total TFR protein was localized in the bottom 4 fractions (7-10) (**Fig 4.2C**). Similar to PLAP, 76.9% of total BCRP protein was found in lipid raft-enriched fractions 2 and 3.

Localization of the BCRP Transporter Following Cholesterol Depletion of BeWo Cells

In order to characterize density gradient fractions collected from BeWo cells, we first assessed total protein and cholesterol. Following centrifugation, 14.0% of total protein was localized to lipid raft fractions (fractions 1-3), while 25.1% of cholesterol (normalized to protein) was localized to the same fractions (**Fig 4.3**). We next analyzed BeWo cells for expression of BCRP in lipid rafts. Analysis of the gradient fractions by Western blotting showed that 46.3% of total PLAP was found in fractions 2 and 3, while 90.3% of total TFR was found in fractions 7-10 (**Fig 4.4**). BCRP co-localized with PLAP in lipid rafts, with 33.6% of total BCRP contained in fractions 2 and 3.

To determine the extent to which cholesterol influences the localization of BCRP in lipid rafts, BeWo cells were treated with the cholesterol sequestrant MβCD. MβCD treatment reduced the content of BCRP and PLAP in lipid raft fractions by 51.4% and 92.6%,

respectively (**Fig 4.4**). This redistribution of BCRP and PLAP was reversed when cells were replenished with cholesterol after MβCD treatment. Greater than 90% of TFR content was localized to the higher density fractions and MβCD treatment did not affect its distribution. Protein analysis showed that BeWo lipid rafts (fractions 1-3) accounted for 13.3% and 12.2% of total protein in MβCD and cholesterol replenished treatment groups, respectively (**Fig 4.3**). By comparison, cholesterol analysis showed that fractions 1-3 accounted for 11.4%, and 40.9% of total cholesterol in MβCD and cholesterol replenished treatment groups, respectively (**Fig 4.3**).

Effects of Cholesterol on BCRP Transport Activity

Initially, we characterized BCRP transport activity in BeWo cells using the fluorescent substrate, Hoechst 33342 (**Fig 4.5B**). Ko143, a specific functional inhibitor of BCRP [32], increased the cellular accumulation of Hoechst 33342 by 172%. To determine whether reduced cholesterol content affected BCRP function, cells were treated with pravastatin and assessed for cholesterol content and Hoechst 33342 retention. Pravastatin treatment (48 h) caused a concentration-dependent decrease in total cellular cholesterol (**Fig 4.5A**), and this resulted in an increase in the retention of Hoechst 33342 up to 47% (**Fig 4.5B**).

To determine if repletion with cholesterol would restore BCRP efflux activity, BeWo cells were treated in a separate set of experiments with MβCD (5 mM, 1 h) or pravastatin (200 μM, 48 h) and then exogenous cholesterol (5 mM MβCD-cholesterol, 30 min). The retention of Hoecsht 33342 and the estrogenic mycotoxin zearalenone were then measured. Treatment of BeWo cells with MβCD and pravastatin reduced cellular cholesterol content by 75.3% and 37.8%, respectively (**Fig 4.6A**), which increased Hoechst 33342 accumulation by 20% (**Fig 4.6B**) and zearalenone retention by 125%

(**Fig 4.6C**) for both treatments. BeWo cells under the same treatment conditions were analyzed for loading of Hoechst 33342 or Rhodamine 123, a fluorescent chemical that is not transported by BCRP (**Supplemental Fig 4.3**). Neither MβCD nor pravastatin showed significant differences in the loading of dyes compared to control. Repletion of cholesterol in MβCD and pravastatin-treated cells restored cellular cholesterol, which lowered the cellular retention of Hoechst 33342 and zearalenone to levels that were not significantly different than control cells (**Fig 4.6A-C**). Ko143 increased the cellular accumulation of both Hoechst 33342 (**Fig 4.6B**) and zearalenone (**Fig 4.6C**), and, as expected, exogenous cholesterol did not reverse the inhibitory effects of Ko143.

Effects of Lowering Cholesterol on BeWo Cell Expression of BCRP

To determine whether the effects of lowering cholesterol on BCRP efflux activity were due to changes in BCRP expression, cells treated with MβCD (5 mM, 1 h) or pravastatin (200 μM, 48 h) were analyzed by Western blotting and flow cytometry. Treatment of BeWo cells with the cholesterol inhibitors did not alter total BCRP expression in the cells (**Supplemental Fig 4.4A**) or its insertion in the plasma membrane (**Supplemental Fig 4.4B**).

1.5 Discussion

Because of BCRP's enrichment in the placenta, and its ability to transport toxicants from the fetus to the maternal circulation, this transporter provides a critical fetoprotective function (Mao, 2008). Our studies demonstrate that BCRP is localized to lipid rafts in syncytiotrophoblasts and BeWo cells. This is based on findings that BCRP can be isolated in detergent-resistant, cholesterol-rich cell membranes after density gradient centrifugation where it co-localizes with PLAP, a well-characterized lipid raft marker (Saslowsky *et al.*, 2002). In BeWo cells, but not MVM, BCRP is also localized in non-lipid raft fractions. BeWo cells are derived from a human choriocarcinoma (Pattillo and Gey, 1968), and differences in the trafficking of BCRP between these cells and primary human tissue may be due to the transformed phenotype. It has also been proposed that some proteins present in lipid raft fractions are simply not as intimately packed within lipid rafts and are susceptible to Triton digestion, which was used only for lipid raft isolation in BeWo cells (Schuck, et al., 2003). Further, it is common that even well-established lipid raft proteins, like caveolin-1, display a bimodal distribution in gradient centrifugation experiments under certain conditions and localize to both raft and nonraft fractions (Chamberlain *et al.*, 2001; Radeva and Sharom, 2004; Yu *et al.*, 2007). It has also been proposed that some fraction of a particular protein can be bound to certain fatty acids that drive the association with lipid rafts (Schuck, et al., 2003). This post-translational modification could, in theory, result in two distinct populations of the same protein: one that associates with rafts and one that does not. Further studies will be needed to determine what drives the bimodal distribution of BCRP, but it is clear that cholesterol plays a functional role in the distribution of BCRP in placental cells.

Our studies measuring efflux transport activity of BCRP used two substrates, Hoechst 33342 and zearalenone. Hoechst 33342 is a fluorescent substrate often used for

measuring BCRP efflux activity (Bircsak, et al., 2013), while zearalenone is an estrogenic mycotoxin produced by fungi that occur naturally on cereal crops. We previously identified zearalenone as a novel substrate for BCRP (Xiao, et al., 2015). *In utero* exposure to zearalenone has been shown to cause developmental toxicities including feminization, mammary epithelial proliferation and precocious puberty (Belli, et al., 2010). The fact that BCRP can efflux zearalenone may make it a critical protein in protecting the fetus against toxicity by this environmental contaminant.

Maternal cholesterol is vital to the development of the fetus. For instance, low maternal serum cholesterol has been noted as a cause of both preterm delivery and lower birth weight (Edison *et al.*, 2007). As indicated above, cholesterol is also crucial to the integrity of lipid rafts, which have been implicated as mediators of a number of key metabolic processes needed for fetal development including transmembrane trafficking of nutrients. For example, lipid raft integrity is important for the maternal-to-fetal transport of folate, a cofactor important in the development of the nervous system (Gelineau-van Waes *et al.*, 2005). In this regard, maternal exposure to fumonisin B1, which is known to disrupt lipid raft integrity in the placenta, has the potential to inhibit receptor-mediated folate transport to the fetus resulting in toxicity (Stevens and Tang, 1997). While it is known that cholesterol and lipid rafts are important in pregnancy, understanding how they modulate efflux transporters such as BCRP will be critical to understanding mechanisms by which the fetus is protected from exposure to xenobiotics. Without affecting BCRP protein expression, both pravastatin and MβCD inhibited most but not all BCRP efflux transport activity by modulating levels of cellular cholesterol, a process that disrupts lipid rafts (Hartel *et al.*, 1998). Further, unlike other statins, pravastatin is not a direct inhibitor of BCRP at the concentrations used (Hirano, et al., 2005). These data indicate that cholesterol is important in regulating BCRP efflux activity. However, the

precise mechanism is not clear. Although lipid rafts may be critical for maximal BCRP activity (see further below), it is also possible that cholesterol modulates BCRP directly. For example, BCRP has been shown to have a cholesterol-binding motif and this may directly influence the change in conformation of BCRP to an active state (Hegedus, et al., 2015). Additionally, it has been postulated that cholesterol aids in the interaction of small, hydrophobic substrates with BCRP, by "filling in" an unoccupied space in the active site (Polgar *et al.*, 2004; Telbisz, et al., 2014). This may, in part, explain why efflux of zearalenone, a small, hydrophobic compound, was more susceptible to the effects of cholesterol reduction than Hoechst 33342, a larger, hydrophilic compound.

Lipid rafts are more ordered than the surrounding phospholipid bilayer and can therefore promote protein-protein interactions. For example, lipid rafts have been reported to enhance the dimerization of glial-cell-derived neurotrophic factor and the high-affinity IgE receptor (Simons and Sampaio, 2011). Efflux of xenobiotics by BCRP is dependent on its dimerization (Krishnamurthy and Schuetz, 2006). Lipid rafts may help to bring BCRP monomers in proximity to one another, while stabilizing a conformation of BCRP that exposes critical cysteine residues needed for dimerization (Kage *et al.*, 2005; Simons and Sampaio, 2011). At the present time, the precise role of raft and non-raft BCRP in BeWo cells in mediating the Hoechst 33342 and zearalenone efflux is not known. It is possible that reducing cellular cholesterol affects both raft and non-raft BCRP, but more studies are needed to clarify this possibility.

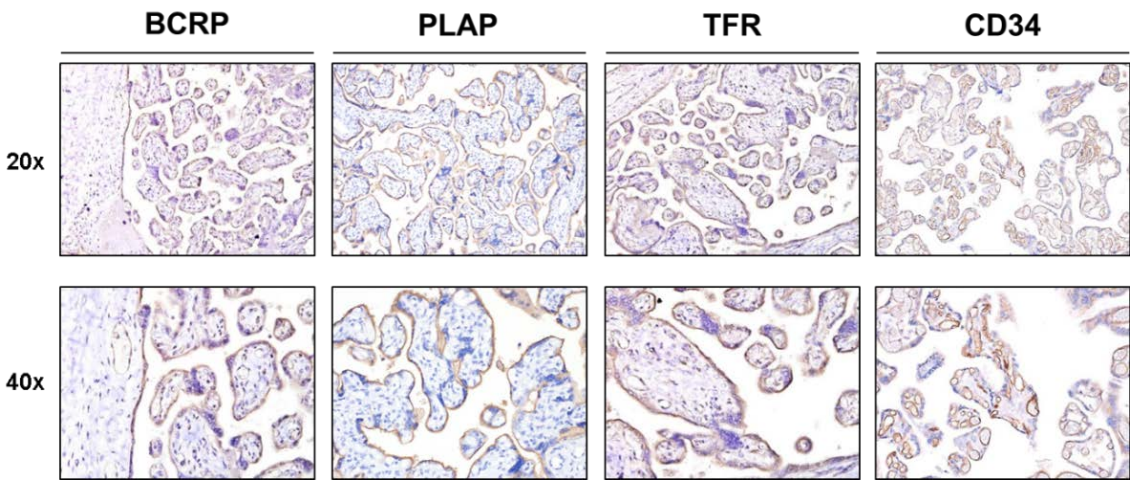

Fig 4.1. Localization of the BCRP transporter and plasma membrane markers in human term placentas.

Healthy, term placentas were fixed in PAXgene tissue stabilizer and then subjected to routine tissue processing and paraffin embedding. Sections (5 µm) were prepared and stained with antibodies against BCRP, PLAP, TFR or CD34 as indicated in the Materials and Methods. Antibody binding was visualized using a Vectastain DAB kit *(brown staining)* and counterstained with hematoxylin *(blue staining)*.

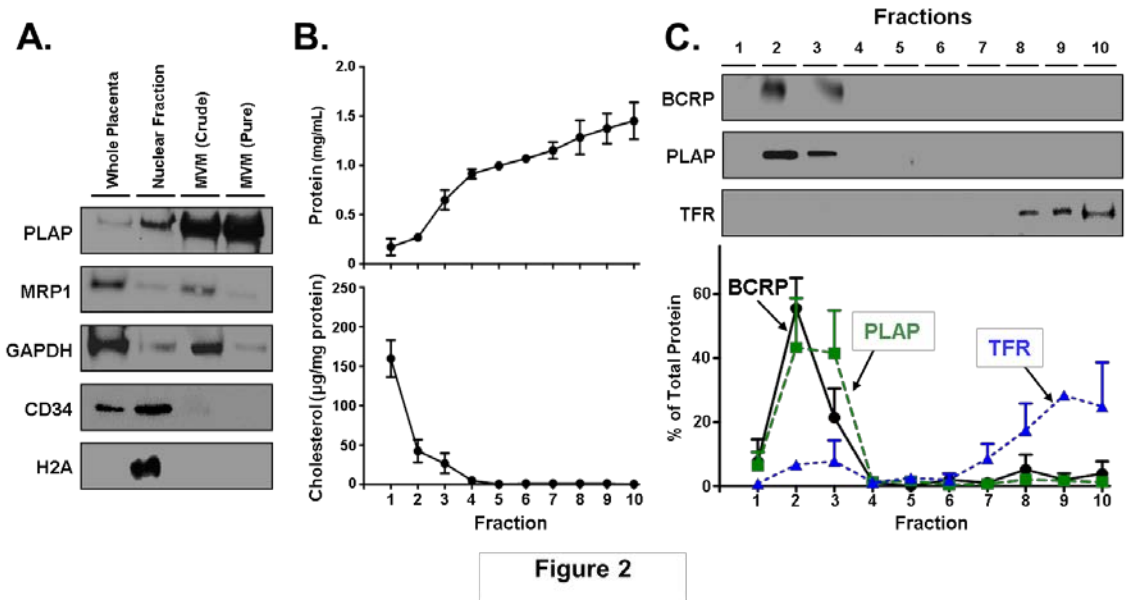

Fig 4.2 Localization of the BCRP transporter in lipid raft-enriched fractions in human term placentas.

A. Western blot of placental MVM. Western blotting was performed on MVM isolated from human term placentas using ultracentrifugation. **B.** Protein and cholesterol analysis of fractions from placental MVM ultracentrifugation. Placenta MVMs were subjected to density gradient ultracentrifugation in order to isolate detergent-resistant lipid rafts. Ten 1.4 mL fractions were collected and analyzed for protein or cholesterol content as described in the Materials and Methods. Data are presented as mean ± SE (n = 3 placentas). **C.** Western blot of fractions from placental MVM ultracentrifugation. Western blots from 1 representative placenta are shown. Data are presented as mean ± SE (n = 3 placentas).

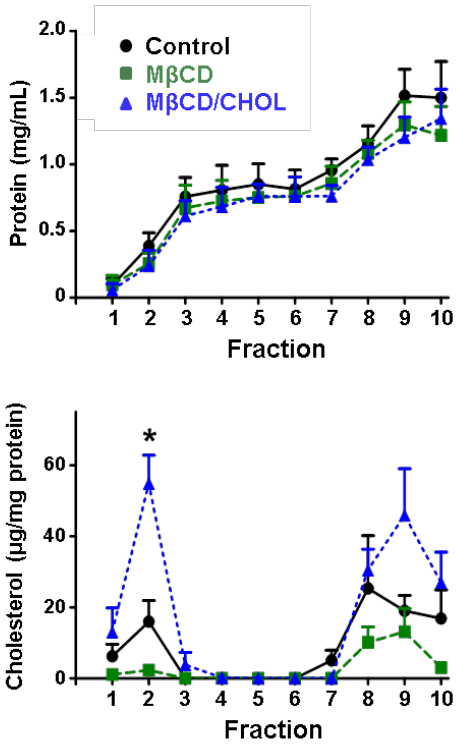

Fig 4.3. Protein and cholesterol content of density gradient fractions from BeWo cells following ultracentrifugation.

Plasma membranes collected from BeWo cells treated with HBSS, MβCD (5 mM, 1 h), or MβCD (5 mM, 1 h) and then MβCD-cholesterol (5 mM, 30 min) were subjected to density gradient ultracentrifugation in order to isolate detergent-resistant lipid rafts. Ten 1.4 mL fractions were collected and analyzed for protein or cholesterol content as described in the Materials and Methods. Data are presented as mean ± SE (n = 3 independent experiments) and were analyzed using a one-way ANOVA followed by Bonferroni post-hoc analysis (*$p < 0.05$ compared to control within fraction).

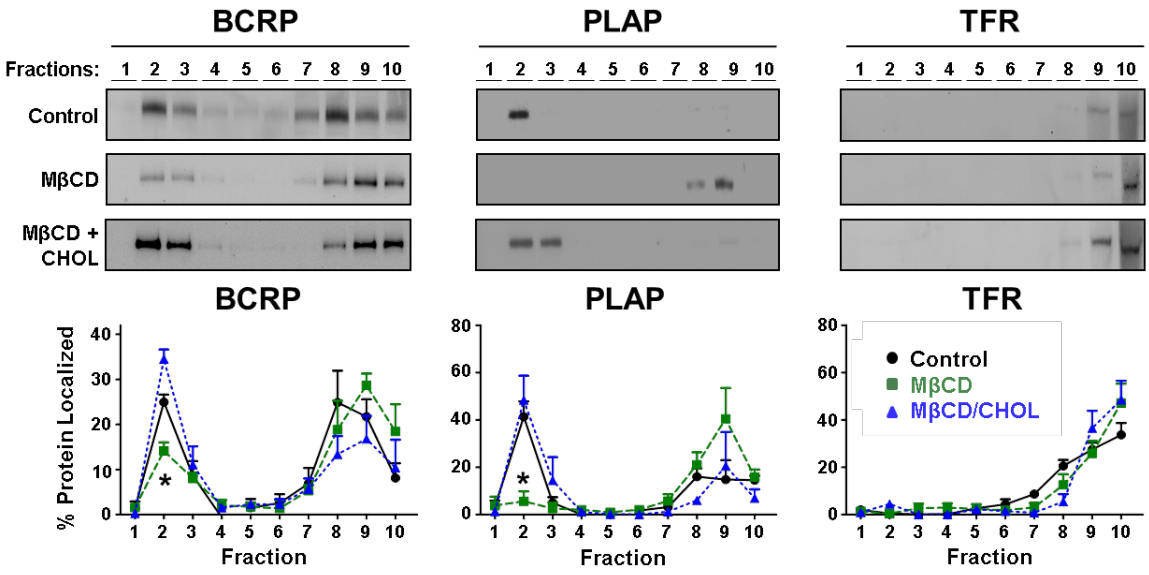

Fig 4.4. Localization of the BCRP transporter following cholesterol depletion of BeWo cells.

Western blots were performed using membrane fractions collected from BeWo cells following treatment with vehicle (Control), 5 mM methyl-β-cyclodextrin (MβCD) for 1 h, or 5 mM MβCD for 1 h and then 5 mM cholesterol-loaded MβCD for 30 min (MβCD + CHOL). Western blots show BCRP along with lipid raft (PLAP) and non-lipid raft (TFR) markers in fractions obtained from 1 representative experiment. Enrichment of proteins in different fractions was semi-quantified using densitometry of Western blots from 3 independent experiments. Data are presented as mean ± SE and were analyzed using a one-way ANOVA followed by Bonferroni post-hoc analysis (*$p < 0.05$ compared to control within fraction).

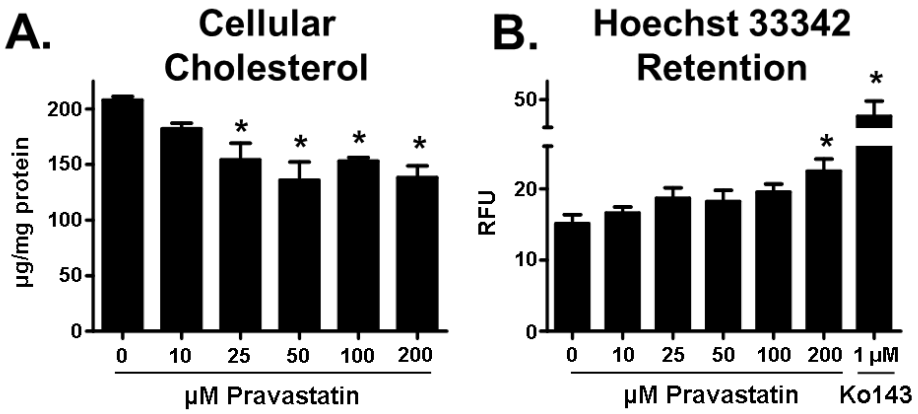

Fig 4.5. Relationship between cholesterol content and BCRP substrate retention in BeWo cells.

BeWo cells were treated with vehicle or pravastatin (10 – 200 µM) for 48 h. **A.** Effects of pravastatin on cholesterol content. Cholesterol was measured in cell lysates using the Amplex Red assay. **B.** Effects of pravastatin on BCRP efflux. Efflux transporter activity was indirectly measured by the ability of cells to retain the BCRP substrate Hoechst 33342. The BCRP substrate was quantified in relative fluorescence units (RFU) using a Nexcelom Cellometer. Data are presented as mean ± SE (n = 3 independent experiments) and were analyzed using a one-way ANOVA followed by Bonferroni post-hoc analysis (*$p < 0.05$ compared to 0 µM).

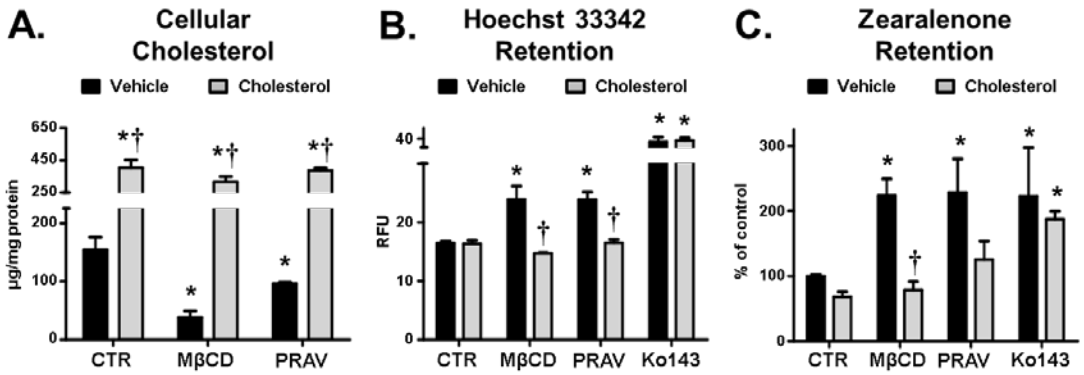

Fig 4.6. Effects of modulating cholesterol on BCRP transporter activity in BeWo cells.

Cholesterol content in BeWo cells was modulated by treatment with MβCD (1 h, 5 mM) or pravastatin (PRAV, 48 h, 200 µM). Cholesterol repletion groups were treated with cholesterol-loaded MβCD (30 min, 5 mM) immediately before the experiment. **A.** Effects of MβCD and pravastatin on BeWo cell cholesterol content. Cells were treated with MβCD or pravastatin, lysates prepared and cholesterol content measured using an Amplex Red assay (n = 3 samples). **B.** Effects of modulating BeWo cell cholesterol on BCRP efflux transporter activity using Hoechst 33342 retention. Efflux transporter activity was measured by the ability of cells to retain the BCRP substrate Hoechst 33342. The BCRP substrate was quantified in relative fluorescence units (RFU) using a Nexcelom Cellometer and expressed as mean ± SD (n = 3 independent experiments). **C.** Effect of modulating BeWo cell cholesterol on BCRP efflux transporter activity using zearalenone retention. Efflux transporter activity was measured by the ability of the cells to retain the BCRP substrate zearalenone. Black bars represent cells where cholesterol was not restored. Grey bars represent cells where cholesterol was restored. Data are presented as mean ± SE (n = 4-6). All data were analyzed using a two-way ANOVA followed by

Bonferroni post-hoc analysis (*$p < 0.05$ compared to control, †$p < 0.05$ compared to vehicle within the same treatment).

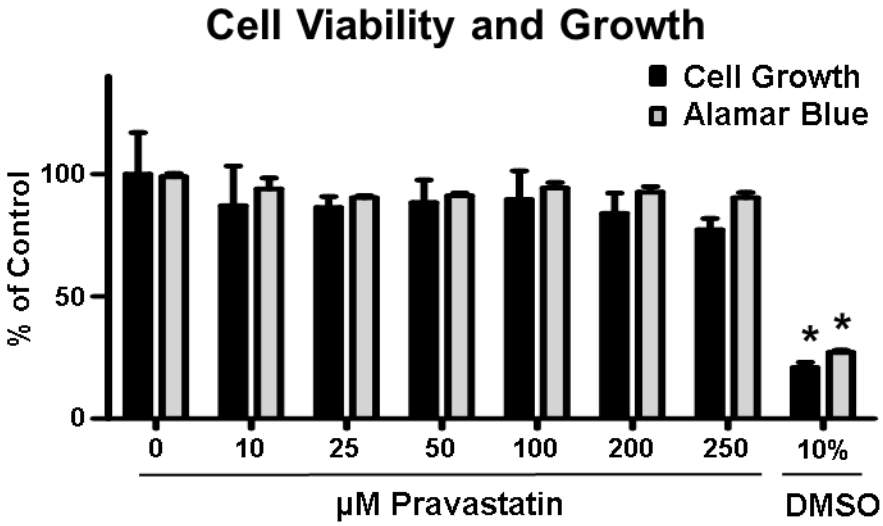

Supplemental Fig 4.1. Effects of pravastatin on BeWo cell viability and growth.

Cells were treated with increasing concentrations of pravastatin (10 – 250 µM). After 48 h, viability was determined using the Alamar Blue assay and cell growth by counting cells using a Coulter Counter. Data are presented as mean ± SE (n = 4) and analyzed using a one-way ANOVA followed by Bonferroni post-hoc analysis (*$p < 0.05$ compared to 0 µM).

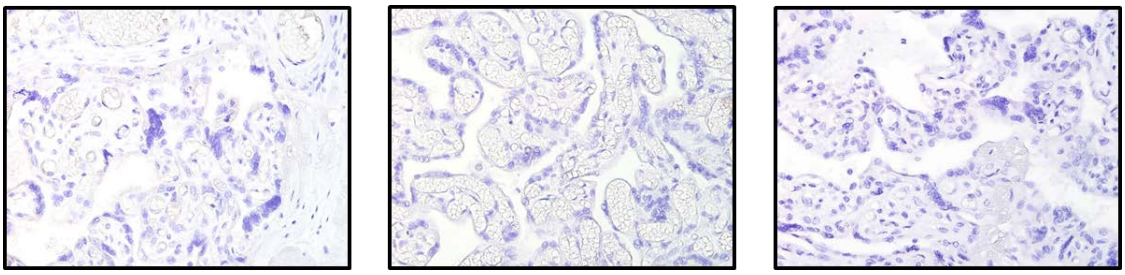

Supplemental Fig 4.2. Negative controls for immunohistochemistry staining.

Healthy, term placentas were fixed in PAXgene tissue stabilizer and then subjected to routine tissue processing and paraffin embedding. Sections (5 μm) were prepared and stained as indicated in the Materials and Methods without primary antibody. Anti-rabbit (left), anti-mouse (center), and anti-rat (right) secondary antibodies were used. Antibody binding was visualized using a Vectastain DAB kit *(brown staining)* and counterstained with hematoxylin *(blue staining)*.

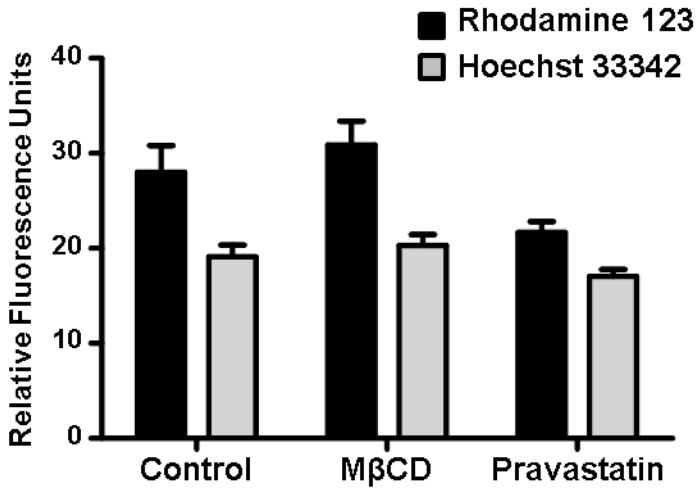

Supplemental Fig 4.3. Effects of altered cholesterol levels in BeWo cells on the cellular loading of fluorescent probes.

BeWo cells were treated with vehicle (control) and MβCD (1 h, 5 mM) or pravastatin (48 h, 200 μM) to lower cellular cholesterol. Cells were then treated with the BCRP substrate (Hoechst 33342) or the non-BCRP substrate (rhodamine) for 30 min and cellular fluorescence quantified using a Nexcelom Cellometer. Data are presented as mean relative fluorescence units ± SE (n = 3).

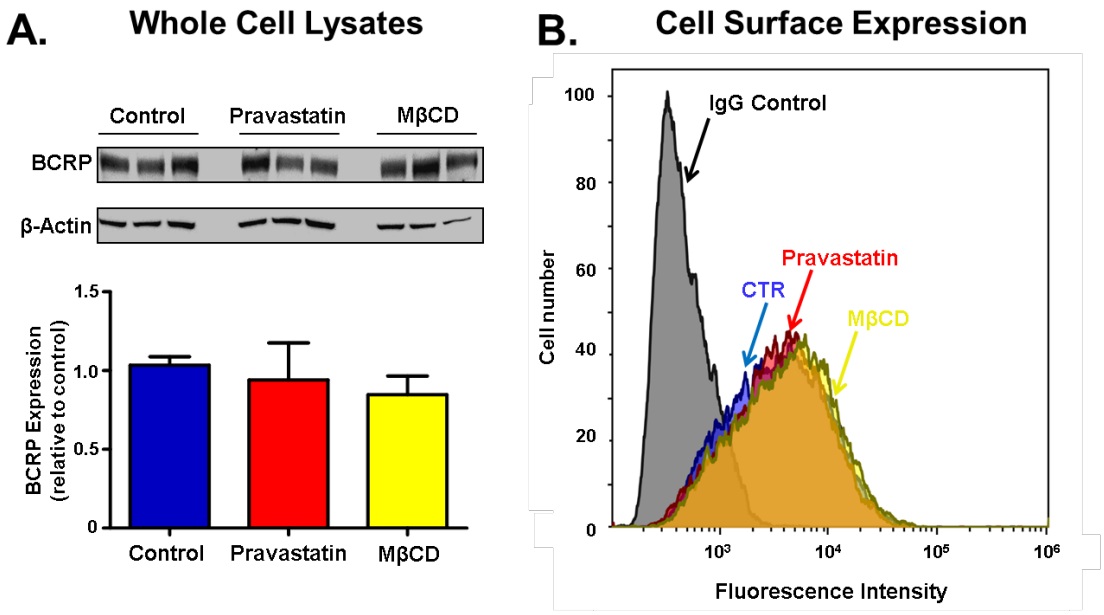

Supplemental Fig 4.4. Expression of the BCRP transporter in BeWo cells following cholesterol depletion.

BeWo cells were treated with vehicle (control), pravastatin (48 h, 200 μM) or MβCD (1 h, 5 mM). **A.** Western blot analysis of pravastatin and MβCD treated BeWo cells. Cell lysates were prepared and analyzed by Western blotting for expression of BCRP (72 kDa). Expression was normalized to the loading control β-actin (42 kDa) and presented as mean ± SE (n = 3). **B.** Flow cytometric analysis of pravastatin and MβCD treated BeWo cells. Treated cells were incubated with phycoerthyrin-labeled anti-BCRP antibody (5D3) or IgG control.

CHAPTER 5: OVERALL DISCUSSION

Summary

The overall objective of this dissertation was to assess the contribution of the placental BCRP transporter in preventing fetal exposure to the mycoestrogen zearalenone and to investigate potential mechanisms that regulate transporter expression, localization, and function. Zearalenone and its metabolites (including zeranol) are prevalent in diets across the globe due to the occurance of *Fusarium* molds in cereal crops and the use of Ralgro as a growth promoter in the beef industry (Zinedine, et al., 2007). This observation coupled with the fact that *in utero* exposure to zearalenone has been shown to interfere with sexual development across species (Belli, et al., 2010; Nikaido *et al.*, 2004) highlights the need to understand transplacental mycoestrogen disposition and factors that may increase fetal exposure.

The data presented in this dissertation support the hypothesis that BCRP limits the maternal-to-fetal transport of zearalenone, a protective mechanism that can be regulated by various lipid-related pathways. This dissertation specifically addressed the contribution of 1) endocannabinoids and 2) membrane cholesterol to the transcriptional and post-transcriptional regulation of BCRP, respectively. Three specific aims were developed to address this hypothesis: 1) comprehensively assess the role of BCRP in preventing the transport of zearalenone and its metabolites across the blood-placenta barrier (**CHAPTER 2**), 2) determine the effect of endocannabinoids on BCRP transcription, expression, and activity (**CHAPTER 3**), and 3) investigate the post-transcriptional regulation of placental BCRP by membrane cholesterol and lipid rafts (**CHAPTER 4**). A graphical summary of chapters 2-4 are presented in **Fig 5.1**.

The first aim thoroughly characterized the role of BCRP on regulating the maternal-to-fetal transfer of zearalenone using *in vivo* and *in vitro* models of the placental barrier. Previous studies using *in vitro* screening methods demonstrated that zearalenone is a potential substrate for BCRP but did not specifically address how BCRP impacts zearalenone disposition during pregnancy (Lin, et al., 2016; Prouillac and Lecoeur, 2010; Xiao, et al., 2015). Using transwell cultures of MDCK and BeWo cells, we demonstrated that BCRP increases the fetal-to-maternal and decreases the maternal-to-fetal transport of zearalenone. *In vivo* pharmacokinetic analysis of zearalenone in wild type and Bcrp$^{-/-}$ mice demonstrated a marked increase of zearalenone and its major metabolites, α-zearalenol and β-zearalenol, in both fetal and placental tissues of knockout mice. Importantly, no changes were observed in the maternal serum concentrations of zearalenone or its metabolites between the two phenotypes. These data confirm that placental BCRP/Bcrp protects the fetus from exposure to zearalenone.

The second aim assessed whether increased exposure to endocannabinoids, signaling molecules implicated in a number of gestational disorders (Costa, 2016a), impact the expression and activity of BCRP in the placenta. A 24 h exposure to the endocannabinoid anandamide decreased BCRP mRNA and protein expression in human placental explants (1 μM anandamide) and human BeWo trophoblast cells (10 μM anandamide). BeWo cells also demonstrated a marked reduction in the BCRP-mediated efflux of H33342 and zearalenone following anandamide treatment. Notably, this study is the first to document the ability of endocannabinoids to influence the expression of a xenobiotic efflux transporter. Both the CB2 receptor inhibitor AM630 and 8-Br-cAMP prevented the anandamide-mediated down-regulation of BCRP expression after 24h. Moreover, anandamide decreased intracellular cAMP, CREB phosphorylation, and p-CREB binding to the *BCRP* promoter element. It is therefore evident that

anandamide down-regulates BCRP by activating the CB2 receptor, which in turn inhibits cAMP production and signaling. This mechanism may explain why placental BCRP expression is down-regulated in certain diseases of pregnancy that also exhibit features of endocannabinoid dysregulation.

The third aim of this dissertation investigated whether placental BCRP localizes to lipid rafts and if BCRP efflux activity is dependent on membrane cholesterol. Density gradient ultracentrifugation was used to isolate and analyze lipid raft fractions from human term placenta and BeWo cells. BCRP was found in lipid raft fractions of placentas and both raft and non-raft fractions in BeWo cells. This observation was highly novel as prior studies have utilized only immortalized cell models rather than intact human tissues. Methyl-β-cyclodextran (5 mM, 1 h), which removes membrane cholesterol, decreased the association of BCRP with lipid raft fractions. Replenishing cholesterol (5 mM cholesterol- Methyl-β-cyclodextran, 30 min) after treatment with methyl-β-cyclodextran restored BCRP association with lipid raft fractions. Reducing cholesterol using methyl-β-cyclodextran (5 mM, 1 h) or pravastatin (100 μM, 48 h) also decreased BCRP efflux of H33342 and zearalenone, and this effect was reversed if cholesterol was replenished (5 mM cholesterol- Methyl-β-cyclodextran, 30 min) after treatment.

Zearalenone

In all *in vitro* and *in vivo* models tested, BCRP/Bcrp decreased the maternal-to-fetal transfer of zearalenone, highlighting its fetoprotective function in the placenta (**CHAPTER 2**). However, it should be noted the dose of zearalenone used was not representative of real world exposures. *In vitro* transwell experiments and *in vivo* mouse experiments used 50 μM or 10 mg/kg of zearalenone, respectively. These concentrations were used in order to ensure that the samples later measured for

zearalenone content would be well above the detectable limit for HPLC-UV/Vis and LC-MS and provide proof-of-concept data supported the interaction of zearalenone and BCRP. Zearalenone is present at much lower concentrations in human serum. For instance, one study of 48 women (31-65 years) detected a mean total zearalenone (zearalenone + all metabolites) concentration of 1.26 ± 0.875 ng/mL in serum (~3 nM) (Mauro *et al.*, 2018). Further, our pharmacokinetic analyses were performed after a single bolus dose of zearalenone. More commonly, zearalenone, a dietary contaminant, is likely to be ingested in small doses over the course of the pregnancy. Utilization of the iv route of administration was advantageous in this study as it bypassed BCRP protein found in the gastrointestinal tract. We hypothesize that oral administration of zearalenone to $Bcrp^{-/-}$ mice would enhance bioavailability by preventing luminal efflux.

The discrepancy in dose between our studies and real world exposure levels may change the pharmacokinetics of zearalenone and the contribution of various transporters to mycoestrogen disposition. It is possible, for instance, that zearalenone has some affinity for other efflux transporters in the placenta that are not as highly expressed as BCRP. While we demonstrated that inhibiting MDR1 in MDCK cells did not impact zearalenone transwell kinetics, it is still possible that zearalenone has some limited affinity for MDR1. BCRP and MDR1 do share a number of substrates including irinotecan, doxorubicin, and methotrexate (Jandu *et al.*, 2016; Louisa *et al.*, 2014; Norris *et al.*, 1996; Park *et al.*, 1994; Sun *et al.*, 2013; Volk *et al.*, 2002a). In a real world exposure scenario, it is possible that zearalenone does not exhibit the same placental disposition in the absence of BCRP because other, albeit less efficient, transport mechanisms play a larger role in regulating disposition.

Future studies with zearalenone should address two questions: 1) how does placental BCRP influence fetal exposure to dietary concentrations of zearalenone and 2) does BCRP protect the fetus from developmental toxicities under these conditions. Measuring zearalenone content in clinical samples (placenta, cord blood, maternal serum) and correlating the data to BCRP expression or known polymorphisms (such as Q141K) may prove useful in understanding the role of BCRP under real-world conditions. These questions can also be addressed feeding Bcrp$^{+/-}$ mice zearalenone daily with concentrations common to human exposure throughout gestation and assessing the pups for zearalenone content or developmental endpoints later in life including mammary proliferation and anogenital distance. It should be noted that using rodent models to understand BCRP function has its own limitations, and, in fact, the placentas of no two mammals are the same (reviewed in Carter, 2007). While it has been shown that many BCRP substrates are similarly transported by human BCRP and murine Bcrp (Bakhsheshian *et al.*, 2013), differences do exist. BPA, for example, is transported by the human BCRP but not rat Bcrp (Mazur, et al., 2012). Moreover, human BCRP is more sensitive to inhibition by fumitremorgin C, a mycotoxin, than mouse Bcrp (Gonzalez-Lobato *et al.*, 2010). These discrepancies may therefore lead to over- or underestimating the role of BCRP in drug disposition relative to other efflux transporters. It is therefore important to consider these differences when interpreting data on Bcrp$^{+/-}$ mice. Importantly, however, knocking out Bcrp in mice does not impact fertility or reproduction, and embryos of Bcrp$^{+/-}$ mice develop normally.

Anandamide

Our findings suggest that dysregulation of the endocannabinoid system in certain diseases of pregnancy may be contributing to reductions in BCRP expression (**CHAPTER 3**). Interestingly, the effects of anandamide are selective for BCRP over

other transporters. BeWo gene expression of MRP1, 2, 5, OATP4A1, OAT2B1, and MDR1 were all analyzed after anandamide treatment alongside BCRP, but no significant changes were observed (data not shown). A limitation of this study is the concentration of anandamide (10 μM) that was used to elicit these effects, particularly in BeWo cells. Circulating anandamide is normally 0.1-10 nM even in pathological pregnancies (Gebeh, et al., 2013; Gouveia-Figueira *et al.*, 2017; Habayeb, et al., 2004; Martins *et al.*, 2015). While the lowest concentration of anandamide used (10 nM) reduced BCRP mRNA expression in human placental explants, the same effect was not evident at the protein level after 24 h (data not shown). This can be explained by the rapid breakdown of anandamide by FAAH (Habayeb, et al., 2008). Without more sustained anandamide signaling, the transcriptional changes seen at lower concentrations of anandamide may be overcome by other mechanisms like ubiquitin-mediated proteolysis. Even with our highest dose of anandamide (10 μM), BCRP mRNA returned to control levels by 48 h, likely due to anandamide turnover. Furthermore, while the circulating concentrations of anandamide during pregnancy have been analyzed, the local concentration of anandamide around the syncytiotrophoblasts is unknown. Because the endometrium secretes anandamide throughout pregnancy (Costa, 2016a), the local concentration of anandamide may be significantly higher than circulating concentrations. It is therefore difficult to accurately recapitulate *in vivo* conditions with *in vitro* cultures using a single dose of anandamide. However, our observations make evident the novel concept that the endocannabinoid system can regulate BCRP expression in the placenta. Future research investigating the impact FAAH dysfunction on placental BCRP function *in vivo*, either through Faah knockout or point mutation, could strengthen the clinical relevance of our findings.

The observations in Chapter 3 are centered around the effects of anandamide on the expression of placental transporters, but endocannabinoids could similarly affect other tissues. Both CB1 and CB2 receptor signal transduction pathways trigger $G\alpha_{i/o}$-mediated inhibition of adenylate cyclase (Bayewitch *et al.*, 1995; Mukhopadhyay and Howlett, 2001), although our results suggest that changes in placental BCRP expression are specifically CB2-dependent. Cannabinoid receptors are expressed in the liver, kidney, gut, and blood-brain barrier (Pagotto, et al., 2006; Vendel and de Lange, 2014). A CB receptor-dependent decrease in BCRP expression in any of these organs could potentially enhance the accumulation and toxicity of BCRP substrates. In hepatocytes for example, BCRP is expressed in the apical membrane and facilitates biliary excretion. Extrapolating our observations beyond the placenta, it is possible that increased endocannabinoid signaling in the liver could down-regulate hepatocyte BCRP expression, decreasing hepatic drug clearance and exacerbating injury from hepatotoxicants such as aflatoxin B1 (van Herwaarden *et al.*, 2006b). If anandamide reduces BCRP expression at the blood-brain barrier, then endocannabinoid dysregulation could intensify the effects of neurotoxic BCRP substrates, like ketamine (Ganguly, et al., 2018). The same mechanism in enterocytes or proximal tubular cells would increase area-under-the-curve exposures for BCRP substrates and exacerbate overall toxicity. However, it cannot be assumed that anandamide signaling would decrease BCRP expression in all tissues with cannabinoid receptors. First, the role of cAMP in BCRP expression has been observed in several *in vitro* models, but this response has not been validated in all BCRP-expressing cell types or *in vivo*. Secondly, cannabinoid receptor signaling does not universally inhibit cAMP production. In fact, anandamide signaling can either decrease or increase cAMP based on the tissue type and model. It is therefore necessary to assess the BCRP response to anandamide in

each tissue type individually before concluding that endocannabinoid signaling enhances BCRP substrate toxicity.

The data presented in Chapter 3 also warrant further investigation into the effects of xenocannabinoids on the placenta. As previously discussed, both CB1 and CB2 receptor agonism can interfere with the development and function of the placenta (Costa, 2016a). It has been reported that 34-60% of women who use cannabis regularly continue smoking marijuana during pregnancy, often to alleviate the symptoms of morning sickness (Jaques, et al., 2014; Moore, et al., 2010; Passey, et al., 2014; Schempf and Strobino, 2008). This is to the detriment of the fetus, as marijuana use is well-documented to decrease fetal growth (Davitian, et al., 2006; El Marroun, et al., 2009; Warner, et al., 2014). The push for "natural" remedies over pharmaceutical intervention and the decriminalization of marijuana are likely to increase the percent of women who use marijuana during pregnancy. The three active components of marijuana, tetrahydrocannabinol, cannabinol and cannabidiol, all interact with the cannabinoid receptors, albeit with different affinities and effects (Pertwee, 2008), and may therefore impact placental drug permeability. For instance, cannabidiol exposure increases BCRP and decreases MDR1 expression in BeWo and Jar cells, another human trophoblast cell line (Feinshtein *et al.*, 2013a). Further, all three compounds can directly inhibit BCRP efflux activity (Holland, et al., 2007). In fact, cannabidiol increases the retention of mitoxantrone in BeWo cells and Jar cells and increases the maternal-to-fetal transport of glyburide in an *ex vivo* placental perfusion model (Feinshtein, et al., 2013b). The problem becomes increasingly complex when considering that marijuana has at 483 known compounds and at least 66 are known or potential cannabinoids (Elsohly and Slade, 2005; Pertwee, 2008).

The advent of synthetic cannabinoids raises concern as well. From 2008 to 2014, over 140 novel synthetic cannabinoids were reported to the European Monitoring Centre for Drugs and Drug Addiction from 2008 to 2014 including the most commonly recognized K2, also known as Spice (Abouchedid *et al.*, 2016). Many of these compounds are largely illegal worldwide, but it is difficult for regulators and scientists to keep up with the synthetic chemists formulating these designer drugs. Many synthetic cannabinoids have a dramatically increased affinity for the cannabinoid receptors over the constituents of marijuana, and the resulting side effects are both unexpected and detrimental to human health (Brents *et al.*, 2011; Fantegrossi *et al.*, 2014). Reported effects of synthetic cannabinoids have included cardiac arrhythmia, severe CNS depression, and seizures (Abouchedid, et al., 2016). These compounds have even been reported to induce intense withdrawal symptoms (Cooper, 2016). Synthetic cannabinoid use worldwide is far beneath that of natural cannabis, but use of Spice during pregnancy cannot be ruled out. One report from The American College of Obstetricians and Gynecologists describes a case of a woman who took Spice while 35 weeks pregnant (2013). She was admitted after suffering a seizure and was found to be ecclamptic. The baby was delivered after emergency caesarian section and survived, but no follow up studies were reported. Because these compounds are so potent, even exposures that do not result in apparent toxicity could have long term effects on placental function and fetal development. Taken together with the data presented in Chapter 3, synthetic cannabinoids could also compromise placental barrier function driven by CB-dependent changes in transporter expression.

The class of cannabinoids encompasses a virtually boundless number of endogenous, natural, and synthetic compounds, and there is limited data on the effects of even the most well-known cannabinoids during pregnancy. It is therefore worthwhile for future

studies to more deeply investigate the relationship between cannabinoids and the placenta.

Cholesterol

In previous studies using BCRP-transfected MDCK cells, BCRP was shown to localize to a subgroup of lipid rafts termed caveolae. Caveolae are small, flask-shaped invaginations in the plasma membrane that participate in functions similar the larger class of lipid rafts (mechanosensing, signal transduction, endocytosis) (reviewed in Das and Das, 2012). Caveolae are especially plentiful in endothelial cells, adipocytes, and embryonic notochord cells. Besides their shape, caveolae are characterized by localized expression of caveolins and cavins, proteins thought to oligomerize in order to form and maintain the unique structure of caveolae. Density gradient ultracentrifugation of MDCK cells demonstrated BCRP in lipid raft fractions along with caveolin-1 (Storch, et al., 2007). Importantly, caveolin also immunoprecipitates with BCRP when a BCRP antibody is used, suggesting that the two proteins physically interact *in situ* (Herzog, et al., 2011). Further, caveolin-1 shRNA knockdown decreased BCRP activity in MDCK cells, as determined by pheophorbide A retention and viability in the presence of mitoxantrone (Herzog, et al., 2011). These data suggested that caveolin-1 was required for BCRP to function fully. However, syncytiotrophoblasts, which have functional BCRP, express little to no caveolin-1 protein, and electron microscopy of the placenta shows plentiful caveolar structures in the fetal endothelium but not in the syncytium (Byrne *et al.*, 2007; Linton *et al.*, 2003; Lyden *et al.*, 2002). While caveolin-1 does contribute to BCRP activity in other cell types, it is unlikely that caveolin-1 is necessary for placental BCRP function. Our study therefore examined that placental BCRP activity is dependent on lipid rafts cholesterol but independent of caveolae formation and caveolin-1 interaction.

The precise mechanism by which BCRP activity is dependent on cholesterol was not determined in our study. Several potential mechanisms were hypothesized in Chapter 4 including 1) cholesterol promotes BCRP oligomerization, 2) cholesterol binds to BCRP to alter its conformation to an active state, and 3) cholesterol fills empty space in the substrate binding site to promote BCRP interaction with small, hydrophobic molecules. Additionally, membrane cholesterol could be directly interacting with hydrophobic BCRP substrates to promote their interaction with the plasma membrane. It has been postulated that BCRP contains multiple binding sites including one (transmembrane helix 2) that can interact with molecules from the inner leaflet in the plasma membrane, rather than the intercellular space (Cai *et al.*, 2010; Rosenberg *et al.*, 2015). In this mechanism of efflux, BCRP activity would depend on how efficiently a substrate enters the membrane and its proximity to the BCRP active site. Because BCRP associates with cholesterol in the plasma membrane (Hegedus, et al., 2015; Telbisz, et al., 2013), lipid rafts may therefore promote the direct interaction between BCRP and its substrates.

Our conclusions rely on certain assumptions about lipid rafts that still remain controversial (summarized in Levental and Veatch, 2016). While it has been firmly established that plasma membranes tend to separate into ordered and disordered liquid phases, it is not clear to what extent lipid rafts *per se* contribute to biological processes. This uncertainty has been rooted in the difficulty of lipid raft detection and the limitations of the methods used to study them. First of all, lipid rafts are not permanent, discrete structures like most organelles. Lipid rafts are instead the result of a dynamic, heterogeneous plasma membrane composed of hundreds of distinct lipids that associate and segregate based on biochemical properties including hydrophobicity and chain length. Cholesterol, for example, can self-aggregate because of hydrogen bonding, therefore decreasing fluidity. Lipid rafts have been hypothesized to exist anywhere from

nanoseconds to milliseconds, and understanding this time resolution can determine if lipid rafts are relevant to biological processes. It is important to note that the methods used to study lipid rafts have noted limitations. Density gradient ultracentrifugation was used to isolate and analyze lipid rafts in Chapter 3, and this is a well-established and frequently used method in the field of lipid raft research. However, it is understood that this technique is not necessarily indicative of cellular conditions *in situ*. It is possible that observations using this technique are instead artifacts of the individual chemical properties of the specific proteins analyzed. Advanced imaging techniques have been employed to study lipid rafts *in situ*, but there still exists no conclusive proof of lipid rafts. Immunofluorescent imaging techniques including fluorescence resonance energy transfer have been used to visualize lipid rafts but often rely on protein-protein interaction rather than lipid-lipid or protein-lipid interactions. Lipid rafts are hypothesized to be 15 to 50 nm in size, and as a result attempts to image the lipids themselves using fluorescent probes and super resolution microscopy have also failed because of the spatial and time resolution required.

In order to work around directly imaging lipid rafts, cholesterol depletion methods have been employed study their functional relevance. Cyclodextrins are often used to sequester cholesterol from the plasma membrane. Using cyclodextrins, cholesterol depletion has been shown to inhibit membrane trafficking, signaling, and immune cell activation (reviewed in Levental and Veatch, 2016). Methyl-β-cyclodextrin was used in Chapter 4 to demonstrate the role of cholesterol in BCRP efflux. However, cholesterol depletion is inherently pleiotropic, impacting membrane permeability, ion polarity, and ultimately cell viability. While all the potential effects of methyl-β-cyclodextrin in BeWo cells cannot be accounted for, the specific role of cholesterol in BCRP activity was also examined using pravastatin. Pravastatin inhibits cholesterol synthesis and is a milder

and slower treatment than methyl-β-cyclodextrin. These experiments also incorporated a cholesterol repletion treatment in an effort to elucidate the specific role of cholesterol in BCRP efflux activity.

Our findings ultimately highlight the importance of adequate circulating cholesterol levels during pregnancy. Cholesterol therefore may be an important factor to consider when prescribing during pregnancy that is not currently taken into account. While cyclodextrins and statins are not currently prescribed during pregnancy, the StAmP clinical trial (Statins for the Amelioration of Preeclampsia) is currently investigating pravastatin as potential therapeutic for preeclamptic patients (ClinicalTrials.gov, 2018). Statins have been observed to exhibit pleiotropic effects beyond lowering cholesterol. For instance, statins promote anti-inflammatory gene expression, nitric oxide production, and endothelial function (Endres *et al.*, 1998; Fox *et al.*, 2011; Grosser *et al.*, 2004; Laufs *et al.*, 1997). Building on the observations in pregnant B6D2F1 mice that pravastatin lowers circulating soluble vascular endothelial growth factor-1 (Kumasawa *et al.*, 2011), a preeclampsia biomarker, pravastatin may soon prove a useful therapeutic in the treatment of preeclampsia. Statins are not currently prescribed during pregnancy, but multiple studies have shown statin administration to be safe during pregnancy (Kazmin *et al.*, 2007; Ofori *et al.*, 2007; Taguchi *et al.*, 2008). It should be noted, however, that, based on the evidence presented in Chapter 4, pravastatin can potentially reduce BCRP function and therefore increase placental drug permeability. This increases the risk of fetal metabolic dysfunction, for instance, if a pregnant mother is prescribed both pravastatin and glyburide. There are also a number of other compounds relevant to a pregnant mother that can interfere with membrane cholesterol and fluidity. For instance, polyunsaturated fatty acids, like those present in fish oil supplements and prescribed prenatal vitamins, are well known to lower cholesterol and can integrate directly into

plasma membranes, increasing membrane fluidity (Shaikh, 2012). Studies in plasma membrane vesicles have also shown that amphipathic compounds like bile acids, menthol, and synthetic detergents can decrease membrane phase separation (indicating a decrease in lipid raft integrity) (Gray *et al.*, 2013; Zhou *et al.*, 2013). Future studies can incorporate these more relevant exposures to determine their impact on placental BCRP activity and drug disposition during pregnancy.

Conclusion

The objective of this dissertation was to improve our understanding of transplacental xenobiotic disposition in order to increase the likelihood of healthy offspring. The observations put forward herein describe the fetoprotective role of the BCRP transporter in limiting *in utero* exposure to the estrogenic mycotoxin, zearalenone. Further, this research proposes that the fetoprotective activity of BCRP in limiting the placental transfer of zearalenone can be regulated by two classes of lipids: endocannabinoids and cholesterol. Taken together, these data highlight the importance of placental xenobiotic transporters to ensuring proper fetal development as well as demonstrate the ability of nutritional and environmental factors to impact the effectiveness of the placental barrier.

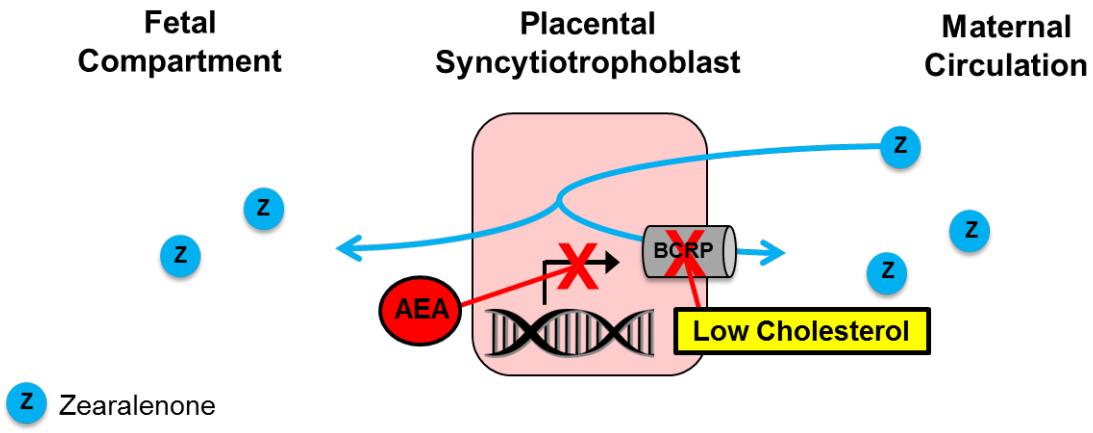

Fig 5.1. Graphical summary of overall project.

APPENDIX 1: SELECTIVE TARGETING OF HEME PROTEIN IN CYTOCHROME P450 AND NITRIC OXIDE SYNTHASE BY DIPHENYLENEIODONIUM

John T. Szilagyi[*], Vladimir Mishin[†], Diane E. Heck[‡], Yi-Hua Jan*, Lauren M. Aleksunes[†], Jason R. Richardson[§], Ned D. Heindel[¶], Debra L. Laskin[†] and Jeffrey D. Laskin*

Affiliations:

*Department of Environmental and Occupational Health, Rutgers University School of Public Health, Piscataway, NJ

[†]Department of Pharmacology and Toxicology, Rutgers University, Piscataway, New Jersey

[‡]Department of Environmental Health Science, New York Medical College, Valhalla, New York

[§]Department of Pharmaceutical Sciences, Northeast Ohio Medical University, Rootstown, OH

[¶]Department of Chemistry, Lehigh University, Bethlehem, PA

A-1.1 Abstract

Cytochrome P450 (CYP) enzymes mediate mixed-function oxidation reactions important in drug metabolism. The aromatic heterocyclic cation, diphenyleneiodonium (DPI) binds flavin in cytochrome P450 reductase and inhibits CYP-mediated activity. DPI also inhibits CYP by directly interacting with heme. Herein we report that DPI effectively inhibits a number of CYP-related monooxygenase reactions including NADPH oxidase, a microsomal enzyme activity that generates hydrogen peroxide in the absence of metabolizing substrates. Inhibition of monooxygenase by DPI was time- and concentration-dependent with IC_{50}'s ranging from 0.06-1.9 μM. Higher (4.6-23.9 μM), but not lower (0.06-1.9 μM), concentrations of DPI inhibited electron flow via cytochrome P450 reductase, as measured by its ability to reduce cytochrome c and mediate quinone redox cycling. Similar results were observed with inducible nitric oxide synthase (iNOS), an enzyme containing a C-terminal reductase domain homologous to cytochrome P450 reductase that mediates reduction of cytochrome c, and an N-terminal heme-thiolate oxygenase domain mediating nitric oxide production. Significantly greater concentrations of DPI were required to inhibit cytochrome c reduction by iNOS (IC_{50} = 30 μM) than nitric oxide production (IC_{50} = 0.2 μM). Difference spectra of liver microsomes, recombinant CYPs and iNOS demonstrated that DPI altered heme-carbon monoxide interactions. In the presence of NADPH, DPI treatment of microsomes and iNOS yielded a type II spectral shift. These data indicate that DPI interacts with both flavin and heme in CYPs and iNOS. Increased sensitivity for inhibition of CYP-mediated metabolism and nitric oxide production by iNOS indicates that DPI targets heme moieties within the enzymes.

Abbreviations

βNF, β-naphthoflavone; CYP, cytochrome P450; DETAPAC, diethylenetriaminepentaacetic acid; DEX, dexamethasone; DPI, diphenyleneiodonium; FAD, flavin adenine dinucleotide; FMN, flavin mononucleotide; iNOS, inducible nitric oxide synthase; ISN, isoniazid; PCN, pregnenolone-16 α-carbonitrile.

A-1.2 Introduction

It is well recognized that microsomal enzyme complexes are essential for carrying out many metabolic reactions including xenobiotic transformation. This process is mediated by several successive steps involving electron transport and oxygen activation (Poulos, 2005). Initially, electrons flow from NADPH to cytochrome P450 reductase, a flavin adenine dinucleotide (FAD) and a flavin mononucleotide (FMN) containing enzyme. Via an interflavin electron transfer between stable semiquinone FAD/FMN intermediates, there is sequential donation of two electrons to the heme containing cytochrome P450 (CYP) enzymes (Gutierrez *et al.*, 2002). This latter reaction can simultaneously generate hydrogen peroxide (H_2O_2), a process referred to as oxidase activity or "uncoupling" of the microsomal electron transport chain (De Matteis *et al.*, 2012; Gillette *et al.*, 1957). Interflavin electron transfer within cytochrome P450 reductase can also mediate the reduction of several substrates including cytochrome c and ferricyanide; it can also mediate quinone redox cycling (Guengerich *et al.*, 2009; Lemaire and Livingstone, 1994; Murataliev *et al.*, 2004; Vermilion and Coon, 1978a).

The diaryliodonium salt, diphenyleneiodonium (DPI), is an aromatic heterocyclic cation and a potent arylating agent (Banks, 1966). It is known to inhibit cytochrome P450 reductase, as well as other flavin-containing enzymes including NADPH oxidase (O'Donnell *et al.*, 1993), xanthine oxidase (Doussiere and Vignais, 1992), protoporphyrinogen oxidase (Arnould and Camadro, 1998), mitochondrial respiratory chain complex I (Majander *et al.*, 1994), and several forms of nitric oxide synthase (Stuehr *et al.*, 1991). DPI is thought to function by reacting with flavin cofactors within these enzymes, a process that interferes with electron transport. In the case of cytochrome P450 reductase, DPI modifies reduced FMN and effectively blocks its ability to reduce cytochrome c and quinone redox cycling (Gray *et al.*, 2007; O'Donnell *et al.*,

1994; Wang *et al.*, 2008c). The flavin cofactor target in nitric oxide synthase is not well characterized (Stuehr, et al., 1991). Alternative sites of action for DPI have also been reported including metal-bound porphyrins and proteins (Doussiere *et al.*, 1999; O'Donnell, et al., 1993). DPI has been shown to generate aryl ferric complexes with a synthetic ferrous tetraphenylporphyrin and the heme porphyrin in microsomal CYPs (Battioni *et al.*, 1988) in a manner generally similar to methyl- and phenylhydrazine (Delaforge *et al.*, 1986).The heme component of neutrophil NADPH oxidase is also a target for DPI (Doussiere, et al., 1999). As CYP-dependent monooxygenase activity requires both flavins in cytochrome P450 reductase and heme in the CYPs, either or both could be a target for DPI. Similarly, nitric oxide synthases are proteins with flavin-containing C-terminal domains homologous to cytochrome P450 reductase, and N-terminal heme-thiolate oxygenase domains (Stuehr, 1999), each of which has the potential to react with DPI (Stuehr, et al., 1991). The present studies show that in CYP enzymes and nitric oxide synthase, DPI targets both flavins and heme. Reactions mediated by heme are more sensitive to inhibition than reactions mediated by flavins indicating that DPI preferentially targets heme in these enzymes.

A-1.3 Materials and Methods

Materials

Recombinant microsomal proteins from baculovirus infected insect cells containing human NADPH cytochrome P450 reductase enzyme or cytochrome P450 reductase co-expressed with either CYP1A2, CYP2E1 or CYP3A4 were obtained from BD Gentest (Woburn, MA). Control liver microsomes and microsomes from pregnenolone-16 α-carbonitrile (PCN)-, dexamethasone (DEX)-, β-naphthoflavone (βNF)-, isoniazid (ISN)-treated Sprague Dawley rats and human liver microsomes from a mixed gender pool of 50 samples were from XenoTech (Lenexa, KS). Amplex Red (10-acetyl-3,7-dihydroxyphenoxazine) was from Molecular Probes (Eugene, OR). Mouse recombinant inducible nitric oxide synthase (iNOS) expressed in *E. coli* (cat #N2783), glucose-6-phosphate dehydrogenase, trichloroacetic acid, p-nitrophenol, horseradish peroxidase, NADPH, glucose, cytochrome c from horse heart, bovine hemin, sodium azide, 30% H_2O_2, ferricyanide, dibenzylfluorescein, methoxyresorufin, ethoxyresorufin, 7-ethoxycoumarin, menadione, diethylenetriaminepentaacetic acid (DETAPAC), and all other chemicals were from Sigma-Aldrich (St. Louis, MO).

Enzyme Assays

All enzyme assays were performed in 96-well flat bottom microwell plates. Data were collected using a SoftMax Pro 6.3 software controlled SpectraMax M3 Multimode Microplate Reader (Molecular Devices, Sunnyvale, CA) and analyzed using GraphPad Prism 5 (La Jolla, CA). Unless otherwise described, the enzymatic activities were measured continuously, and linear rates of product formation were analyzed in triplicate. Unless otherwise indicated, DPI, prepared in DMSO (1% final concentration), was added to reaction mixtures prior to NADPH.

For CYP metabolic assays, dibenzylfluorescein, 7-methoxyresorufin, and 7-ethoxyresorufin were used to assess CYP3A, CYP1A2, and CYP1A1 activity,

respectively (Ghosal *et al.*, 2003). In order to assess CYP2E1 metabolic activity, either 7-ethoxycoumarin or p-nitrophenol was used as the substrate. Briefly, reaction mixtures contained 100 mM potassium phosphate buffer (pH 7.4), 1.0 mM DETAPAC, 5 µM dibenzylfluorescein, methoxyresorufin or ethoxyresorufin, or 500 µM 7-ethoxycoumarin, and 50-100 µg/mL liver microsomal or 25 µg/mL recombinant enzyme proteins in a final volume of 0.1 mL. Reactions were initiated by the addition of NADPH and an NADPH regenerating system (200 µM NADPH, 5.0 mM glucose-6-phosphate and 1 U/mL glucose-6-phosphate dehydrogenase, final concentrations). The excitation and emission wavelengths used for CYP substrates were 485 nm and 530 nm for dibenzylfluorescein, 535 nm and 580 nm for resorufin, and 380 nm and 460 nm for 7-hydroxycoumarin. In pre-incubation experiments, reaction mixtures contained DPI, microsomal proteins, NADPH and an NADPH regenerating system and were initiated by the addition of the CYP substrate.

The CYP2E1-dependent conversion of p-nitrophenol to p-nitrocatechol was assayed by high performance liquid chromatography using a LUNA 250x2 column as described previously (Mishin *et al.*, 1996). Briefly, reaction mixtures contained 100 mM potassium phosphate buffer (pH 6.9), 1.0 mM DETAPAC, 20 µM p-nitrophenol, and 500 µg/mL liver microsomal proteins in a final volume of 0.1 mL. Reactions were initiated by the addition of NADPH (200 µM). Reactions were terminated using 10 µL 20% trichloroacetic acid and centrifuged at 4000 x g for 20 min before analysis. The amounts of p-nitrocathecol formed were calculated using CLASS-VP V5 software.

Cytochrome P450 reductase-mediated reduction of cytochrome c was assayed by monitoring changes in absorbance at 550 nm as described by Guengerich et al. (2009). Briefly, reaction mixtures contained 100 mM potassium phosphate buffer (pH 7.8), 40

μM cytochrome c and 40 μg/mL microsomal proteins, 1 μg/mL recombinant enzymes or 1 μg/mL iNOS in a final volume of 0.2 mL. Reactions were initiated by the addition of NADPH and an NADPH regenerating system. In pre-incubation studies, reaction mixtures contained DPI, microsomal proteins, NADPH and an NADPH regenerating system and were initiated by the addition of cytochrome c. Cytochrome P450 reductase-mediated reduction of ferricyanide was assayed by measuring changes in absorbance at 420 nm as described by Vermilion et al. (1981). Reaction mixtures contained 100 mM potassium phosphate buffer (pH 7.8), 0.5 mM ferricyanide and 200 μg/mL microsomal or 50 μg/mL recombinant enzyme proteins in a final volume of 0.1 mL. Reactions were initiated by the addition of NADPH and an NADPH regenerating system.

The Amplex Red reaction was used to measure CYP-mediated H_2O_2 formation in NADPH oxidase assays and in cytochrome P450 reductase-mediated menadione redox cycling assays as previously described (Fussell *et al.*, 2011a; Mishin *et al.*, 2010). Briefly, reaction mixtures contained 100 mM potassium phosphate buffer (pH 7.8), 1.0 mM sodium azide, 1.0 mM DETAPAC, and 40 μg/mL microsomal or 10 μg/mL recombinant enzyme protein in a final volume of 0.1 mL. Reactions were initiated by the addition of NADPH and an NADPH regenerating system. For cytochrome P450 reductase mediated chemical redox cycling, reactions were supplemented with 200 μM menadione, and the linear rate of resorufin formation in the presence of horseradish peroxidase (2.75 units/mL) and Amplex Red (50 μM) was continuously monitored on the microplate reader using excitation and emission wavelengths of 530 nm and 585 nm, respectively. H_2O_2 formation by CYP enzymes was measured by adding horseradish peroxidase (2.75 units/mL) and Amplex Red (50 μM) five min after the start of the reactions and immediately recording the fluorescence at a single time point. iNOS as recombinant enzyme was used in the present studies since it was readily available from

commercial sources. Nitric oxide production by iNOS in enzyme assays was quantified using an Ionics/Sievers nitric oxide analyzer (GE Instruments, Boulder, CO) (Shi *et al.*, 2013). Briefly, reaction mixtures in a final volume of 50 µL contained 100 mM potassium phosphate buffer (pH 7.4), 1 mM arginine, 20 µM tetrahydrobiopterin and 180 µM DTT. Reactions were initiated by the addition of NADPH and an NADPH regenerating system. After 5 min, 20 µL of the reaction mixture was assayed for nitrate by reduction-linked chemiluminescence using the nitric oxide analyzer. Argon purged vanadium chloride in 1 M HCl at 95°C was used as a reducing agent. Data are presented as the concentration of nitric oxide produced by the reaction mixture after 5 min, and assays were performed in triplicate.

The decrease of absorbance at 340 nm was used to analyze the conversion of NADPH to $NADP^+$ by CYP enzymes in the absence of substrate (Wang, et al., 2008c). Briefly, reaction mixtures contained 100 mM potassium phosphate buffer (pH 7.8), 1.0 mM sodium azide, 1.0 mM DETAPAC, and 0.5 mg/mL microsomal protein or 0.1 mg/mL recombinant protein in a final volume of 0.1 mL. Reactions were initiated by the addition of 200 µM NADPH.

Spectral Studies

Heme binding spectra and carbon monoxide difference spectra were recorded on the SpectraMax M3 Multi-mode Microplate Reader as previously described (Guengerich, et al., 2009; Locuson *et al.*, 2007). Reaction mixtures for all spectra contained 100 mM potassium phosphate buffer (pH 7.4), 10% glycerol, 0.5 mM EDTA and either 2 mg/mL rat liver microsomes from β-NF treated rats, 40 µM hemin, or 1 mg/mL recombinant iNOS in one mL cuvettes. Reactions mixtures were incubated in the presence of DPI or vehicle for 10 min in the dark at room temperature. The reference cuvette for each

spectrum contained all components of the reaction mixture except for carbon monoxide. For binding spectra, the sample cuvette contained DPI and the reference cuvette contained vehicle control. Reaction mixtures were incubated in the dark and, after 10 min at room temperature, 100 μM NADPH or a few grains of sodium dithionite was added to both cuvettes and the mixture incubated for an additional 10 min before analysis with or without carbon monoxide.

A-1.4 Results

Effects of DPI on Microsomal CYP Enzyme Activities

Initially, we examined the effects of DPI on the CYP activity of rat liver microsomes from β-NF treated rats. Using methoxyresorufin as the substrate for CYP1A2, we found that formation of the product, resorufin, was time- and NADPH-dependent (**Fig A1.1** and not shown). DPI (10 μM) blocked CYP1A2 activity in a time-dependent manner; thus, pre-incubation of the microsomes with DPI and NADPH for 0 to 20 min increased their sensitivity to inhibition (IC_{50} = 0.56 μM, 0.15 μM, and 0.03 μM for 0, 5 and 20 min pre-treatments with DPI and NADPH, respectively) (**Fig A1.1**). Pre-incubation of the microsomes with DPI in the absence of NADPH did not increase their sensitivity to inhibition (IC_{50} = 0.99 μM, 0.79 μM, and 0.81 μM for 0, 5 and 20 min pre-treatments with DPI, respectively) (not shown). These data suggest that DPI binds irreversibly to microsomal electron transport complexes. The reduction of cytochrome c, a marker for cytochrome P450 reductase activity in β-NF microsomes, was also found to be time- and NADPH-dependent (**Fig A1.1** and not shown). Higher concentrations of DPI (100 μM) were required to inhibit cytochrome c reduction. As observed with CYP1A2 activity, pre-incubation of microsomes with DPI and NADPH for 0 to 20 min increased the sensitivity of cytochrome c reductase activity to inhibition (IC_{50} = 8.5 μM, 0.79 μM, and 0.15 μM for 0, 5 and 20 min pre-treatments with DPI and NADPH, respectively). However, at each pre-incubation time with DPI and NADPH (0, 5 or 20 min), CYP1A2 activity was significantly more sensitive to inhibition than cytochrome c reductase activity in the microsomes. Pre-incubation of the microsomes with DPI in the absence of NADPH did not increase their sensitivity to inhibition (IC_{50} = 5.48 μM, 8.33 μM, and 6.30 μM for 0, 5 and 20 min pre-treatments with DPI, respectively) (not shown).

Similar time-dependent effects of DPI pretreatments were observed with cytochrome P450 reductase and CYP activities in other microsomal preparations and recombinant CYP preparations. In each case, activity associated with CYP was more sensitive to DPI than activity associated with cytochrome P450 reductase (not shown). Enzymatic assays performed to assess the inhibitory potency of DPI on CYP- and cytochrome P450 reductase-dependent activities were thus carried out without pre-incubation with DPI and NADPH. **Fig A1.2** and **Table A1.1** compare the effects of DPI on rat and human liver microsomes as well as recombinant human CYPs when NADPH is added at time zero. CYP1A1 and CYP3A1/2 activities in β-NF microsomes were 11-19-fold more sensitive to DPI than cytochrome c reductase activity (**Table A1.1**, IC_{50} = 0.77 and 0.44 μM, vs. 8.50 μM respectively). CYP3A1 activity in PCN- and DEX-treated rat liver microsomes was 85- and 143-fold more sensitive to inhibition by DPI than cytochrome c reductase activity (**Table A1.1**, IC_{50} = 0.06 and 0.07 μM, vs. 5.10 μM and 10.0 μM, respectively). CYP2E1 activity in ISN rat liver microsomes was 16-25-fold more sensitive to DPI than cytochrome c reductase activity (**Table A1.1** and **Fig A1.2**, IC_{50} = 0.62 μM using 7-ethoxycoumarin as the substrate and 0.99 μM using p-nitrophenol as the substrate vs. 15.70 μM). It should be noted that, although 1% DMSO is known to inhibit CYP2E1 activity, the presence of this solvent did not affect the sensitivity of 7-ethoxycoumarin hydroxylase activity in ISN rat liver microsomes to DPI (IC_{50} = 0.32 μM, 0.33 μM, and 0.31 μM in the presence of 1%, 0.1%, and 0% DMSO, respectively) (not shown). CYP3A1/2 activity in ISN rat liver microsomes was 14-fold more sensitive to DPI than cytochrome c reductase activity (**Table A1.1** and **Fig A1.2**, IC_{50} = 1.16 μM vs. 15.70 μM), and CYP3A2 activity in control rat liver microsomes was 16-fold more sensitive than cytochrome c reductase activity (IC_{50} = 0.29 μM vs. 4.60 μM). CYP activity in human liver microsomes and human recombinant CYPs (1A2, 2E1 and 3A4) were also more sensitive to DPI than cytochrome c reductase activity. Thus, we found that CYP

activity was 11-12-fold more sensitive to DPI for these enzymes, when compared to activity for cytochrome c reduction (**Table A1.1** and **Fig A1.2**). The sensitivity of cytochrome c reductase activity to DPI in human recombinant cytochrome P450 reductase was generally similar to the rat and human microsomes and the human recombinant CYPs co-expressed with cytochrome P450 reductase (**Table A1.1** and **Fig A1.2**, IC_{50} = 16.7 μM).

It is well recognized that the CYPs also exhibit NADPH-dependent "oxidase" activity where the spontaneous oxidation of NADPH leads to the formation of H_2O_2 (Mishin *et al.*, 2014). Each of the microsomal preparations and human recombinant CYPs readily generated H_2O_2 (**Fig A1.1**, **Table A1.1** and not shown). Both substrate-independent H_2O_2 formation and NADPH oxidation by microsomes were blocked by DPI (**Figs A1.1 and A1.2** and **Table A1.1**). The sensitivity of these activities to DPI was similar to the CYP metabolic activity (IC_{50} = 0.17 – 1.70 μM for H_2O_2 formation and 0.22 – 0.56 μM for NADPH oxidation, respectively), and significantly more sensitive to inhibition than cytochrome P450 reductase mediated reduction of cytochrome c.

Cytochrome P450 reductase is also known to mediate chemical redox cycling, a process that generates H_2O_2 (Wang *et al.*, 2010). Using menadione as a redox cycling quinone, we found that the sensitivity of rat and human liver microsomes, as well as recombinant human cytochrome P450 reductase and CYP preparations, to DPI, was generally similar to their sensitivity to cytochrome c reduction by DPI (IC_{50} = 4.84 μM – 23.61 μM) (**Figs A1.1, A1.2** and **Table A1.1**). This was significantly less than their sensitivity to inhibition of CYP metabolic activity, as well as oxidase activity, by DPI. Cytochrome P450 reductase also reduces ferricyanide in the presence of NADPH (Vermilion and Coon, 1978b). Under our experimental conditions, DPI (up to 100 μM) had no significant

effect on reduction of ferricyanide in any of the microsomal preparations or recombinant enzymes examined (**Fig A1.2** and **Table A1.1**).

Spectral Analysis of CYP450 and iNOS

The reduced and oxidized intermediate states of heme containing proteins can be identified by specific spectral characteristics and interconversion of these different states provides insights into reaction mechanisms. Spectral intermediates are identified based on changes in the Soret bands of heme, as well as in the visible spectrum. We next examined the spectral characteristics of CYP heme and free hemin following DPI treatment using difference spectrophotometry. The difference spectrum of carbon monoxide-bound CYP heme and free hemin displayed characteristic peaks at 450 nm and 412 nm, respectively (**Fig A1.3**). DPI caused a concentration-dependent reduction in the height of peaks at concentrations as low as 5 μM for hemin and 0.1 μM for the microsomes. A characteristic type II spectral shift with a trough at 416 nm and peak at 426 nm was present in the difference spectrum of CYP in the presence of NADPH and DPI (**Fig A1.3**). In the absence of NADPH, DPI did not induce any spectral changes in rat liver microsomes (not shown). In free hemin, DPI induced a similar spectral shift with a trough at 366 nm and a peak at 426 nm. The intensity of the spectral changes was dependent on the concentration of DPI with both CYP heme and free hemin. With both microsomes and hemin, the effects of DPI were time dependent (**Fig A1.3**, insets).

Nitric oxide synthase is a dual flavin-containing cytochrome c reductase; it also possesses heme-dependent nitric oxide generating activity (White and Marletta, 1992). We found that DPI inhibits both the cytochrome c reductase and the nitric oxide generating activity of iNOS (**Fig A1.4**). Approximately 20-fold higher concentrations of DPI were required to inhibit cytochrome c reductase activity of iNOS when compared to

nitric oxide production (IC_{50} = 3.50 and 0.16 μM, respectively). DPI was also found to alter the spectral properties of iNOS. Reduced iNOS generated a carbon monoxide spectrum with a characteristic peak at 447 nm. A concentration-dependent decrease in peak height was noted in the presence of DPI (**Fig A1.4**).

A-1.5 Discussion

DPI is an arylating agent that acts via a radical based mechanism. Initial abstraction of an electron from a nucleophile by DPI generates a phenyl radical, this radical then adds back to a nucleophile to form covalent adducts (O'Donnell, et al., 1994). The best characterized DPI adducts are with flavin cofactors in enzymes and based on these data, DPI has been widely used as a flavoenzyme inhibitor (Basu *et al.*, 2014; Chiapella *et al.*, 2000; Cross *et al.*, 1990; Venkatachalam *et al.*, 2008). However, the actions of DPI are not enzyme specific; thus many flavoenzymes, including cytochrome P450 reductase, are inhibited by DPI (O'Donnell, et al., 1994). The present studies confirmed that DPI is an effective inhibitor of cytochrome P450 reductase in rat and human liver microsomes, in recombinant cytochrome P450 reductase, and in recombinant CYPs co-expressed with cytochrome P450 reductase. Inhibition of cytochrome P450 reductase by DPI was also found to block electron transfer to CYPs resulting in inhibition of their monooxygenase activity. Inhibition of these enzyme activities was time-dependent. These findings are consistent with the idea that DPI is a mechanism-based inhibitor (McGuire *et al.*, 1998).

In earlier studies, DPI was also shown to modify heme moieties in microsomal CYPs and neutrophil NADPH oxidase (Battioni, et al., 1988; Doussiere, et al., 1999). In the case of NADPH oxidase, two components of the enzyme, FAD and heme *b*, could be modified by DPI (Doussiere, et al., 1999). However, our spectral studies showed that DPI caused a decrease in NADPH oxidase activity that was directly correlated with decreases in the

absorbance of the Soret peak of flavocytochrome *b* in NADPH-treated neutrophil membranes, indicating that heme is the predominant target for DPI.

Our studies also showed that DPI reacts with CYP heme in liver microsomes generating characteristic type II difference spectra, as well as decreases in the carbon monoxide difference spectra. These data indicate that DPI can alter the CYP heme thiolate structure (Locuson, et al., 2007; Omura and Sato, 1964). Changes in the heme spectra occurred at concentrations of DPI that inhibited CYP, but not cytochrome P450 reductase, also supporting the idea the heme is an important target for DPI. The actions of DPI were not limited to CYP heme as the difference spectrum of hemin, a simple ferric iron ion containing protoporphyrin IX with a chloride ligand, showed similar changes in its type II spectra and carbon monoxide difference spectra after DPI treatment. Taken together, these data provide additional support for the idea that DPI reacts with heme structures.

As CYP-mediated reactions require both the flavoenzyme cytochrome P450 reductase as the electron donor, and heme containing CYP for monooxygenase activity, a question arises as to whether DPI preferentially targets the flavoenzyme or heme in the CYPs. To address this, we performed a dose-response analysis of the different metabolic reactions carried out by the two components of the CYP complexes. For cytochrome P450 reductase, we quantified the effects of DPI on cytochrome c reduction and menadione redox cycling, and for CYP, we measured CYP-mediated substrate metabolism, NADPH oxidation and oxidase activity. In all liver microsomal preparations including human microsomes, control rat microsomes and microsomes from rats treated with DEX, PCN, βNF or ISN, as well as human recombinant CYP1A2, 2E1 and 3A4, reactions mediated by CYP heme were markedly more sensitive to inhibition by DPI than the flavin-dependent reactions mediated by cytochrome P450 reductase. The activities of

recombinant cytochrome P450 reductase were similar to those of the recombinant enzymes and the microsomes. Of the best characterized CYP system reactions (reduction of cytochrome c and CYP monooxygenase activity), DPI-mediated inhibition of CYP activity was 9.4-22.3-fold more sensitive than inhibition of cytochrome c reduction in recombinant enzymes and 11.0-143-fold more sensitive in the liver microsomes. These data, together with our findings that concentrations of DPI that inhibit CYP activity, but not cytochrome P450 reductase activity, induce a type II difference spectra, support the idea that DPI selectively targets heme in the CYP complex. Also of note were our findings that differences in sensitivity to DPI in reactions mediated by cytochrome P450 reductase and CYP were independent of DPI pretreatments of the enzyme preparations. Thus, while the sensitivity of each of the reactions increased following pre-treatment with the inhibitor, CYP-mediated reactions remained more sensitive to DPI than cytochrome P450 reductase-mediated reactions. These data further support the idea of similar reactivity via a mechanism-based reaction to the flavin and heme binding sites of the CYP complex.

When comparing reactions in different recombinant CYP preparations, sensitivity to DPI was generally similar. However, with microsomal preparations, more variation was noted, presumably due to greater variability in content of CYP complex enzymes, as well as non-CYP components in the microsomes. Of particular interest were our findings that DPI was unable to inhibit reduction of ferricyanide in any of the recombinant or microsomal preparations (IC_{50} > 100 μM). It has long been recognized that cytochrome P450 reductase mediates the one electron reduction of ferricyanide in a reaction mediated by FAD (Kurzban and Strobel, 1986; Vermilion, et al., 1981; Vermilion and Coon, 1978b). In fact, FMN-free cytochrome P450 reductase retains the ability to reduce ferricyanide, but not reduction of cytochrome c (Vermilion et al. 1981). Similarly,

site-directed mutagenesis of Tyr-178 in cytochrome P450 reductase blocks FMN binding and cytochrome c reductase activity; however, the mutant enzyme retains ferricyanide reductase activity in direct correlation with its FAD content (Shen *et al.*, 1989). Similarly, mutations in neuronal nitric oxide synthase acidic and aromatic residues in the FMN binding domain destabilizes FMN enzyme binding, which also results in a loss of cytochrome c reductase activity but not ferricyanide reductase activity (Adak *et al.*, 1999). These data are consistent with earlier findings that DPI directly binds to FMN in cytochrome P450 reductase and the fact FMN is critical for mediating the one electron reduction of cytochrome c (Huang *et al.*, 2015; Tew, 1993). As the one electron reduction of menadione during redox cycling is also inhibited by DPI, it appears that FMN is required for this reaction. In this regard, menadione redox cycling has also been reported to be inhibited in FMN-depleted cytochrome P450 reductase (Gherasim *et al.*, 2008; Vermilion, et al., 1981). Similarly, in another diflavin oxidoreductase, methionine synthase reductase, which is known to possess cytochrome c reductase and menadione redox cycling activity, a mutant enzyme with destabilized FMN binding, displays only a limited capacity to carry out these reactions (Gherasim, et al., 2008; Vermilion, et al., 1981), further supporting the idea that FMN mediates quinone redoxy cycling.

Like the CYP complex, nitric oxide synthases contain a reductase domain homologous to cytochrome P450 reductase that mediates electron transfer from NADPH to a heme-thiolate oxygenase domain; in the case of nitric oxide synthase, this domain mediates nitric oxide production from L-arginine. Using iNOS, we found that significantly greater concentrations of DPI were required to inhibit cytochrome c reduction (IC_{50} = 30 µM) than nitric oxide production (IC_{50} = 0.2 µM). Difference spectra using recombinant iNOS demonstrated that DPI altered the interaction between heme and carbon monoxide causing a decrease in the magnitude of the absorption peak at 450 nm. Overall, our

data indicate that DPI interacts with both flavin and heme in CYPs and iNOS. Increased sensitivity for inhibition of CYP-mediated metabolism and nitric oxide production by iNOS indicates that DPI selectively targets heme moieties in the enzymes.

It should be noted that, in addition to the CYPs, cytochrome P450 reductase is an electron donor protein for heme oxygenase and several other enzymes including cytochrome b5, squalene monooxygenase and 7-dehydrocholesterol reductase (Porter, 2012). Targeting flavin in cytochrome P450 reductase by DPI would be expected to inhibit these enzyme activities. However, heme oxygenase is also a heme containing protein (Schuller *et al.*, 1999; Strittmatter, 1960). A comparison of DPI binding sites in this enzyme complex is required to determine if, like CYP and iNOS, there is preferential targeting of heme. Although cytochrome b5 also contains heme, it is unlikely to be a target for DPI due to biscoordination with His residues at its 5^{th} and 6^{th} ligands (Delaforge, et al., 1986).

Based on its ability to react with heme and inhibit heme-dependent reactions over flavin-dependent cytochrome P450 reductase- and iNOS-related reactions, we conclude that DPI preferentially binds to heme. At the present time, mechanisms mediating targeting of heme in the CYP system and iNOS are not known. It may be that the reaction of DPI with heme is kinetically more favorable than reactions with flavin in the enzymes. Alternatively, heme may be more accessible to modification in the enzymes, possibly through their substrate access channels. Cationic pathways for DPI-induced modifications with biological targets have also been proposed. These pathways, along with radical mediated pathways, are supported by data with arylations taking place on SP2 aromatic carbons, enolic methylenes, and a variety of other nucleophiles (Aggarwal and Olofsson, 2005; Chakraborty and Massey, 2002; Jalalian *et al.*, 2011; Modha and

Greaney, 2015; Wen *et al.*, 2012)**.** It is possible that the mechanism by which DPI reacts with flavins is distinct from its reactions with heme. Further studies are needed to more precisely define the mechanism(s) by which DPI interacts with CYP and iNOS to alter their functioning.

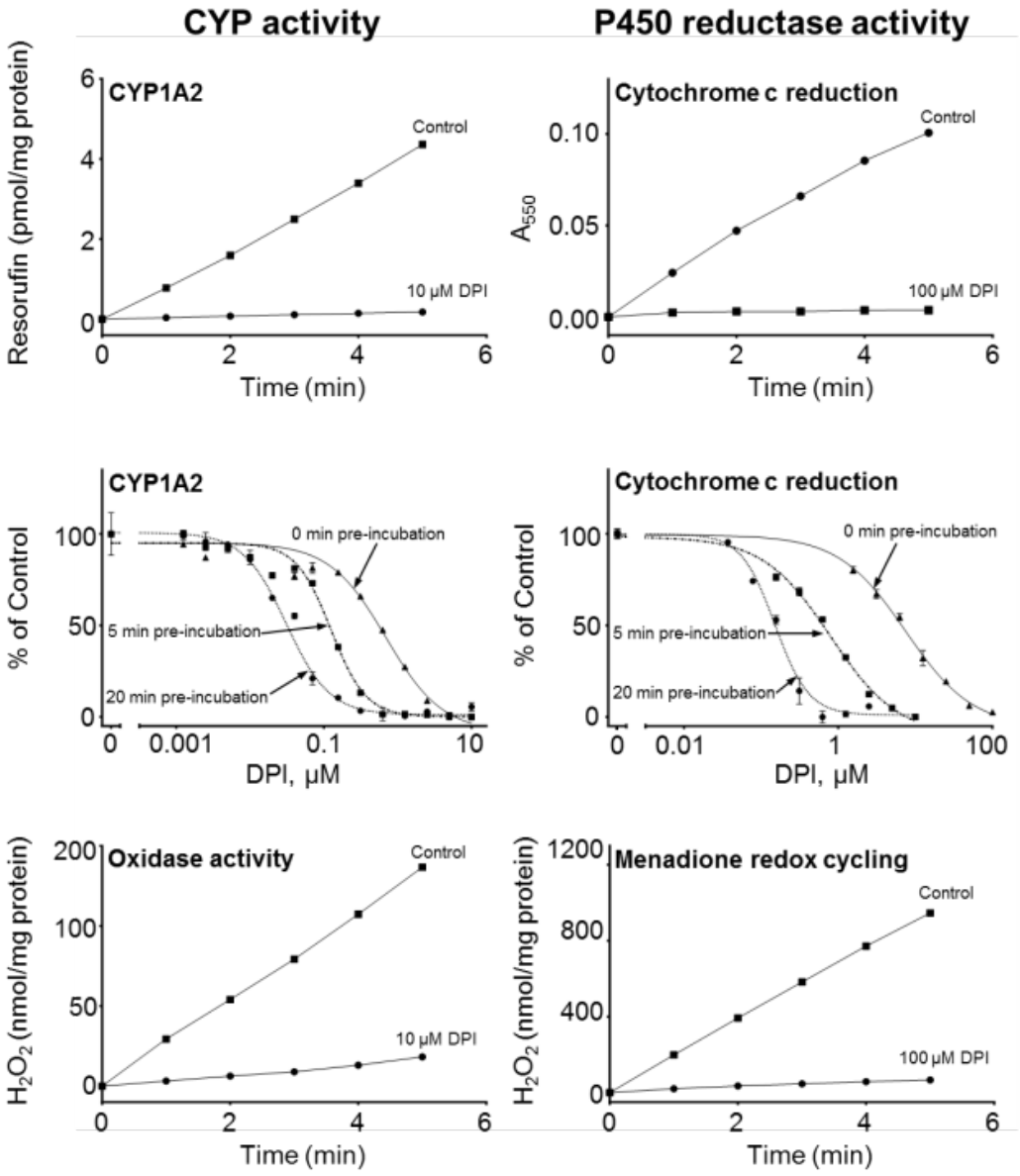

Fig A1.1. Effects of DPI on enzymatic activities of microsomes from β-NF treated rats.

Upper panels: CYP1A2 and cytochrome c reductase activity in microsomes from β-NF treated rats in the absence or presence of DPI. **Center panels:** Time-dependent inhibition of CYP1A2 and cytochrome c reductase activity. Microsomes were pre-

incubated with DPI and NADPH for 0, 5 and 20 min. Data are the mean ± SE (n = 3). **Lower panels:** CYP-mediated oxidase activity and cytochrome P450 reductase-mediated menadione redox cycling. Assays were run in the absence or presence of DPI. H_2O_2 formation was measured using the Amplex Red assay.

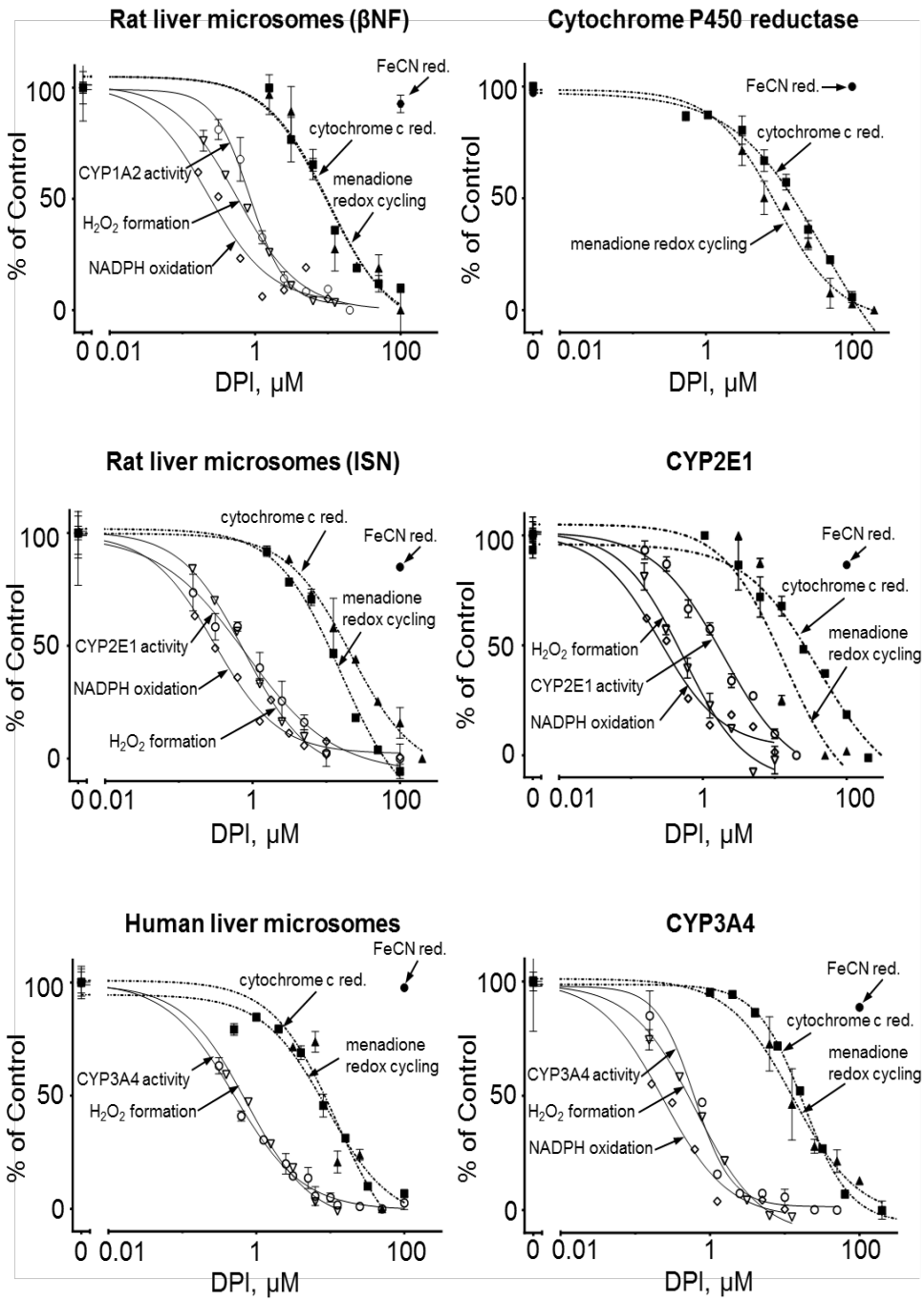

Fig A1.2. Effects of DPI on cytochrome P450 reductase and CYP activities in native liver microsomes and recombinant enzymes.

All enzyme assays were performed as described in the Materials and Methods. Black symbols represent cytochrome P450 reductase-mediated activities; white symbols represent CYP-mediated activities. Data for NADPH oxidation are results of duplicate measurements. Data in all other assays are the mean ± SE (n = 3). Enzyme reactions were run without pre-incubations with DPI.

Table A1.1. Summary of the effects of DPI on the cytochrome P450 reductase and CYP enzyme reactions in recombinant CYP450 enzymes, human liver microsomes and rat liver microsomes

		Cytochrome P450 reductase-mediated activity			CYP-mediated activity				$\frac{IC_{50}(cyt\ c)}{IC_{50}(CYP)}$
		Menadione redox cycling	Cytochrome c reduction	Ferricyanide reduction[b]	NADPH oxidation	H_2O_2 formation	CYP activity[d]		
		IC_{50} (μM)[a]			IC_{50} (μM)				
Rat liver microsomes	CTL[c]	4.84	4.60	>100	ND	0.17	0.29	3A2	15.90
	DEX	23.61	10.00	>100	0.31	0.48	0.07	3A1	142.90
	PCN	13.76	5.10	>100	0.35	0.90	0.06	3A1	85.00
	βNF	9.72	8.50	>100	0.22	0.60	0.77 0.56 0.44	1A1 1A2 3A1/2	11.00 15.20 19.30
	ISN	21.32	15.70	>100	0.31	0.81	0.62[e] (0.99)[f] 1.16	2E1 3A1/2	25.30[e] (15.89)[f] 13.50
Human enzymes	P450 Reductase[g]	9.28	16.70	>100	-	-	-		9.40
	CYP1A2	6.06	18.00	>100	0.56	1.40	1.90	1A2	61.30
	CYP2E1	12.39	23.91	>100	0.25	1.70	0.39	2E1	22.30
	CYP3A4	12.90	14.50	>100	0.24	0.39	0.65	3A4	11.90
	Liver Microsomes	12.15	8.90	>100	ND[h]	0.51	1.20 0.82 1.10[e] 0.75	1A1 1A2 2E1 3A4/5	7.40 10.85 8.09 9.40

a. IC_{50} values were measured without pre-incubations with DPI and NADPH
b. DPI did not inhibit the reduction of ferricyanide by cytochrome P450 reductase
c. Control (CTL), β-NF and ISN microsomes were from male rats. PCN and DEX microsomes were from female rats
d. Substrates used to evaluate CYP1A1, CYP1A2, and CYP3A activities were 7-ethoxyresorufin, 7-methoxyresorufin, and dibenzylfluorescein, respectively
e. Determined using 7-ethoxycoumarin as the substrate. 7-ethoxycoumarin is also known to be metabolized by CYP1A1, 1A2, and 2B1 in rat liver microsomes and 1A2 in human liver microsomes.
f. Determined using p-nitrophenol as the substrate.
g. P450 reductase, CYP1A2, CYP2E1 and CYP3A4 are recombinant human enzymes expressed in baculovirus infected insect cells
h. ND, not determined

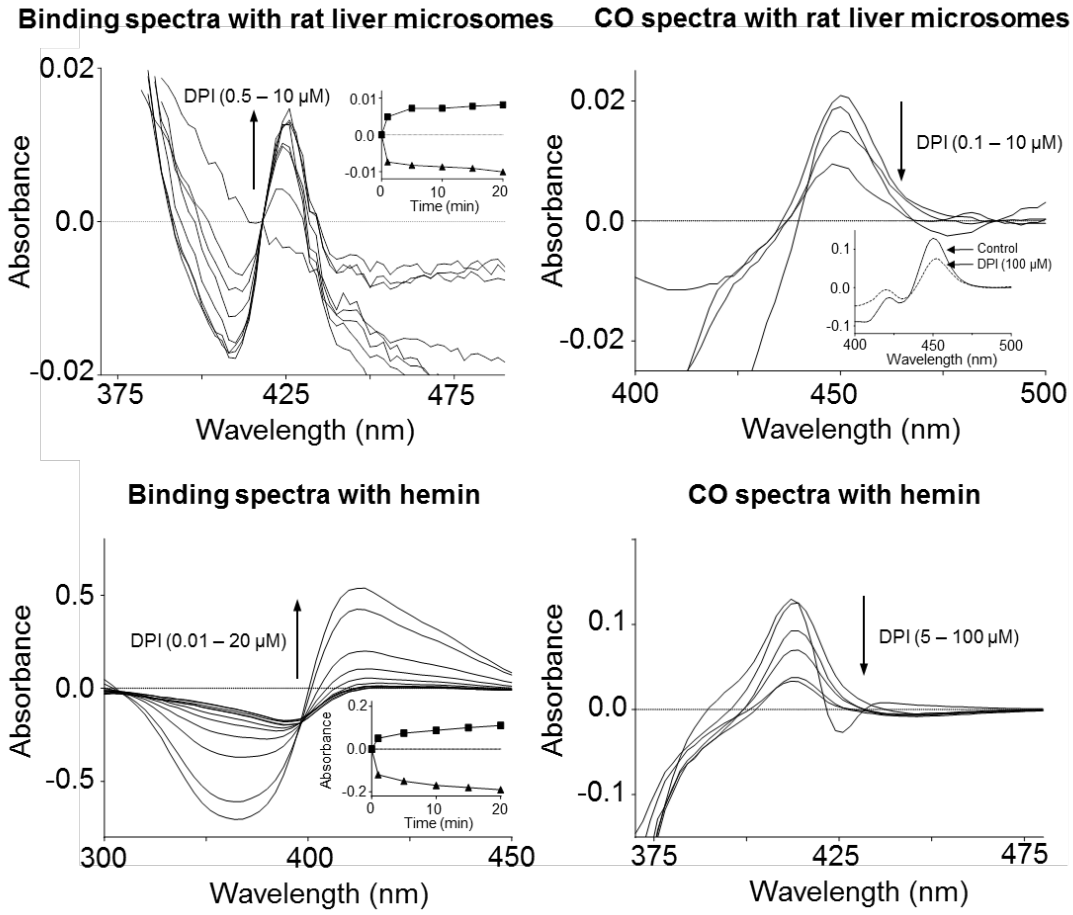

Fig A1.3. Effects of DPI on the spectral properties of rat liver microsomes and hemin.

Spectra were recorded using liver microsomes from β-NF treated rats (upper panels) and hemin (lower panels). Carbon monoxide (CO) difference spectra (right panels) and binding spectra (left panels) were performed as described in Materials and Methods. CO difference spectra included NADPH as the reductant for rat liver microsomes and sodium dithionite for hemin, respectively. The reference cuvette for CO spectra contained all components in the sample cuvette except CO. Binding spectra for microsomes included NADPH as the reductant; no reductant was used for the hemin

binding spectra. The reference cuvette for binding spectra contained all components in the sample cuvette except DPI. **Insets: Left panels, t**ime-dependent effects of DPI (1 μM) on the absorbance at the trough (▲, 410 and 366 nm for microsomes and hemin, respectively) and peak (■, 424 and 426 for microsomes and hemin, respectively) of the binding spectra of rat liver microsomes and hemin. Reactions with microsomes and hemin were initiated with the addition of 100 μM NADPH or DPI, respectively. **Upper right panel,** dithionite reduced CO spectra in the presence and absence of DPI.

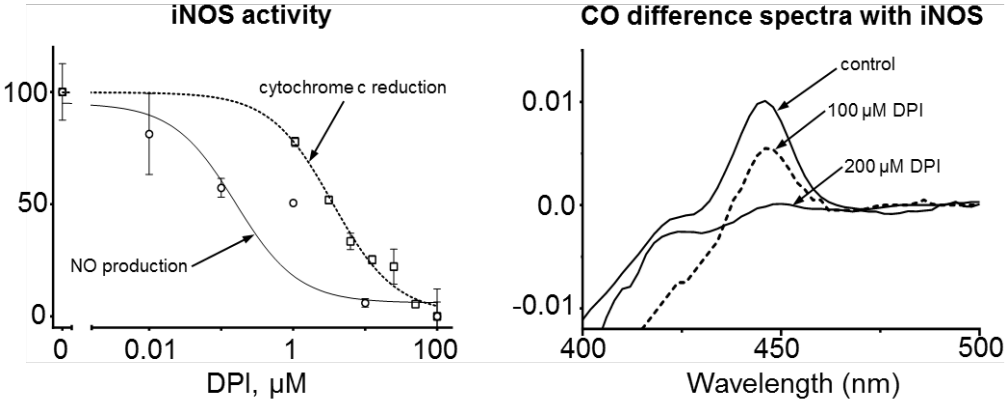

Fig A1.4. Effects of DPI on iNOS.

Left panel. The effects if DPI on nitric oxide production and cytochrome c reduction by iNOS were were measured as described in the Materials and Methods using sodium dithionite as a reductant. Data are the mean ± SE (n = 3). **Right panel.** The carbon monoxide (CO) difference spectra of iNOS were recorded in the absence and presence of DPI. Assays were run without preincubations with DPI

APPENDIX 2: QUINONE AND NITROFURANTOIN REDOX CYCLING BY RECOMBINANT CYTOCHROME B_5 REDUCTASE

John T. Szilagyi*, Karma C. Fussell†, Yun Wang*, Yi-Hua Jan*, Vladimir Mishin†, Jason R. Richardson^, Diane E. Heck‡, Shaojun Yang†, Lauren M. Aleksunes†, Debra L. Laskin† and Jeffrey D. Laskin*

*Department of Environmental and Occupational Health, Rutgers University School of Public Health, Piscataway, NJ 08854

†Department of Pharmacology and Toxicology, Ernest Mario School of Pharmacy, Rutgers University, Piscataway, NJ 08854

^Department of Pharmaceutical Sciences, Northeast Ohio Medical University, Rootstown, OH 44272

‡Department of Environmental Health Science, New York Medical College, Valhalla, NY 10595

A-2.1 Abstract

NADH cytochrome b_5 reductase mediates electron transfer from NADH to cytochrome b_5 utilizing flavin adenine dinucleotide as a redox cofactor. Reduced cytochrome b_5 is an important cofactor in many metabolic reactions including cytochrome P450-mediated xenobiotic metabolism, steroid biosynthesis and fatty acid metabolism, hemoglobin reduction, and methionine and plasmalogen synthesis. Using recombinant human enzyme, we discovered that cytochrome b5 reductase mediates redox cycling of a variety of quinones generating superoxide anion, hydrogen peroxide, and, in the presence of transition metals, hydroxyl radicals. Redox cycling activity was oxygen-dependent and preferentially utilized NADH as a co-substrate; NADH was 5-10 times more active than NADPH in supporting redox cycling. Redox cycling activity was greatest for 9,10-phenanthrenequinone and 1,2-naphthoquinone, followed by 1,4-naphthoquinone and 2-methyl-1,4-naphthoquinone (menadione), nitrofurantoin and 2-hydroxyestradiol. Using menadione as the substrate, quinone redox cycling was found to inhibit reduction of cytochrome b_5 by cytochrome b_5 reductase, as measured by heme spectral changes in cytochrome b_5. Under anaerobic conditions where redox cycling is inhibited, menadione had no effect on the reduction of cytochrome b_5. Chemical redox cycling by cytochrome b_5 reductase may be important in generating cytotoxic reactive oxygen species in target tissues. This activity, together with the inhibition of cytochrome b_5 reduction by redox-active chemicals and consequent deficiencies in available cellular cytochrome b_5, are likely to contribute to tissue injury following exposure to quinones and related redox active chemicals.

Abbreviations

NADH, reduced nicotinamide adenine dinucleotide; NADPH, reduced nicotinamide adenine dinucleotide phosphate; EDTA, ethylenediaminetetraacetic acid; FAD, flavin adenine dinucleotide; PHEN, 9,10-phenanthrene quinone; NFT, nitrofurantoin; MD, menadione; 1,4 NQ, 1,4-napthoquinone; 2-OH E2, 2-OH estradiol; TPT, terephthalate.

A-2.2 Introduction

Cytochrome b_5 reductase is an FAD-containing enzyme that mediates electron transfer from NADH to cytochrome b_5 (Elahian *et al.*, 2014; Strittmatter, 1965). Reduced cytochrome b_5 serves as a redox partner in an array of metabolic processes including cytochrome P450-mediated xenobiotic metabolism and steroid biosynthesis, fatty acid metabolism, hemoglobin reduction, and methionine and plasmalogen synthesis (Guengerich, 2005). Cytochrome b_5 reductase/cytochrome b_5 has also recently been reported to reduce cytoglobin, a heme containing protein thought to be important in protecting cells against hypoxia (Amdahl *et al.*, 2017). The importance of cytochrome b_5 reductase *in vivo* is illustrated by findings that endoplasmic reticulum-associated b_5 knockout mice display phenotypic abnormalities that include alterations in hepatic fatty acid metabolism and the development of diabetes and lipoatrophy (Xu *et al.*, 2011). Genetic deficiencies in cytochrome b_5 reductase in humans have also been linked to methemoglobinemia which is associated with accumulation of oxidized Fe^{+3} and a reduced oxygen carrying capacity of blood as well as neurodevelopmental disorders (Fermo *et al.*, 2008; Galeeva *et al.*, 2013; Hudspeth *et al.*, 2010; Nagai *et al.*, 1993).

Earlier studies demonstrated that cytochrome b_5 reductase can mediate the one electron reduction of quinones to their semiquinone form (Iyanagi *et al.*, 1984; Iyanagi and Yamazaki, 1969; Iyanagi and Yamazaki, 1970). Semiquinone intermediates are unstable and donate an electron to diatomic oxygen, forming superoxide anion and returning to the native quinone state (O'Brien, 1991) (see **Fig A2.1** for reaction scheme). The ability of a quinone to be reduced again by cytochrome b_5 reductase, cycling back and forth between redox states, a process referred to as chemical redox cycling or futile redox cycling, can result in tissue injury. The formation of superoxide anion through redox cycling generates cytotoxic oxidizing species including hydrogen

peroxide (H_2O_2), hydroxyl radicals and, in the presence of nitric oxide, peroxynitrite; in cells this process can lead to oxidative and/or nitrosative stress (Wink *et al.*, 1997).

Quinone redox cycling is an energetically favorable reaction which can inhibit the enzymes mediating this process. For example, quinone redox cycling is also known to be mediated by NADPH cytochrome P450 reductase, an enzyme that donates electrons to the cytochrome P450s (Szilagyi et al., 2016). Redox cycling preferentially uses electrons from NADPH at the expense of their supply to the cytochrome P450s which in turn inhibits their monooxygenase activities (Jan et al., 2015). Similarly, sepiapterin reductase, the rate limiting enzyme in tetrahydrobiopterin biosynthesis, is a mediator of quinone redox cycling, a process that readily inhibits activity of this enzyme (Yang et al., 2013). In the present studies, we characterized chemical redox cycling using recombinant human cytochrome b_5 reductase and determined if this process interferes with electron flow from NADH to cytochrome b_5.

A-2.3 Materials and Methods

Chemicals and Reagents

Amplex red (10-acetyl-3,7-dihydroxyphenoxazine) was obtained from Invitrogen (Eugene, OR). Cytochrome b_5, acetylated cytochrome c, 9,10-phenanthrenequinone, 2-methyl-1,4-naphthquinone (menadione), 1,4-naphthoquinone, nitrofurantoin (N-(5-nitro-2-furfurylidene)-1-aminohydantoin), 2-hydroxyestradiol, diethylenetriaminepentaacetic acid (DETAPAC) and all other chemicals were from Sigma-Aldrich (St. Louis, MO). cDNA expressing recombinant N-terminal histidine tagged human cytochrome b_5 reductase was a generous gift of Dr. Lauren Trepanier (University of Wisconsin-Madison, Madison, WI). The enzyme was expressed in *E. coli* as previously described (Kurian *et al.*, 2004) and purified using Ni-ion chromatography (Invitrogen, Carlsbad, CA) according to the manufacturer's instructions. Stock solutions of the enzyme ranged from 1-4 mg/ml and were >98% pure as determined by SDS-polyacrylamide gel electrophoresis followed by silver staining. The specific enzyme activity was assessed using the ferricyanide assay as previously published (Mihara and Sato, 1975) where 1 U of cytochrome b_5 reductase reduces 1 µmole of ferricyanide per min.. Enzyme protein was quantified using the DC protein assay kit (Bio-Rad, Hercules, CA) with bovine serum albumin as the standard.

Enzyme Assays

Unless otherwise stated, all assays were performed in 96-well flat bottom microwell plates at 37^{o}C; changes in absorbance/fluorescence were measured using a SpectraMax M3 fluorescent microplate reader (Molecular Devices, Sunnyvale, CA). Data were collected using SoftMax Pro 6.3 software and analyzed using GraphPad Prism 5 (La Jolla, CA). Reactions were initiated using NADH or NADPH (200 µM final

concentration) as reducing cofactors. Enzyme concentrations in reaction mixes ranged from 0.02-12 U/mL, as specified in Fig legends.

Measurements of Reactive Oxygen Species in Enzyme Assays

Changes in absorbance at 550 nm of acetylated cytochrome c were used to monitor production of superoxide anion (Azzi *et al.*, 1975). Briefly, reaction mixtures contained 100 mM potassium phosphate buffer (pH 7.8), 50 μM acetylated cytochrome c, 1 U/mL recombinant cytochrome b_5 reductase and 100 μM menadione in a final volume of 0.1 ml. Unless otherwise stated, reactions were initiated by the addition of NAD(P)H (200 μM). To demonstrate the specificity of the assay, superoxide dismutase (1000 U/mL) was used as a scavenger of superoxide anion. H_2O_2 generation was measured using the continuous Amplex red/horseradish peroxidase method as previously described (Mishin, et al., 2010). Briefly, reaction mixtures contained 100 mM potassium phosphate buffer (pH 7.8), 0.2 U/mL recombinant cytochrome b_5 reductase, 100 μM Amplex red, 1 U/mL horseradish peroxidase, and redox cycling compounds in a final volume of 0.1 mL. Reactions were initiated by the addition of NAD(P)H. To demonstrate the specificity of the assay, catalase (1000 U/mL) was used as a scavenger of H_2O_2. The fluorescence increase due to formation of resorufin (excitation 535 nm/emission 580 nm), was recorded, and the rates were calculated based on the linear phase of reactions after background subtraction. The terephthalate-based assay was used to measure the formation of hydroxyl radicals (Son *et al.*, 2015). In this assay, hydroxyl radicals are formed due to the reaction of H_2O_2 with Fe^{2+} and scavenged by the non-fluorescent substrate terephthalate, producing the fluorescent 2-hydroxyterephthalate (2-OH-TPT, excitation 315 nm/emission 425 nm). Reactions were run in the presence of 1 U/mL recombinant cytochrome b_5 reductase, 100 μM $FeCl_3$, 110 μM EDTA and 1 mM

terephthalate. To demonstrate the specificity of the assay, in some experiments DMSO (1%, ~125 mM) was used as a trap for hydroxyl radicals.

Analysis of NAD(P)H Consumption and Oxygen Utilization in Enzyme Assays

Oxygen uptake was measured using an Oxygraph Plus System fitted with a Clark-type oxygen electrode (Hansatech Instruments Ltd, UK) as previously described (Yang *et al.*, 2013). Decreases in absorbance at 340 nm were used to analyze the rates of NADH utilization initiated by cytochrome b_5 reductase (Bergmeyer, 1975). Briefly, reaction mixtures contained 100 mM potassium phosphate buffer (pH 7.8), 1.0 mM sodium azide, 1.0 mM DETAPAC, and 600 µM NADH in a final volume of 0.1 ml. In these experiments the reactions were initiated by the addition of 1U/mL cytochrome b_5 reductase.

Spectral Analysis of Cytochrome b_5 Heme

The oxidation state of heme containing proteins can be characterized using visible-wavelength spectral analysis (Lewis, 1954; North *et al.*, 1996). Previous research has shown that reduction of purified cytochrome b_5, a heme containing protein, results in a red shift of its Soret peak from 412 to 425 nm and the formation of additional peaks at 526 and 556 nm (Aoyama *et al.*, 1990; Arinc and Cakir, 1999; Strittmatter and Velick, 1956). Heme-binding difference spectra were recorded on the microplate reader as previously described (Szilagyi, et al., 2016)**.** Reaction mixtures for all spectral measurements contained 100 mM potassium phosphate buffer (pH 7.5), 0.1% Triton X-100, 12 U/mL cytochrome b_5 reductase and 12 ng/mL cytochrome b_5. Prior to the addition of NADH, each sample served as its own reference cuvette. Reaction mixtures were incubated in the dark and, after 10 min at room temperature, 200 µM NADH was added and the mixture incubated for an additional 10 min. The optical absorbance from 300-500 nm was before and after the addition of NADH. Difference spectra were

generated by subtracting the absolute oxidized spectra from the absolute reduced spectra. Where applied, anaerobic conditions in the wells were generated by incubating reaction mixtures with 25 U/mL catalase, 50 mM glucose, and 12.5 U/mL glucose oxidase for 20 min prior to initiating spectral analysis (Penketh *et al.*, 2015).

A-2.4 Results

In initial studies, we characterized redox cycling by recombinant human cytochrome b_5 reductase. Redox cycling of quinones generates a semiquinone radical that reacts with molecular oxygen to regenerate the parent compound (O'Brien, 1991). Using menadione as the redox active quinone, the enzyme was found to readily consume oxygen in the presence of NADH (**Fig A2.2A**). Both oxygen utilization and NADH consumption were time-dependent (**Figs A2.2A-B**). The redox cycling process actively generated superoxide anion and H_2O_2 (**Figs A2.2C-D**). Formation of reactive oxygen species was also dependent on time and the concentration of menadione. NADH was significantly more active in supplying reducing equivalents to cytochrome b_5 reductase for redox cycling when compared to NADPH (**Fig 2.2E**); the rate of H_2O_2 formation in the presence of menadione (100 µM) per unit of cytochrome b_5 reductase for NADH and NADPH was 595.8 ± 18.1 and 58.8 ± 7.8 pmole/min/U B_5R (n = 3 ± SD), respectively. In the presence of Fe^{3+}/EDTA complexes, redox cycling corresponded with generation of hydroxyl radicals (**Fig A2.2F**). Accumulation of superoxide anion and H_2O_2 in redox cycling assays was abolished by superoxide dismutase and catalase, respectively, while hydroxyl radical production was inhibited by DMSO, a hydroxyl radical trap (Eberhardt and Colina, 1988).

Several additional redox active chemicals generated reactive oxygen species also by redox cycling with cytochrome b_5 reductase including 9,10-phenanthrenequinone, 1,4-naphthoquinone, and the catechol estrogen, 2-hydroxyestradiol and nitrofurantoin (**Fig A2.3** and **Table 2.1**). Of these chemicals, 9,10-phenanthrenequinone was most active (Km = 5.7 µM, kcat = 5.8 min^{-1}, kcat/Km = 1.0 $min^{-1}µM^{-1}$). Less activity was noted for 1,4-naphthoquinone (Km = 5.7 µM, kcat = 5.8 min^{-1}, kcat/Km = 1.0 $min^{-1}µM^{-1}$), 2-hydroxyestradiol (Km = 5.7 µM, kcat = 5.8 min^{-1}, kcat/Km = 1.0 $min^{-1}µM^{-1}$), menadione

(Km = 5.7 µM, kcat = 5.8 min^{-1}, kcat/Km = 1.0 $min^{-1}µM^{-1}$) and nitrofurantoin (Km = 5.7 µM, kcat = 5.8 min^{-1}, kcat/Km = 1.0 $min^{-1}µM^{-1}$). Cytochrome b_5 reductase-mediated redox cycling was also observed with other catechol estrogens, including 4-hydroxyestradiol, 4-hydroxyestrone and 2-hydroxyestriol. The parent estrogens, estradiol, estrone, and estriol, and the methoxy-estrogen metabolite 2-methoxyestradiol were not able to redox cycle with the enzyme (data not shown).

Cytochrome b_5 is an endogenous ligand for cytochrome b_5 reductase (Strittmatter, 1965). As a heme-containing protein, reduction of cytochrome b_5 by cytochrome b_5 reductase can be monitored by difference spectroscopy (Aoyama, et al., 1990; Strittmatter and Velick, 1956). In this assay, reduction of cytochrome b_5 by cytochrome b_5 reductase results in a red shift of its Soret peak from 410 nm to 425 nm (**Fig A2.4**)(Aoyama, et al., 1990). We found that by redox cycling with cytochrome b_5 reductase, both menadione (10 µM and 100 µM) and 2-hydroxyestradiol (100 µM) blocked reduction of cytochrome b_5 (**Fig A2.5A-B**). As redox cycling is oxygen-dependent, we next analyzed the effects of depleting oxygen on cytochrome b_5-mediated reduction of cytochrome b_5 in reaction mixtures. In the presence of NADH, cytochrome b_5 reductase effectively supplied electrons to cytochrome b_5 under both aerobic and anaerobic conditions, as measured by distinctive changes in the cytochrome b_5 difference spectra. However, under anaerobic conditions, menadione was unable to inhibit the reduction of cytochrome b_5 (**Fig A2.5C**).

A-2.5 Discussion

The present studies demonstrate that a variety of redox active chemicals including quinones and nitrofurantoin, redox cycle with purified recombinant cytochrome b_5 reductase. These data are consistent with earlier studies using electron spin resonance, which demonstrated that cytochrome b_5 reductase catalyzes the one electron reduction of quinones including menadione (Iyanagi and Yamazaki, 1969; 1970). The generation of reactive oxygen species during chemical redox cycling is an important mechanism contributing to tissue injury (Hochstein, 1983). Hydroxyl radicals derived from superoxide anion and H_2O_2 are highly reactive; modifications on cellular macromolecules can disrupt cellular function. Reactive oxygen species can also initiate lipid peroxidation, a process that can disrupt lipid membranes and generate cytotoxic lipid peroxidation end products. In addition to cytochrome b_5 reductase, a number of other enzymes have been reported to mediate redox cycling, including various aldo-keto reductases, nitric oxide synthases and thioredoxin reductases, cytochrome P450 reductase, sepiapterin reductase and dicarbonyl/l-xylulose reductase (Garner *et al.*, 1999; Gray, et al., 2007; Shultz *et al.*, 2011; Szilagyi, et al., 2016; Yang, et al., 2013; Yang *et al.*, 2017). At the present time, the individual contributions of the enzymes to tissue injury in response to different quinones and other redox active chemicals as a consequence of redox cycling, is unknown. It is likely that toxicity depends, not only on the relative ability of individual enzymes to generate reactive oxygen species during redox cycling, but also on enzyme concentrations and their subcellular distribution in different cell types. In this regard, the ability of microsomal forms of cytochrome b_5 reductase and cytochrome P450 reductase to generate reactive oxygen species during redox cycling may compromise microsomal functioning including xenobiotic metabolism. However, redox cycling enzymes such as various aldo-keto reductases and cytochrome P450s can also metabolize various redox active chemicals. Together with various cellular antioxidants, these detoxifying enzymes

are important in limiting tissue damage resulting from exposure to redox active chemicals.

It is well recognized that estrogens are an important risk factor for the development of breast cancer (Santen *et al.*, 2015). Estrogens can be metabolized to catechols, as well as reactive quinones and semiquinones (Parl *et al.*, 2009). Catechol estrogens are known to redox cycle, and their ability to generate cytotoxic reactive oxygen species may contribute to the carcinogenic process (Parl, et al., 2009). Both breast cancer epithelial cells and purified NADPH cytochrome P450 reductase mediate catechol estrogen redox cycling and generate reactive oxygen species (Fussell *et al.*, 2011b). The present studies demonstrate that cytochrome b_5 reductase mediates redox cycling of certain catechol estrogens. Depending on the localized concentrations of catechol estrogens and enzymes that mediate redox cycling such as cytochrome b_5 reductase, this may be an important mechanism contributing to the development of breast cancer.

Nitrofurantoin is a commonly used nitroaromatic redox-active antibiotic; it has also been used as an antitumor agent (Kamat and Lamm, 2004; Oscier *et al.*, 2002). Adverse reactions to the drug, which include liver injury (Paiva *et al.*, 1992), pulmonary fibrosis (Witten, 1989), hematological disorders (Gait, 1990), and peripheral polyneuropathy (Jacknowitz *et al.*, 1977), are thought to be due to the generation of reactive oxygen species during redox cycling (Martin, 1983; Rossi *et al.*, 1988). Our data showing that cytochrome b_5 reductase mediates nitrofurantoin redox cycling indicates that this enzyme may be an off-target for the drug. Redox cycling by cytochrome b_5 reductase, as well as other enzymes reported to redox cycle nitroaromatic compounds, including nitric oxide synthase (Boelsterli *et al.*, 2006), thioredoxin reductase (Cenas *et al.*, 2006), ferredoxin:NADP+ reductase (Miskiniene *et al.*, 1997) and cytochrome P450 reductase

(Wang, et al., 2008c) may contribute to cytotoxicity of nitrofurantoin. Inhibition of the production of reactive oxygen species by these enzymes during redox cycling might translate into improved medical use of nitrofurantoin and related drugs.

Of interest were our findings that chemical redox cycling was associated with inhibition of the cytochrome b_5 reduction by cytochrome b_5 reductase. This was oxygen-dependent, a finding consistent with the fact that oxygen is required for quinone redox cycling by cytochrome b_5 reductase. Cytochrome b_5 reductase catalyzes electron transfer from NADH, a two electron carrier, to cytochrome b_5, a one electron carrier, via FAD binding domains (Strittmatter, 1965). Transfer of electrons from NADH generates a fully reduced form of FAD while transfer of single electrons to cytochrome b_5 generates FAD semiquinone intermediates. Redox cycling presumably occurs via single electron transfer between FAD, semiquinones and the redox active chemical. Inhibition of cytochrome b_5 reduction of cytochrome b_5 as a result of redox cycling is likely because this is an energetically favorable process (Iyanagi, et al., 1984). Thus, electrons preferentially transfer to redox active chemicals at the expense of the reduction of cytochrome b_5. Inhibition of cytochrome b_5 reduction may result in deficiencies in processes dependent on this cofactor including fatty acid and cholesterol synthesis, methemoglobin and cytoglobin reduction, and xenobiotic oxidation (Amdahl, et al., 2017; Galeeva, et al., 2013; Guengerich, 2005; Hudspeth, et al., 2010; Nagai, et al., 1993; Xu, et al., 2011). The extent to which redox cycling affects different metabolic pathways mediated by cytochrome b_5 reductase remains to be determined.

In summary, the present studies show that cytochrome b_5 reductase-mediated redox cycling, not only generates cytotoxic reactive oxygen species, but also has the capacity to reduce localized concentrations of intracellular oxygen and reducing equivalents from pyridine nucleotide cofactors, which can contribute to tissue damage. These activities,

together with the inhibition of cytochrome b_5 reduction, are likely to contribute to cytotoxicity following exposure to quinones and other redox active chemicals. However, further studies are needed to determine how redox active chemicals bind to cytochrome b_5 reductase and the precise mechanism of electron transfer during redox cycling reactions.

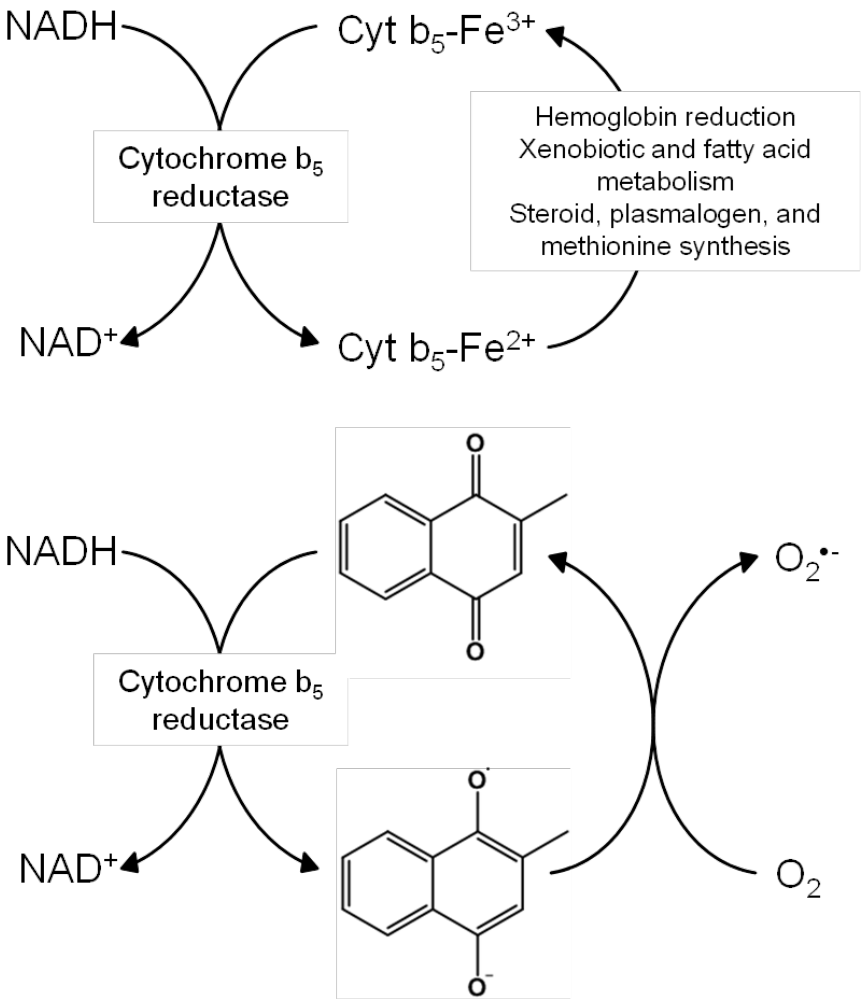

Fig A2.1. Reactions mediated by cytochrome b5 reductase.

Upper panel: Reduced cytochrome b5 (Cytb5-Fe^{+3}) serves as a redox partner for a variety of enzymes including those mediating reduction of hemoglobin, xenobiotics and fatty acid/lipid metabolism and steroid, plasmalogen, and methionine biosynthesis. Cytochrome b_5 is maintained in the reduced state by cytochrome b_5 reductase at the expense of reducing equivalents supplied by NADH. *Lower panel*: Cytochrome b5 reductase also mediates chemical redox cycling. In this reaction, the enzyme forms semiquinone radicals from redox active quinones such as menadione (2-methyl-1,4-naphthoquinone) from electrons donated by NADH. Reaction of the semiquinone with

molecular oxygen regenerates the parent compound and in the process, generates superoxide anion. Spontaneous and enzyme supported dismutation of superoxide anion generates H_2O_2 and, in the presence of a transition metal, hydroxyl radicals.

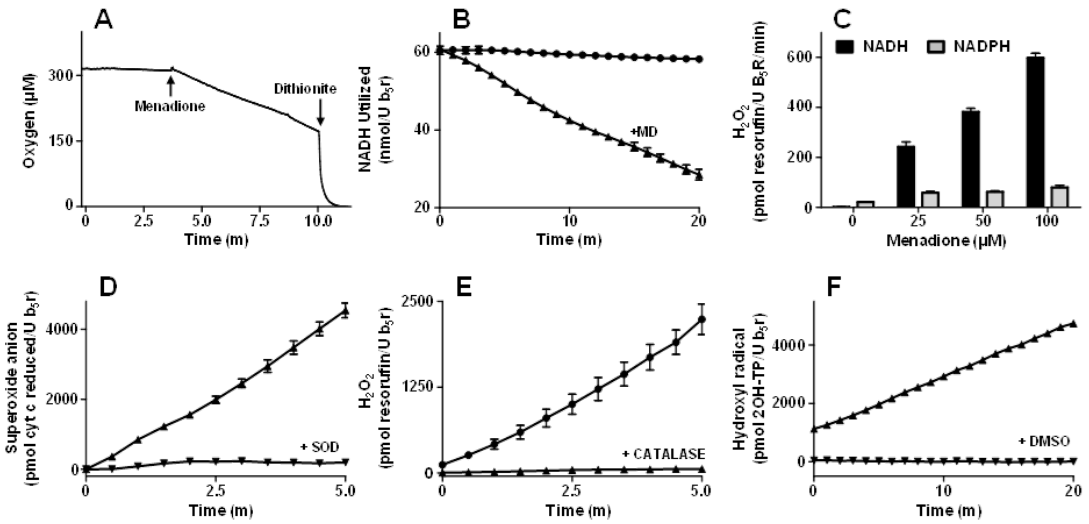

Fig A2.2. Characterization of redox cycling by cytochrome b_5 reductase.

Formation of reactive oxygen species by cytochrome b_5 reductase during redox cycling was initiated in the presence of menadione. *Panel A*, Oxygen consumption activated by menadione redox cycling was measured using a Clark oxygen electrode. Reaction mixtures contained 0.2 U/mL cytochrome b_5 reductase, 100 μM menadione, and 200 μM NADH. Note that the addition of menadione to the reaction mix, as indicated by the arrow, initiated oxygen consumption. Oxygen calibration was performed with the addition of several grains of sodium dithionite, as indicated by the arrow. *Panel B,* Consumption of NADH by cytochrome b_5 reductase (1 U/mL) in the presence and absence of 100 μM menadione. Then the reactions were initiated by adding NADH to a final concentration of 600 μM. Reactions were initiated by adding NADH to a final concentration of 600 μM. *Panel C*, NADH is a more effective electron donor in cytochrome b_5 reductase-mediated redox cycling. Reactions contained 0.2 U/ml cytochrome b_5 reductase, 200 μM NADH or NADPH, and increasing concentrations of menadione. Rates of H_2O_2 formation are

presented as the mean ± SD (n = 3). *Panels D and E*, Time-dependent formation of superoxide anion and H_2O_2 during menadione redox cycling. Reaction mixtures contained 100 µM menadione, 200 µM NADH and 1 U/mL cytochrome b_5 reductase to measure formation of superoxide anion or 0.2 U/mL cytochrome b_5 reductase to measure formation of H_2O_2 formation. Superoxide anion was assayed using acetylated cytochrome c as described in the Materials and Methods. As indicated in some experiments, superoxide dismutase (10^3 U/mL) or catalase (10^3 U/ml) was added to the reaction mixtures to demonstrate the specificity of the assays. *Panel F*, Production of hydroxyl radicals in the presence of Fe^{2+} during menadione redox cycling. Reactions contained 100 µM menadione, 200 µM NADH, 1 U/mL cytochrome b_5 reductase, 100 µM $FeCl_3$, and 110 µM EDTA. In some reactions, DMSO (1%) was added as a hydroxyl radical trap.

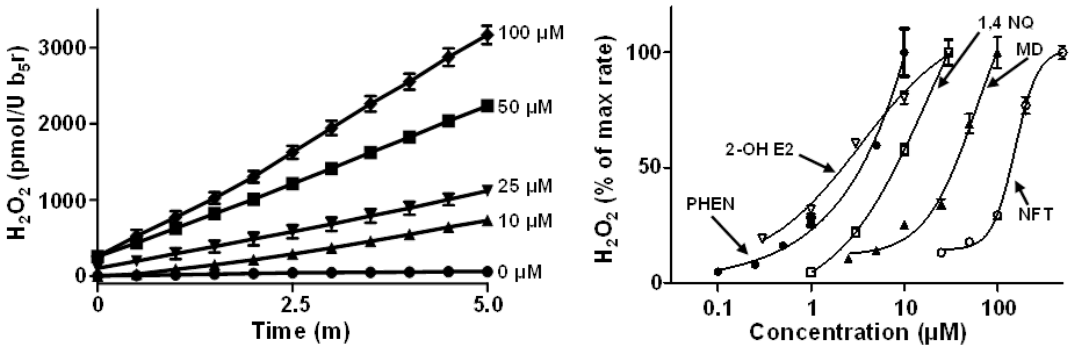

Fig A2.3. Comparison of chemical redox cycling by cytochrome b_5 reductase using different redox active quinones and nitrofurantoin.

Reaction mixtures contained 0.2 U/mL cytochrome b_5 reductase and were initiated by the addition of NADH to a final concentration of 200 µM. *Left panel*, H_2O_2 concentrations at various times were measuring in reaction mixtures contained increasing concentrations of menadione. Data are the mean ± SD (n = 3). *Right panel*, Reactions were run in the presence of increasing concentrations of 2-hydroxyestradiol (2-OH E2), 9,10-phenanthrenequinone (PHEN), 1,4-napthoquinone (1,4 NQ), menadione (MD), and nitrofurantoin (NFT). H_2O_2 concentrations were measured after 5 min.

Table A2.1. Kinetic constants for NADH-cytochrome b_5 reductase-mediated H_2O_2 generation by redox cycling agents

Compound	K_M (μM)	k_{cat} (min^{-1})	k_{cat}/K_M ($min^{-1}\mu M^{-1}$)
Menadione	77	3.5	0.046
9,10-Phenanthrenequinone	5.7	5.8	1.0
1,4-Napthoquinone	9.8	0.99	0.10
Nitrofurantoin	270	0.99	0.0037
2OHE2	2.6	0.17	0.065

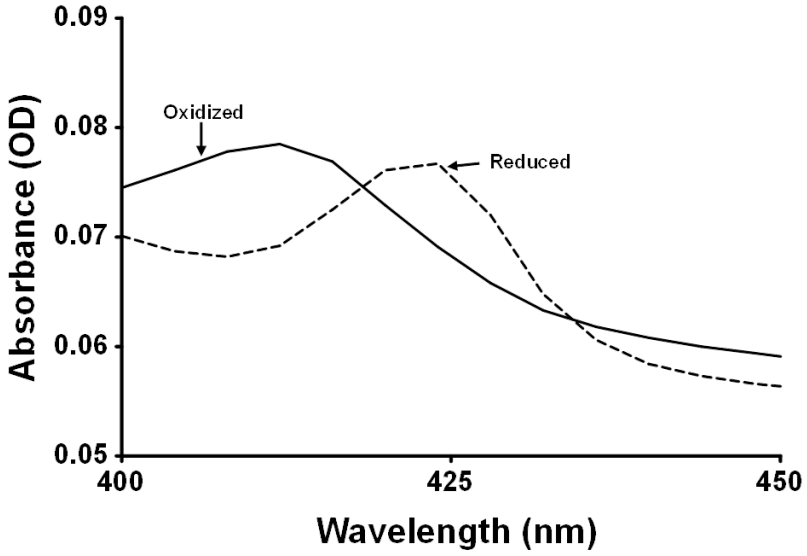

Fig A2.4. Spectral properties of oxidized and reduced cytochrome b_5.

Absolute spectra were recorded as described in Materials and Methods. Reaction mixtures contained 12 U/mL cytochrome b_5 reductase and 12 ng/mL cytochrome b_5. Oxidized and reduced spectra were recorded in the presence and absence of NADH (200 μM final concentration), respectively. Reduction of cytochrome b_5 is characterized by a shift in its Soret peak from 414 to 425 nm (Mihara and Sato, 1975; Strittmatter, 1965).

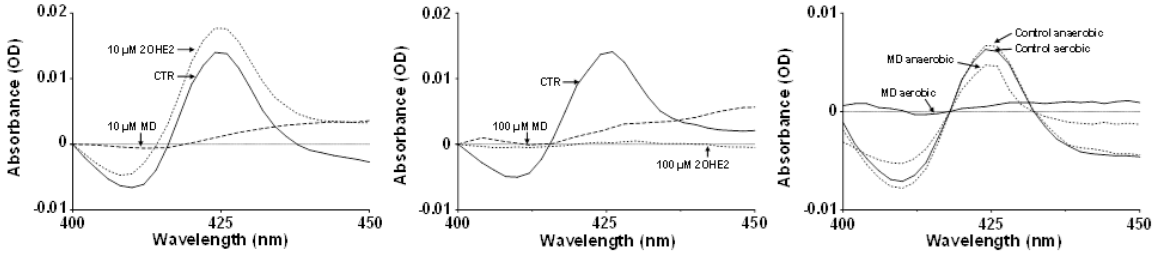

Fig A2.5. Effects of redox cycling agents on the reduction of cytochrome b_5 by cytochrome b_5 reductase.

Difference spectra were recorded as described in Materials and Methods. Reaction mixtures contained 12 U/mL cytochrome b_5 reductase, 12 ng/mL cytochrome b_5, and menadione or 2OHE2 (*Left panel,* 10 μM; *Center panel,* 100 μM). The spectrum of each sample was recorded before and after the addition of NADH to a final concentration of 200 μM. Spectra in the absence of NADH for each sample served as the reference. *Right panel*, Reduction of cytochrome b_5 by cytochrome b_5 reductase in the presence and absence of menadione under aerobic and anaerobic conditions. Reaction mixtures contained 12 U/mL cytochrome b_5 reductase, 12 ng/mL cytochrome b_5, and 100 μM menadione. Anaerobic conditions were generated *in situ* using the glucose/glucose oxidase method as described in the Materials and Methods.

REFERENCES

Aban, C., Leguizamon, G. F., Cella, M., Damiano, A., Franchi, A. M., and Farina, M. G. (2013). Differential expression of endocannabinoid system in normal and preeclamptic placentas: Effects on nitric oxide synthesis. *Placenta* **34**, 67-74.

Aban, C., Martinez, N., Carou, C., Albamonte, I., Toro, A., Seyahian, A., Franchi, A., Leguizamon, G., Trigubo, D., Damiano, A., and Farina, M. (2016). Endocannabinoids participate in placental apoptosis induced by hypoxia inducible factor-1. *Apoptosis* **21**, 1094-1105.

Abouchedid, R., Ho, J. H., Hudson, S., Dines, A., Archer, J. R., Wood, D. M., and Dargan, P. I. (2016). Acute toxicity associated with use of 5f-derivations of synthetic cannabinoid receptor agonists with analytical confirmation. *J Med Toxicol* **12**, 396-401.

Adak, S., Ghosh, S., Abu-Soud, H. M., and Stuehr, D. J. (1999). Role of reductase domain cluster 1 acidic residues in neuronal nitric-oxide synthase. Characterization of the fmn-free enzyme. *J Biol Chem* **274**, 22313-22320.

Agarwal, S., Sane, R., Ohlfest, J. R., and Elmquist, W. F. (2011). The role of the breast cancer resistance protein (abcg2) in the distribution of sorafenib to the brain. *J Pharmacol Exp Ther* **336**, 223-233.

Aggarwal, V. K., and Olofsson, B. (2005). Enantioselective alpha-arylation of cyclohexanones with diaryl iodonium salts: Application to the synthesis of (-)-epibatidine. *Angew Chem Int Ed Engl* **44**, 5516-5519.

Aguirre, C. A., Castillo, V. A., and Llanos, M. N. (2012). Excess of the endocannabinoid anandamide during lactation induces overweight, fat accumulation and insulin resistance in adult mice. *Diabetol Metab Syndr* **4**, 35.

Albekairi, N. A., Al-Enazy, S., Ali, S., and Rytting, E. (2015). Transport of digoxin-loaded polymeric nanoparticles across bewo cells, an in vitro model of human placental trophoblast. *Therapeutic Delivery* **6**, 1325-1334.

Allen, J. D., Van Dort, S. C., Buitelaar, M., van Tellingen, O., and Schinkel, A. H. (2003). Mouse breast cancer resistance protein (bcrp1/abcg2) mediates etoposide resistance and transport, but etoposide oral availability is limited primarily by p-glycoprotein. *Cancer Research* **63**, 1339-1344.

Allikmets, R., Schriml, L. M., Hutchinson, A., Romano-Spica, V., and Dean, M. (1998a). A human placenta-specific atp-binding cassette gene (abcp) on chromosome 4q22 that is involved in multidrug resistance. *Cancer Res* **58**, 5337-5339.

Allikmets, R., Schriml, L. M., Hutchinson, A., Romano-Spica, V., and Dean, M. (1998b). A human placenta-specific atp-binding cassette gene (abcp) on chromosome 4q22 that is involved in multidrug resistance. *Cancer Research* **58**, 5337-5339.

Amdahl, M. B., Sparacino-Watkins, C. E., Corti, P., Gladwin, M. T., and Tejero, J. (2017). Efficient reduction of vertebrate cytoglobins by the cytochrome b5/cytochrome b5 reductase/nadh system **56**, 3993-4004.

An, G., and Morris, M. E. (2011). The sulfated conjugate of biochanin a is a substrate of breast cancer resistant protein (abcg2). *Biopharm Drug Dispos* **32**, 446-457.

Ando, T., Kusuhara, H., Merino, G., Alvarez, A. I., Schinkel, A. H., and Sugiyama, Y. (2007). Involvement of breast cancer resistance protein (abcg2) in the biliary excretion mechanism of fluoroquinolones. *Drug Metab Dispos* **35**, 1873-1879.

Aoyama, T., Nagata, K., Yamazoe, Y., Kato, R., Matsunaga, E., Gelboin, H. V., and Gonzalez, F. J. (1990). Cytochrome b5 potentiation of cytochrome p-450 catalytic activity demonstrated by a vaccinia virus-mediated in situ reconstitution system. *Proc Natl Acad Sci U S A* **87**, 5425-5429.

Appelgren, L. E., Arora, R. G., and Larsson, P. (1982). Autoradiographic studies of [3h]zearalenone in mice. *Toxicology* **25**, 243-253.

Arinc, E., and Cakir, D. (1999). Simultaneous purification and characterization of cytochrome b5 reductase and cytochrome b5 from sheep liver. *Int J Biochem Cell Biol* **31**, 345-362.

Arnould, S., and Camadro, J. M. (1998). The domain structure of protoporphyrinogen oxidase, the molecular target of diphenyl ether-type herbicides. *Proc Natl Acad Sci U S A* **95**, 10553-10558.

Azzi, A., Montecucco, C., and Richter, C. (1975). The use of acetylated ferricytochrome c for the detection of superoxide radicals produced in biological membranes. *Biochem Biophys Res Commun* **65**, 597-603.

Bai, M., Ma, Z., Sun, D., Zheng, C., Weng, Y., Yang, X., Jiang, T., and Jiang, H. (2017). Multiple drug transporters mediate the placental transport of sulpiride. *Arch Toxicol* **91**, 3873-3884.

Bakhsheshian, J., Hall, M. D., Robey, R. W., Herrmann, M. A., Chen, J.-Q., Bates, S. E., and Gottesman, M. M. (2013). Overlapping substrate and inhibitor specificity of human and murine abcg2. *Drug Metabolism and Disposition* **41**, 1805-1812.

Balogh, A., Pozsgay, J., Matko, J., Dong, Z., Kim, C. J., Varkonyi, T., Sammar, M., Rigo, J., Jr., Meiri, H., Romero, R., Papp, Z., and Than, N. G. (2011). Placental protein 13 (pp13/galectin-13) undergoes lipid raft-associated subcellular redistribution in the syncytiotrophoblast in preterm preeclampsia and hellp syndrome. *Am J Obstet Gynecol* **205**, 156.e151-114.

Bandera, E. V., Chandran, U., Buckley, B., Lin, Y., Isukapalli, S., Marshall, I., King, M., and Zarbl, H. (2011). Urinary mycoestrogens, body size and breast development in new jersey girls. *Sci Total Environ* **409**, 5221-5227.

Barakat, S., Gayet, L., Dayan, G., Labialle, S., Lazar, A., Oleinikov, V., Coleman, A. W., and Baggetto, L. G. (2005). Multidrug-resistant cancer cells contain two populations of p-

glycoprotein with differently stimulated p-gp atpase activities: Evidence from atomic force microscopy and biochemical analysis. *Biochem J* **388**, 563-571.

Bartels, Ä., and O'Donoghue, K. (2011). Cholesterol in pregnancy: A review of knowns and unknowns. *Obstetric Medicine* **4**, 147-151.

Barth, F., and Rinaldi-Carmona, M. (1999). The development of cannabinoid antagonists. *Curr Med Chem* **6**, 745-755.

Basu, S., Rajakaruna, S., Dickinson, B. C., Chang, C. J., and Menko, A. S. (2014). Endogenous hydrogen peroxide production in the epithelium of the developing embryonic lens. *Mol Vis* **20**, 458-467.

Battioni, J.-P., Dupré, D., Delaforge, M., Jaouen, M., and Mansuy, D. (1988). Réactions des dérivés de l'iode(iii) avec les ferroporphyrines et le cytochrome p-450: Formation de complexes σ-aryles du fer(iii) et de n-aryl-porphyrines du fer(ii) à partir de sels de diaryliodonium. *Journal of Organometallic Chemistry* **358**, 389-400.

Battista, N., Bari, M., and Maccarrone, M. (2015). Endocannabinoids and reproductive events in health and disease. *Handb Exp Pharmacol* **231**, 341-365.

Baumann, M. U., Schneider, H., Malek, A., Palta, V., Surbek, D. V., Sager, R., Zamudio, S., and Illsley, N. P. (2014). Regulation of human trophoblast glut1 glucose transporter by insulin-like growth factor i (igf-i). *PLoS One* **9**, e106037.

Bayewitch, M., Avidor-Reiss, T., Levy, R., Barg, J., Mechoulam, R., and Vogel, Z. (1995). The peripheral cannabinoid receptor: Adenylate cyclase inhibition and g protein coupling. *FEBS Lett* **375**, 143-147.

Bayyareddy, K., Zhu, X., Orlando, R., and Adang, M. J. (2012). Proteome analysis of cry4ba toxin-interacting aedes aegypti lipid rafts using gelc-ms/ms. *Journal of proteome research* **11**, 5843-5855.

Beery, E., Rajnai, Z., Abonyi, T., Makai, I., Bansaghi, S., Erdo, F., Sziraki, I., Heredi-Szabo, K., Kis, E., Jani, M., Marki-Zay, J., Toth, G. K., and Krajcsi, P. (2012). Abcg2 modulates chlorothiazide permeability--in vitro-characterization of its interactions. *Drug Metab Pharmacokinet* **27**, 349-353.

Belli, P., Bellaton, C., Durand, J., Balleydier, S., Milhau, N., Mure, M., Mornex, J. F., Benahmed, M., and Le Jan, C. (2010). Fetal and neonatal exposure to the mycotoxin zearalenone induces phenotypic alterations in adult rat mammary gland. *Food Chem Toxicol* **48**, 2818-2826.

Bergmeyer, H. U. (1975). [new values for the molar extinction coefficients of nadh and nadph for the use in routine laboratories (author's transl)]. *Z Klin Chem Klin Biochem* **13**, 507-508.

Bernhoft, A., Behrens, G. H., Ingebrigtsen, K., Langseth, W., Berndt, S., Haugen, T. B., and Grotmol, T. (2001). Placental transfer of the estrogenic mycotoxin zearalenone in rats. *Reprod Toxicol* **15**, 545-550.

Bircsak, K. M., and Aleksunes, L. M. (2015). Interaction of isoflavones with the bcrp/abcg2 drug transporter. *Curr Drug Metab* **16**, 124-140.

Bircsak, K. M., Gibson, C. J., Robey, R. W., and Aleksunes, L. M. (2013). Assessment of drug transporter function using fluorescent cell imaging. *Curr Protoc Toxicol* **57**, Unit 23.26.

Bircsak, K. M., Gupta, V., Yuen, P. Y., Gorczyca, L., Weinberger, B. I., Vetrano, A. M., and Aleksunes, L. M. (2016). Genetic and dietary regulation of glyburide efflux by the human placental breast cancer resistance protein transporter. *J Pharmacol Exp Ther* **357**, 103-113.

Bircsak, K. M., Moscovitz, J. E., Wen, X., Archer, F., Yuen, P. Y. S., Mohammed, M., Memon, N., Weinberger, B. I., Saba, L. M., Vetrano, A. M., and Aleksunes, L. M. (2018). Interindividual regulation of the breast cancer resistance protein/abcg2 transporter in term human placentas. *Drug Metab Dispos* **46**, 619-627.

Boelsterli, U. A., Ho, H. K., Zhou, S., and Leow, K. Y. (2006). Bioactivation and hepatotoxicity of nitroaromatic drugs. *Curr Drug Metab* **7**, 715-727.

Brangi, M., Litman, T., Ciotti, M., Nishiyama, K., Kohlhagen, G., Takimoto, C., Robey, R., Pommier, Y., Fojo, T., and Bates, S. E. (1999). Camptothecin resistance: Role of the atp-binding cassette (abc), mitoxantrone-resistance half-transporter (mxr), and potential for glucuronidation in mxr-expressing cells. *Cancer Research* **59**, 5938-5946.

Bream, E. N., Leppellere, C. R., Cooper, M. E., Dagle, J. M., Merrill, D. C., Christensen, K., Simhan, H. N., Fong, C. T., Hallman, M., Muglia, L. J., Marazita, M. L., and Murray, J. C. (2013). Candidate gene linkage approach to identify DNA variants that predispose to preterm birth. *Pediatr Res* **73**, 135-141.

Brent, R. L. (2001). The cause and prevention of human birth defects: What have we learned in the past 50 years? *Congenital Anomalies* **41**, 3-21.

Brents, L. K., Reichard, E. E., Zimmerman, S. M., Moran, J. H., Fantegrossi, W. E., and Prather, P. L. (2011). Phase i hydroxylated metabolites of the k2 synthetic cannabinoid jwh-018 retain in vitro and in vivo cannabinoid 1 receptor affinity and activity. *PLoS One* **6**, e21917.

Brown, D. A., and London, E. (1998). Functions of lipid rafts in biological membranes. *Annu Rev Cell Dev Biol* **14**, 111-136.

Burger, H., van Tol, H., Boersma, A. W. M., Brok, M., Wiemer, E. A. C., Stoter, G., and Nooter, K. (2004). Imatinib mesylate (sti571) is a substrate for the breast cancer resistance protein (bcrp)/abcg2 drug pump. *Blood* **104**, 2940-2942.

Byrne, S., Ahenkorah, J., Hottor, B., Lockwood, C., and Ockleford, C. D. (2007). Immuno-electron microscopic localisation of caveolin 1 in human placenta. *Immunobiology* **212**, 39-46.

Cai, X., Bikadi, Z., Ni, Z., Lee, E. W., Wang, H., Rosenberg, M. F., and Mao, Q. (2010). Role of basic residues within or near the predicted transmembrane helix 2 of the human breast cancer resistance protein in drug transport. *J Pharmacol Exp Ther* **333**, 670-681.

Carter, A. M. (2007). Animal models of human placentation--a review. *Placenta* **28 Suppl A**, S41-47.

Ceckova, M., Libra, A., Pavek, P., Nachtigal, P., Brabec, M., Fuchs, R., and Staud, F. (2006). Expression and functional activity of breast cancer resistance protein (bcrp, abcg2) transporter in the human choriocarcinoma cell line bewo. *Clin Exp Pharmacol Physiol* **33**, 58-65.

Ceckova, M., Reznicek, J., Ptackova, Z., Cerveny, L., Muller, F., Kacerovsky, M., Fromm, M. F., Glazier, J. D., and Staud, F. (2016). Role of abc and solute carrier transporters in the placental transport of lamivudine. *Antimicrob Agents Chemother* **60**, 5563-5572.

Cella, M., Leguizamón, G. F., Sordelli, M. S., Cervini, M., Guadagnoli, T., Ribeiro, M. L., Franchi, A. M., and Farina, M. G. (2008). Dual effect of anandamide on rat placenta nitric oxide synthesis. *Placenta* **29**, 699-707.

Cenas, N., Prast, S., Nivinskas, H., Sarlauskas, J., and Arner, E. S. (2006). Interactions of nitroaromatic compounds with the mammalian selenoprotein thioredoxin reductase and the relation to induction of apoptosis in human cancer cells. *J Biol Chem* **281**, 5593-5603.

Cerf, E., Gasper, R., Belani, J. D., Rychnovsky, S., Chang, X. B., Buyse, F., and Ruysschaert, J. M. (2007). Multidrug resistance protein 1 is not associated to detergent-resistant membranes. *Biochem Biophys Res Commun* **355**, 1025-1030.

Chakraborty, S., and Massey, V. (2002). Reaction of reduced flavins and flavoproteins with diphenyliodonium chloride. *J Biol Chem* **277**, 41507-41516.

Chamberlain, L. H., Burgoyne, R. D., and Gould, G. W. (2001). Snare proteins are highly enriched in lipid rafts in pc12 cells: Implications for the spatial control of exocytosis. *Proc Natl Acad Sci U S A* **98**, 5619-5624.

Chamley, L. W., Bhalla, A., Stone, P. R., Liddell, H., O'Carroll, S., Kearn, C., and Glass, M. (2008). Nuclear localisation of the endocannabinoid metabolizing enzyme fatty acid amide hydrolase (faah) in invasive trophoblasts and an association with recurrent miscarriage. *Placenta* **29**, 970-975.

Chan, H. W., McKirdy, N. C., Peiris, H. N., Rice, G. E., and Mitchell, M. D. (2013). The role of endocannabinoids in pregnancy. *Reproduction* **146**, R101-109.

Chen, Z. S., Robey, R. W., Belinsky, M. G., Shchaveleva, I., Ren, X. Q., Sugimoto, Y., Ross, D. D., Bates, S. E., and Kruh, G. D. (2003). Transport of methotrexate, methotrexate polyglutamates, and 17beta-estradiol 17-(beta-d-glucuronide) by abcg2: Effects of acquired mutations at r482 on methotrexate transport. *Cancer Research* **63**, 4048-4054.

Chiapella, C., Radovan, R. D., Moreno, J. A., Casares, L., Barbe, J., and Llagostera, M. (2000). Plant activation of aromatic amines mediated by cytochromes p450 and flavin-containing monooxygenases. *Mutat Res* **470**, 155-160.

Christensen, B. (2000). Which antibiotics are appropriate for treating bacteriuria in pregnancy? *J Antimicrob Chemother* **46 Suppl A**, 29-34.

Christopoulos, A., and Wilson, K. (2001). Interaction of anandamide with the m1 and m4 muscarinic acetylcholine receptors. *Brain Research* **915**, 70-78.

Cinar, R., Gochuico, B. R., Iyer, M. R., Jourdan, T., Yokoyama, T., Park, J. K., Coffey, N. J., Pri-Chen, H., Szanda, G., Liu, Z., Mackie, K., Gahl, W. A., and Kunos, G. (2017). Cannabinoid cb1 receptor overactivity contributes to the pathogenesis of idiopathic pulmonary fibrosis. *JCI Insight* **2**.

ClinicalTrials.gov (2018). Pravastatin for the prevention of preeclampsia in high-risk women: A phase i pilot study [pravastatin for prevention of preeclampsia]. In (

Commision, E. (2006). Commission regulation (ec) no 1881/2006 of 19 december 2006 setting maximum levels for certain contaminants in foodstuffs. *Off. J. Eur. Union* **L364**, 5-24.

Cooper, Z. D. (2016). Adverse effects of synthetic cannabinoids: Management of acute toxicity and withdrawal. *Curr Psychiatry Rep* **18**, 52.

Cooray, H. C., Janvilisri, T., van Veen, H. W., Hladky, S. B., and Barrand, M. A. (2004a). Interaction of the breast cancer resistance protein with plant polyphenols. *Biochem. Biophys. Res. Commun.* **317**, 269-275.

Cooray, H. C., Janvilisri, T., van Veen, H. W., Hladky, S. B., and Barrand, M. A. (2004b). Interaction of the breast cancer resistance protein with plant polyphenols. *Biochem Biophys Res Commun* **317**, 269-275.

Costa, M. A. (2016a). The endocannabinoid system: A novel player in human placentation. *Reprod Toxicol* **61**, 58-67.

Costa, M. A. (2016b). The endocrine function of human placenta: An overview. *Reprod Biomed Online* **32**, 14-43.

Costa, M. A., Fonseca, B. M., Mendes, A., Braga, J., Teixeira, N. A., and Correia da Silva, G. (2015a). The endocannabinoid anandamide affects the synthesis of human syncytiotrophoblast-related proteins. *Cell Tissue Res* **362**, 441-446.

Costa, M. A., Fonseca, B. M., Teixeira, N. A., and Correia-da-Silva, G. (2015b). The endocannabinoid anandamide induces apoptosis in cytotrophoblast cells: Involvement of both mitochondrial and death receptor pathways. *Placenta* **36**, 69-76.

Cross, A. R., Henderson, L., Jones, O. T., Delpiano, M. A., Hentschel, J., and Acker, H. (1990). Involvement of an nad(p)h oxidase as a po2 sensor protein in the rat carotid body. *Biochem J* **272**, 743-747.

Cunningham, F. G., Leveno, K. J., Bloom, S. L., Spong, C. Y., Dashe, J. S., Hoffman, B. L., Casey, B. M., and Sheffield, J. S. (2014). *Williams obstetrics, 24th edition*. McGraw-Hill Education, Columbus, OH.

Dankers, A. C., Roelofs, M. J., Piersma, A. H., Sweep, F. C., Russel, F. G., van den Berg, M., van Duursen, M. B., and Masereeuw, R. (2013). Endocrine disruptors differentially target atp-binding cassette transporters in the blood-testis barrier and affect leydig cell testosterone secretion in vitro. *Toxicol Sci* **136**, 382-391.

Das, M., and Das, D. K. (2012). Caveolae, caveolin, and cavins: Potential targets for the treatment of cardiac disease. *Ann Med* **44**, 530-541.

Davitian, C., Uzan, M., Tigaizin, A., Ducarme, G., Dauphin, H., and Poncelet, C. (2006). [maternal cannabis use and intra-uterine growth restriction]. *Gynecol Obstet Fertil* **34**, 632-637. First published on Consommation maternelle de cannabis et retard de croissance intra-uterin.

De Baere, S., Osselaere, A., Devreese, M., Vanhaecke, L., De Backer, P., and Croubels, S. (2012). Development of a liquid-chromatography tandem mass spectrometry and ultra-high-performance liquid chromatography high-resolution mass spectrometry method for the quantitative determination of zearalenone and its major metabolites in chicken and pig plasma. *Anal Chim Acta* **756**, 37-48.

de Gooijer, M. C., de Vries, N. A., Buckle, T., Buil, L. C. M., Beijnen, J. H., Boogerd, W., and van Tellingen, O. (2018). Improved brain penetration and antitumor efficacy of temozolomide by inhibition of abcb1 and abcg2. *Neoplasia* **20**, 710-720.

De Matteis, F., Ballou, D. P., Coon, M. J., Estabrook, R. W., and Haines, D. C. (2012). Peroxidase-like activity of uncoupled cytochrome p450: Studies with bilirubin and toxicological implications of uncoupling. *Biochem Pharmacol* **84**, 374-382.

de Vries, N. A., Buckle, T., Zhao, J., Beijnen, J. H., Schellens, J. H., and van Tellingen, O. (2012). Restricted brain penetration of the tyrosine kinase inhibitor erlotinib due to the drug transporters p-gp and bcrp. *Invest New Drugs* **30**, 443-449.

Delaforge, M., Battioni, P., Mahy, J. P., and Mansuy, D. (1986). In vivo formation of sigma-methyl- and sigma-phenyl-ferric complexes of hemoglobin and liver-cytochrome p-450 upon treatment of rats with methyl- and phenylhydrazine. *Chem Biol Interact* **60**, 101-113.

Delidaki, M., Gu, M., Hein, A., Vatish, M., and Grammatopoulos, D. K. (2011). Interplay of camp and mapk pathways in hcg secretion and fusogenic gene expression in a trophoblast cell line. *Mol Cell Endocrinol* **332**, 213-220.

Demeule, M., Jodoin, J., Gingras, D., and Beliveau, R. (2000). P-glycoprotein is localized in caveolae in resistant cells and in brain capillaries. *FEBS Lett* **466**, 219-224.

Di Marzo, V., Capasso, R., Matias, I., Aviello, G., Petrosino, S., Borrelli, F., Romano, B., Orlando, P., Capasso, F., and Izzo, A. A. (2008). The role of endocannabinoids in the regulation of gastric emptying: Alterations in mice fed a high-fat diet. *British Journal of Pharmacology* **153**, 1272-1280.

Dlugos, A., Childs, E., Stuhr, K. L., Hillard, C. J., and de Wit, H. (2012). Acute stress increases circulating anandamide and other n-acylethanolamines in healthy humans. *Neuropsychopharmacology* **37**, 2416-2427.

Dornetshuber, R., Heffeter, P., Sulyok, M., Schumacher, R., Chiba, P., Kopp, S., Koellensperger, G., Micksche, M., Lemmens-Gruber, R., and Berger, W. (2009). Interactions between abc-transport proteins and the secondary fusarium metabolites enniatin and beauvericin. *Mol Nutr Food Res* **53**, 904-920.

Doussiere, J., Gaillard, J., and Vignais, P. V. (1999). The heme component of the neutrophil nadph oxidase complex is a target for aryliodonium compounds. *Biochemistry* **38**, 3694-3703.

Doussiere, J., and Vignais, P. V. (1992). Diphenylene iodonium as an inhibitor of the nadph oxidase complex of bovine neutrophils. Factors controlling the inhibitory potency of diphenylene iodonium in a cell-free system of oxidase activation. *Eur J Biochem* **208**, 61-71.

Doyle, L. A., Yang, W., Abruzzo, L. V., Krogmann, T., Gao, Y., Rishi, A. K., and Ross, D. D. (1998a). A multidrug resistance transporter from human mcf-7 breast cancer cells. *Proc Natl Acad Sci U S A* **95**, 15665-15670.

Doyle, L. A., Yang, W., Abruzzo, L. V., Krogmann, T., Gao, Y., Rishi, A. K., and Ross, D. D. (1998b). A multidrug resistance transporter from human mcf-7 breast cancer cells. *Proc. Natl. Acad. Sci.* **95**, 15665-15670.

Durmus, S., Sparidans, R. W., Wagenaar, E., Beijnen, J. H., and Schinkel, A. H. (2012). Oral availability and brain penetration of the b-rafv600e inhibitor vemurafenib can be enhanced by the p-glycoprotein (abcb1) and breast cancer resistance protein (abcg2) inhibitor elacridar. *Mol Pharm* **9**, 3236-3245.

Duzyj, C. M., Buhimschi, I. A., Motawea, H., Laky, C. A., Cozzini, G., Zhao, G., Funai, E. F., and Buhimschi, C. S. (2015). The invasive phenotype of placenta accreta extravillous trophoblasts associates with loss of e-cadherin. *Placenta* **36**, 645-651.

Eberhardt, M. K., and Colina, R. (1988). The reaction of oh radicals with dimethyl sulfoxide. A comparative study of fenton's reagent and the radiolysis of aqueous dimethyl sulfoxide solutions. *The Journal of Organic Chemistry* **53**, 1071-1074.

Edison, R. J., Berg, K., Remaley, A., Kelley, R., Rotimi, C., Stevenson, R. E., and Muenke, M. (2007). Adverse birth outcome among mothers with low serum cholesterol. *Pediatrics* **120**, 723-733.

El Marroun, H., Tiemeier, H., Steegers, E. A., Jaddoe, V. W., Hofman, A., Verhulst, F. C., van den Brink, W., and Huizink, A. C. (2009). Intrauterine cannabis exposure affects fetal growth trajectories: The generation r study. *J Am Acad Child Adolesc Psychiatry* **48**, 1173-1181.

Elahian, F., Sepehrizadeh, Z., Moghimi, B., and Mirzaei, S. A. (2014). Human cytochrome b5 reductase: Structure, function, and potential applications. *Crit Rev Biotechnol* **34**, 134-143.

Elsohly, M. A., and Slade, D. (2005). Chemical constituents of marijuana: The complex mixture of natural cannabinoids. *Life Sci* **78**, 539-548.

Endres, M., Laufs, U., Huang, Z., Nakamura, T., Huang, P., Moskowitz, M. A., and Liao, J. K. (1998). Stroke protection by 3-hydroxy-3-methylglutaryl (hmg)-coa reductase inhibitors mediated by endothelial nitric oxide synthase. *Proc Natl Acad Sci U S A* **95**, 8880-8885.

Engeli, S., Böhnke, J., Feldpausch, M., Gorzelniak, K., Janke, J., Bátkai, S., Pacher, P., Harvey-White, J., Luft, F. C., Sharma, A. M., and Jordan, J. (2005). Activation of the peripheral endocannabinoid system in human obesity. *Diabetes* **54**, 2838-2843.

Enokizono, J., Kusuhara, H., and Sugiyama, Y. (2007). Effect of breast cancer resistance protein (bcrp/abcg2) on the disposition of phytoestrogens. *Mol. Pharmacol.* **72**, 967-975.

Eshkoli, T., Sheiner, E., Ben-Zvi, Z., and Holcberg, G. (2011). Drug transport across the placenta. *Curr Pharm Biotechnol* **12**, 707-714.

Evseenko, D. A., Murthi, P., Paxton, J. W., Reid, G., Emerald, B. S., Mohankumar, K. M., Lobie, P. E., Brennecke, S. P., Kalionis, B., and Keelan, J. A. (2007a). The abc transporter bcrp/abcg2 is a placental survival factor, and its expression is reduced in idiopathic human fetal growth restriction. *Faseb j* **21**, 3592-3605.

Evseenko, D. A., Paxton, J. W., and Keelan, J. A. (2007b). The xenobiotic transporter abcg2 plays a novel role in differentiation of trophoblast-like bewo cells. *Placenta* **28 Suppl A**, S116-120.

Fantegrossi, W. E., Moran, J. H., Radominska-Pandya, A., and Prather, P. L. (2014). Distinct pharmacology and metabolism of k2 synthetic cannabinoids compared to delta(9)-thc: Mechanism underlying greater toxicity? *Life Sci* **97**, 45-54.

Feinshtein, V., Erez, O., Ben-Zvi, Z., Erez, N., Eshkoli, T., Sheizaf, B., Sheiner, E., Huleihel, M., and Holcberg, G. (2013a). Cannabidiol changes p-gp and bcrp expression in trophoblast cell lines. *PeerJ* **1**, e153.

Feinshtein, V., Erez, O., Ben-Zvi, Z., Eshkoli, T., Sheizaf, B., Sheiner, E., and Holcberg, G. (2013b). Cannabidiol enhances xenobiotic permeability through the human placental barrier by direct inhibition of breast cancer resistance protein: An ex vivo study. *Am J Obstet Gynecol* **209**, 573.e571-573.e515.

Fermo, E., Bianchi, P., Vercellati, C., Marcello, A. P., Garatti, M., Marangoni, O., Barcellini, W., and Zanella, A. (2008). Recessive hereditary methemoglobinemia: Two novel mutations in the nadh-cytochrome b5 reductase gene. *Blood Cells Mol Dis* **41**, 50-55.

Fezza, F., Oddi, S., Di Tommaso, M., De Simone, C., Rapino, C., Pasquariello, N., Dainese, E., Finazzi-Agro, A., and Maccarrone, M. (2008). Characterization of biotin-anandamide, a novel tool for the visualization of anandamide accumulation. *J Lipid Res* **49**, 1216-1223.

Fields, R. D., and Lancaster, M. V. (1993). Dual-attribute continuous monitoring of cell proliferation/cytotoxicity. *Am Biotechnol Lab* **11**, 48-50.

Fleck, S. C., Churchwell, M. I., Doerge, D. R., and Teeguarden, J. G. (2016). Urine and serum biomonitoring of exposure to environmental estrogens ii: Soy isoflavones and zearalenone in pregnant women. *Food Chem Toxicol* **95**, 19-27.

Fonseca, B. M., Battista, N., Correia-da-Silva, G., Rapino, C., Maccarrone, M., and Teixeira, N. A. (2014). Activity of anandamide (aea) metabolic enzymes in rat placental bed. *Reprod Toxicol* **49**, 74-77.

Fox, K. A., Longo, M., Tamayo, E., Kechichian, T., Bytautiene, E., Hankins, G. D., Saade, G. R., and Costantine, M. M. (2011). Effects of pravastatin on mediators of vascular function in a mouse model of soluble fms-like tyrosine kinase-1-induced preeclampsia. *Am J Obstet Gynecol* **205**, 366.e361-365.

Francois, L. N., Gorczyca, L., Du, J., Bircsak, K. M., Yen, E., Wen, X., Tu, M. J., Yu, A. M., Illsley, N. P., Zamudio, S., and Aleksunes, L. M. (2017). Down-regulation of the placental bcrp/abcg2 transporter in response to hypoxia signaling. *Placenta* **51**, 57-63.

Fugedi, G., Molnar, M., Rigo, J., Jr., Schonleber, J., Kovalszky, I., and Molvarec, A. (2014). Increased placental expression of cannabinoid receptor 1 in preeclampsia: An observational study. *BMC Pregnancy Childbirth* **14**, 395.

Fussell, K. C., Udasin, R. G., Gray, J. P., Mishin, V., Smith, P. J., Heck, D. E., and Laskin, J. D. (2011a). Redox cycling and increased oxygen utilization contribute to diquat-induced oxidative stress and cytotoxicity in chinese hamster ovary cells overexpressing nadph-cytochrome p450 reductase. *Free Radic Biol Med* **50**, 874-882.

Fussell, K. C., Udasin, R. G., Smith, P. J., Gallo, M. A., and Laskin, J. D. (2011b). Catechol metabolites of endogenous estrogens induce redox cycling and generate reactive oxygen species in breast epithelial cells. *Carcinogenesis* **32**, 1285-1293.

Gahir, S. S., and Piquette-Miller, M. (2011). Gestational and pregnane x receptor-mediated regulation of placental atp-binding cassette drug transporters in mice. *Drug Metab Dispos* **39**, 465-471.

Gait, J. E. (1990). Hemolytic reactions to nitrofurantoin in patients with glucose-6-phosphate dehydrogenase deficiency: Theory and practice. *Dicp* **24**, 1210-1213.

Galeeva, N. M., Voevoda, M. I., Spiridonova, M. G., Stepanov, V. A., and Poliakov, A. V. (2013). [population frequency and age of c.806c > t mutation in cyb5r3 gene as cause of recessive congenital methemoglobinemia in yakutia]. *Genetika* **49**, 523-530.

Galiegue, S., Mary, S., Marchand, J., Dussossoy, D., Carriere, D., Carayon, P., Bouaboula, M., Shire, D., Le Fur, G., and Casellas, P. (1995). Expression of central and

peripheral cannabinoid receptors in human immune tissues and leukocyte subpopulations. *Eur J Biochem* **232**, 54-61.

Ganguly, S., Panetta, J. C., Roberts, J. K., and Schuetz, E. G. (2018). Ketamine pharmacokinetics and pharmacodynamics are altered by p-glycoprotein and breast cancer resistance protein efflux transporters in mice. *Drug Metab Dispos* **46**, 1014-1022.

Garner, A. P., Paine, M. J., Rodriguez-Crespo, I., Chinje, E. C., Ortiz De Montellano, P., Stratford, I. J., Tew, D. G., and Wolf, C. R. (1999). Nitric oxide synthases catalyze the activation of redox cycling and bioreductive anticancer agents. *Cancer Res* **59**, 1929-1934.

Gayet, L., Dayan, G., Barakat, S., Labialle, S., Michaud, M., Cogne, S., Mazane, A., Coleman, A. W., Rigal, D., and Baggetto, L. G. (2005). Control of p-glycoprotein activity by membrane cholesterol amounts and their relation to multidrug resistance in human cem leukemia cells. *Biochemistry* **44**, 4499-4509.

Gebeh, A. K., Willets, J. M., Bari, M., Hirst, R. A., Marczylo, T. H., Taylor, A. H., Maccarrone, M., and Konje, J. C. (2013). Elevated anandamide and related n-acylethanolamine levels occur in the peripheral blood of women with ectopic pregnancy and are mirrored by changes in peripheral fatty acid amide hydrolase activity. *J Clin Endocrinol Metab* **98**, 1226-1234.

Gebeh, A. K., Willets, J. M., Marczylo, E. L., Taylor, A. H., and Konje, J. C. (2012). Ectopic pregnancy is associated with high anandamide levels and aberrant expression of faah and cb1 in fallopian tubes. *J Clin Endocrinol Metab* **97**, 2827-2835.

Gedeon, C., Anger, G., Piquette-Miller, M., and Koren, G. (2008). Breast cancer resistance protein: Mediating the trans-placental transfer of glyburide across the human placenta. *Placenta* **29**, 39-43.

Gedeon, C., Behravan, J., Koren, G., and Piquette-Miller, M. (2006). Transport of glyburide by placental abc transporters: Implications in fetal drug exposure. *Placenta* **27**, 1096-1102.

Gelineau-van Waes, J., Starr, L., Maddox, J., Aleman, F., Voss, K. A., Wilberding, J., and Riley, R. T. (2005). Maternal fumonisin exposure and risk for neural tube defects: Mechanisms in an in vivo mouse model. *Birth Defects Res A Clin Mol Teratol* **73**, 487-497.

Gelsomino, G., Corsetto, P. A., Campia, I., Montorfano, G., Kopecka, J., Castella, B., Gazzano, E., Ghigo, D., Rizzo, A. M., and Riganti, C. (2013). Omega 3 fatty acids chemosensitize multidrug resistant colon cancer cells by down-regulating cholesterol synthesis and altering detergent resistant membranes composition. *Mol Cancer* **12**, 137.

Gherasim, C. G., Zaman, U., Raza, A., and Banerjee, R. (2008). Impeded electron transfer from a pathogenic fmn domain mutant of methionine synthase reductase and its responsiveness to flavin supplementation. *Biochemistry* **47**, 12515-12522.

Ghosal, A., Hapangama, N., Yuan, Y., Lu, X., Horne, D., Patrick, J. E., and Zbaida, S. (2003). Rapid determination of enzyme activities of recombinant human cytochromes p450, human liver microsomes and hepatocytes. *Biopharm Drug Dispos* **24**, 375-384.

Giang, D. K., and Cravatt, B. F. (1997). Molecular characterization of human and mouse fatty acid amide hydrolases. *Proc Natl Acad Sci U S A* **94**, 2238-2242.

Gibson, C. J., Hossain, M. M., Richardson, J. R., and Aleksunes, L. M. (2012). Inflammatory regulation of atp binding cassette efflux transporter expression and function in microglia. *J Pharmacol Exp Ther* **343**, 650-660.

Gillette, J. R., Brodie, B. B., and La Du, B. N. (1957). The oxidation of drugs by liver microsomes: On the role of tpnh and oxygen. *J Pharmacol Exp Ther* **119**, 532-540.

Glodkowska-Mrowka, E., Mrowka, P., Basak, G. W., Niesiobedzka-Krezel, J., Seferynska, I., Wlodarski, P. K., Jakobisiak, M., and Stoklosa, T. (2014). Statins inhibit abcb1 and abcg2 drug transporter activity in chronic myeloid leukemia cells and potentiate antileukemic effects of imatinib. *Exp Hematol* **42**, 439-447.

Gluckman, P. D., and Hanson, M. A. (2004). Living with the past: Evolution, development, and patterns of disease. *Science* **305**, 1733-1736.

Godoy, V., and Riquelme, G. (2008). Distinct lipid rafts in subdomains from human placental apical syncytiotrophoblast membranes. *J Membr Biol* **224**, 21-31.

Goncalves, P., Gregorio, I., and Martel, F. (2011). The short-chain fatty acid butyrate is a substrate of breast cancer resistance protein. *Am J Physiol Cell Physiol* **301**, C984-994.

Gong, I., E. Mansell, S., and B. Kim, R. (2018). *Role of efflux transporters mdr1 and bcrp in rivaroxaban drug disposition*.

Gonzalez-Lobato, L., Real, R., Prieto, J. G., Alvarez, A. I., and Merino, G. (2010). Differential inhibition of murine bcrp1/abcg2 and human bcrp/abcg2 by the mycotoxin fumitremorgin c. *Eur J Pharmacol* **644**, 41-48.

Gormley, M., Ona, K., Kapidzic, M., Garrido-Gomez, T., Zdravkovic, T., and Fisher, S. J. (2017). Preeclampsia: Novel insights from global rna profiling of trophoblast subpopulations. *Am J Obstet Gynecol* **217**, 200 e201-200 e217.

Gouveia-Figueira, S., Goldin, K., Hashemian, S. A., Lindberg, A., Persson, M., Nording, M. L., Laurell, K., and Fowler, C. J. (2017). Plasma levels of the endocannabinoid anandamide, related n-acylethanolamines and linoleic acid-derived oxylipins in patients with migraine. *Prostaglandins Leukot Essent Fatty Acids* **120**, 15-24.

Gowland, P. A., Francis, S. T., Duncan, K. R., Freeman, A. J., Issa, B., Moore, R. J., Bowtell, R. W., Baker, P. N., Johnson, I. R., and Worthington, B. S. (1998). In vivo perfusion measurements in the human placenta using echo planar imaging at 0.5 t. *Magn Reson Med* **40**, 467-473.

Gray, E., Karslake, J., Machta, B. B., and Veatch, S. L. (2013). Liquid general anesthetics lower critical temperatures in plasma membrane vesicles. *Biophys J* **105**, 2751-2759.

Gray, J. P., Heck, D. E., Mishin, V., Smith, P. J., Hong, J. Y., Thiruchelvam, M., Cory-Slechta, D. A., Laskin, D. L., and Laskin, J. D. (2007). Paraquat increases cyanide-insensitive respiration in murine lung epithelial cells by activating an nad(p)h:Paraquat oxidoreductase: Identification of the enzyme as thioredoxin reductase. *J Biol Chem* **282**, 7939-7949.

Grinwich, D. L., Ham, E. A., Hichens, M., and Behrman, H. R. (1976). Binding of human chorionic gonadotropin and response of cyclic nucleotides to luteinizing hormone in luteal tissue from rats treated with prostaglandin f2alpha. *Endocrinology* **98**, 146-150.

Grosser, N., Hemmerle, A., Berndt, G., Erdmann, K., Hinkelmann, U., Schurger, S., Wijayanti, N., Immenschuh, S., and Schroder, H. (2004). The antioxidant defense protein heme oxygenase 1 is a novel target for statins in endothelial cells. *Free Radic Biol Med* **37**, 2064-2071.

Guengerich, F. P. (2005). Reduction of cytochrome b5 by nadph-cytochrome p450 reductase. *Arch Biochem Biophys* **440**, 204-211.

Guengerich, F. P., Martin, M. V., Sohl, C. D., and Cheng, Q. (2009). Measurement of cytochrome p450 and nadph-cytochrome p450 reductase. *Nat Protoc* **4**, 1245-1251.

Gunness, P., Aleksa, K., and Koren, G. (2011). Acyclovir is a substrate for the human breast cancer resistance protein (bcrp/abcg2): Implications for renal tubular transport and acyclovir-induced nephrotoxicity. *Can J Physiol Pharmacol* **89**, 675-680.

Gupta, S. K., Malhotra, S. S., Malik, A., Verma, S., and Chaudhary, P. (2016). Cell signaling pathways involved during invasion and syncytialization of trophoblast cells. *Am J Reprod Immunol* **75**, 361-371.

Gutierrez, A., Paine, M., Wolf, C. R., Scrutton, N. S., and Roberts, G. C. (2002). Relaxation kinetics of cytochrome p450 reductase: Internal electron transfer is limited by conformational change and regulated by coenzyme binding. *Biochemistry* **41**, 4626-4637.

Habayeb, O. M., Taylor, A. H., Bell, S. C., Taylor, D. J., and Konje, J. C. (2008). Expression of the endocannabinoid system in human first trimester placenta and its role in trophoblast proliferation. *Endocrinology* **149**, 5052-5060.

Habayeb, O. M., Taylor, A. H., Evans, M. D., Cooke, M. S., Taylor, D. J., Bell, S. C., and Konje, J. C. (2004). Plasma levels of the endocannabinoid anandamide in women--a potential role in pregnancy maintenance and labor? *J Clin Endocrinol Metab* **89**, 5482-5487.

Hahnova-Cygalova, L., Ceckova, M., and Staud, F. (2011). Fetoprotective activity of breast cancer resistance protein (bcrp, abcg2): Expression and function throughout pregnancy. *Drug Metab Rev* **43**, 53-68.

Hartel, S., Diehl, H. A., and Ojeda, F. (1998). Methyl-beta-cyclodextrins and liposomes as water-soluble carriers for cholesterol incorporation into membranes and its evaluation by a microenzymatic fluorescence assay and membrane fluidity-sensitive dyes. *Anal Biochem* **258**, 277-284.

He, J., Wei, C., Li, Y., Liu, Y., Wang, Y., Pan, J., Liu, J., Wu, Y., and Cui, S. (2018). Zearalenone and alpha-zearalenol inhibit the synthesis and secretion of pig follicle stimulating hormone via the non-classical estrogen membrane receptor gpr30. *Mol Cell Endocrinol* **461**, 43-54.

Hegedus, C., Telbisz, A., Hegedus, T., Sarkadi, B., and Ozvegy-Laczka, C. (2015). Lipid regulation of the abcb1 and abcg2 multidrug transporters. *Adv Cancer Res* **125**, 97-137.

Hemauer, S. J., Patrikeeva, S. L., Nanovskaya, T. N., Hankins, G. D. V., and Ahmed, M. S. (2010). Role of human placental apical membrane transporters in the efflux of glyburide, rosiglitazone, and metformin. *American journal of obstetrics and gynecology* **202**, 383.e381-383.e387.

Herzog, M., Storch, C. H., Gut, P., Kotlyar, D., Fullekrug, J., Ehehalt, R., Haefeli, W. E., and Weiss, J. (2011). Knockdown of caveolin-1 decreases activity of breast cancer resistance protein (bcrp/abcg2) and increases chemotherapeutic sensitivity. *Naunyn Schmiedebergs Arch Pharmacol* **383**, 1-11.

Heyman, E., Gamelin, F. X., Goekint, M., Piscitelli, F., Roelands, B., Leclair, E., Di Marzo, V., and Meeusen, R. (2012). Intense exercise increases circulating endocannabinoid and bdnf levels in humans--possible implications for reward and depression. *Psychoneuroendocrinology* **37**, 844-851.

Hidalgo, I. J., Raub, T. J., and Borchardt, R. T. (1989). Characterization of the human colon carcinoma cell line (caco-2) as a model system for intestinal epithelial permeability. *Gastroenterology* **96**, 736-749.

Hilakivi-Clarke, L., Cho, E., and Clarke, R. (1998). Maternal genistein exposure mimics the effects of estrogen on mammary gland development in female mouse offspring. *Oncol Rep* **5**, 609-616.

Hillyard, D. Z., Nutt, C. D., Thomson, J., McDonald, K. J., Wan, R. K., Cameron, A. J. M., Mark, P. B., and Jardine, A. G. (2007). Statins inhibit nk cell cytotoxicity by membrane raft depletion rather than inhibition of isoprenylation. *Atherosclerosis* **191**, 319-325.

Hines, M. (2011). Prenatal endocrine influences on sexual orientation and on sexually differentiated childhood behavior. *Frontiers in Neuroendocrinology* **32**, 170-182.

Hinrichs, J. W., Klappe, K., Hummel, I., and Kok, J. W. (2004). Atp-binding cassette transporters are enriched in non-caveolar detergent-insoluble glycosphingolipid-enriched membrane domains (digs) in human multidrug-resistant cancer cells. *J Biol Chem* **279**, 5734-5738.

Hirano, M., Maeda, K., Matsushima, S., Nozaki, Y., Kusuhara, H., and Sugiyama, Y. (2005). Involvement of bcrp (abcg2) in the biliary excretion of pitavastatin. *Mol Pharmacol* **68**, 800-807.

Hochstein, P. (1983). Futile redox cycling: Implications for oxygen radical toxicity. *Fundam Appl Toxicol* **3**, 215-217.

Hodin, S., Basset, T., Jacqueroux, E., Delezay, O., Clotagatide, A., Perek, N., Mismetti, P., and Delavenne, X. (2018). In vitro comparison of the role of p-glycoprotein and breast cancer resistance protein on direct oral anticoagulants disposition **43**, 183-191.

Holder, B. S., Tower, C. L., Abrahams, V. M., and Aplin, J. D. (2012). Syncytin 1 in the human placenta. *Placenta* **33**, 460-466.

Holland, M. L., Lau, D. T., Allen, J. D., and Arnold, J. C. (2007). The multidrug transporter abcg2 (bcrp) is inhibited by plant-derived cannabinoids. *Br J Pharmacol* **152**, 815-824.

Huang, L., Wang, Y., and Grimm, S. (2006). Atp-dependent transport of rosuvastatin in membrane vesicles expressing breast cancer resistance protein. *Drug Metab Dispos* **34**, 738-742.

Huang, R., Zhang, M., Rwere, F., Waskell, L., and Ramamoorthy, A. (2015). Kinetic and structural characterization of the interaction between the fmn binding domain of cytochrome p450 reductase and cytochrome c. *J Biol Chem* **290**, 4843-4855.

Hudspeth, M. P., Joseph, S., and Holden, K. R. (2010). A novel mutation in type ii methemoglobinemia. *J Child Neurol* **25**, 91-93.

Imai, Y., Asada, S., Tsukahara, S., Ishikawa, E., Tsuruo, T., and Sugimoto, Y. (2003a). Breast cancer resistance protein exports sulfated estrogens but not free estrogens. *Mol. Pharmacol.* **64**, 610-618.

Imai, Y., Asada, S., Tsukahara, S., Ishikawa, E., Tsuruo, T., and Sugimoto, Y. (2003b). Breast cancer resistance protein exports sulfated estrogens but not free estrogens. *Mol Pharmacol* **64**, 610-618.

Imai, Y., Nakane, M., Kage, K., Tsukahara, S., Ishikawa, E., Tsuruo, T., Miki, Y., and Sugimoto, Y. (2002). C421a polymorphism in the human breast cancer resistance protein gene is associated with low expression of q141k protein and low-level drug resistance. *Mol Cancer Ther* **1**, 611-616.

Imai, Y., Tsukahara, S., Asada, S., and Sugimoto, Y. (2004). Phytoestrogens/flavonoids reverse breast cancer resistance protein/abcg2-mediated multidrug resistance. *Cancer Research* **64**, 4346-4352.

Iqbal, S. Z., Asi, M. R., Jinap, S., and Rashid, U. (2014). Detection of aflatoxins and zearalenone contamination in wheat derived products. *Food Control* **35**, 223-226.

Ito, Y., and Ohtsubo, K. (1994). Effects of neonatal administration of zearalenone on the reproductive physiology of female mice. *J Vet Med Sci* **56**, 1155-1159.

Iyanagi, T., Watanabe, S., and Anan, K. F. (1984). One-electron oxidation-reduction properties of hepatic nadh-cytochrome b5 reductase. *Biochemistry* **23**, 1418-1425.

Iyanagi, T., and Yamazaki, I. (1969). One-electron-transfer reactions in biochemical systems. 3. One-electron reduction of quinones by microsomal flavin enzymes. *Biochim Biophys Acta* **172**, 370-381.

Iyanagi, T., and Yamazaki, I. (1970). One-electron-transfer reactions in biochemical systems. V. Difference in the mechanism of quinone reduction by the nadh dehydrogenase and the nad(p)h dehydrogenase (dt-diaphorase). *Biochim Biophys Acta* **216**, 282-294.

Jacknowitz, A. I., Le Frock, J. L., and Prince, R. A. (1977). Nitrofurantoin polyneuropathy: Report of two cases. *Am J Hosp Pharm* **34**, 759-762.

Jackson, S. M., Manolaridis, I., and Kowal, J. (2018). Structural basis of small-molecule inhibition of human multidrug transporter abcg2 **25**, 333-340.

Jalalian, N., Ishikawa, E. E., Silva, L. F., Jr., and Olofsson, B. (2011). Room temperature, metal-free synthesis of diaryl ethers with use of diaryliodonium salts. *Org Lett* **13**, 1552-1555.

Jandu, H., Aluzaite, K., Fogh, L., Thrane, S. W., Noer, J. B., Proszek, J., Do, K. N., Hansen, S. N., Damsgaard, B., Nielsen, S. L., Stougaard, M., Knudsen, B. R., Moreira, J., Hamerlik, P., Gajjar, M., Smid, M., Martens, J., Foekens, J., Pommier, Y., Brunner, N., Schrohl, A. S., and Stenvang, J. (2016). Molecular characterization of irinotecan (sn-38) resistant human breast cancer cell lines. *BMC Cancer* **16**, 34.

Jani, M., Ambrus, C., Magnan, R., Jakab, K. T., Beery, E., Zolnerciks, J. K., and Krajcsi, P. (2014). Structure and function of bcrp, a broad specificity transporter of xenobiotics and endobiotics. *Arch Toxicol* **88**, 1205-1248.

Janvilisri, T., Shahi, S., Venter, H., Balakrishnan, L., and van Veen, Hendrik W. (2005). Arginine-482 is not essential for transport of antibiotics, primary bile acids and unconjugated sterols by the human breast cancer resistance protein (abcg2). *Biochemical Journal* **385**, 419-426.

Jaques, S. C., Kingsbury, A., Henshcke, P., Chomchai, C., Clews, S., Falconer, J., Abdel-Latif, M. E., Feller, J. M., and Oei, J. L. (2014). Cannabis, the pregnant woman and her child: Weeding out the myths. *J Perinatol* **34**, 417-424.

Jebbink, J., Veenboer, G., Boussata, S., Keijser, R., Kremer, A. E., Elferink, R. O., van der Post, J., Afink, G., and Ris-Stalpers, C. (2015a). Total bile acids in the maternal and fetal compartment in relation to placental abcg2 expression in preeclamptic pregnancies complicated by hellp syndrome. *Biochim Biophys Acta* **1852**, 131-136.

Jebbink, J., Veenboer, G., Boussata, S., Keijser, R., Kremer, A. E., Elferink, R. O., van der Post, J., Afink, G., and Ris-Stalpers, C. (2015b). Total bile acids in the maternal and fetal compartment in relation to placental abcg2 expression in preeclamptic pregnancies complicated by hellp syndrome. *Biochimica et Biophysica Acta (BBA) - Molecular Basis of Disease* **1852**, 131-136.

Jefferson, W. N., and Williams, C. J. (2011). Circulating levels of genistein in the neonate, apart from dose and route, predict future adverse female reproductive outcomes. *Reprod Toxicol* **31**, 272-279.

Jimenez, V., Henriquez, M., Llanos, P., and Riquelme, G. (2004). Isolation and purification of human placental plasma membranes from normal and pre-eclamptic pregnancies. A comparative study. *Placenta* **25**, 422-437.

Johns, D. G., Behm, D. J., Walker, D. J., Ao, Z., Shapland, E. M., Daniels, D. A., Riddick, M., Dowell, S., Staton, P. C., Green, P., Shabon, U., Bao, W., Aiyar, N., Yue, T. L., Brown, A. J., Morrison, A. D., and Douglas, S. A. (2007). The novel endocannabinoid receptor gpr55 is activated by atypical cannabinoids but does not mediate their vasodilator effects. *British Journal of Pharmacology* **152**, 825-831.

Jonker, J. W., Buitelaar, M., Wagenaar, E., Van Der Valk, M. A., Scheffer, G. L., Scheper, R. J., Plosch, T., Kuipers, F., Elferink, R. P., Rosing, H., Beijnen, J. H., and Schinkel, A. H. (2002a). The breast cancer resistance protein protects against a major chlorophyll-derived dietary phototoxin and protoporphyria. *Proc Natl Acad Sci U S A* **99**, 15649-15654.

Jonker, J. W., Buitelaar, M., Wagenaar, E., Van Der Valk, M. A., Scheffer, G. L., Scheper, R. J., Plosch, T., Kuipers, F., Elferink, R. P., Rosing, H., Beijnen, J. H., and Schinkel, A. H. (2002b). The breast cancer resistance protein protects against a major chlorophyll-derived dietary phototoxin and protoporphyria. *Proc. Natl. Acad. Sci. U.S.A.* **99**, 15649-15654.

Kage, K., Fujita, T., and Sugimoto, Y. (2005). Role of cys-603 in dimer/oligomer formation of the breast cancer resistance protein bcrp/abcg2. *Cancer Sci* **96**, 866-872.

Kahya, N., Brown, D. A., and Schwille, P. (2005). Raft partitioning and dynamic behavior of human placental alkaline phosphatase in giant unilamellar vesicles. *Biochemistry* **44**, 7479-7489.

Kamat, A. M., and Lamm, D. L. (2004). Antitumor activity of common antibiotics against superficial bladder cancer. *Urology* **63**, 457-460.

Kamau, S. W., Kramer, S. D., Gunthert, M., and Wunderli-Allenspach, H. (2005). Effect of the modulation of the membrane lipid composition on the localization and function of p-glycoprotein in mdr1-mdck cells. *In Vitro Cell Dev Biol Anim* **41**, 207-216.

Kawamura, K., Yamasaki, T., Yui, J., Hatori, A., Konno, F., Kumata, K., Irie, T., Fukumura, T., Suzuki, K., Kanno, I., and Zhang, M. R. (2009). In vivo evaluation of p-glycoprotein and breast cancer resistance protein modulation in the brain using [(11)c]gefitinib. *Nucl Med Biol* **36**, 239-246.

Kazmin, A., Garcia-Bournissen, F., and Koren, G. (2007). Risks of statin use during pregnancy: A systematic review. *J Obstet Gynaecol Can* **29**, 906-908.

Khunweeraphong, N., Stockner, T., and Kuchler, K. (2017). The structure of the human abc transporter abcg2 reveals a novel mechanism for drug extrusion. *Sci Rep* **7**, 13767.

Kimura, T., Ohta, T., Watanabe, K., Yoshimura, H., and Yamamoto, I. (1998). Anandamide, an endogenous cannabinoid receptor ligand, also interacts with 5-hydroxytryptamine (5-ht) receptor. *Biological & Pharmaceutical Bulletin* **21**, 224-226.

Kis, E., Nagy, T., Jani, M., Molnar, E., Janossy, J., Ujhellyi, O., Nemet, K., Heredi-Szabo, K., and Krajcsi, P. (2009). Leflunomide and its metabolite a771726 are high affinity substrates of bcrp: Implications for drug resistance. *Ann Rheum Dis* **68**, 1201-1207.

Klaassen, C. D., and Aleksunes, L. M. (2010). Xenobiotic, bile acid, and cholesterol transporters: Function and regulation. *Pharmacol Rev* **62**, 1-96.

Klappe, K., Dijkhuis, A. J., Hummel, I., van Dam, A., Ivanova, P. T., Milne, S. B., Myers, D. S., Brown, H. A., Permentier, H., and Kok, J. W. (2010). Extensive sphingolipid depletion does not affect lipid raft integrity or lipid raft localization and efflux function of the abc transporter mrp1. *Biochem J* **430**, 519-529.

Klappe, K., Hummel, I., Hoekstra, D., and Kok, J. W. (2009). Lipid dependence of abc transporter localization and function. *Chem Phys Lipids* **161**, 57-64.

Knerr, I., Beinder, E., and Rascher, W. (2002). Syncytin, a novel human endogenous retroviral gene in human placenta: Evidence for its dysregulation in preeclampsia and hellp syndrome. *Am J Obstet Gynecol* **186**, 210-213.

Knofler, M., Saleh, L., Strohmer, H., Husslein, P., and Wolschek, M. F. (1999). Cyclic amp- and differentiation-dependent regulation of the proximal alphahcg gene promoter in term villous trophoblasts. *Mol Hum Reprod* **5**, 573-580.

Koraichi, F., Videmann, B., Mazallon, M., Benahmed, M., Prouillac, C., and Lecoeur, S. (2012). Zearalenone exposure modulates the expression of abc transporters and nuclear receptors in pregnant rats and fetal liver. *Toxicol Lett* **211**, 246-256.

Koritzinsky, M., Magagnin, M. G., van den Beucken, T., Seigneuric, R., Savelkouls, K., Dostie, J., Pyronnet, S., Kaufman, R. J., Weppler, S. A., Voncken, J. W., Lambin, P., Koumenis, C., Sonenberg, N., and Wouters, B. G. (2006). Gene expression during acute and prolonged hypoxia is regulated by distinct mechanisms of translational control. *Embo j* **25**, 1114-1125.

Krishnamurthy, P., Ross, D. D., Nakanishi, T., Bailey-Dell, K., Zhou, S., Mercer, K. E., Sarkadi, B., Sorrentino, B. P., and Schuetz, J. D. (2004). The stem cell marker bcrp/abcg2 enhances hypoxic cell survival through interactions with heme. *J. Biol. Chem.* **279**, 24218-24225.

Krishnamurthy, P., and Schuetz, J. D. (2006). Role of abcg2/bcrp in biology and medicine. *Annu Rev Pharmacol Toxicol* **46**, 381-410.

Krishnamurthy, U., Yadav, B. K., Jella, P. K., Haacke, E. M., Hernandez-Andrade, E., Mody, S., Yeo, L., Hassan, S. S., Romero, R., and Neelavalli, J. (2017). Quantitative flow imaging in human umbilical vessels in utero using nongated 2d phase contrast mri. *J Magn Reson Imaging*.

Kruijtzer, C. M., Beijnen, J. H., Rosing, H., ten Bokkel Huinink, W. W., Schot, M., Jewell, R. C., Paul, E. M., and Schellens, J. H. (2002). Increased oral bioavailability of topotecan in combination with the breast cancer resistance protein and p-glycoprotein inhibitor gf120918. *J Clin Oncol* **20**, 2943-2950.

Kuan, C. Y., Walker, T. H., Luo, P. G., and Chen, C. F. (2011). Long-chain polyunsaturated fatty acids promote paclitaxel cytotoxicity via inhibition of the mdr1 gene in the human colon cancer caco-2 cell line. *J Am Coll Nutr* **30**, 265-273.

Kudo, Y., Boyd, C. A., Millo, J., Sargent, I. L., and Redman, C. W. (2003). Manipulation of cd98 expression affects both trophoblast cell fusion and amino acid transport activity during syncytialization of human placental bewo cells. *J Physiol* **550**, 3-9.

Kuiper-Goodman, T., Scott, P. M., and Watanabe, H. (1987). Risk assessment of the mycotoxin zearalenone. *Regul Toxicol Pharmacol* **7**, 253-306.

Kumasawa, K., Ikawa, M., Kidoya, H., Hasuwa, H., Saito-Fujita, T., Morioka, Y., Takakura, N., Kimura, T., and Okabe, M. (2011). Pravastatin induces placental growth factor (pgf) and ameliorates preeclampsia in a mouse model. *Proc Natl Acad Sci U S A* **108**, 1451-1455.

Kunimatsu, S., Mizuno, T., Fukudo, M., and Katsura, T. (2013). Effect of p-glycoprotein and breast cancer resistance protein inhibition on the pharmacokinetics of sunitinib in rats. *Drug Metab Dispos* **41**, 1592-1597.

Kurian, J. R., Bajad, S. U., Miller, J. L., Chin, N. A., and Trepanier, L. A. (2004). Nadh cytochrome b5 reductase and cytochrome b5 catalyze the microsomal reduction of xenobiotic hydroxylamines and amidoximes in humans. *J Pharmacol Exp Ther* **311**, 1171-1178.

Kurzban, G. P., and Strobel, H. W. (1986). Preparation and characterization of fad-dependent nadph-cytochrome p-450 reductase. *J Biol Chem* **261**, 7824-7830.

Lagas, J. S., van der Kruijssen, C. M., van de Wetering, K., Beijnen, J. H., and Schinkel, A. H. (2009). Transport of diclofenac by breast cancer resistance protein (abcg2) and stimulation of multidrug resistance protein 2 (abcc2)-mediated drug transport by diclofenac and benzbromarone. *Drug Metab Dispos* **37**, 129-136.

Lahouar, A., Jedidi, I., Sanchis, V., and Said, S. (2018). Aflatoxin b1, ochratoxin a and zearalenone in sorghum grains marketed in tunisia. *Food Addit Contam Part B Surveill*, 1-8.

Laufs, U., Fata, V. L., and Liao, J. K. (1997). Inhibition of 3-hydroxy-3-methylglutaryl (hmg)-coa reductase blocks hypoxia-mediated down-regulation of endothelial nitric oxide synthase. *J Biol Chem* **272**, 31725-31729.

Lee, Y. J., Kusuhara, H., Jonker, J. W., Schinkel, A. H., and Sugiyama, Y. (2005). Investigation of efflux transport of dehydroepiandrosterone sulfate and mitoxantrone at the mouse blood-brain barrier: A minor role of breast cancer resistance protein. *J Pharmacol Exp Ther* **312**, 44-52.

Lemaire, P., and Livingstone, D. R. (1994). Inhibition studies on the involvement of flavoprotein reductases in menadione- and nitrofurantoin-stimulated oxyradical production by hepatic microsomes of flounder (platichthys flesus). *J Biochem Toxicol* **9**, 87-95.

Levental, I., and Veatch, S. (2016). The continuing mystery of lipid rafts. *J Mol Biol* **428**, 4749-4764.

Lewis, U. J. (1954). Acid cleavage of heme proteins. *J Biol Chem* **206**, 109-120.

Li, H., van Ravenzwaay, B., Rietjens, I. M., and Louisse, J. (2013a). Assessment of an in vitro transport model using bewo b30 cells to predict placental transfer of compounds. *Arch Toxicol* **87**, 1661-1669.

Li, J., Wang, Y., and Hidalgo, I. J. (2013b). Kinetic analysis of human and canine p-glycoprotein-mediated drug transport in mdr1-mdck cell model: Approaches to reduce false-negative substrate classification. *J Pharm Sci* **102**, 3436-3446.

Li, X., Pan, Y. Z., Seigel, G. M., Hu, Z. H., Huang, M., and Yu, A. M. (2011). Breast cancer resistance protein bcrp/abcg2 regulatory microrna s (hsa-mir-328, -519c and -520h) and their differential expression in stem-like abcg2+ cancer cells. *Biochem Pharmacol* **81**, 783-792.

Licht, P., Cao, H., Lei, Z. M., Rao, C. V., and Merz, W. E. (1993). Novel self-regulation of human chorionic gonadotropin biosynthesis in term pregnancy human placenta. *Endocrinology* **133**, 3014-3025.

Lin, L. S., Roberts, V. J., and Yen, S. S. (1995). Expression of human gonadotropin-releasing hormone receptor gene in the placenta and its functional relationship to human chorionic gonadotropin secretion. *J Clin Endocrinol Metab* **80**, 580-585.

Lin, S. L., Chien, C. W., Han, C. L., Chen, E. S., Kao, S. H., Chen, Y. J., and Liao, F. (2010). Temporal proteomics profiling of lipid rafts in ccr6-activated t cells reveals the integration of actin cytoskeleton dynamics. *J Proteome Res* **9**, 283-297.

Lin, Y., Bircsak, K. M., Gorczyca, L., Wen, X., and Aleksunes, L. M. (2016). Regulation of the placental bcrp transporter by ppar gamma. *J Biochem Mol Toxicol*.

Lingwood, D., and Simons, K. (2010). Lipid rafts as a membrane-organizing principle. *Science* **327**, 46-50.

Linton, E. A., Rodriguez-Linares, B., Rashid-Doubell, F., Ferguson, D. J., and Redman, C. W. (2003). Caveolae and caveolin-1 in human term villous trophoblast. *Placenta* **24**, 745-757.

Litman, T., Brangi, M., Hudson, E., Fetsch, P., Abati, A., Ross, D. D., Miyake, K., Resau, J. H., and Bates, S. E. (2000). The multidrug-resistant phenotype associated with overexpression of the new abc half-transporter, mxr (abcg2). *J. Cell. Sci.* **113 (Pt 11)**, 2011-2021.

Liu, J., Wang, L., Harvey-White, J., Huang, B. X., Kim, H. Y., Luquet, S., Palmiter, R. D., Krystal, G., Rai, R., Mahadevan, A., Razdan, R. K., and Kunos, G. (2008). Multiple pathways involved in the biosynthesis of anandamide. *Neuropharmacology* **54**, 1-7.

Liu, W. M., Duan, E. K., and Cao, Y. J. (2002). Effects of anandamide on embryo implantation in the mouse. *Life Sci* **71**, 1623-1632.

Locuson, C. W., Hutzler, J. M., and Tracy, T. S. (2007). Visible spectra of type ii cytochrome p450-drug complexes: Evidence that "incomplete" heme coordination is common. *Drug Metab Dispos* **35**, 614-622.

Louisa, M., Soediro, T. M., and Suyatna, F. D. (2014). In vitro modulation of p-glycoprotein, mrp-1 and bcrp expression by mangiferin in doxorubicin-treated mcf-7 cells. *Asian Pac J Cancer Prev* **15**, 1639-1642.

Lowry, O. H., Rosebrough, N. J., Farr, A. L., and Randall, R. J. (1951). Protein measurement with the folin phenol reagent. *J Biol Chem* **193**, 265-275.

Lozovaya, N., Yatsenko, N., Beketov, A., Tsintsadze, T., and Burnashev, N. (2005). Glycine receptors in cns neurons as a target for nonretrograde action of cannabinoids. *The Journal of Neuroscience* **25**, 7499-7506.

Lucero, H. A., and Robbins, P. W. (2004). Lipid rafts-protein association and the regulation of protein activity. *Arch Biochem Biophys* **426**, 208-224.

Lyden, T. W., Anderson, C. L., and Robinson, J. M. (2002). The endothelium but not the syncytiotrophoblast of human placenta expresses caveolae. *Placenta* **23**, 640-652.

Lye, P., Bloise, E., Dunk, C., Javam, M., Gibb, W., Lye, S. J., and Matthews, S. G. (2013). Effect of oxygen on multidrug resistance in the first trimester human placenta. *Placenta* **34**, 817-823.

Maccarrone, M., Di Rienzo, M., Battista, N., Gasperi, V., Guerrieri, P., Rossi, A., and Finazzi-Agro, A. (2003). The endocannabinoid system in human keratinocytes. Evidence that anandamide inhibits epidermal differentiation through cb1 receptor-dependent inhibition of protein kinase c, activation protein-1, and transglutaminase. *J Biol Chem* **278**, 33896-33903.

Mader, T. L. (1994). Effect of implant sequence and dose on feedlot cattle performance. *J Anim Sci* **72**, 277-282.

Majander, A., Finel, M., and Wikstrom, M. (1994). Diphenyleneiodonium inhibits reduction of iron-sulfur clusters in the mitochondrial nadh-ubiquinone oxidoreductase (complex i). *J Biol Chem* **269**, 21037-21042.

Maliepaard, M., Scheffer, G. L., Faneyte, I. F., van Gastelen, M. A., Pijnenborg, A. C., Schinkel, A. H., van De Vijver, M. J., Scheper, R. J., and Schellens, J. H. (2001). Subcellular localization and distribution of the breast cancer resistance protein transporter in normal human tissues. *Cancer Res* **61**, 3458-3464.

Maliepaard, M., van Gastelen, M. A., de Jong, L. A., Pluim, D., van Waardenburg, R. C., Ruevekamp-Helmers, M. C., Floot, B. G., and Schellens, J. H. (1999). Overexpression of the bcrp/mxr/abcp gene in a topotecan-selected ovarian tumor cell line. *Cancer Res* **59**, 4559-4563.

Mao, Q. (2008). Bcrp/abcg2 in the placenta: Expression, function and regulation. *Pharm Res* **25**, 1244-1255.

Martin, W. J., 2nd (1983). Nitrofurantoin: Evidence for the oxidant injury of lung parenchymal cells. *Am Rev Respir Dis* **127**, 482-486.

Martins, C. J., Genelhu, V., Pimentel, M. M., Celoria, B. M., Mangia, R. F., Aveta, T., Silvestri, C., Di Marzo, V., and Francischetti, E. A. (2015). Circulating endocannabinoids and the polymorphism 385c>a in fatty acid amide hydrolase (faah) gene may identify the obesity phenotype related to cardiometabolic risk: A study conducted in a brazilian population of complex interethnic admixture. *PLoS One* **10**, e0142728.

Mason, C. W., Buhimschi, I. A., Buhimschi, C. S., Dong, Y., Weiner, C. P., and Swaan, P. W. (2011). Atp-binding cassette transporter expression in human placenta as a function of pregnancy condition. *Drug Metabolism and Disposition* **39**, 1000-1007.

Mason, C. W., Lee, G. T., Dong, Y., Zhou, H., He, L., and Weiner, C. P. (2014). Effect of prostaglandin e2 on multidrug resistance transporters in human placental cells. *Drug Metab Dispos* **42**, 2077-2086.

Mastorakos, G., and Ilias, I. (2003). Maternal and fetal hypothalamic-pituitary-adrenal axes during pregnancy and postpartum. *Ann N Y Acad Sci* **997**, 136-149.

Matsumoto, H., Sato, Y., Horie, A., Suginami, K., Tani, H., Hattori, A., Araki, Y., Kagami, K., Konishi, I., and Fujiwara, H. (2016). Cd9 suppresses human extravillous trophoblast invasion. *Placenta* **47**, 105-112.

Matsuo, M. (2010). Atp-binding cassette proteins involved in glucose and lipid homeostasis. *Biosci Biotechnol Biochem* **74**, 899-907.

Matsushima, S., Maeda, K., Kondo, C., Hirano, M., Sasaki, M., Suzuki, H., and Sugiyama, Y. (2005). Identification of the hepatic efflux transporters of organic anions using double-transfected madin-darby canine kidney ii cells expressing human organic anion-transporting polypeptide 1b1 (oatp1b1)/multidrug resistance-associated protein 2, oatp1b1/multidrug resistance 1, and oatp1b1/breast cancer resistance protein. *J Pharmacol Exp Ther* **314**, 1059-1067.

Mauro, T., Hao, L., Pop, L. C., Buckley, B., Schneider, S. H., Bandera, E. V., and Shapses, S. A. (2018). Circulating zearalenone and its metabolites differ in women due to body mass index and food intake. *Food Chem Toxicol* **116**, 227-232.

Mazur, C. S., Marchitti, S. A., Dimova, M., Kenneke, J. F., Lumen, A., and Fisher, J. (2012). Human and rat abc transporter efflux of bisphenol a and bisphenol a glucuronide: Interspecies comparison and implications for pharmacokinetic assessment. *Toxicol Sci* **128**, 317-325.

McGuire, J. J., Anderson, D. J., McDonald, B. J., Narayanasami, R., and Bennett, B. M. (1998). Inhibition of nadph-cytochrome p450 reductase and glyceryl trinitrate biotransformation by diphenyleneiodonium sulfate. *Biochem Pharmacol* **56**, 881-893.

Memon, N., Bircsak, K. M., Archer, F., Gibson, C. J., Ohman-Strickland, P., Weinberger, B. I., Parast, M. M., Vetrano, A. M., and Aleksunes, L. M. (2014). Regional expression of the bcrp/abcg2 transporter in term human placentas. *Reprod Toxicol* **43**, 72-77.

Merino, G., Alvarez, A. I., Pulido, M. M., Molina, A. J., Schinkel, A. H., and Prieto, J. G. (2006). Breast cancer resistance protein (bcrp/abcg2) transports fluoroquinolone antibiotics and affects their oral availability, pharmacokinetics, and milk secretion. *Drug Metab Dispos* **34**, 690-695.

Merino, G., Jonker, J. W., Wagenaar, E., van Herwaarden, A. E., and Schinkel, A. H. (2005). The breast cancer resistance protein (bcrp/abcg2) affects pharmacokinetics, hepatobiliary excretion, and milk secretion of the antibiotic nitrofurantoin. *Mol. Pharmacol.* **67**, 1758-1764.

Meszaros, P., Klappe, K., Hummel, I., Hoekstra, D., and Kok, J. W. (2011). Function of mrp1/abcc1 is not dependent on cholesterol or cholesterol-stabilized lipid rafts. *Biochem J* **437**, 483-491.

Mi, S., Lee, X., Li, X., Veldman, G. M., Finnerty, H., Racie, L., LaVallie, E., Tang, X. Y., Edouard, P., Howes, S., Keith, J. C., Jr., and McCoy, J. M. (2000). Syncytin is a captive retroviral envelope protein involved in human placental morphogenesis. *Nature* **403**, 785-789.

Mihara, K., and Sato, R. (1975). Purification and properties of the intact form of nadh-cytochrome b5 reductase from rabbit liver microsomes. *J Biochem* **78**, 1057-1073.

Miller, R. K., Genbacev, O., Turner, M. A., Aplin, J. D., Caniggia, I., and Huppertz, B. (2005). Human placental explants in culture: Approaches and assessments. *Placenta* **26**, 439-448.

Mishin, V., Gray, J. P., Heck, D. E., Laskin, D. L., and Laskin, J. D. (2010). Application of the amplex red/horseradish peroxidase assay to measure hydrogen peroxide generation by recombinant microsomal enzymes. *Free Radic Biol Med* **48**, 1485-1491.

Mishin, V., Heck, D. E., Laskin, D. L., and Laskin, J. D. (2014). Human recombinant cytochrome p450 enzymes display distinct hydrogen peroxide generating activities during substrate independent nadph oxidase reactions. *Toxicol Sci* **141**, 344-352.

Mishin, V. M., Koivisto, T., and Lieber, C. S. (1996). The determination of cytochrome p450 2e1-dependent p-nitrophenol hydroxylation by high-performance liquid chromatography with electrochemical detection. *Anal Biochem* **233**, 212-215.

Miskiniene, V., Dickancaite, E., Nemeikaite, A., and Cenas, N. (1997). Nitroaromatic betulin derivatives as redox cycling agents. *Biochem Mol Biol Int* **42**, 391-397.

Mitra, P., and Audus, K. L. (2010). Mrp isoforms and bcrp mediate sulfate conjugate efflux out of bewo cells. *Int J Pharm* **384**, 15-23.

Modha, S. G., and Greaney, M. F. (2015). Atom-economical transformation of diaryliodonium salts: Tandem c-h and n-h arylation of indoles. *J Am Chem Soc* **137**, 1416-1419.

Mohrmann, K., van Eijndhoven, M. A., Schinkel, A. H., and Schellens, J. H. (2005). Absence of n-linked glycosylation does not affect plasma membrane localization of breast cancer resistance protein (bcrp/abcg2). *Cancer Chemother Pharmacol* **56**, 344-350.

Molvarec, A., Fugedi, G., Szabo, E., Stenczer, B., Walentin, S., and Rigo, J., Jr. (2015). Decreased circulating anandamide levels in preeclampsia. *Hypertens Res* **38**, 413-418.

Montminy, M. R., and Bilezikjian, L. M. (1987). Binding of a nuclear protein to the cyclic-amp response element of the somatostatin gene. *Nature* **328**, 175-178.

Moore, D. G., Turner, J. D., Parrott, A. C., Goodwin, J. E., Fulton, S. E., Min, M. O., Fox, H. C., Braddick, F. M., Axelsson, E. L., Lynch, S., Ribeiro, H., Frostick, C. J., and Singer, L. T. (2010). During pregnancy, recreational drug-using women stop taking ecstasy (3,4-methylenedioxy-n-methylamphetamine) and reduce alcohol consumption, but continue to smoke tobacco and cannabis: Initial findings from the development and infancy study. *J Psychopharmacol* **24**, 1403-1410.

Mudd, L. M., Holzman, C. B., Catov, J. M., Senagore, P. K., and Evans, R. W. (2012). Maternal lipids at mid-pregnancy and the risk of preterm delivery. *Acta Obstet Gynecol Scand* **91**, 726-735.

Muhl, D., Kathmann, M., Hoyer, C., Kranaster, L., Hellmich, M., Gerth, C. W., Faulhaber, J., Schlicker, E., and Leweke, F. M. (2014). Increased cb2 mrna and anandamide in human blood after cessation of cannabis abuse. *Naunyn-Schmiedeberg's Archives of Pharmacology* **387**, 691-695.

Mukherjee, D., Royce, S. G., Alexander, J. A., Buckley, B., Isukapalli, S. S., Bandera, E. V., Zarbl, H., and Georgopoulos, P. G. (2014). Physiologically-based toxicokinetic modeling of zearalenone and its metabolites: Application to the jersey girl study. *PLoS ONE* **9**, e113632.

Mukhopadhyay, S., and Howlett, A. C. (2001). Cb1 receptor-g protein association. Subtype selectivity is determined by distinct intracellular domains. *Eur J Biochem* **268**, 499-505.

Murataliev, M. B., Feyereisen, R., and Walker, F. A. (2004). Electron transfer by diflavin reductases. *Biochim Biophys Acta* **1698**, 1-26.

Myllynen, P., Kummu, M., Kangas, T., Ilves, M., Immonen, E., Rysa, J., Pirila, R., Lastumaki, A., and Vahakangas, K. H. (2008). Abcg2/bcrp decreases the transfer of a food-born chemical carcinogen, 2-amino-1-methyl-6-phenylimidazo[4,5-b]pyridine (phip) in perfused term human placenta. *Toxicol Appl Pharmacol* **232**, 210-217.

Nagai, T., Shirabe, K., Yubisui, T., and Takeshita, M. (1993). Analysis of mutant nadh-cytochrome b5 reductase: Apparent "type iii" methemoglobinemia can be explained as type i with an unstable reductase. *Blood* **81**, 808-814.

Nakamura, U., and Kadokawa, H. (2015). The nonsteroidal mycoestrogen zearalenone and its five metabolites suppress lh secretion from the bovine anterior pituitary cells via the estradiol receptor gpr30 in vitro. *Theriogenology* **84**, 1342-1349.

Nakayama, A., Matsuo, H., Takada, T., Ichida, K., Nakamura, T., Ikebuchi, Y., Ito, K., Hosoya, T., Kanai, Y., Suzuki, H., and Shinomiya, N. (2011). Abcg2 is a high-capacity urate transporter and its genetic impairment increases serum uric acid levels in humans. *Nucleosides, Nucleotides and Nucleic Acids* **30**, 1091-1097.

Neradugomma, N. K., Liao, M. Z., and Mao, Q. (2017). Buprenorphine, norbuprenorphine, r-methadone, and s-methadone upregulate bcrp/abcg2 expression by activating aryl hydrocarbon receptor in human placental trophoblasts. *Mol Pharmacol* **91**, 237-249.

Nikaido, Y., Yoshizawa, K., Danbara, N., Tsujita-Kyutoku, M., Yuri, T., Uehara, N., and Tsubura, A. (2004). Effects of maternal xenoestrogen exposure on development of the reproductive tract and mammary gland in female cd-1 mouse offspring. *Reprod Toxicol* **18**, 803-811.

Nishizawa, H., Ota, S., Suzuki, M., Kato, T., Sekiya, T., Kurahashi, H., and Udagawa, Y. (2011). Comparative gene expression profiling of placentas from patients with severe pre-eclampsia and unexplained fetal growth restriction. *Reprod Biol Endocrinol* **9**, 107.

Nixon, B., Bielanowicz, A., McLaughlin, E. A., Tanphaichitr, N., Ensslin, M. A., and Aitken, R. J. (2009). Composition and significance of detergent resistant membranes in mouse spermatozoa. *J Cell Physiol* **218**, 122-134.

Nkabinde, L. A., Shoba-Zikhali, L. N., Semete-Makokotlela, B., Kalombo, L., Swai, H. S., Hayeshi, R., Naicker, B., Hillie, T. K., and Hamman, J. H. (2012). Permeation of plga nanoparticles across different in vitro models. *Curr Drug Deliv* **9**, 617-627.

Norris, M. D., De Graaf, D., Haber, M., Kavallaris, M., Madafiglio, J., Gilbert, J., Kwan, E., Stewart, B. W., Mechetner, E. B., Gudkov, A. V., and Roninson, I. B. (1996). Involvement of mdr1 p-glycoprotein in multifactorial resistance to methotrexate. *Int J Cancer* **65**, 613-619.

North, J. A., Rein, D., and Tappel, A. L. (1996). Multicomponent analysis of heme protein spectra in biological materials. *Anal Biochem* **233**, 115-123.

Nothdurfter, C., Tanasic, S., Di Benedetto, B., Rammes, G., Wagner, E. M., Kirmeier, T., Ganal, V., Kessler, J. S., Rein, T., Holsboer, F., and Rupprecht, R. (2010). Impact of lipid raft integrity on 5-ht3 receptor function and its modulation by antidepressants. *Neuropsychopharmacology* **35**, 1510-1519.

O'Brien, P. J. (1991). Molecular mechanisms of quinone cytotoxicity. *Chem Biol Interact* **80**, 1-41.

O'Donnell, Smith, G. C., and Jones, O. T. (1994). Involvement of phenyl radicals in iodonium inhibition of flavoenzymes. *Mol Pharmacol* **46**, 778-785.

O'Donnell, Tew, D. G., Jones, O. T., and England, P. J. (1993). Studies on the inhibitory mechanism of iodonium compounds with special reference to neutrophil nadph oxidase. *Biochem J* **290**, 41-49.

Ofori, B., Rey, E., and Berard, A. (2007). Risk of congenital anomalies in pregnant users of statin drugs. *Br J Clin Pharmacol* **64**, 496-509.

Ogunyemi, D. A., Fong, A., Rad, S., Fong, S., and Kjos, S. L. (2011). Attitudes and practices of healthcare providers regarding gestational diabetes: Results of a survey conducted at the 2010 meeting of the international association of diabetes in pregnancy study group (iadpsg). *Diabet Med* **28**, 976-986.

Ok, H. E., Choi, S. W., Kim, M., and Chun, H. S. (2014). Hplc and uplc methods for the determination of zearalenone in noodles, cereal snacks and infant formula. *Food Chem* **163**, 252-257.

Oka, S., Nakajima, K., Yamashita, A., Kishimoto, S., and Sugiura, T. (2007). Identification of gpr55 as a lysophosphatidylinositol receptor. *Biochemical and Biophysical Research Communications* **362**, 928-934.

Omura, T., and Sato, R. (1964). The carbon monoxide-binding pigment of liver microsomes. I. Evidence for its hemoprotein nature. *J Biol Chem* **239**, 2370-2378.

Oscier, D., Bramble, J., Hodges, E., and Wright, D. (2002). Regression of mucosa-associated lymphoid tissue lymphoma of the bladder after antibiotic therapy. *J Clin Oncol* **20**, 882.

Oz, M., Ravindran, A., Diaz-Ruiz, O., Zhang, L., and Morales, M. (2003). The endogenous cannabinoid anandamide inhibits α₇ nicotinic acetylcholine receptor-mediated responses in xenopus oocytes. *Journal of Pharmacology and Experimental Therapeutics* **306**, 1003-1010.

Page, B., Page, M., and Noel, C. (1993). A new fluorometric assay for cytotoxicity measurements in-vitro. *Int J Oncol* **3**, 473-476.

Pagotto, U., Marsicano, G., Cota, D., Lutz, B., and Pasquali, R. (2006). The emerging role of the endocannabinoid system in endocrine regulation and energy balance. *Endocr Rev* **27**, 73-100.

Paiva, L. A., Wright, P. J., and Koff, R. S. (1992). Long-term hepatic memory for hypersensitivity to nitrofurantoin. *Am J Gastroenterol* **87**, 891-893.

Pan, G., Giri, N., and Elmquist, W. F. (2007). Abcg2/bcrp1 mediates the polarized transport of antiretroviral nucleosides abacavir and zidovudine. *Drug Metab Dispos* **35**, 1165-1173.

Park, B., Gibbons, H. M., Mitchell, M. D., and Glassa, M. (2003). Identification of the cb1 cannabinoid receptor and fatty acid amide hydrolase (faah) in the human placenta. *Placenta* **24**, 473-478.

Park, J. G., Lee, S. K., Hong, I. G., Kim, H. S., Lim, K. H., Choe, K. J., Kim, W. H., Kim, Y. I., Tsuruo, T., and Gottesman, M. M. (1994). Mdr1 gene expression: Its effect on drug resistance to doxorubicin in human hepatocellular carcinoma cell lines. *J Natl Cancer Inst* **86**, 700-705.

Parl, F. F., Dawling, S., Roodi, N., and Crooke, P. S. (2009). Estrogen metabolism and breast cancer a risk model. *Annals of the New York Academy of Sciences* **1155**, 68-75.

Passey, M. E., Sanson-Fisher, R. W., D'Este, C. A., and Stirling, J. M. (2014). Tobacco, alcohol and cannabis use during pregnancy: Clustering of risks. *Drug Alcohol Depend* **134**, 44-50.

Pattillo, R. A., and Gey, G. O. (1968). The establishment of a cell line of human hormone-synthesizing trophoblastic cells in vitro. *Cancer Research* **28**, 1231-1236.

Pattillo, R. A., Gey, G. O., Delfs, E., and Mattingly, R. F. (1968). Human hormone production in vitro. *Science* **159**, 1467-1469.

Pavek, P., Merino, G., Wagenaar, E., Bolscher, E., Novotna, M., Jonker, J. W., and Schinkel, A. H. (2005). Human breast cancer resistance protein: Interactions with steroid drugs, hormones, the dietary carcinogen 2-amino-1-methyl-6-phenylimidazo(4,5-b)pyridine, and transport of cimetidine. *J. Pharmacol. Exp. Ther.* **312**, 144-152.

Peng, L., Yoo, B., Gunewardena, S. S., Lu, H., Klaassen, C. D., and Zhong, X.-b. (2012). Rna sequencing reveals dynamic changes of mrna abundance of cytochromes p450 and their alternative transcripts during mouse liver development. *Drug Metabolism and Disposition* **40**, 1198-1209.

Penketh, P. G., Shyam, K., Baumann, R. P., Ratner, E. S., and Sartorelli, A. C. (2015). A simple and inexpensive method to control oxygen concentrations within physiological and neoplastic ranges. *Anal Biochem* **491**, 1-3.

Pertwee, R. G. (2008). The diverse cb1 and cb2 receptor pharmacology of three plant cannabinoids: Delta9-tetrahydrocannabinol, cannabidiol and delta9-tetrahydrocannabivarin. *Br J Pharmacol* **153**, 199-215.

Pertwee, R. G. (2015). Endocannabinoids and their pharmacological actions. *Handb Exp Pharmacol* **231**, 1-37.

Pisanti, S., Picardi, P., D'Alessandro, A., Laezza, C., and Bifulco, M. (2013a). The endocannabinoid signaling system in cancer. *Trends Pharmacol Sci* **34**, 273-282.

Pisanti, S., Picardi, P., D'Alessandro, A., Laezza, C., and Bifulco, M. (2013b). The endocannabinoid signaling system in cancer. *Trends in Pharmacological Sciences* **34**, 273-282.

Polgar, O., Robey, R. W., Morisaki, K., Dean, M., Michejda, C., Sauna, Z. E., Ambudkar, S. V., Tarasova, N., and Bates, S. E. (2004). Mutational analysis of abcg2: Role of the gxxxg motif. *Biochemistry* **43**, 9448-9456.

Pollex, E., Lubetsky, A., and Koren, G. (2008). The role of placental breast cancer resistance protein in the efflux of glyburide across the human placenta. *Placenta* **29**, 743-747.

Porcelli, L., Giovannetti, E., Assaraf, Y. G., Jansen, G., Scheffer, G. L., Kathman, I., Azzariti, A., Paradiso, A., and Peters, G. J. (2014). The egfr pathway regulates bcrp expression in nsclc cells: Role of erlotinib. *Curr Drug Targets* **15**, 1322-1330.

Porter, T. D. (2012). New insights into the role of cytochrome p450 reductase (por) in microsomal redox biology. *Acta Pharmaceutica Sinica B* **2**, 102-106.

Poulos, T. L. (2005). Intermediates in p450 catalysis. *Philos Trans A Math Phys Eng Sci* **363**, 793-806; discussion 1035-1040.

Prasad, B., Lai, Y., Lin, Y., and Unadkat, J. D. (2013). Interindividual variability in the hepatic expression of the human breast cancer resistance protein (bcrp/abcg2): Effect of age, sex, and genotype. *J Pharm Sci* **102**, 787-793.

Prouillac, C., and Lecoeur, S. (2010). The role of the placenta in fetal exposure to xenobiotics: Importance of membrane transporters and human models for transfer studies. *Drug Metab Dispos* **38**, 1623-1635.

Prouillac, C., Videmann, B., Mazallon, M., and Lecoeur, S. (2009). Induction of cells differentiation and abc transporters expression by a myco-estrogen, zearalenone, in human choriocarcinoma cell line (bewo). *Toxicology* **263**, 100-107.

Prueksaritanont, T., Chu, X., Gibson, C., Cui, D., Yee, K. L., Ballard, J., Cabalu, T., and Hochman, J. (2013). Drug–drug interaction studies: Regulatory guidance and an industry perspective. *The AAPS Journal* **15**, 629-645.

Rabindran, S. K., He, H., Singh, M., Brown, E., Collins, K. I., Annable, T., and Greenberger, L. M. (1998a). Reversal of a novel multidrug resistance mechanism in human colon carcinoma cells by fumitremorgin c. *Cancer Research* **58**, 5850-5858.

Rabindran, S. K., He, H., Singh, M., Brown, E., Collins, K. I., Annable, T., and Greenberger, L. M. (1998b). Reversal of a novel multidrug resistance mechanism in human colon carcinoma cells by fumitremorgin c. *Cancer Res* **58**, 5850-5858.

Radeva, G., and Sharom, F. J. (2004). Isolation and characterization of lipid rafts with different properties from rbl-2h3 (rat basophilic leukaemia) cells. *Biochem J* **380**, 219-230.

Reyner, E. L., Sevidal, S., West, M. A., Clouser-Roche, A., Freiwald, S., Fenner, K., Ullah, M., Lee, C. A., and Smith, B. J. (2013). In vitro characterization of axitinib interactions with human efflux and hepatic uptake transporters: Implications for disposition and drug interactions. *Drug Metab Dispos* **41**, 1575-1583.

Riquelme, G. (2011). Review: Placental syncytiotrophoblast membranes--domains, subdomains and microdomains. *Placenta* **32 Suppl 2**, S196-202.

Riquelme, G., de Gregorio, N., Vallejos, C., Berrios, M., and Morales, B. (2012). Differential expression of potassium channels in placentas from normal and pathological pregnancies: Targeting of the k(ir) 2.1 channel to lipid rafts. *J Membr Biol* **245**, 141-150.

Riquelme, G., Vallejos, C., de Gregorio, N., Morales, B., Godoy, V., Berrios, M., Bastias, N., and Rodriguez, C. (2011). Lipid rafts and cytoskeletal proteins in placental microvilli membranes from preeclamptic and iugr pregnancies. *J Membr Biol* **241**, 127-140.

Robey, R. W., Steadman, K., Polgar, O., Morisaki, K., Blayney, M., Mistry, P., and Bates, S. E. (2004). Pheophorbide a is a specific probe for abcg2 function and inhibition. *Cancer Research* **64**, 1242-1246.

Roland, C. S., Hu, J., Ren, C. E., Chen, H., Li, J., Varvoutis, M. S., Leaphart, L. W., Byck, D. B., Zhu, X., and Jiang, S. W. (2016). Morphological changes of placental syncytium and their implications for the pathogenesis of preeclampsia. *Cell Mol Life Sci* **73**, 365-376.

Rosenberg, M. F., Bikadi, Z., Hazai, E., Starborg, T., Kelley, L., Chayen, N. E., Ford, R. C., and Mao, Q. (2015). Three-dimensional structure of the human breast cancer resistance protein (bcrp/abcg2) in an inward-facing conformation. *Acta Crystallogr D Biol Crystallogr* **71**, 1725-1735.

Ross, R. A., Brockie, H. C., Stevenson, L. A., Murphy, V. L., Templeton, F., Makriyannis, A., and Pertwee, R. G. (1999). Agonist-inverse agonist characterization at cb1 and cb2 cannabinoid receptors of l759633, l759656, and am630. *Br J Pharmacol* **126**, 665-672.

Rossi, L., Silva, J. M., McGirr, L. G., and O'Brien, P. J. (1988). Nitrofurantoin-mediated oxidative stress cytotoxicity in isolated rat hepatocytes. *Biochem Pharmacol* **37**, 3109-3117.

Ruebner, M., Langbein, M., Strissel, P. L., Henke, C., Schmidt, D., Goecke, T. W., Faschingbauer, F., Schild, R. L., Beckmann, M. W., and Strick, R. (2012). Regulation of the human endogenous retroviral syncytin-1 and cell–cell fusion by the nuclear hormone receptors pparγ/rxrα in placentogenesis. *Journal of Cellular Biochemistry* **113**, 2383-2396.

Ryberg, E., Larsson, N., Sjögren, S., Hjorth, S., Hermansson, N. O., Leonova, J., Elebring, T., Nilsson, K., Drmota, T., and Greasley, P. J. (2007). The orphan receptor gpr55 is a novel cannabinoid receptor. *British Journal of Pharmacology* **152**, 1092-1101.

Saito, S., and Nakashima, A. (2014). A review of the mechanism for poor placentation in early-onset preeclampsia: The role of autophagy in trophoblast invasion and vascular remodeling. *J Reprod Immunol* **101-102**, 80-88.

Santen, R. J., Yue, W., and Wang, J. P. (2015). Estrogen metabolites and breast cancer. *Steroids* **99**, 61-66.

Saslowsky, D. E., Lawrence, J., Ren, X., Brown, D. A., Henderson, R. M., and Edwardson, J. M. (2002). Placental alkaline phosphatase is efficiently targeted to rafts in supported lipid bilayers. *J Biol Chem* **277**, 26966-26970.

Scharenberg, C. W., Harkey, M. A., and Torok-Storb, B. (2002). The abcg2 transporter is an efficient hoechst 33342 efflux pump and is preferentially expressed by immature human hematopoietic progenitors. *Blood* **99**, 507-512.

Schempf, A. H., and Strobino, D. M. (2008). Illicit drug use and adverse birth outcomes: Is it drugs or context? *J Urban Health* **85**, 858-873.

Schrickx, J., Lektarau, Y., and Fink-Gremmels, J. (2006). Ochratoxin a secretion by atp-dependent membrane transporters in caco-2 cells. *Arch Toxicol* **80**, 243-249.

Schrickx, J. A., and Fink-Gremmels, J. (2007). Danofloxacin-mesylate is a substrate for atp-dependent efflux transporters. *Br J Pharmacol* **150**, 463-469.

Schuck, S., Honsho, M., Ekroos, K., Shevchenko, A., and Simons, K. (2003). Resistance of cell membranes to different detergents. *Proc Natl Acad Sci U S A* **100**, 5795-5800.

Schuller, D. J., Wilks, A., Ortiz de Montellano, P. R., and Poulos, T. L. (1999). Crystal structure of human heme oxygenase-1. *Nat Struct Biol* **6**, 860-867.

Sesink, A. L., Arts, I. C., de Boer, V. C., Breedveld, P., Schellens, J. H., Hollman, P. C., and Russel, F. G. (2005). Breast cancer resistance protein (bcrp1/abcg2) limits net intestinal uptake of quercetin in rats by facilitating apical efflux of glucuronides. *Mol. Pharmacol.* **67**, 1999-2006.

Shaikh, S. R. (2012). Biophysical and biochemical mechanisms by which dietary n-3 polyunsaturated fatty acids from fish oil disrupt membrane lipid rafts. *J Nutr Biochem* **23**, 101-105.

Shao, Z., Yin, J., Chapman, K., Grzemska, M., Clark, L., Wang, J., and Rosenbaum, D. M. (2016). High-resolution crystal structure of the human cb1 cannabinoid receptor. *Nature*.

Shen, A. L., Porter, T. D., Wilson, T. E., and Kasper, C. B. (1989). Structural analysis of the fmn binding domain of nadph-cytochrome p-450 oxidoreductase by site-directed mutagenesis. *J Biol Chem* **264**, 7584-7589.

Shi, J. D., Golden, T., Guo, C.-J., Tu, S. P., Scott, P., Lee, M.-J., Yang, C. S., and Gow, A. J. (2013). Tocopherol supplementation reduces no production and pulmonary inflammatory response to bleomycin. *Nitric Oxide* **34**, 27-36.

Shin, B. S., Hong, S. H., Bulitta, J. B., Hwang, S. W., Kim, H. J., Lee, J. B., Yang, S. D., Kim, J. E., Yoon, H. S., Kim, D. J., and Yoo, S. D. (2009a). Disposition, oral bioavailability, and tissue distribution of zearalenone in rats at various dose levels. *J Toxicol Environ Health A* **72**, 1406-1411.

Shin, B. S., Hong, S. H., Bulitta, J. B., Lee, J. B., Hwang, S. W., Kim, H. J., Yang, S. D., Yoon, H. S., Kim, D. J., Lee, B. M., and Yoo, S. D. (2009b). Physiologically based pharmacokinetics of zearalenone. *J Toxicol Environ Health A* **72**, 1395-1405.

Shultz, C. A., Quinn, A. M., Park, J. H., Harvey, R. G., Bolton, J. L., Maser, E., and Penning, T. M. (2011). Specificity of human aldo-keto reductases, nad(p)h:Quinone oxidoreductase, and carbonyl reductases to redox-cycle polycyclic aromatic hydrocarbon diones and 4-hydroxyequilenin-o-quinone. *Chem Res Toxicol* **24**, 2153-2166.

Silver, B. J., Bokar, J. A., Virgin, J. B., Vallen, E. A., Milsted, A., and Nilson, J. H. (1987). Cyclic amp regulation of the human glycoprotein hormone alpha-subunit gene is mediated by an 18-base-pair element. *Proc Natl Acad Sci U S A* **84**, 2198-2202.

Simon, V., and Cota, D. (2017). Mechanisms in endocrinology: Endocannabinoids and metabolism: Past, present and future. *Eur J Endocrinol* **176**, R309-r324.

Simons, K., and Sampaio, J. L. (2011). Membrane organization and lipid rafts. *Cold Spring Harb Perspect Biol* **3**, a004697.

Simons, K., and Toomre, D. (2000). Lipid rafts and signal transduction. *Nat Rev Mol Cell Biol* **1**, 31-39.

Sitras, V., Paulssen, R. H., Gronaas, H., Leirvik, J., Hanssen, T. A., Vartun, A., and Acharya, G. (2009). Differential placental gene expression in severe preeclampsia. *Placenta* **30**, 424-433.

Smart, E. J., Ying, Y. S., Mineo, C., and Anderson, R. G. (1995). A detergent-free method for purifying caveolae membrane from tissue culture cells. *Proc Natl Acad Sci U S A* **92**, 10104-10108.

Son, Y., Mishin, V., Welsh, W., Lu, S. E., Laskin, J. D., Kipen, H., and Meng, Q. (2015). A novel high-throughput approach to measure hydroxyl radicals induced by airborne particulate matter. *Int J Environ Res Public Health* **12**, 13678-13695.

Spiro, A. S., Wong, A., Boucher, A. A., and Arnold, J. C. (2012). Enhanced brain disposition and effects of delta9-tetrahydrocannabinol in p-glycoprotein and breast cancer resistance protein knockout mice. *PLoS One* **7**, e35937.

Stevens, V. L., and Tang, J. (1997). Fumonisin b1-induced sphingolipid depletion inhibits vitamin uptake via the glycosylphosphatidylinositol-anchored folate receptor. *J Biol Chem* **272**, 18020-18025.

Storch, C. H., Ehehalt, R., Haefeli, W. E., and Weiss, J. (2007). Localization of the human breast cancer resistance protein (bcrp/abcg2) in lipid rafts/caveolae and modulation of its activity by cholesterol in vitro. *J Pharmacol Exp Ther* **323**, 257-264.

Strittmatter, P. (1960). The nature of the heme binding in microsomal cytochrome b5. *J Biol Chem* **235**, 2492-2497.

Strittmatter, P. (1965). Protein and coenzyme interactions in the nadh-cytochrome b5 reductase system. *Fed Proc* **24**, 1156-1163.

Strittmatter, P., and Velick, S. F. (1956). The isolation and properties of microsomal cytochrome. *The Journal of biological chemistry* **221**, 253-264.

Stuehr, D. J. (1999). Mammalian nitric oxide synthases. *Biochim Biophys Acta* **1411**, 217-230.

Stuehr, D. J., Fasehun, O. A., Kwon, N. S., Gross, S. S., Gonzalez, J. A., Levi, R., and Nathan, C. F. (1991). Inhibition of macrophage and endothelial cell nitric oxide synthase by diphenyleneiodonium and its analogs. *FASEB J* **5**, 98-103.

Sun, X., Xie, H., Yang, J., Wang, H., Bradshaw, H. B., and Dey, S. K. (2010). Endocannabinoid signaling directs differentiation of trophoblast cell lineages and placentation. *Proc Natl Acad Sci U S A* **107**, 16887-16892.

Sun, Z. W., Wang, X. C., Gao, J., Li, J., Li, Y. Y., Dang, Y. Z., and Shen, L. (2013). [correlation of mdr1 and abcg2 genetic polymorphisms with the efficacy and adverse events of irinotecan chemotherapy in patients with colorectal cancer]. *Zhonghua Wei Chang Wai Ke Za Zhi* **16**, 524-528.

Szilagyi, J. T., Mishin, V., Heck, D. E., Jan, Y. H., Aleksunes, L. M., Richardson, J. R., Heindel, N. D., Laskin, D. L., and Laskin, J. D. (2016). Selective targeting of heme protein in cytochrome p450 and nitric oxide synthase by diphenyleneiodonium. *Toxicol Sci* **151**, 150-159.

Szilagyi, J. T., Vetrano, A. M., Laskin, J. D., and Aleksunes, L. M. (2017). Localization of the placental bcrp/abcg2 transporter to lipid rafts: Role for cholesterol in mediating efflux activity. *Placenta* **55**, 29-36.

Tachampa, K., Takeda, M., Khamdang, S., Noshiro-Kofuji, R., Tsuda, M., Jariyawat, S., Fukutomi, T., Sophasan, S., Anzai, N., and Endou, H. (2008). Interactions of organic anion transporters and organic cation transporters with mycotoxins. *J Pharmacol Sci* **106**, 435-443.

Taguchi, N., Rubin, E. T., Hosokawa, A., Choi, J., Ying, A. Y., Moretti, M. E., Koren, G., and Ito, S. (2008). Prenatal exposure to hmg-coa reductase inhibitors: Effects on fetal and neonatal outcomes. *Reprod Toxicol* **26**, 175-177.

Tailor, C. S., Nouri, A., Zhao, Y., Takeuchi, Y., and Kabat, D. (1999). A sodium-dependent neutral-amino-acid transporter mediates infections of feline and baboon endogenous retroviruses and simian type d retroviruses. *J Virol* **73**, 4470-4474.

Takemura, H., Shim, J.-Y., Sayama, K., Tsubura, A., Ting Zhu, B., and Shimoi, K. (2007). *Characterization of the estrogenic activities of zearalenone and zeranol in vivo and in vitro*.

Tal, R. (2012). The role of hypoxia and hypoxia-inducible factor-1alpha in preeclampsia pathogenesis. *Biol Reprod* **87**, 134.

Tang, C., Mei, L., Pan, L., Xiong, W., Zhu, H., Ruan, H., Zou, C., Tang, L., Iguchi, T., and Wu, X. (2015). Hedgehog signaling through gli1 and gli2 is required for epithelial-mesenchymal transition in human trophoblasts. *Biochim Biophys Acta* **1850**, 1438-1448.

Taylor, N. M. I., Manolaridis, I., Jackson, S. M., Kowal, J., Stahlberg, H., and Locher, K. P. (2017). Structure of the human multidrug transporter abcg2. *Nature* **546**, 504-509.

Telbisz, A., Hegedus, C., Varadi, A., Sarkadi, B., and Ozvegy-Laczka, C. (2014). Regulation of the function of the human abcg2 multidrug transporter by cholesterol and bile acids: Effects of mutations in potential substrate and steroid binding sites. *Drug Metab Dispos* **42**, 575-585.

Telbisz, A., Muller, M., Ozvegy-Laczka, C., Homolya, L., Szente, L., Varadi, A., and Sarkadi, B. (2007). Membrane cholesterol selectively modulates the activity of the human abcg2 multidrug transporter. *Biochim Biophys Acta* **1768**, 2698-2713.

Telbisz, A., Ozvegy-Laczka, C., Hegedus, T., Varadi, A., and Sarkadi, B. (2013). Effects of the lipid environment, cholesterol and bile acids on the function of the purified and reconstituted human abcg2 protein. *Biochem J* **450**, 387-395.

Tew, D. G. (1993). Inhibition of cytochrome p450 reductase by the diphenyliodonium cation. Kinetic analysis and covalent modifications. *Biochemistry* **32**, 10209-10215.

The American College of Obstetricians and Gynecologists (2013). News release: Synthetic marijuana mimics preeclampsia and eclampsia during pregnancy.

To, K. K., Hu, M., and Tomlinson, B. (2014). Expression and activity of abcg2, but not abcb1 or oatp1b1, are associated with cholesterol levels: Evidence from in vitro and in vivo experiments. *Pharmacogenomics* **15**, 1091-1104.

Toth, A., Blumberg, P. M., and Boczan, J. (2009). Anandamide and the vanilloid receptor (trpv1). *Vitam Horm* **81**, 389-419.

Trabucco, E., Acone, G., Marenna, A., Pierantoni, R., Cacciola, G., Chioccarelli, T., Mackie, K., Fasano, S., Colacurci, N., Meccariello, R., Cobellis, G., and Cobellis, L. (2009). Endocannabinoid system in first trimester placenta: Low faah and high cb1 expression characterize spontaneous miscarriage. *Placenta* **30**, 516-522.

Tralamazza, S. M., Bemvenuti, R. H., Zorzete, P., de Souza Garcia, F., and Correa, B. (2016). Fungal diversity and natural occurrence of deoxynivalenol and zearalenone in freshly harvested wheat grains from brazil. *Food Chem* **196**, 445-450.

Vähäkangas, K., and Myllynen, P. (2009). Drug transporters in the human blood-placental barrier. *British Journal of Pharmacology* **158**, 665-678.

van Herwaarden, A. E., Wagenaar, E., Karnekamp, B., Merino, G., Jonker, J. W., and Schinkel, A. H. (2006a). Breast cancer resistance protein (bcrp1/abcg2) reduces systemic exposure of the dietary carcinogens aflatoxin b1, iq and trp-p-1 but also mediates their secretion into breast milk. *Carcinogenesis* **27**, 123-130.

van Herwaarden, A. E., Wagenaar, E., Karnekamp, B., Merino, G., Jonker, J. W., and Schinkel, A. H. (2006b). Breast cancer resistance protein (bcrp1/abcg2) reduces systemic exposure of the dietary carcinogens aflatoxin b1, iq and trp-p-1 but also mediates their secretion into breast milk. *Carcinogenesis* **27**, 123-130.

van Herwaarden, A. E., Wagenaar, E., Merino, G., Jonker, J. W., Rosing, H., Beijnen, J. H., and Schinkel, A. H. (2007). Multidrug transporter abcg2/breast cancer resistance protein secretes riboflavin (vitamin b2) into milk. *Mol Cell Biol* **27**, 1247-1253.

Vardhana, P. A., and Illsley, N. P. (2002). Transepithelial glucose transport and metabolism in bewo choriocarcinoma cells. *Placenta* **23**, 653-660.

Vendel, E., and de Lange, E. C. (2014). Functions of the cb1 and cb 2 receptors in neuroprotection at the level of the blood-brain barrier. *Neuromolecular Med* **16**, 620-642.

Venkatachalam, P., de Toledo, S. M., Pandey, B. N., Tephly, L. A., Carter, A. B., Little, J. B., Spitz, D. R., and Azzam, E. I. (2008). Regulation of normal cell cycle progression by flavin-containing oxidases. *Oncogene* **27**, 20-31.

Vermilion, J. L., Ballou, D. P., Massey, V. L., and Coon, M. J. (1981). Separate roles for fmn and fad in catalysis by liver microsomal nadph-cytochrome p-450 reductase. *J Biol Chem* **256**, 266-277.

Vermilion, J. L., and Coon, M. J. (1978a). Identification of the high and low potential flavins of liver microsomal nadph-cytochrome p-450 reductase. *J Biol Chem* **253**, 8812-8819.

Vermilion, J. L., and Coon, M. J. (1978b). Purified liver microsomal nadph-cytochrome p-450 reductase. Spectral characterization of oxidation-reduction states. *J Biol Chem* **253**, 2694-2704.

Videmann, B., Mazallon, M., Prouillac, C., Delaforge, M., and Lecoeur, S. (2009). Abcc1, abcc2 and abcc3 are implicated in the transepithelial transport of the myco-estrogen zearalenone and its major metabolites. *Toxicol Lett* **190**, 215-223.

Volk, E. L., Farley, K. M., Wu, Y., Li, F., Robey, R. W., and Schneider, E. (2002a). Overexpression of wild-type breast cancer resistance protein mediates methotrexate resistance. *Cancer Res* **62**, 5035-5040.

Volk, E. L., Farley, K. M., Wu, Y., Li, F., Robey, R. W., and Schneider, E. (2002b). Overexpression of wild-type breast cancer resistance protein mediates methotrexate resistance. *Cancer Research* **62**, 5035-5040.

Waldeck-Weiermair, M., Zoratti, C., Osibow, K., Balenga, N., Goessnitzer, E., Waldhoer, M., Malli, R., and Graier, W. F. (2008). Integrin clustering enables anandamide-induced ca²⁺ signaling in endothelial cells via gpr55 by protection against cb₁-receptor-triggered repression. *Journal of Cell Science* **121**, 1704-1717.

Walsh, D. R., Nolin, T. D., and Friedman, P. A. (2015). Drug transporters and na(+)/h(+) exchange regulatory factor psd-95/drosophila discs large/zo-1 proteins. *Pharmacological Reviews* **67**, 656-680.

Wang, H., Segal, S. J., and Koide, S. S. (1988). Purification and characterization of an incompletely glycosylated form of human chorionic gonadotropin from human placenta. *Endocrinology* **123**, 795-803.

Wang, H., Unadkat, J. D., and Mao, Q. (2008a). Hormonal regulation of bcrp expression in human placental bewo cells. *Pharm Res* **25**, 444-452.

Wang, H., Xie, H., and Dey, S. K. (2008b). Loss of cannabinoid receptor cb1 induces preterm birth. *PLoS One* **3**, e3320.

Wang, H., Zhou, L., Gupta, A., Vethanayagam, R. R., Zhang, Y., Unadkat, J. D., and Mao, Q. (2006). Regulation of bcrp/abcg2 expression by progesterone and 17beta-estradiol in human placental bewo cells. *Am J Physiol Endocrinol Metab* **290**, E798-807.

Wang, J., Paria, B. C., Dey, S. K., and Armant, D. R. (1999). Stage-specific excitation of cannabinoid receptor exhibits differential effects on mouse embryonic development. *Biol Reprod* **60**, 839-844.

Wang, Y., Gray, J. P., Mishin, V., Heck, D. E., Laskin, D. L., and Laskin, J. D. (2008c). Role of cytochrome p450 reductase in nitrofurantoin-induced redox cycling and cytotoxicity. *Free Radic Biol Med* **44**, 1169-1179.

Wang, Y., Gray, J. P., Mishin, V., Heck, D. E., Laskin, D. L., and Laskin, J. D. (2010). Distinct roles of cytochrome p450 reductase in mitomycin c redox cycling and cytotoxicity. *Mol Cancer Ther* **9**, 1852-1863.

Warner, T. D., Roussos-Ross, D., and Behnke, M. (2014). It's not your mother's marijuana: Effects on maternal-fetal health and the developing child. *Clin Perinatol* **41**, 877-894.

Wen, J., Zhang, R. Y., Chen, S. Y., Zhang, J., and Yu, X. Q. (2012). Direct arylation of arene and n-heteroarenes with diaryliodonium salts without the use of transition metal catalyst. *J Org Chem* **77**, 766-771.

White, K. A., and Marletta, M. A. (1992). Nitric oxide synthase is a cytochrome p-450 type hemoprotein. *Biochemistry* **31**, 6627-6631.

Willoughby, K. A., Moore, S. F., Martin, B. R., and Ellis, E. F. (1997). The biodisposition and metabolism of anandamide in mice. *J Pharmacol Exp Ther* **282**, 243-247.

Wink, D. A., Cook, J. A., Kim, S. Y., Vodovotz, Y., Pacelli, R., Krishna, M. C., Russo, A., Mitchell, J. B., Jourd'heuil, D., Miles, A. M., and Grisham, M. B. (1997). Superoxide modulates the oxidation and nitrosation of thiols by nitric oxide-derived reactive intermediates. Chemical aspects involved in the balance between oxidative and nitrosative stress. *J Biol Chem* **272**, 11147-11151.

Witten, C. M. (1989). Pulmonary toxicity of nitrofurantoin. *Arch Phys Med Rehabil* **70**, 55-57.

Wood, J. T., Williams, J. S., Pandarinathan, L., Courville, A., Keplinger, M. R., Janero, D. R., Vouros, P., Makriyannis, A., and Lammi-Keefe, C. J. (2008). Comprehensive profiling of the human circulating endocannabinoid metabolome: Clinical sampling and sample storage parameters. *Clinical chemistry and laboratory medicine : CCLM / FESCC* **46**, 1289-1295.

Woodhams, S. G., Sagar, D. R., Burston, J. J., and Chapman, V. (2015). The role of the endocannabinoid system in pain. *Handb Exp Pharmacol* **227**, 119-143.

Wu, B., Jiang, W., Yin, T., Gao, S., and Hu, M. (2012). A new strategy to rapidly evaluate kinetics of glucuronide efflux by breast cancer resistance protein (bcrp/abcg2). *Pharm Res* **29**, 3199-3208.

Xiao, J., Wang, Q., Bircsak, K. M., Wen, X., and Aleksunes, L. M. (2015). Screening of environmental chemicals identifies zearalenone as a novel substrate of the placental bcrp/ transporter. *Toxicol Res (Camb)* **4**, 695-706.

Xie, H., Sun, X., Piao, Y., Jegga, A. G., Handwerger, S., Ko, M. S., and Dey, S. K. (2012). Silencing or amplification of endocannabinoid signaling in blastocysts via cb1 compromises trophoblast cell migration. *J Biol Chem* **287**, 32288-32297.

Xie, Y., Nakanishi, T., Natarajan, K., Safren, L., Hamburger, A. W., Hussain, A., and Ross, D. D. (2015). Functional cyclic amp response element in the breast cancer resistance protein (bcrp/abcg2) promoter modulates epidermal growth factor receptor pathway- or androgen withdrawal-mediated bcrp/abcg2 transcription in human cancer cells. *Biochimica et biophysica acta* **1849**, 317-327.

Xiong, W., Hosoi, M., Koo, B. N., and Zhang, L. (2008). Anandamide inhibition of 5-ht3a receptors varies with receptor density and desensitization. *Molecular Pharmacology* **73**, 314-322.

Xu, M., Wang, W., Frontera, J. R., Neely, M. C., Lu, J., Aires, D., Hsu, F. F., Turk, J., Swerdlow, R. H., Carlson, S. E., and Zhu, H. (2011). Ncb5or deficiency increases fatty acid catabolism and oxidative stress. *J Biol Chem* **286**, 11141-11154.

Yang, M., Lei, Z. M., and Rao Ch, V. (2003). The central role of human chorionic gonadotropin in the formation of human placental syncytium. *Endocrinology* **144**, 1108-1120.

Yang, S., Jan, Y. H., Gray, J. P., Mishin, V., Heck, D. E., Laskin, D. L., and Laskin, J. D. (2013). Sepiapterin reductase mediates chemical redox cycling in lung epithelial cells. *J Biol Chem* **288**, 19221-19237.

Yang, S., Jan, Y. H., Mishin, V., Heck, D. E., Laskin, D. L., and Laskin, J. D. (2017). Diacetyl/l-xylulose reductase mediates chemical redox cycling in lung epithelial cells **30**, 1406-1418.

Yang, X., Ma, Z., Zhou, S., Weng, Y., Lei, H., Zeng, S., Li, L., and Jiang, H. (2016). Multiple drug transporters are involved in renal secretion of entecavir. *Antimicrobial Agents and Chemotherapy* **60**, 6260-6270.

Yoshie, M., Kaneyama, K., Kusama, K., Higuma, C., Nishi, H., Isaka, K., and Tamura, K. (2010). Possible role of the exchange protein directly activated by cyclic amp (epac) in the cyclic amp-dependent functional differentiation and syncytialization of human placental bewo cells. *Hum Reprod* **25**, 2229-2238.

Yu, H., Wakim, B., Li, M., Halligan, B., Tint, G. S., and Patel, S. B. (2007). Quantifying raft proteins in neonatal mouse brain by 'tube-gel' protein digestion label-free shotgun proteomics. *Proteome Sci* **5**, 17.

Zaher, H., Khan, A. A., Palandra, J., Brayman, T. G., Yu, L., and Ware, J. A. (2006). Breast cancer resistance protein (bcrp/abcg2) is a major determinant of sulfasalazine absorption and elimination in the mouse. *Mol Pharm* **3**, 55-61.

Zamber, C. P., Lamba, J. K., Yasuda, K., Farnum, J., Thummel, K., Schuetz, J. D., and Schuetz, E. G. (2003). Natural allelic variants of breast cancer resistance protein (bcrp) and their relationship to bcrp expression in human intestine. *Pharmacogenetics* **13**, 19-28.

Zamek-Gliszczynski, M. J., Day, J. S., Hillgren, K. M., and Phillips, D. L. (2011). Efflux transport is an important determinant of ethinylestradiol glucuronide and ethinylestradiol sulfate pharmacokinetics. *Drug Metab Dispos* **39**, 1794-1800.

Zhang, D., He, K., Herbst, J. J., Kolb, J., Shou, W., Wang, L., Balimane, P. V., Han, Y. H., Gan, J., Frost, C. E., and Humphreys, W. G. (2013). Characterization of efflux transporters involved in distribution and disposition of apixaban. *Drug Metab Dispos* **41**, 827-835.

Zhang, Y., Bressler, J. P., Neal, J., Lal, B., Bhang, H. E., Laterra, J., and Pomper, M. G. (2007a). Abcg2/bcrp expression modulates d-luciferin based bioluminescence imaging. *Cancer Res* **67**, 9389-9397.

Zhang, Y., Hu, X., Gao, G., Wang, Y., Chen, P., and Ye, Y. (2016). Autophagy protects against oxidized low density lipoprotein-mediated inflammation associated with preeclampsia. *Placenta* **48**, 136-143.

Zhang, Y., Qu, X., Teng, Y., Li, Z., Xu, L., Liu, J., Ma, Y., Fan, Y., Li, C., Liu, S., Wang, Z., Hu, X., Zhang, J., and Liu, Y. (2015). Cbl-b inhibits p-gp transporter function by preventing its translocation into caveolae in multiple drug-resistant gastric and breast cancers. *Oncotarget* **6**, 6737-6748.

Zhang, Y., Wang, H., Unadkat, J. D., and Mao, Q. (2007b). Breast cancer resistance protein 1 limits fetal distribution of nitrofurantoin in the pregnant mouse. *Drug Metab Dispos* **35**, 2154-2158.

Zhao, F., Li, R., Xiao, S., Diao, H., Viveiros, M. M., Song, X., and Ye, X. (2013). Postweaning exposure to dietary zearalenone, a mycotoxin, promotes premature onset of puberty and disrupts early pregnancy events in female mice. *Toxicological Sciences* **132**, 431-442.

Zheng, R., Po, I., Mishin, V., Black, A. T., Heck, D. E., Laskin, D. L., Sinko, P. J., Gerecke, D. R., Gordon, M. K., and Laskin, J. D. (2013a). The generation of 4-

hydroxynonenal, an electrophilic lipid peroxidation end product, in rabbit cornea organ cultures treated with uvb light and nitrogen mustard. *Toxicology and Applied Pharmacology* **272**, 345-355.

Zheng, R., Po, I., Mishin, V., Black, A. T., Heck, D. E., Laskin, D. L., Sinko, P. J., Gerecke, D. R., Gordon, M. K., and Laskin, J. D. (2013b). The generation of 4-hydroxynonenal, an electrophilic lipid peroxidation end product, in rabbit cornea organ cultures treated with uvb light and nitrogen mustard. *Toxicol Appl Pharmacol* **272**, 345-355.

Zhou, L., Naraharisetti, S. B., Wang, H., Unadkat, J. D., Hebert, M. F., and Mao, Q. (2008). The breast cancer resistance protein (bcrp1/abcg2) limits fetal distribution of glyburide in the pregnant mouse: An obstetric-fetal pharmacology research unit network and university of washington specialized center of research study. *Mol Pharmacol* **73**, 949-959.

Zhou, L., Schmidt, K., Nelson, F. R., Zelesky, V., Troutman, M. D., and Feng, B. (2009). The effect of breast cancer resistance protein and p-glycoprotein on the brain penetration of flavopiridol, imatinib mesylate (gleevec), prazosin, and 2-methoxy-3-(4-(2-(5-methyl-2-phenyloxazol-4-yl)ethoxy)phenyl)propanoic acid (pf-407288) in mice. *Drug Metab. Dispos.* **37**, 946-955.

Zhou, Y., Maxwell, K. N., Sezgin, E., Lu, M., Liang, H., Hancock, J. F., Dial, E. J., Lichtenberger, L. M., and Levental, I. (2013). Bile acids modulate signaling by functional perturbation of plasma membrane domains. *J Biol Chem* **288**, 35660-35670.

Zinedine, A., Soriano, J. M., Moltó, J. C., and Mañes, J. (2007). Review on the toxicity, occurrence, metabolism, detoxification, regulations and intake of zearalenone: An oestrogenic mycotoxin. *Food and Chemical Toxicology* **45**, 1-18.